Proceedings, 15th Applied Stochastic Models and Data Analysis (ASMDA2013)
International Conference, Mataró (Barcelona), Spain 25 - 28 June 2013

Regression Models for Repairable Systems

Petr Novák

Charles University in Prague, Faculty of Mathematics and Physics, Department of Probability and Mathematical Statistics, Sokolovská 83, 186 75 Praha 8, Czech Republic
(E-mail: novakp@karlin.mff.cuni.cz)

Abstract. When operating a device which is a subject to degradation, we want to estimate the distribution of the time to failure for maintenance optimization. Our aim is to describe the dependency of the failure time distribution on applicable regression variables. Models commonly used in survival analysis, such as the Cox model or the Accelerated failure time model, need to be adjusted to accommodate repairs and maintenance. For instance, we may use the number of repairs or maintenance actions or their cost as time-varying covariates. In this work we describe such models and demonstrate their application on real data.
Keywords: Reliability analysis, Repair models, Regression.

1 Introduction

We study data describing a service record of one ore more devices which degrade over time. When a device breaks down, it is necessary to perform a repair. We want to avoid breakdowns by performing preventive maintenance, and to optimize the maintenance costs, it is desirable to estimate the time to failure distribution with the help of available information. In this work we focus on methods of modeling the life time of the device with available regression models of survival analysis with suitable covariates. The models need to be adjusted to accommodate recurring repairs and maintenance actions. One such approach was described by Percy and Kobbacy[8] and Percy and Alkali[6] for the Cox proportional hazards model with covariates multiplicatively influencing a parametric baseline hazard. In a similar way, we show the use the Accelerated failure time model with time-varying covariates (Lin and Ying[4]), which states that the covariates influence multiplicatively the flow of the internal time of the device. Further, we show methods of estimating the cumulative baseline hazard nonparametrically if we have data on more devices, which allows us to estimate the regression parameters without assumptions on the shape of the baseline. Finally, we show the application of all described methods on real data from oil industry.

2 Modeling the life time of one device

Let $T_1, ..., T_n$ be random variables representing the ordered times of actions (repair or maintenance). Denote $\Delta_1, ..., \Delta_n$ the indicators whether in j-th time a repair ($\Delta_j = 1$) or a maintenance ($\Delta_j = 0$) was performed and let $X(t)$ be an explanatory variable, possibly time-varying.

We work with counting processes denoting the number of repairs and maintenance actions up to time t:

$$N_\bullet(t) = \sum_{j=1}^{n} I(T_j \le t, \Delta_j = 1), \qquad M_\bullet(t) = \sum_{j=1}^{n} I(T_j \le t, \Delta_j = 0).$$

Denote the hazard function

$$\lambda(t) = \lim_{h \to 0} P(N_\bullet(t+h) - N_\bullet(t) \ge 1 | \mathcal{H}(t))/h$$

where $\mathcal{H}(t)$ is the history of events up to time t. Further denote the cumulative hazard function $\Lambda(t) = \int_0^t \lambda(s)ds$ and $S(t) = \exp(-\Lambda(t))$ and $f(t) = -S'(t)$ corresponding survival function and density of the time to failure distribution. We assume that a repair returns the device to working state and that it affects the hazard function. The aim is to determine whether repairs and maintenance actions increase or decrease the hazard and by how much. We parametrize the hazard function and estimate the parameters using maximum likelihood method. The likelihood can be written as

$$L = \prod_{j=1}^{n} \left(\frac{f(T_j^-)}{S(T_{j-1})} \right)^{\Delta_j} \left(\frac{S(T_j)}{S(T_{j-1})} \right)^{1-\Delta_j} = \prod_{j=1}^{n} \lambda(T_j^-)^{\Delta_j} \cdot S(T_n)$$

and the log-likelihood has the form

$$l = \sum_{j=1}^{n} \Delta_j \log \lambda(T_j^-) - \int_0^{T_n} \lambda(t)dt.$$

Cox model

In the Cox model the covariates affect the hazard function multiplicatively. We assume that each repair or maintenance action multiplicatively increases or decreases the baseline hazard and so do other explanatory variables. We work with the hazard function in the form (Percy and Alkali[6])

$$\lambda(t) = \lambda_0(t) e^{M_\bullet(t)\rho + N_\bullet(t)\sigma + X(t)\beta} = \lambda_0(t)(e^\rho)^{M_\bullet(t)}(e^\sigma)^{N_\bullet(t)}(e^\beta)^{X(t)}.$$

As the explanatory variable $X(t)$ we can use for instance the cost of the last repair. If the covariate values change only in the times of observed events and the baseline hazard $\lambda_0(t)$ is parametric, it is possible to insert the hazard function into the log-likelihood and maximize.

Accelerated failure time model

We can also assume that each repair or maintenance causes that the internal time of the device flows faster or slower (Accelerated Failure Time model, AFT). We use the time transformation (Lin and Ying[4])

$$t \to \int_0^t e^{M_\bullet(s)\rho + N_\bullet(s)\sigma + X(s)\beta} ds =: h(t, \boldsymbol{\beta}),$$

where $\boldsymbol{\beta} = (\rho, \sigma, \beta)^T$. The hazard function has the form

$$\lambda(t) = \lambda_0(h(t, \boldsymbol{\beta}))e^{M_\bullet(t)\rho + N_\bullet(t)\sigma + X(t)\beta}.$$

If the baseline hazard function is constant (corresponding with the exponential distribution), both models coincide.

3 Inference when observing more devices

If we have data on n independent devices, we work with joint likelihood. We can either parametrize the baseline hazard and proceed as above, or estimate the baseline nonparametrically. This may be desirable, since we do not need to pose any assumptions on the form of the baseline and focus on the regression parameters. Let us have $\lambda_i(t)$, T_{ij}, Δ_{ij}, $j = 1, ...n_i$ and $X_i(t)$ the hazard function, times of events, repair indicators and covariate values for the i-th device respectively. Denote

$$N_{ij}(t) = \Delta_{ij} I(T_{ij} \leq t),$$
$$M_{ij}(t) = (1 - \Delta_{ij}) I(T_{ij} \leq t),$$
$$Y_{ij}(t) = I(T_{i,j-1} < t \leq T_{ij}).$$

We get the log-likelihood in form

$$l = \sum_{ij} \int_0^\infty \Big(\log \lambda_i(t^-) dN_{ij}(t) - Y_{ij}(t)\lambda_i(t^-)dt \Big).$$

The hazard function λ_i will contain the counts of repairs and maintenance actions $N_{i\bullet}$ and $M_{i\bullet}$, where $\bullet$ means the sum over corresponding index.

Semiparametric Cox model

Denote $\mathbf{X}_i^T(t) = (N_{i\bullet}(t), M_{i\bullet}(t), X_i(t))$. Then the likelihood and score function under the Cox model are

$$l = \sum_{ij} \int_0^\infty \Big((\log \lambda_0(t^-) + \mathbf{X}_i^T(t^-)\boldsymbol{\beta}) dN_{ij}(t) - Y_{ij}(t) e^{\mathbf{X}_i^T(t^-)\boldsymbol{\beta}} \lambda_0(t^-) dt \Big),$$

$$U(\boldsymbol{\beta}) = \sum_{ij} \int_0^\infty \Big(\mathbf{X}_i^T(t^-) dN_{ij}(t) - Y_{ij}(t) \mathbf{X}_i^T(t^-) e^{\mathbf{X}_i^T(t^-)\boldsymbol{\beta}} d\Lambda_0(t) \Big).$$

The score depends on an unknown cumulative baseline hazard $\Lambda_0(t)$. This can be replaced by the Nelson-Aalen estimate

$$\hat{\Lambda}_0(t, \boldsymbol{\beta}) = \int_0^t \frac{dN_{\bullet\bullet}(s)}{\sum_{ij} e^{\mathbf{X}_i^T(s^-)\boldsymbol{\beta}} Y_{ij}(s)}.$$

Inserting the estimate we get the score function in form

$$U(\boldsymbol{\beta}) = \sum_{ij} \int_0^\infty \left(\mathbf{X}_i(t^-) - \frac{\sum_{ij} \mathbf{X}_i(t^-) e^{\mathbf{X}_i^T(t^-)\boldsymbol{\beta}} Y_{ij}(t)}{\sum_{ij} e^{\mathbf{X}_i^T(t^-)\boldsymbol{\beta}} Y_{ij}(t)} \right) dN_{ij}(t)$$

and we find the parameter estimates by solving the equations $U(\boldsymbol{\beta}) = \mathbf{0}$.

Semiparametric AFT model

For each device we have the time transformation $t \to h_i(t, \boldsymbol{\beta})$. We work with time-transformed processes

$$N^*_{ij}(t, \boldsymbol{\beta}) = \Delta_{ij} I(h_i(T_{ij}, \boldsymbol{\beta}) \leq t),$$

$$M^*_{ij}(t, \boldsymbol{\beta}) = (1 - \Delta_{ij}) I(h_i(T_{ij}, \boldsymbol{\beta}) \leq t),$$

$$Y^*_{ij}(t, \boldsymbol{\beta}) = I(h_i(T_{i,j-1}, \boldsymbol{\beta}) < t \leq h_i(T_{ij}, \boldsymbol{\beta})),$$

$$X^*_i(t, \boldsymbol{\beta}) = X_i(h_i^{-1}(t, \boldsymbol{\beta})).$$

The exact score has a more complicated form, but it can be replaced by the approximate score (Lin and Ying[4])

$$U(\boldsymbol{\beta}) = \sum_{ij} \int_0^\infty \mathbf{X}^*_i(t^-, \boldsymbol{\beta}) \left(dN^*_{ij}(t, \boldsymbol{\beta}) - Y^*_{ij}(t, \boldsymbol{\beta}) d\Lambda_0(t) \right)$$

and we can again insert the estimate of the cumulative baseline hazard function

$$\hat{\Lambda}_0(t, \boldsymbol{\beta}) = \int_0^t \frac{dN^*_{\bullet\bullet}(s, \boldsymbol{\beta})}{\sum_{ij} Y^*_{ij}(t, \boldsymbol{\beta})}.$$

We get

$$U(\boldsymbol{\beta}) = \sum_{ij} \int_0^\infty \left(\mathbf{X}^*_i(t^-, \boldsymbol{\beta}) - \frac{\sum_{ij} \mathbf{X}^*_i(t^-, \boldsymbol{\beta}) Y^*_{ij}(t, \boldsymbol{\beta})}{\sum_{ij} Y^*_{ij}(t, \boldsymbol{\beta})} \right) dN^*_{ij}(t, \boldsymbol{\beta}).$$

Because the score is not continuous in $\boldsymbol{\beta}$, we obtain the parameter estimates by minimizing $\|U(\boldsymbol{\beta})\|$.

4 Modeling lifetime of oil pumps

We explore data on service of oil pumps during several years (Kobbacy *et al.*[1] and Percy and Alkali[7]). For one device we have detailed data on $n_1 = 65$ times of repairs, maintenance actions and the cost of each action in man-hours. This data has been studied by Percy and Alkali[6] using the Cox model. We try to model the lifetime using both the Cox and the AFT model as shown above with various parametrized baseline hazard functions and compare the results. In the parametric case, it is possible to directly maximize the likelihood for all cases and see in which it was largest.

For four other pumps we have only the times of actions at disposal, with $(n_2, ..., n_5) = (51, 90, 30, 30)$. We use both the semiparametric methods and parametrized baseline hazards with the two described models to estimate the regression parameters utilizing data of all the five pumps. The likelihood in semiparametric methods depends on the unknown baseline hazard and therefore is not available for comparison of the used methods.

Parametric modeling of one pump service

We have the times of repairs, maintenance actions and cost of each action for one pump. Using methods from section 2 we estimate the parameters ρ, σ and β in both the Cox model and the AFT model. We try to maximize the likelihood for exponential, Weibull $\lambda_0(t) = a\lambda^a t^{a-1}$, gamma $f(t) \propto t^{a-1}e^{-\lambda t}$, truncated Gumbel $\lambda_0(t) = \lambda a^t$ and log-normal baseline distributions.

Model	λ_0	log - lik	$e^{\hat{\rho}}$	$e^{\hat{\sigma}}$	$e^{\hat{\beta}}$	$\hat{\lambda}$	$\hat{a}$
	Exp.	-213.8	1.407	0.980	1.0066	0.0015	–
Cox	Weibull	-213.5	1.266	0.924	1.0064	0.0017	1.672
	Gamma	-213.8	1.405	0.918	1.0066	0.0016	1.027
	Gumbel	**-210.2**	0.701	0.745	1.0063	0.0006	1.010
	LN	-214.8	1.541	0.913	1.0069	$\hat{\mu}$=6.3	$\hat{\sigma}$=1.66
AFT	Weibull	-212.7	1.278	0.918	1.0061	0.0014	1.639
	Gamma	-213.8	1.418	0.916	1.0066	0.0014	0.918
	Gumbel	**-210.2**	1.318	0.877	1.0050	0.0005	1.001
	LN	-218.1	1.300	1.050	1.0070	$\hat{\mu}$=5.25	$\hat{\sigma}$=0.89

Table 1. The log-likelihood and parameter estimates from parametric models of the lifetime of one oil pump.

Comparing the likelihood values in Table 1 we find that it is highest for both the Cox and AFT model with the truncated Gumbel distribution. Further we see that the more each action did cost, the more it increased the hazard function or accelerated the internal time, because $e^{\hat{\beta}} > 1$. Each man-hour of the action means an increase of hazard or acceleration of time by about $0.5 - 0.7\%$. A repair itself has a positive influence ($e^{\hat{\sigma}} < 1$), with the exception of the AFT model with log-normal baseline distribution, but that is the case with the lowest likelihood value. It is interesting that according to all cases except the Gumbel distribution in Cox model, the maintenance actions tend to have a negative influence ($e^{\hat{\rho}} > 1$). This could be due to repairs often taking much more man-hours than maintenances, resulting in negative influence of both.

Semiparametric modeling of the lifetime of five pumps

For five devices we have only the times of repairs and maintenances available. The data on the cost of the actions was not available for all pumps, therefore we estimate only the regression parameters ρ and σ. We tried the Cox and the AFT models, both parametric with the same baseline distributions as above and semiparametric. In the parametric cases we maximize the log-likelihood whereas in the semiparametric approach we insert the estimate of the cumulative baseline hazard into the score function and solve the equations $U(\boldsymbol{\beta}) = \mathbf{0}$ for the Cox model and minimize $\|U(\boldsymbol{\beta})\|$ for the AFT model.

Model	λ_0	log - lik	$e^{\hat{\rho}}$	$e^{\hat{\sigma}}$	$\hat{\lambda}$	$\hat{a}$
	Exp.	-880.3	0.985	1.016	0.016	–
Cox	Weibull	-880.2	0.976	1.016	0.014	1.063
	Gamma	-880.1	0.988	1.016	0.015	0.811
	Gumbel	-880.3	0.994	1.016	0.016	0.999
	LN	-894.4	1.090	1.016	$\hat{\mu}$=3.22	$\hat{\sigma}$=0.89
AFT	Weibull	-880.2	0.980	1.015	0.014	1.038
	Gamma	-880.1	0.988	1.016	0.015	0.812
	Gumbel	**-875.1**	1.022	1.036	0.013	0.999
	LN	-879.5	1.284	1.158	$\hat{\mu}$=2.67	$\hat{\sigma}$=1.56
Cox	nonparam.	–	1.043	1.020	–	–
AFT	nonparam.	–	1.028	1.084	–	–

Table 2. The log-likelihood and parameter estimates from modeling the lifetime of five pumps.

In Table 2 we see that in all cases a repair increases the hazard or accelerates the internal time ($e^{\hat{\sigma}} > 1$). Among the parametric models, the Gumbel distribution with AFT model has the highest likelihood. In that case and also in the cases with log-normal baseline hazard and the semiparametric models, the maintenance actions have also a negative influence, whereas in the other cases it is positive. In Figure 1 we see the estimates of the cumulative baseline hazard for both Cox and AFT models. The time in the AFT model is on the transformed scale $t \to h(t, \hat{\boldsymbol{\beta}})$.

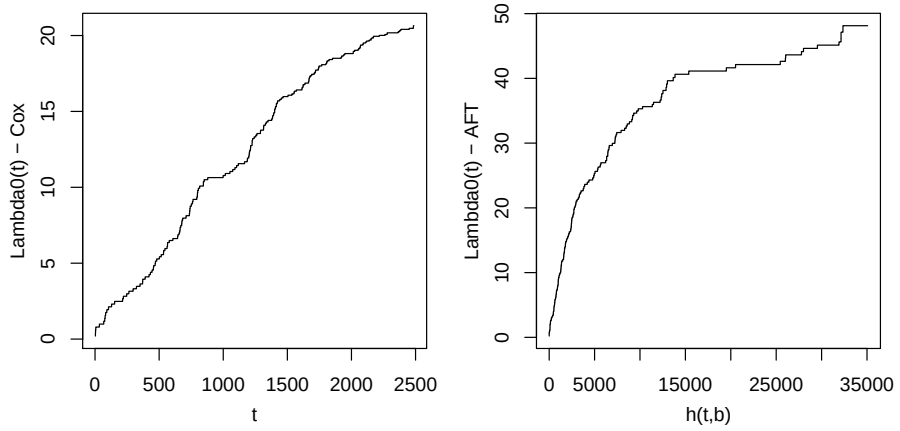

Fig. 1. Estimates of the cumulative baseline hazard in semiparametric Cox and AFT models.

Possible model selection and validation methods

When comparing two models, it is possible to perform a χ^2 test based on scaled deviance $D = 2 \cdot (l_1 - l_2)$ to see for instance whether an added covariate significantly improves a model. For the one pump data using Cox model with Gumbel baseline, no significant improvement was found when adding the influence of the cost of the action (β) to a model containing only the regression parameters ρ and σ (Percy and Alkali[6]), while it can be argued that the covariate still adds some relevant information.

Aside from the likelihood value, we do not have a direct means to determine which model fits the data best, especially when comparing the parametric and semiparametric approaches. For classic survival regression data, goodness-of-fit tests have been developed for parametric versions of both models by Lin and Spiekerman[2], for the semiparametric Cox model by Lin *et al.*[3] and for the semiparametric AFT model by Novák[5]. This methods could be adapted to accommodate repairs and maintenance actions. They are however, based on resampling approach and asymptotic convergence of certain martingale processes, and therefore it remains to be seen how well they would perform in such cases as with above data representing only a few independent devices.

5 Conclusion

We explored methods for modeling the influence of maintenance and repairs on the lifetime of the observed device. In the Cox model the covariates representing the count and size of repairs and maintenance actions influence the hazard function multiplicatively, whereas in the AFT model they accelerate or decelerate the flow of the internal time of the device. When we parametrize the baseline hazard function, the service record of one device is enough to obtain the estimates of the regression parameters. If we have data on more devices, it is possible to estimate the cumulative baseline hazard function nonparametrically. Further research could concern developing goodness-of-fit tests or testing whether a nonparametric estimate may be replaced by a suitable parametrized baseline hazard. It would be also possible to explore other transformations in the accelerated failure time model.

Acknowledgement

This work was supported by grants SVV 261315/2013 and GAUK 11122/2013.

References

1.K.A.H. Kobbacy, B.B. Fawzi, D.F. Percy and H.E. Ascher. A full history proportional hazards model for preventive maintenance scheduling. *Quality and Reliability Engineering Intl.*, 13, 187-198, 1997.

2.D.Y.Lin and C.F. Spiekerman. Model checking techniques for parametric regression with censored data. *Scandinavian Journal of Statistics*, 23, 157–177, 1996.
3.D.Y. Lin, L.J. Wei and Z. Ying. Checking the Cox model with cumulative sums of martingale-based residuals. *Biometrika* 80(3), 557–572, 1993.
4.D.Y. Lin and Z. Ying. Semiparametric inference for the accelerated life model with time-dependent covariates. *Journal od Statistical Planning and Inference*, 44, 47–63, 1995.
5.P. Novák. Goodness-of-fit test for the Accelerated Failure Time model based on martingale residuals *Kybernetika* 49(1), 40–59, 2013.
6.D.F. Percy and B.M. Alkali. Generalized proportional intensities models for repairable systems. *IMA Journal of Management Mathematics* 17, 171–185, 2005.
7.D.F. Percy and B.M. Alkali. Scheduling preventive maintenance for oil pumps using generalized proportional intensities models. *International Transactions of Operational Research* 14, 547–563, 2007.
8.D.F. Percy and K.A.H. Kobbacy. Using proportional-intensities models to schedule preventive-maintenance intervals *IMA Journal of Mathematics Applied in Business & Industry*, 9, 289–302, 1998.

Proceedings, 15th Applied Stochastic Models and Data Analysis (ASMDA2013)
International Conference, Mataró (Barcelona), Spain 25 - 28 June 2013

Stochastic modeling of hydraulic operating parameters in pipeline systems

N.N. Novitsky [1], O.V. Vanteyeva [2]

[1] Energy Systems Institute, Siberian Branch of the Russian Academy of Sciences, 130, Lermontov st., Irkutsk, 664033, Russia (e-mail: pipenet@isem.sei.irk.ru)

[2] Energy Systems Institute, Siberian Branch of the Russian Academy of Sciences, 130, Lermontov st., Irkutsk, 664033, Russia (e-mail: vanteeva@isem.sei.irk.ru)

Introduction. The problems of calculating hydraulic operating parameters are the basic problems in the analysis of operating conditions of pipeline systems when designed, operated, and controlled. These problems are traditionally solved using models and methods, which, however, do not allow us to quantitatively assess the satisfiability of operating conditions when consumption is random, which is typical of many practical situations. This is explained by high complexity and dimensionality of pipeline systems (heat-, water-, gas supply systems, etc.) as modeling objects, excessive efforts necessary to apply general methods of stochastic modeling (such as the Monte-Carlo method), and difficulties in obtaining initial statistical data.

The paper presents an approach, a set of mathematical models and methods for modeling the operating parameters of pipeline systems that were developed in terms of stochastics and dynamics of consumption processes and the established rules of their control, which make it possible to rationally combine the adequacy of modeling and its high computational efforts [1, 2].

Problem statement of the probabilistic calculation of hydraulic operating parameters. Probabilistic description of definite hydraulic operating parameters is reduced to the probability density function, which is denoted here by $p(R,\phi_R)$, where R – the value of a random vector of operating parameters (pressure, flow rate, etc.); ϕ_R – distribution parameters. Most of the practical cases allow us to use the hypothesis about normal distribution of R. Then $\phi_R=\{\bar{R},C_R\}$ and the probabilistic description of hydraulic operating parameters can be reduced to the specification of values of mathematical expectation ($\bar{R}$) and covariance matrix (C_R) for value *R*.

Not every combination of R components is acceptable, since they should satisfy the equations of flow distribution model $U(R)=0$ (where U – non-linear vector function). These equations result from general physical conservation laws, and hence should be solved deterministically.

The traditional deterministic model of steady hydraulic operating parameters in a pipeline system as a hydraulic circuit with lumped parameters can be represented as [3]

$$U(R)=U(X,Y)=U(x,Q,P,\alpha)=\begin{pmatrix} Ax-Q \\ A^{\mathrm{T}}P-f(x,\alpha)\end{pmatrix}=0. \qquad (1)$$

Here the first subsystem of equations represents the conditions of material balance at the nodes of hydraulic circuit (equations of the first Kirchhoff law); the second subsystem – the equations of the second Kirchhoff law; X – boundary conditions; Y – unknown operating parameters; T – transposition sign; A – $m\times n$ - incidence matrix with elements $a_{ji}=1(-1)$, if node j is the initial (end) node for branch i, $a_{ji}=0$, if branch i is not incident to node j; *m, n* – number of nodes and branches of the hydraulic circuit; x – *n*-dimensional vector of flow rate in branches, Q,P – *m*-dimensional vectors of nodal pressures and flow rates, $f(x,\alpha)$ – *n*-dimensional vector-function with components $f_i(x_i,\alpha_i)$, reflecting the laws of hydraulic flow for the branches; α – n_α-dimensional vector of parameters of these characteristics. For instance, if $f_i(x_i,\alpha_i)=s_i x_i\,|\,x_i\,|-H_i$, then $\alpha_i=\{s_i,H_i\}$, where x_i – flow rate in the *i*-th branch; s_i – hydraulic resistance of the branch; $H_i>0$ – increase in pressure in the case of an active branch (e.g. a branch representing a pumping station); $H_i=0$ in the case of a passive branch (e.g. a branch representing a pipeline section). If in (1) all parameters s_i, H_i, $i=\overline{1,n}$ are set deterministically, then $R=(x^{\mathrm{T}},\bar{Q}^{\mathrm{T}},\bar{P}^{\mathrm{T}})^{\mathrm{T}}$. Thus, the probabilistic model of steady flow distribution can be represented as $U(R)=0$, $R\sim N_r(\bar{R},C_R)$, where N_r – *r* –dimensional normal probability distribution; r – dimensional of vector *R*. In the case of normal distribution of X, if we neglect the non-linear distortion of distribution $p[Y(X),\phi_{Y(X)}]$ (where $Y(X)$ – implicit function given by the flow distribution equations), the problem can be reduced to the determination of $\varphi_R=\{\bar{R},C_R\}$ with the given function $\varphi_X=\{\bar{X},C_X\}$ and under condition $U(R)=U(X,Y)=0$. Moreover, the composition of X should provide solvability of equations $U(X,Y)=0$ with respect to Y, i.e. $\dim(Y)=\dim(U)=\mathrm{rank}(\partial U/\partial Y)$, where $\partial U/\partial Y$ – Jacobian matrix (of partial derivatives) under fixed boundary conditions X^* in the neighborhood of the solution point Y^*, $\dim(\cdot)$ – vector dimensional, $\mathrm{rank}(\cdot)$ – matrix rank.

Methodological approach. Let $\xi_X=(X-\bar{X})$ be a random deviation of possible realization of boundary conditions from its mathematical expectation $\bar{X}$. After linearizing function $Y(X)$ in the neighborhood of $\bar{X}$, we

obtain $Y \approx Y(\bar{X}) + (\partial Y / \partial X)\xi_X$, where $\partial Y / \partial X$ is derivative matrix at point $\bar{X}$. Since $E(Y) = \bar{Y}$ and $E(\xi_X) = 0$, where E is the operation of mathematical expectation, then $\bar{Y} = Y(\bar{X})$. Thus, the mathematical expectation of unknown operating parameters ($\bar{Y}$) is the function of flow distribution equations under boundary conditions $\bar{X}$. Correspondingly,

$$\bar{R} = \begin{pmatrix} \bar{X} \\ \bar{Y} \end{pmatrix} = \begin{pmatrix} \bar{X} \\ Y(\bar{X}) \end{pmatrix} \tag{2}$$

and $C_R = E\left[\begin{pmatrix} \xi_X \\ \xi_Y \end{pmatrix}\begin{pmatrix} \xi_X \\ \xi_Y \end{pmatrix}^{\mathrm{T}}\right] = \left[\begin{array}{c|c} C_X & C_{XY} \\ \hline C_{YX} & C_Y \end{array}\right]$, where $C_Y = E\left[\xi_Y \xi_Y^{\mathrm{T}}\right] \approx E\left[\frac{\partial Y}{\partial X}\xi_X \xi_X^{\mathrm{T}}\left(\frac{\partial Y}{\partial X}\right)^{\mathrm{T}}\right] = \frac{\partial Y}{\partial X} C_X \left(\frac{\partial Y}{\partial X}\right)^{\mathrm{T}}$,

$C_{XY} = C_{YX}^{\mathrm{T}} = E(\xi_X \xi_Y^{\mathrm{T}}) = E\left(\xi_X \xi_X^{\mathrm{T}}\left(\frac{\partial Y}{\partial X}\right)^{\mathrm{T}}\right) = C_X \left(\frac{\partial Y}{\partial X}\right)^{\mathrm{T}}$, $\xi_Y = (Y - \bar{Y})$.

Thus, *the general scheme for solving the problem of probabilistic calculation of hydraulic parameters* is reduced to the following: 1) to obtain vector $\bar{Y}$ by traditional methods for calculating the flow distribution with the given $\bar{X}$; 2) to determine matrix C_R, whose individual blocks are determined using the known matrix C_X and derivative matrix $\partial Y / \partial X$ at point $\bar{X}$.

Here two main questions arise: 1) based on what do we set the distribution parameters of boundary conditions ($\varphi_X = \{\bar{X}, C_X\}$); 2) what is the final form of relationships for the resultant covariance matrices in different variants of the division of R into X and Y, since in the traditional methods for the flow distribution calculation the derivatives $\partial Y / \partial X$ are not calculated in explicit form, which represents a separate problem.

Probabilistic description of consumer loads. A typical example of pipeline systems operating under the conditions of stochastic consumer loads is water supply systems. The approach applied to the probabilistic description of these stochastic conditions is based on the use of the queuing theory methods and on results of the studies [4, 5, etc.], which found their reflection in the regulatory documents [6]. According to these results, the probability of using plumbing units (p_{hr}) can be described by Erlang formulas, which demonstrate a discrete limit distribution of used channels, depending on the characteristics of the flow of requests and the performance of the queuing system.

The suggested technique for calculating the mathematical expectation of consumer flow rates ($\bar{q}_{hr}$) and their variances ($\sigma^2_{q,hr}$) consist in the following:

1. Knowing the number of plumbing units at the consumption node (N) and the probability of using them p_{hr} [6], we can calculate $m = \bar{m}_{hr}$ such that maximum value ($p_{\max}(m)$) acquires the probability

$$p(m) = \left(\frac{\left(N\, p_{hr}\right)^m}{m!}\right) \Big/ Z \;,\; m = 0,1,...,N \;, \tag{3}$$

where $Z = \sum_{k=0}^{N} \frac{\left(N\, p_{hr}\right)^k}{k!}$, m is the number of simultaneously used plumbing units; Np_{hr} is their usage rate.

2. We should determine the average hourly flow rate $\bar{q}_{hr} = \bar{m}_{hr}\, q_{0,h}$, where $q_{0,h} = q_{0,hr} / 1000$ – hourly water flow rate by one device, m^3/h; $\bar{q}_{hr}$ – can be interpreted as the mathematical expectation of flow rate at the consumption node; $q_{0,hr}$ – standardized value, l/h.

3. When approximating the discrete Erlang distribution by the continuous normal distribution, we should calculate the equivalent variance by formula $\sigma^2_{m,hr} = 1 / 2\pi p^2_{\max}(m)$.

4. The variance of the average hourly flow rate will be determined as $\sigma^2_{q,hr} = q^2_{0,h}\, \sigma^2_{m,hr}$.

Figure 1 presents a diagram of function (3), where N =270 and p_{hr} =0.023. The diagram shows that the maximum probability density function corresponds to $\bar{m}_{hr}$, whose average hourly flow rate is $\bar{q}_{hr}$.

General scheme of obtaining the covariance matrix consists of three stages: 1) to linearize system (1) at point $\bar{X}$; 2) to reduce linearized system $\frac{\partial U}{\partial R}\xi_R = 0$ to $\xi_Y = \frac{\partial Y}{\partial X}\xi_X$; 3) to obtain covariance matrix of the vector of unknown operating parameters C_R using the operation $E\left[\begin{pmatrix} \xi_X \\ \xi_Y \end{pmatrix}\begin{pmatrix} \xi_X \\ \xi_Y \end{pmatrix}^{\mathrm{T}}\right]$.

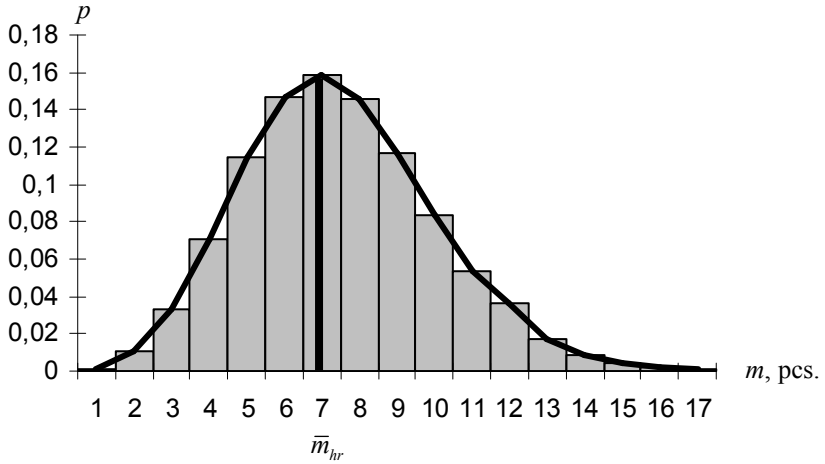

Fig. 1. Continuous approximation of Erlang distribution for the probability of simultaneously used devices for the case where N=270 and p_{hr}=0.023.

Thus, for the case, where $X = Q$, $Y = \begin{pmatrix} x \\ P \end{pmatrix}$, $P_m = \text{const}$, $\alpha = \text{const}$: $\dfrac{\partial U}{\partial R} = \left[\begin{array}{c|c} A & 0 \\ \hline f' & A^{\mathrm{T}} \end{array}\right]$;

$$\begin{pmatrix} \xi_x \\ \xi_P \end{pmatrix} = \left[\begin{array}{c} (f_x')^{-1} A^{\mathrm{T}} M^{-1} \\ \hline M^{-1} \end{array}\right] \xi_Q;$$

$$C_R = \left[\begin{array}{c|c|c} C_Q & C_{Qx} & C_{QP} \\ \hline C_{xQ} & C_x & C_{xP} \\ \hline C_{PQ} & C_{Px} & C_P \end{array}\right] = \left[\begin{array}{c|c|c} C_Q & C_Q M^{-1} A (f_x')^{-1} & C_Q M^{-1} \\ \hline (f_x')^{-1} A^{\mathrm{T}} M^{-1} C_Q & (f_x')^{-1} A^{\mathrm{T}} M^{-1} C_Q M^{-1} A (f_x')^{-1} & (f_x')^{-1} A^{\mathrm{T}} M^{-1} C_Q M^{-1} \\ \hline M^{-1} C_Q & M^{-1} C_Q M^{-1} A (f_x')^{-1} & M^{-1} C_Q M^{-1} \end{array}\right],$$

where f_x' – diagonal matrix with elements $\partial f_i(x_i, \alpha_i) / \partial x_i$; C_Q – known covariance matrix of nodal flow rate; C_P, C_x – covariance matrix of nodal pressure and covariance matrix of flow rate in branches; $C_{Qx} = C_{xQ}^{\mathrm{T}}$ – covariance matrix of nodal flow rate and flow rate in branches; $C_{PQ} = C_{QP}^{\mathrm{T}}$ – covariance matrix of nodal pressure and flow rate; $C_{Px} = C_{xP}^{\mathrm{T}}$ – covariance matrix of nodal pressure and flow rate in branches. Thus, knowing $C_X = C_Q$, we can calculate C_R. No special requirements are imposed on matrix C_Q, however, in practice it is usually taken as a diagonal matrix from considerations of statistical independence of consumer loads. This means that $\text{cov}(Q_j, Q_i) = \sigma_{Q_j}^2$ for $j = t$, and $\text{cov}(Q_j, Q_i) = 0$ for $j \neq t$.

Covariance matrix for the general case of setting boundary conditions $X = (Q_X^{\mathrm{T}}, P_X^{\mathrm{T}}, \alpha_X^{\mathrm{T}})^{\mathrm{T}}$, where at each node we can set either the flow rate or the pressure, and each branch is characterized by $n_{\alpha,i}$-dimensional vector (e.g. $\alpha_i = \{s_i, H_i\}$, $n_{\alpha,i} = 2$) of hydraulic parameters, which is specified in the probabilistic form in full or partially [1, 2].

Divide the set of nodes in the design scheme into subsets of nodes with the given flow rate (J_Q) and pressure (J_P), and the set of branches into subsets of branches with hydraulic parameters given in the probabilistic (I_V) and deterministic (I_D) forms. We omit the conclusion and give the finite expressions for the covariance matrix of unknown operating parameters:

1) Covariance matrix of unknown nodal pressure

$$C_{PY} = \mathrm{E}\left[\xi_{PY},\ \xi_{PY}^{\mathrm{T}}\right] = \frac{\partial P_Y}{\partial Q_X} A_{QV} \frac{\partial x_V}{\partial \alpha_V} C_{\alpha V} \frac{\partial x_V}{\partial \alpha_V} A_{QV}^{\mathrm{T}} \left(\frac{\partial P_Y}{\partial Q_X}\right)^{\mathrm{T}} + \frac{\partial P_Y}{\partial Q_X} C_{QX} \left(\frac{\partial P_Y}{\partial Q_X}\right)^{\mathrm{T}} + \frac{\partial P_Y}{\partial P_X} C_{PX} \left(\frac{\partial P_Y}{\partial P_X}\right)^{\mathrm{T}};$$

2) Covariance matrix of flow rate in the branches with deterministically specified characteristics

$$C_{x,D} = \mathrm{E}\left[\xi_{x,D}, \xi_{x,D}^{\mathrm{T}}\right] = \frac{\partial x_D}{\partial P_Y} C_{PY} \left(\frac{\partial x_D}{\partial P_Y}\right)^{\mathrm{T}} + \frac{\partial x_D}{\partial P_X} C_{PX} \left(\frac{\partial x_D}{\partial P_X}\right)^{\mathrm{T}};$$

3) Covariance matrix of flow rate in the branches with probabilistically specified characteristics

$$C_{xV} = \mathrm{E}\left[\xi_{\boldsymbol{x}V}, \xi_{\boldsymbol{x}V}^{\mathrm{T}}\right] = \frac{\partial x_V}{\partial P_Y} C_{PY} \left(\frac{\partial x_V}{\partial P_Y}\right)^{\mathrm{T}} + \frac{\partial x_V}{\partial P_X} C_{PX} \left(\frac{\partial x_V}{\partial P_X}\right)^{\mathrm{T}} + \frac{\partial x_V}{\partial \alpha_V} C_{\alpha V} \left(\frac{\partial x_V}{\partial \alpha_V}\right)^{\mathrm{T}};$$

4) Covariance matrix of unknown nodal flow rates

$$C_{QY} \equiv \mathrm{E}\left[\xi_{QY}, \xi_{QY}^{\mathrm{T}}\right] = A_{PD} C_{xD} A_{PD}^{\mathrm{T}} + A_{PV} C_{xV} A_{PV}^{\mathrm{T}},$$

where A_{QD} – $(m_Q \times n_D)$-dimensional incidence matrix with elements a_{ji}, $j \in J_Q$, $i \in I_D$; A_{QV} – $(m_Q \times n_V)$-dimensional incidence matrix with elements a_{ji}, $j \in J_Q, i \in I_V$; A_{PD} – $(m_P \times n_D)$-dimensional incidence matrix with elements a_{ji}, $j \in J_P$, $i \in I_D$; A_{PV} – $(m_P \times n_V)$-dimensional incidence matrix with elements a_{ji}, $j \in J_P$, $i \in I_V$; $\frac{\partial x_D}{\partial P_Y} = \left(\frac{\partial f_{xD}}{\partial x_D}\right)^{-1} A_{QD}^{\mathrm{T}}$, $\frac{\partial x_D}{\partial P_X} = \left(\frac{\partial f_{xD}}{\partial x_D}\right)^{-1} A_{PD}^{\mathrm{T}}$, $\frac{\partial x_V}{\partial P_Y} = \left(\frac{\partial f_{xV}}{\partial x_V}\right)^{-1} A_{QV}^{\mathrm{T}}$, $\frac{\partial x_V}{\partial P_X} = \left(\frac{\partial f_{xV}}{\partial x_V}\right)^{-1} A_{PV}^{\mathrm{T}}$, $\frac{\partial x_V}{\partial \alpha_V} = \left(\frac{\partial f_{xV}}{\partial x_V}\right)^{-1} \frac{\partial f_{xV}}{\partial \alpha_V}$ – matrices of partial derivatives of the corresponding combinations of parameters, which implicitly depend on three matrices only: $\frac{\partial f_{xD}}{\partial x_D}$, $\frac{\partial f_{xV}}{\partial x_V}$ and $\frac{\partial f_{xV}}{\partial \alpha_V}$, whose structure is determined by the type of branch characteristics. Moreover, the first two of them are diagonal, and therefore, easily invertible.

Thus, based on the given relations, we can sequentially calculate the covariance matrices of all the operating parameters, if we know the covariance matrices of nodal flow rate set in the probabilistic form (C_{QX}), nodal pressure (C_{PX}), and hydraulic characteristics of branches ($C_{\alpha V}$).

Probabilistic calculation of dynamics of hydraulic operating parameters. Stochastic boundary conditions initiate the change in hydraulic operating parameters with time. As a result we face the problem of probabilistic modeling and analysis of operating parameter dynamics $R(t), 0 \le t \le T$ as a random process for the calculation period T.

Figure 2 presents the graphs of realization-frequency distribution of two hydraulic operating parameters (the nodal flow rate and the nodal pressure). The first parameter can be considered as a disturbance, the second – as a response. Figure 2a shows the graph of water flow rate frequencies for an individual residential building in the water supply system that is constructed based on the experimental data. Figure 2b shows the graph of pressure frequencies at the connection node of the reservoir in the water supply system in one of the Irkutsk districts that is obtained by processing the data of the dispatching department for 490 days.

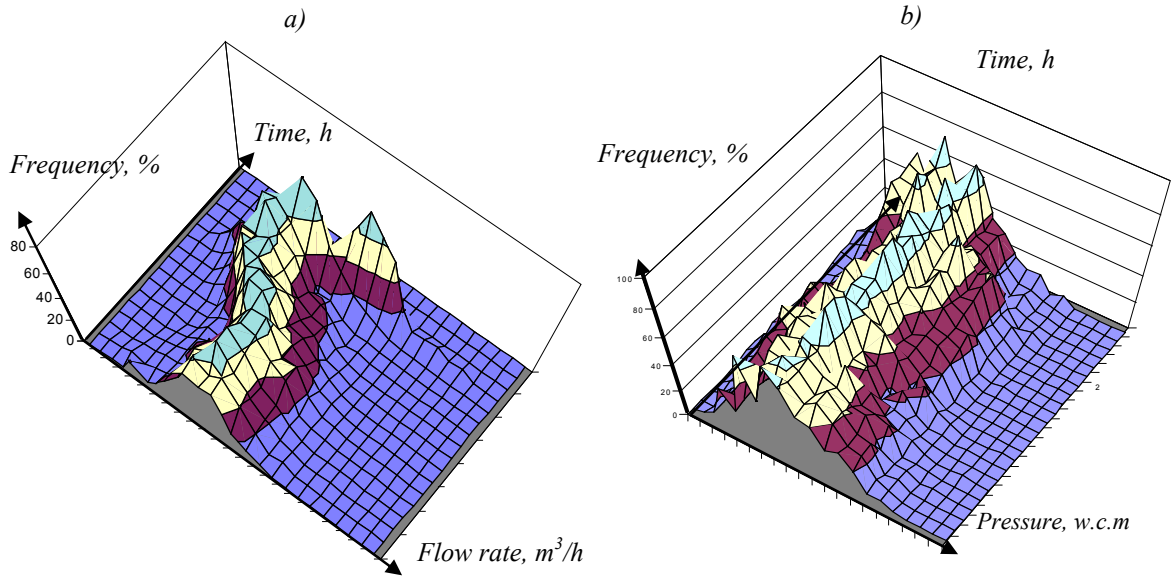

Fig. 2. Daily change in the frequency distribution of hydraulic operating parameters

a) For the nodal flow rate, b) For the nodal pressure

Analysis of both processes in Fig. 2 indicates that: 1) the frequency distribution at any cross-section of both processes is approximated by the normal (Gaussian) distribution satisfactorily enough; 2) the variance of every process (σ^2) is practically invariable. The root-mean-square deviation (σ) for daily water flow rate changes negligibly, i.e. within 10 per cent (Table 1), for pressure – within 7 per cent; 3) the mathematical expectation for both processes changes during a day (Fig. 3a); 4) the autocorrelation function stabilizes at the zero value (for the nodal value in Fig. 3b) fast enough.

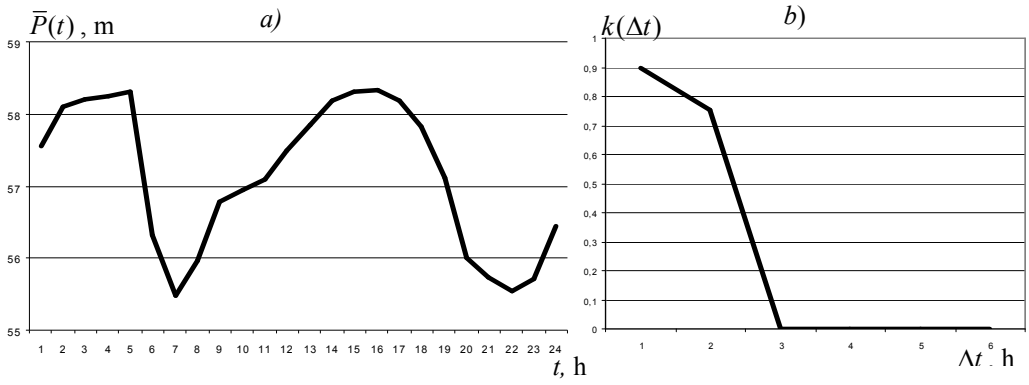

Fig. 3. Statistical characteristics of change in the nodal pressure as a random process
a) Dynamics of mathematical expectation;
b) Graph of the autocorrelation function of pressure in the reservoir

Table 1. Values of mathematical expectations and root-mean-square deviations of the nodal flow rate during day hours for the conditions in Fig. 2a.

Day hour	$\bar{Q}$, m^3/h	σ	$\frac{\sigma}{\bar{\sigma}}100\%$	Day hour	$\bar{Q}$, m^3/h	σ	$\frac{\sigma}{\bar{\sigma}}100\%$
1	4.60	2.14	3.11	13	11.97	2.25	8,41.
2	2.32	1.94	6.52	14	11.77	2.2	6.00
3	1.88	1.99	4.12	15	11.28	2.15	3.59
4	1.66	1.94	6.52	16	11.16	2.07	0.26
5	1.87	1.84	7.97	17	11.53	2.0	3.63
6	3.28	2.2	6.00	18	12.32	2.09	0.70
7	7.88	2.02	2.67	19	12.35	2.17	4.56
8	10.80	2.08	0.22	20	13.34	2.05	1.22
9	10.88	1.96	5.56	21	13.68	2.04	1.71
10	12.40	2.26	8.89	22	14.34	2.02	2.67
11	12.48	2.02	2.67	23	12.51	1.85	10.86
12	12.13	2.28	9.86	24	9.10	2.18	5.04

The hydraulic operating parameters vary in time in response to three main disturbing actions (boundary conditions): 1) random actions of regular character (consumer loads); 2) deterministic actions of regular character (control actions); 3) random actions of irregular character (fires, accidents). The second type of disturbances is taken into account algorithmically on the basis of the specified control rules. Analysis of the consequences of relatively rare disturbances of the third type is the subject of the reliability theory of pipeline systems and is not carried out here.

Dynamics of hydraulic operating parameters $R(t)$, $0 \le t \le T$ may be considered as a random process with the discrete time (a quasidynamic approach). At each time instant of the process the operating parameters obey the normal distribution. Variation of the operating parameters at the adjacent instants may be considered as insignificant and the flow distribution – as steady. Thus, the problem of probabilistic calculation of hydraulic operating parameter dynamics is reduced to the determination of $\bar{\mathbf{R}} = [\bar{R}(0)^{\mathrm{T}}, \bar{R}(1)^{\mathrm{T}}, ..., \bar{R}(T)^{\mathrm{T}}]^{\mathrm{T}}$ and $\mathbf{C}_{\mathbf{R}} = E\left[\xi_R \xi_R^{\mathrm{T}}\right]$ based on the specified parameters $\bar{\mathbf{X}} = [\bar{X}(0)^{\mathrm{T}}, \bar{X}(1)^{\mathrm{T}}, ..., \bar{X}(T)^{\mathrm{T}}]^{\mathrm{T}}$, $\mathbf{C}_{\mathbf{X}}$ and the conditions $A(t)x(t) = Q(t,P)$, $\bar{A}(t)^{\mathrm{T}} \bar{P}^{\mathrm{T}}(t) = y(t)$, $y(t) = f\left(x(t), \alpha(t)\right)$, $t = 0, ..., T$. In this case the suggested analytical probabilistic models and the calculation methods can be applied to each calculation instant, which will sharply decrease computational efforts. The computing experiments in Table 1 have shown the decrease in running time by tens of times.

Table 2. Time required for probabilistic calculation by the Monte Carlo and analytical methods [7]

Number of scheme nodes and branches	Time for method		$t_{\text{Ì -Ê}} / t_{\text{âí àëèò.}}$
	analytical	Monte Carlo	
6 nodes and 8 branches	3.2 s	3 min	56.25
12 nodes and 19 branches	4.8 s	28.5 min	356.25
12 nodes and 29 branches	16.2 s	1.25 h	277.77

In some cases such as availability of reservoirs it is important to take account of the lagging factor of internal responses of pipeline systems, when the successive operating condition depends on the prehistory of conditions. Availability of reservoirs can be taken into account by using the additional dynamic relation $P_{j,k} = P_{j,k-1} + \rho g(\Delta t / F_j) Q_{k,j}$, where Δt – duration of the k-th condition; F_j – liquid surface area in the reservoir; j – index of the node with a reservoir; g – gravitational acceleration; ρ – liquid density. The reservoir operation can be modeled by insertion of a dummy branch connected to a dummy node with zero (or air) pressure. The hydraulic characteristic of such a branch has the form: $y_{i,k} = s_{i,k} x_{i,k} - H_{i,k}$, where $H_{i,k} = P_{j,k-1}$, $s_{i,k} = \rho g \Delta t / F_j$. Let H_k^f be a vector of dummy pressure rises in the branches that represent all the reservoirs. The covariance matrix of vector H_k^f that is used at the k-th calculation step will have the form: $C_{H_f}(t_k) = C^*_{PY}(t_{k-1})$, where $C^*_{PY}(t_{k-1})$ – block of covariance matrix C_{PY} that was calculated at the previous step and is attributed to the pressures at the nodes with reservoirs.

Calculation of probabilistic operating parameters of pipeline systems. The suggested approach to the calculation of statistical parameters of pipeline system operation offers an opportunity to obtain probabilistic estimates of virtually any operating parameters of pipeline systems depending on their operating conditions by the known formulas of the probability theory. For example the probability that any "nondegenerate" subset of operating parameters belongs to a given range at the time t_k will be determined by the formula

$$p_{Rk} = \frac{1}{\sqrt{(2\pi)^n |C_{Rk}|}} \int_{\underline{v}_n}^{\overline{v}_n} \dots \int_{\underline{v}_1}^{\overline{v}_1} \exp\left\{-\frac{1}{2}\left(R_k - \overline{R}_k\right)^{\mathrm{T}} \mathrm{C}_{Rk}^{-1} \left(R_k - \overline{R}_k\right)\right\} dR_1 \mathrm{K}\, dR_n, \quad (4)$$

where R_k – n-dimensional vector (subvector) of operating parameter values at the time instant t_k; $\overline{R}_k$ – n-dimensional vector of mathematical expectation R_k; C_{Rk} – $(n \times n)$-dimensional covariance matrix for R_k; p_{Rk} – probability that R_k belongs to a specified range $[\overline{v}, \underline{v}]$; $\overline{v} = [\overline{v}_1, \dots, \overline{v}_n]^{\mathrm{T}}$ and $\underline{v} = [\underline{v}_1, \dots, \underline{v}_n]^{\mathrm{T}}$ – vectors of upper and lower boundaries of the studied range, whose components can take infinite values to take account of one-sided intervals or their absence.

The assessment of probability that R_k belongs to a specified range $[\overline{v}_r, \underline{v}_r]$ during period T will be determined by the formula

$$p_{RT} = \sum_{k=1}^{K} \left(p_{Rk} \Delta t_k\right) \Big/ \sum_{k=1}^{K} \Delta t_k = \sum_{k=1}^{K} \left(p_{Rk} \Delta t_k\right) \Big/ T, \quad (5)$$

where K – the number of calculated periods over period $T = \sum_{k=1}^{K} \Delta t_k$; Δt_k – duration of the k-th condition.

Equations (4) and (5) can be applied to estimate the operation of pipeline system, its fragments or individual components in a definite operating condition or over the period of time, for example in terms of the extent to which they are loaded, consumer demand is satisfied, or process constraints are met, etc.

Numerical example

Let us consider a numerical example of calculating the stochastics of the hydraulic operating parameters for the network presented in Fig.4. The network consists of 7 nodes and 11 branches of which: one node has a fixed pressure; two nodes have lumped loads; two nodes are nonfixed loads depending on pressure; one branch represents a pumping station with an increasing head H_0=21 m; one dummy branch simulates a reservoir (water level in the reservoir H^f=16.4 m); two dummy branches simulate nonfixed loads, their resistances are random values. Thus, this example illustrates the possibilities of the suggested approach in terms of the random composition of boundary conditions.

The input information specified in the probabilistic form is: $X = (Q_X^{\mathrm{T}}, P_X^{\mathrm{T}}, \alpha_X^{\mathrm{T}})^{\mathrm{T}} = (\overline{Q}_4, \overline{Q}_5, \overline{P}_7, \overline{s}_9, \overline{s}_{10}) =$ (5.2, 1.8, 0, 0.30359, 1.2407); C_X – a diagonal matrix with nonzero elements (1.065, 0.3969, 0.0001, 0,059, 0.51564).

Resistances in the dummy branches 9 and 10, that simulate nonfixed flow rates at consumers are determined by the formula [1, 2] $\overline{s}_i = P_j^r / (Q_j^r)^2$, and variances – $\sigma_{s,i}^2 = \left(4 (P_j^r)^2 / (Q_j^r)^6\right) \sigma_{Qr,j}^2$, where P_j^r, Q_j^r – design (required) pressures and flow rates for this consumer, j – index of the initial node of the i-th branch. Correspondingly in the example $Q_2^r = 7.7$, $\sigma_2^2 = 9.61$, $P_2^r = 18$, $Q_3^r = 7.11$, $\sigma_3^2 = 0.81$, $P_3^r = 12$.

Resistances in the branches that were specified deterministically are: $s_1 = 0.00257$, $s_2 = 0.8996$, $s_3 = 0.00408$, $s_4 = 0.095$, $s_5 = 0.67$, $s_6 = 0.067$, $s_7 = 0.0957$, $s_8 = 0.00646$, $s_{11} = 0.014$.

The calculation results for nodes are presented in Table 3 and for branches – in Table 4.

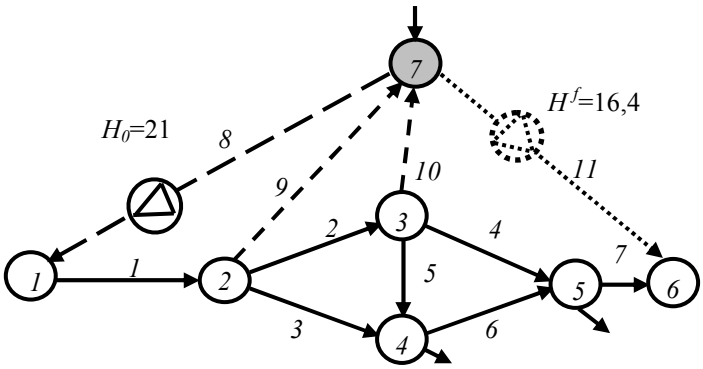

Fig.4. Example of the calculated scheme of the pipeline system for the general case of boundary conditions

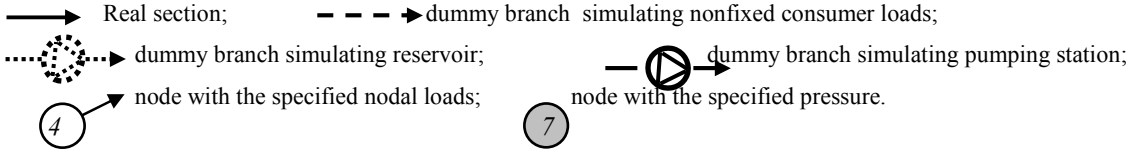

Table 3. Calculation results for nodes

j	Parameters			
	P_j, *Mwc*	$\sigma_{P,j}$	Q_j, m^3/h	$\sigma_{Q,j}$
1	18.22	0.89	–	–
2	17.11	1.25	9.19	4.03
3	14.96	1.21	6.48	1.08
4	16.70	1.25	–	–
5	16.01	0.83	–	–
6	16.37	0.02	–	–
7	–	–	22.67	9.07

Table 4. Calculation results for branches

i	Parameters	
	x_i, m^3/h	$\sigma^2_{x,i}$
1	20.75	3.29
2	1.54	0.02
3	10.01	0.03
4	-3.32	0.59
5	-1.61	0.02
6	3.20	0.98
7	-1.92	2.21
8	20.75	3.29
9	9.19	4.03
10	6.48	1.08
11	1.82	0.66

Figure 5 presents a graphical interpretation of the calculated probability of providing consumers with a required flow rate. For example for the consumer at the second node $p(0 < \bar{Q}_2 < Q_2^r) \approx 0.3442$ or $p(Q_2^r < \bar{Q}_2 < +\infty) \approx 0.64446$, and at the third node $p(0 < \bar{Q}_3 < Q_3^r) \approx 0.71914$ or $p(Q_3^r < \bar{Q}_3 < +\infty) \approx 0.28083$, where Q^r is the required flow rate.

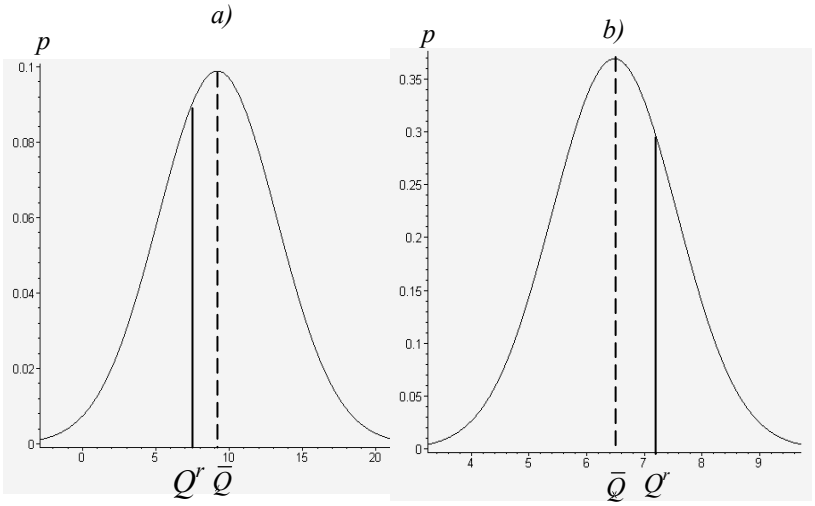

Figure 5. Illustration to the calculation of probability of providing consumer with a required flow rate: a) at node 2, b) at node 3.

$\bar{Q}$ – Calculated value of mathematical expectation of consumer flow rate considering its dependence on nodal pressure, Q^r – required value of consumer flow rate.

Conclusions.

1. The paper presents:
   - a technique for apriori calculation of statistical characteristics of a probabilistic process of the transported medium consumption as a queuing process;
   - a general scheme for probabilistic calculation of pipeline system hydraulic operating parameters. The calculation suggests determining statistical characteristics of the operating parameters by specified characteristics of boundary conditions and flow distribution model. It is shown that such a calculation is reduced to solving a traditional problem of flow distribution at the point of mathematical expectation of boundary conditions in combination with an additional procedure for calculating covariance matrices of operating parameters;
   - a technique for obtaining the analytical expressions for covariance matrices of operating parameters as well as the expressions for the general case of specifying boundary conditions;
   - a technique for probabilistic modeling of changes in the hydraulic operating parameters on the basis of developed analytical probabilistic flow distribution models. This technique provides a considerable reduction in computational efforts against the known methods of simulation modeling.
2. The suggested technique for modeling pipeline systems provides the possibility of obtaining probabilistic estimates of practically any pipeline system operating parameters that depend on operating conditions.
3. A numerical example of probabilistic calculation of the steady flow distribution in the pipeline system is given for the general case of boundary conditions. The example illustrates the suggested probabilistic approach.

References

1. Novitsky N.N., Vanteyeva O.V. Problems and methods of probabilistic modeling of hydraulic conditions of pipeline systems // Scientific technical bulletin of StPSU. – 2008. – No.1. – P. 68-75.
2. Novitsky N.N., Vanteyeva O.V. Modeling of stochastic flow distribution in hydraulic circuits // Izv RAN . Energetika. – 2011. – No.2. – P.145-154.
3. Merenkov A.P., Khasilev V.Y. Theory of hydraulic circuits. – M.Nauka, 1985. – 280 p.
4. Abramov N.N. Reliability of water supply systems M.Stroiizdat, 1979. – p.231.
5. Shopensky L.A. Study on the operating conditions of water pipelines in residential buildings: PhD dissertation thesis. M., 1968.
6. Internal sanitation of buildings (Construction Norms and Rules 2.04.01-85*) – M.: CITP Gosstroi Rossii, 2004. – 58 c.
7. Vanteyeva O.V. Probabilistic models and methods for analysis of pipeline system operating conditions. PhD dissertation. – Irkutsk, 2011. – 139 p.

Proceedings, 15th Applied Stochastic Models and Data Analysis (ASMDA2013)
International Conference, Mataró (Barcelona), Spain 25 - 28 June 2013

An empirical study on the index of satisfaction of student allocation in the Portuguese undergraduate engineering courses

Raquel Oliveira[1], A. Manuela Gonçalves[2], and Rosa M. Vasconcelos[3]

[1]Faculty of Social Sciences, Catholic University of Portugal, Braga, Portugal (E-mail: roliveira@braga.ucp.pt)
[2]Department of Mathematics and Applications, CMAT - Centre of Mathematics of University of Minho, Portugal (E-mail: mneves@math.uminho.pt)
[3]Department of Textile Engineering, 2C2T - Centre for Textile Science and Technology, University of Minho, Portugal (E-mail: rosa@det.uminho.pt)

Abstract. This paper aims to describe and characterize student allocation in the Portuguese public higher education system, namely in the academic engineering programs. The application of multivariate methodologies for the evaluation of the students' satisfaction index detects natural clusters of academic programs and identifies some determinants of students' choices concerning higher education. These determinants may be used as explanatory variables of a model for the access to higher education engineering programs. The data used in this paper concerns the academic year of 2010/2011 and was provided by the Portuguese Ministry of Education.

Keywords: Students' index satisfaction, higher education, education policy, clusters analysis;

1 Introduction

The implementation of the Bologna Process in Portugal was led by the Portuguese Ministry of Science Technology and Higher Education (MSTHE), and it was a part of a process of reorganization and rationalization of the higher education system, OCDE[1]. The Bologna Declaration of June 19, 1999 - Joint Declaration of European Ministers of Education had, among its many objectives, the standardization of degrees conferred in the European space based on three cycles: Bachelor, Master, PhD. This process also intended the recognition and comparability of degrees, the promotion of students, teachers and researchers' mobility, in order to ensure teaching quality and the incorporation of the European dimension in higher education[2].

The MSTHE instructed the higher education institutions that they could restructure their study programs according to the Bologna principles, beginning in 2006/2007 and with a deadline extended to 2008/2009. This implementation brought about profound modifications in the Higher Education system, European Ministers of Education[3].This study aims to describe and characterize students' allocation in the academic engineering programs in the Portuguese public higher education system through the analysis of the satisfaction index of the academic programs offered by the Portuguese higher education institutions.
This document is organized as follows: in section 2 we give a description of the Portuguese higher education system with regard to organization and admission procedure; in section 3 we present the data set in consideration and the main results that characterize the available data. Section 4 concerns the statistics techniques used and the results; and finally in Section 5 are presented the conclusions and future work.

2 Portuguese higher education system

This section presents, in brief, the Higher Education system in Portugal, as well as the description of the application process to higher education.
Portugal has a binary higher education system, consisting of university and polytechnic education, each with distinct purposes that translate into specific curricular concepts, http://www.dges.mctes.pt [1][4].
University education, guided by a constant perspective of promoting research and knowledge creation, aims at ensuring a solid scientific and cultural preparation, at providing a technical training that qualifies for the exercise of professional and cultural activities and at promoting the development of design capabilities, innovation and critical analysis.
Polytechnic education, guided by a constant perspective of applied research and development aims at understanding and solving concrete problems, at providing a solid cultural and technical level, at developing the capacity for innovation, critical analysis scientific theoretical and practical in nature and its applications for the pursuit of professional activities.
As to their nature, higher education institutions may be public or private.
This study focuses on the publicly funded higher education system offering engineering study programs, since these programs include the majority of the candidates and they are also representative in terms of supply of the land area.
The MSTHE (presently the MEC-Ministry of Education and Science), and more specifically the Department of Higher Education (Direção Geral do Ensino Superior-DGES), is in charge of the higher education sector and regulates access to the higher education system. Currently, the access to higher education

[1] As well as the military and police institutions, integrated in the National Network of Public Higher Education Institutions

is conditioned by system of *numerus clausus*, which defines the maximum number of students for each study program in both the public and the private sectors. This number is defined by each institution, in fixed dates, and is subject to approval of the MSTHE. *Numerus clausus* works as a restriction on the supply side of the system, affecting the size and composition of the tertiary education sector, Oliveira *et al*[5].

Access to higher education, for the public sector, is done through a national contest. The national competition is based on the students' revealed preferences in the application. Each student ranks a maximum of six study program/institution pairs, from the most preferred (the first one) to the least preferred (the last one) alternative. The ensuing nationwide competition allocates the candidates based on their grade point average and the stated ranking of preferences, Oliveira *et al*[5].

3 Methodology

The used data is available online, on a web site of the DGES[6] designed to disseminate the results of the candidates allocation in the national competition. The data was collected for the academic year of 2010/11, and the following variables are available: overall demand for each program (total number of students listing the pair institution/program among their preferences, irrespective of their ranking), as well as the number of students who have selected each program as their first choice, second choice and so forth (up to a maximum of six choices); number of vacancies available at each program in the first stage of the application process; classification of the classification of the last student allocated, number of applicants allocated in the six choices, program size (first cycle or integrated master), and the index satisfaction (ratio of the number of students allocated in the first choice and the number of vacancies available at each program).
This data set comprises 14 universities (U) and 20 polytechnics institutes (PI), from the public education sector, offering 275 academic engineering programs of which 58 are integrated masters and 217 are first cycles.

4 Data analysis and results

The used data set comprises 34 Institutions of Higher Education (IHE), universities and polytechnics institutes. The engineering courses were organized according to the National Classification of Areas of Education and Training (Classificação Nacional de Áreas de Educação e Formação-CNAEF)[7], as is shown in Figure 1.
Figure 2 displays the satisfaction index considering de type of institution.

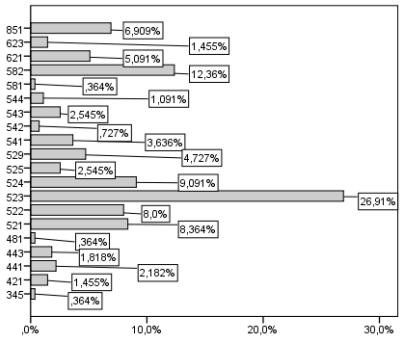

Fig. 1. Areas of Education and Training[2]

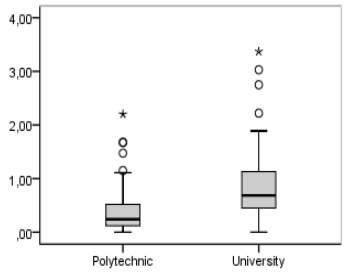

Fig. 2. Satisfaction index by type of institution

Taking into account the distribution of satisfaction index by the Areas of Education and Training of the academic engineering programs, was considered the satisfaction index mean, the results obtained are shown in Figure 3.

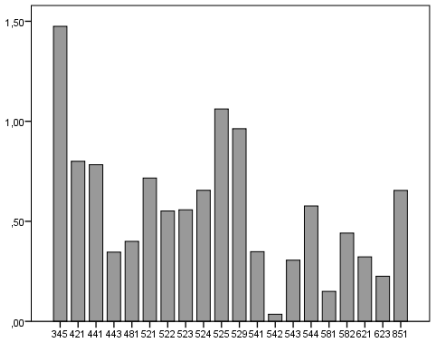

Fig. 3. Distribution of satisfaction index mean by Areas of Education and Training

A few Mann-Whitney and Kruskal-Wallis tests were performed in order to analyze if the satisfaction index depends on the type of institution, on the

[2] The Areas of Education and Training are the following: Management and Administration (345), Biology and Biochemistry (421), Physics (441), Earth Sciences (443), Computer Science (481), Metallurgy and Metalworking (521), Power and Energy (522), Electronics and Automation (523), Chemical Process Technology (524), Construction and Repair of Motor Vehicles (525), Engineering and Similar Techniques (529), Food Industries (541), Industries of the Textile, Clothing, Footwear and Leather (542), Materials (Manufacturing of Wood, Cork, Paper, Plastic, Glass and others) (543), Extractive Industries (544), Architecture and Urbanism (581), Construction and Civil Engineering (582), Agricultural and Animal Production (621), Forestry and Hunting (623), Technology of Environmental Protection (851).

program size (first cycle or integrated master) or on the Areas of Education and Training, Conover[8].
The results of the Mann-Whitney test indicates that the satisfaction index depends on the type of the HIS (test statistics= -8.367; p-value=0.00) and on the program size (test statistics= -8.069; p-value=0.00). A similar situation happens when comparing the Areas of Education and Training. Kruskal-Wallis results show that the satisfaction index also depends on the Areas of Education and Training (test statistics= 34.852; p-value=0.015).
These analyses emphasize the idea that the index of allocation satisfaction is highly related with all variables considered.
A hierarchical agglomerative cluster analysis was performed on the data satisfaction index by using the variables Areas of Education and Training and academic engineering programs, Gore[9]. Euclidean distance was used. The final result of the obtained groups was discussed according to the Ward linkage method, Barnet[10].
The obtained dendrogram and the clusters representation are shown in Figure 4.

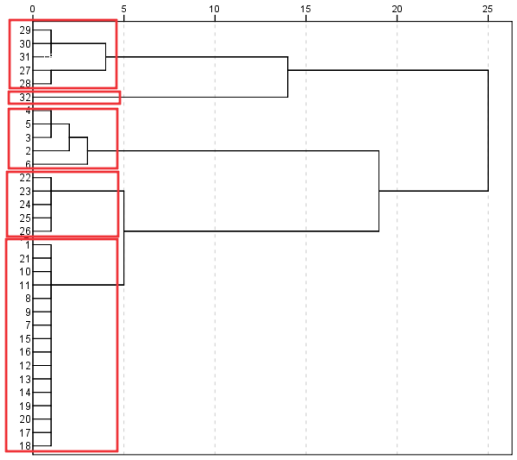

Fig. 4. Dendrogram according to Ward Method

According to the dendrogram analysis, was decided to form the clusters at a cut distance of d=4.7, thus obtaining five well-differenced clusters defined in Table 1. The resulting dendrogram has a cophenetic correlation coefficient of 0.87 (correlation coefficient between the distance matrix and the "cophenetic matrix"), which validates the clustering procedure.

Table1. Cluster identification[3]

Cluster1	27,28,28,30,31
Cluster2	32
Cluster3	2,3,4,5,6
Cluster4	22,23,24,25,26
Cluster5	1,7,8,9,10,11,12,13,14,15,16,17,18,19,20,21

Taking into consideration the index satisfaction averages within each cluster, they are ranked in this order: Cluster 2, Cluster 5, Cluster 1, Cluster 3 and Cluster 4. The results confirm previous knowledge about the ratio existent between the number of vacancies and the number of students allocated in the first choice – satisfaction index, i.e. the cluster better classified is the one corresponding to the academic programs with fewer candidates.

Conclusions and future work

This document contributes to a better understanding of student allocation and the respective satisfaction index in the Portuguese undergraduate engineering courses. This empirical study confirms that index satisfaction is an important indicator of the determinants of students' choices concerning higher education. Although, this issue deserves a much more detailed and careful analysis and

[3]Management and Industrial Engineering (1), Biological Engineering (2), Physics Engineering (3), Geographic Engineering (4), Geological Engineering (5), Systems Engineering (6), Mechanical Engineering (7), Metallurgical and Materials Engineering (8), Industrial Engineering (9), Electromechanical Engineering/Energy Engineering/Renewable Energy Engineering/Energy and Environment Engineering (10), Electrical Engineering/Electrical and Electronics Engineering (11), Computer Engineering/Network Engineering and Systems/Electronics Maritime Systems Engineering (12), Electronics and Telecommunications Engineering/Electrical Engineering and Telecommunications/Electrical and Computer Engineering/Electrical Engineering/Electronics and Computers (13), Telematics and Computer Engineering/Computer Science and Telecommunications/Telecommunications Engineering and Computer/Network Engineering Communications/Communications Engineering (14), Mechatronics Engineering/Macro and Nanotechnologies Engineering/Computer Engineering and Medical Instrumentation (15), Metrology and Instrumentation Engineering/Automation, Control and Instrumentation Engineering (16), Chemical Engineering/Chemistry and Biochemistry/Chemistry and Biological (17), Biomedical Engineering/Bioengineering/Biotechnology (18), Aeronautical Engineering/Aerospace Engineering/Automotive Engineering/Automotive Mechanics Engineering (19), Engineering and Naval Architecture (20), Engineering and Industrial Management/Engineering Sciences/Civil Eng + Eng Electr Eng Informatics and Telec + Design + Interactive Media (21), Food Engineering /Biological and Food (22), Textile Engineering (23), Materials Engineering (24), Polymer Engineering (25), Mining and Geological Engineering/Science Engineering/Mining and Geoenvironment Engineering/Geotechnical and Geoenvironment Engineering (26), Topographic engineering (27), Civil Engineering/Civil Engineering Sciences (28), Agronomic Engineering/Engineering and Agro-Livestock (29), Zootechnical Engineering/Production Animal Engineering (30), Forestry and Natural Resources/Forestry (31), Environmental Engineering/Environmental Engineering and Management (32)

should be the subject of further research, namely extend the study applying other multivariate methodologies with more variables available.

References

1. OECD, Organization for economic co-operation and Development (2006). *Reviews of National policies for education: Tertiary education in Portugal. Examiner's Report*. Available at http://www.dges.mctes.pt/NR/rdonlyres/8B016D34-DAAB-4B50-ADBB-25AE105AEE88/2564/Backgoundreport.pdf.
2. http://www.europa.eu
3. European Ministers of Education. *The Bologna Declaration*, 1999.
4. http://www.dges.mctes.pt
5. Raquel Oliveira, A. Manuela Gonçalves and Rosa M. Vasconcelos *"A statistical model for the demand of undergraduate engineering courses in Portugal: A first study of Bologna Process impact"*, AIP Conference Proceedings, American Institute of Physics (Ed.) DOI: 10.1063/1.4756505, NUMERICAL ANALYSIS AND APPLIED MATHEMATICS ICNAAM 2012: International Conference on Numerical Analysis and Applied Mathematics, Kos, Greece, September 19-25, 1479, 1, 1724-1727, 2012.
6. http://www.dges.mctes.pt/DGES/pt/Estudantes/Acesso
7. http://www.dados.gov.pt/PT/CatalogoDados/Dados.aspx?name=ClassNacionaldeareasdeeducacaoeformacao
8. W.J. Conover. *Practical Nonparametric Statistics*. Third Edition, John Wiley & Sons: New York, 269-300, 1999.
9. P.A. Gore. *Cluster analysis*. In Handbook of applied multivariate statistics and mathematical modeling, ed. H.E.A. Tinsley and S.D. Brown, 297–321. San Diego, CA: Academic Press, 2000.
10. V. Barnett. *Interpreting Multivariate Data*. Sheffield: John Wiley & Sons, 1981.

Proceedings, 15th Applied Stochastic Models and Data Analysis (ASMDA2013)
International Conference, Mataró (Barcelona), Spain 25 - 28 June 2013

Comparisons of multistate models with discrete-time pure-birth process for recurrent events and uncertain parameters

Eva Maria Ortega[2], Encarnacion Ortega-Quiles[3], and Jose Alonso[4]

[1] Residencia Universitaria Oblatas, Murcia, Spain
(E-mail: emariaop@gmail.com)
[2] Colegio Hnas. Carmelitas, Elche, Spain
(E-mail: salvenc@hotmail.com)
[3] Hospital Virgen Caridad, Cartagena, Murcia, Spain
(E-mail: salvenc@hotmail.com)

Abstract. This paper presents a multistate model with recurrent events that are modeled by a discrete-time pure birth process. The probability distribution of the multistate model is based on random sums with support on N and with geometric summands. Exact distributions are given in Belzunce et al. (2009) for independent inter-arrival times. These models are analyzed by stochastic orderings in the case of independent geometric, arbitrarily distributed, and positively correlated inter-arrival times. Some multivariate extensions are described. Motivations are provided in reliability, economics, biology and demography, in particular, the discrete-time pure birth shock model by Belzunce et al. (2009), where the lifetime of a system subjected to shocks (failures) arriving randomly is analyzed. Also, we provide results for some qualitative properties of the kind 'new better than used' of the multistate model assuming independent and identically distributed summands, that are illustrated.
60E15, 62P05.
Keywords: multistate models, discrete-time pure birth process, recurrent events, unobserved heterogeneity, stochastic orderings, demography.

1 Introduction and preliminaries

The multistate models have become a central tool in population biology, medicine and demography for estimating some parameters under incomplete observation or imperfect detection of individuals. Frequentist probability theory, counting processes, maximum likelihood estimation, bayesian methods, Markov chain Monte Carlo simulation are several of the approaches that have been used in the literature to study movements between states that determine the lifetime (age) of an individual, the population size of microorganisms growing or the migration transitions (see Courgeau and Lelivre (1992), Commenges (1999), Rondeau et al. (2003), among others). A multistate model is defined as a stochastic process, which at any time point remains in one of a set of discrete states. The illness-death model is the most commonly applied multistate model in population biology. For such kind of models, there are three states: healthy, illness and death. The individuals start out healthy and from this state the transitions may be to the illness or to the death. Ill individuals may die or become healthy again. Similarly, most of multistate models have three types of

states, which are determined by environmental conditions: the initial state (or the state where the individuals may enter the experimental study), the states where the individuals are studied from their transitions to move to other states, and the states where the individuals are not interesting for the experimental study since such condition is reached. Many multistate modeling concepts are connected with the Markov chain theory, where the previous states can be interpreted as initial, transient and absorbing. Theoretically, the multistate models extend the univariate survival model in two ways: parallel events (where one individual may experience multiple simultaneous events, or where several individuals that may experience an event are grouped in a cluster), and recurrent events (where a single individual may experience the same event several times). In this paper we are interested in multistate models for recurrent events data (see a review in Cook and Lawless (2007)), for instance, the fertility histories of women where the state corresponds to the number of children that a woman has given birth to at any time (or age), and from each birth she moves to the next state. There are three classical event history models: the independent increment model of Andersen and Gill (1982), the marginal model by Wei et al. (1989) and the conditional model of Prentice et al. (1981). For the marginal and conditional models, each occurrence of the event is modeled as a separate event, but for the independent increment model all the events of one individual are identical. For such event history models, a matter of interest is the choice of the time scale, as well as the risk-interval.

Some of the classical and the recent literature deals with incorporation of unobserved heterogeneity in the models for recurrent events, that arises, for example, when not all the individuals have an event before they are lost to follow-up or the study ends. Some authors have incorporated the unobserved heterogeneity by frailty modeling (see Vaupel et al. (1979), Nielsen et al. (1992), Oakes (1992) and Hougaard (2000), among others). On the other hand, modeling and analyzing the number of occurrences of the events by a stochastic process constitutes a matter of interest. For the Markov models, the transition rate only depends on the state where an individual is in, but neither on the time that an individual has been in that state nor on any other events that occurred before entering that state. Several extensions have addressed how to extend Markov models to let the transition rates depend on some features on the events occurred before entering the state, the order or occurrence of the particular state, recurrent events effects, by introducing specific duration distributions, or specific covariate effects (see e.g., Nielsen et al. (1992)).

In this paper, we introduce the discrete-time pure birth process for describing the number of recurrent events, that does not assume the Markov property, and allows that if the event occurred j times, then the probability that the recurrent event will occur depends on j. The main objective of the paper is to analyze a multistate model with recurrent events that are modeled by a discrete-time pure birth process. Its probability distribution is based on random sums with support N and with geometric summands. Specifically, let $\{U_j|j \geq 1\}$ be a sequence of independent random variables, that have the geometric distribution, with parameter α_j, with $0 < \alpha_j < 1$, for all $j \in N \cup \{0\}$ (that is, $\Pr[U_{j+1} = k] = \alpha_j \beta_j^k$, for $k \in N \cup \{0\}$, where $\beta_j = 1 - \alpha_j$, for any

$j \in N$), and let $\{M_j | j \geq 1\}$ be a sequence of positive integer-valued random variables defined on the same probability space, and furthermore, assume that the random variables M_j, $j \geq 1$ are independent of all the independent random variables U_j, $j \geq 1$. The random sums defined by $T_{M_n} = \sum_{j=1}^{M_n} U_j$ for $n = 1, ...,$ and $T_0 = 0$, have been investigated in applied probability for a long time (see e.g, Feller (1971)), with special applications in reliability theory to model the duration of systems with defective components. For instance, the sum of n geometric random variables represents the number of good items inspected before the n-th defective is observed, when the inspection is performed on an assembly line and the chance of a defective item is given initially by $\beta_1 = 1 - \alpha_1$, and subsequently (after adjustments) by $\beta_j = 1 - \alpha_j$, $j = 2, 3, ...$ Other applications of random sums and convolutions of geometric random variables can be found in queueing theory, biology, medicine, insurance and finance (see e.g., Rolski et al. (1999) and Cook and Lawless (2007)).

In the general multistate model, the random sum T_{M_n} represents the number of transitions made by an individual along his/her life. Some extensions of the model are described for incorporating unobserved heterogeneity by random event probabilities. Some motivations are provided in demography. The origin model is based on the discrete-time pure birth shock model by *Belzunce, Ortega and Ruiz (2009) Ageing properties of a discrete-time failure and repair model. IEEE Transactions Reliability, 58, 161-171*, to study the lifetime of a system (measured by the number of tasks executed by a system) which is submitted to shocks (failures) arriving randomly, and the lifetime is a random sum with geometric summands, describing the inter-arrival times of the shock arrival process. The multistate model aforementioned is analyzed by stochastic orderings in the case of independent inter-arrival times. Some of these results can be generalized in three directions: to inter-arrival times having arbitrary distribution (not necessarily geometric), to correlated inter-arrival times and to multivariate populations. The results in the case of independent inter-arrival times can be found with alternative proofs in *Belzunce, Ortega and Ruiz (2001). A note on stochastic comparisons in the discrete pure birth shock model. Technical Report, N. I-2001-17.* The results in the case of correlated inter-arrival times via random environments can be found with alternative proofs in *Escudero, Ortega and Alonso (2010). Variability comparisons for some mixture models with stochastic environments in biosciences and engineering. Stochastic Environmental Research and Risk Assessment 24, 199-209.* Some similar results to those in the case of arbitrarily distributed number of recurrent events can be found in Ortega, Alonso, Ortega (2013). Stochastic comparisons of parametric families in stochastic epidemics. *Mathematical Biosciences, doi: 10.1016/j.mbs.2012.12.006.* Several exact and numerical bounds of transformations of the probability distributions of the multistate model can be derived from the earlier stochastic comparisons. These bounds provide a statistical knowledge to select a better scenario via variations of the recurrent event distribution. In addition, we provide results for some qualitative properties of the kind 'new better than used' of the multistate model assuming independent and identically distributed summands. The organization of the paper is as follows. In Section 2 we introduce the multistate model with discrete-time pure

birth process for recurrent events. Several extensions of the origin model and some motivations in demography are provided. In Section 3 we study stochastic ordering of the multistate model with discrete-time pure birth process for recurrent events, based on results for random sums with geometric summands, and some ageing notions of the multistate model in a particular case. From now on, $X \sim \mathcal{G}(\alpha)$ denotes a geometric random variable, with parameter α, with $0 < \alpha < 1$; and *iid* is used as a shorthand for independent and identically distributed, 'increasing' and 'decreasing' stand for non-decreasing and non-increasing, respectively, and we will assume that the expectation is finite, whenever it is used. In general, we will consider a non-negative integer-valued random variable X, with survival function $\overline{P}_k = Pr[X \geq k]$, for $k \in N \cup \{0\}$, and probability mass function $p_k = \overline{P}_k - \overline{P}_{k+1}$, $k \in N$, with $p_0 = 0$ and notice that the previous definition for the discrete survival function follows the general lines for probability distributions in Roy (1997). For the definitions on stochastic ordering concepts, their implications, as well as, their main properties we will refer to Shaked and Shanthikumar (2007), and for the ageing notions we will refer to Barlow and Proschan (1981) and Lai and Xie (2006).

2 A multistate model with recurrent events

In this section, we introduce the multistate model with a discrete-time pure birth process for recurrent events, which is motivated by Belzunce et al. (2009).

2.1 Mathematical description

Consider an individual that makes sequentially transitions between the states labelled by $1, 2, ..., \omega$, and is subjected to recurrent events, which influence on the stochastic process that describes the movement of the individual. Assume that the events occur randomly in time, according to a discrete-time process $R = \{R(m), m = 1, 2, ...\}$, where $R(m)$ represents the number of events until the $m - th$ transition, for $m \in N$. We notice that the number of transitions made by the individual is considered here as the timescale. The occurrence of the recurrent events has influence time on the transitions that is negligible. The events arrival process R can be described in terms of a sequence of independent geometric interarrival times U_1, U_2, ..., where U_{j+1} is a geometric random variable, with parameter α_j, with $0 < \alpha_j < 1$. This means that if j events have occurred, then the following recurrent event will occur with probability α_j, for $j = 1, 2, ...$ Let now $\overline{P}_k$ denote the probability that the individual makes another transition having experienced the first k events, for $k \in N \cup \{0\}$. Assuming that $1 = \overline{P}_0 \geq \overline{P}_1 \geq \overline{P}_2 \geq ...$ then $\overline{P}_k$, can be considered as the survival function at $k \in N \cup \{0\}$ of an integer-valued positive random variable M, involved with making another transition when the individual has experienced a number of recurrent events M. Then, the random variable $X = \sum_{j=1}^{M} U_j$, describes the number of transitions made by the individual along his/her lifetime. Assuming that U_1, U_2, ... and M are independent, and if we denote by $T_n = \sum_{j=1}^{n} U_j$, for any $n \in N$, then $X = T_M$, is a mixture of

the family $\{T_n|n \in N\}$ with mixing distribution given by M. Throughout this paper, we call T_M *the multistate model with a discrete-time pure birth process for recurrent events.*

2.2 Some examples of multistate models in demography

The fertility histories of women are processes that the demographers have dealt with for a long time. Consider the life course of a woman through her fertility age $A = \{15, 16, ..., \omega\}$ and the multistate model for which each state is defined by her age and each birth is a recurrent event such that from each birth she moves to the next state. If we model the births according to a discrete-time pure birth process $R = \{R(m), m = 1, 2, ...\}$, where $R(m)$ represents the number of children that a woman has given birth to at age m, for $m \in A$, having geometric inter-arrival times $U_1(\alpha_0)$, $U_2(\alpha_1)$, ..., where $0 < \alpha_j < 1$ represents the probability of a birth given that the woman had j children. If $\overline{P}_k$ denotes the probability that the woman had k live children, for $k \in N \cup \{0\}$, for an integer-valued positive random variable M, then $X = \sum_{j=1}^{M} U_j$, describes the age of the woman. Conditioning on a given number of children, X is a convolution of geometric random variables. The bounds for the age of the woman can be calculated by straighforward calculation. Migration and changes in marital status are other transitions that can be studied by using the multistate models above.

2.3 Probabilistic properties of the model

The properties of the probability distribution of T_M are studied in Belzunce et al. (2009) assuming that T_M has support on N and that M and U_1, U_2,..., are independent random variables. This representation will be used in the results. We recall some distributional properties. For $M = k$, then $T_k = \sum_{j=1}^{k} U_j$, $k \in N$, and $\{R(m) \leq k\}$ if and only if $\{T_{k+1} \geq m\}$. We will use the notation

$$z_k(m) = \Pr[R(m) = k] = \Pr[T_k < m \leq T_{k+1}].$$

The function $z_k(m)$ is a totally positive in $(k, m) \in N \times N \cup \{0\}$ (see Karlin (1968)), and a recursive equation for computing $z_k(m)$ is given in Lemma 6 in Belzunce et al. (2009). Assuming that T_M has support on N and that M and U_1, U_2,..., are independent random variables, an exact distribution in terms of $z_k(m)$ can be stated, for $m \in N$, the survival function for T_M is given by

$$\overline{H}(m) = \Pr[T_M \geq m] = \sum_{k=0}^{\infty} z_k(m)\overline{P}_k. \quad (1)$$

Some extensions of the earlier multistate model can be derived in several ways. To introduce the heterogeneity, first we consider that the parameters α_j are random for any $j \in N$ (see Escudero et al. (2010)). Then the random variable that describes the number of transitions made by the individual along his/her lifetime is a random sum by $X = T_M(\alpha_1, ..., \alpha_m, ...) = \sum_{j=1}^{M} \mathcal{G}(\alpha_j)$, and conditioning on $M = m$ it is a mixture of $\{T_m = \sum_{j=1}^{m} \mathcal{G}(\alpha_j)|(\alpha_1, ..., \alpha_m) \in (0, 1)^m\}$ with mixing distribution given by $(\alpha_1, ..., \alpha_m)$. Extensions of the multistate model in the multivariate case will be discussed in Section 3.

3 The results

In this section we provide results on stochastic comparisons of multistate models with discrete-time process for recurrent events. In the following results let M, N be positive integer-valued random variables and $U_1(\alpha_1)$, $U_2(\alpha_2)$,... be a sequence of independent or positively correlated random variables, that are independent of M and of N. Consider the random sums $T_M = \sum_{j=1}^{M} U_j(\alpha_j)$ and $T_N = \sum_{j=1}^{N} U_j(\alpha_j)$ to describe multistate models with a counting process for recurrent events, under two scenarios determined by the distribution of the number of recurrent events M and N, respectively, experienced before making a new transition.

3.1 Some theoretical results

As a starting point, we give a discrete version of a classical result for absolutely continuous random variables.

Theorem 1. *Let $U_1 \sim \mathcal{G}(\alpha_1)$, $U_2 \sim \mathcal{G}(\alpha_2)$,... be a sequence of independent geometric random variables. Denote $\beta_n = 1 - \alpha_n$ and $T_n = \sum_{j=1}^{n} U_j$, for any $n \in N$. The following assertions hold:*
(i) if $\beta_i \leq \beta_{i+1}$, for any $i \in N$ then $U_i \leq_{LR} U_{i+1}$, for any $i \in N$.
(ii) $T_n \leq_{LR} T_{n+1}$, for any $n \in N$.

3.2 The case of independent inter-arrival times.

Next, we obtain results for several stochastic orderings. Some related results can be found in Ross and Schechner (1984), Kochar (1990), Pellerey (1993), and Ortega (2009), among others.

Theorem 2. *Let $U_1 \sim \mathcal{G}(\alpha_1)$, $U_2 \sim \mathcal{G}(\alpha_2)$,... be a sequence of independent geometric random variables, that are independent of M and of N. Consider the random sums $T_M = \sum_{j=1}^{M} U_j(\alpha_j)$ and $T_N = \sum_{j=1}^{N} U_j(\alpha_j)$.*
i) If $M \leq_{LR} N$, then $T_M \leq_{LR} T_N$.
ii) If $M \leq_{FR} N$, then $T_M \leq_{FR} T_N$.
iii) If $M \leq_{RHR} N$, then $T_M \leq_{RHR} T_N$.
iv) If $M \leq_{ST} N$, then $T_M \leq_{ST} T_N$.
v) If $\beta_i \leq \beta_{i+1}$, for any $i \in N$ and $M \leq_{ICX} N$, then $T_M \leq_{ICX} T_N$.
vi) If $\beta_i \leq \beta_{i+1}$, for any $i \in N$; and $M \leq_{Lt} N$, then $T_M \leq_{Lt} T_N$.
vii) If $\left(\sum_{j=k}^{\infty} \frac{\beta_j}{\alpha_j} \overline{P}_j\right) / \left(\sum_{j=k}^{\infty} \frac{\beta_j}{\alpha_j} \overline{Q}_j\right)$ is decreasing in $k = 0, 1, ..., T_M \leq_{MR} T_N$.

The previous results provide technical conditions to be checked for ranking multistate models. Also, these conditions enable us to construct analytical bounds for the multistate models based on parametric families used to describe the survival for recurrent events.

Proceedings, 15th Applied Stochastic Models and Data Analysis (ASMDA2013)
International Conference, Mataró (Barcelona), Spain 25 - 28 June 2013

3.3 The case of arbitrarily distributed number of recurrent events

In this subsection we deal with the case of independent inter-arrival times having arbitrary distribution (not necessarily geometric) and having the ILR property, for which the main assertions in Theorem 2 also hold.

Theorem 3. *Consider the random sums* $T_M = \sum_{j=1}^{M} U_j(\alpha_j)$ *and* $T_N = \sum_{j=1}^{N} U_j(\alpha_j)$, *where the summands are independent random variables with an arbitrary distribution.*
i) If U_1, U_2,... *have the* ILR *property, if* $M \leq_{LR} N$, *then* $T_M \leq_{LR} T_N$.
ii) If U_1, U_2,... *have the* IFR *property, if* $M \leq_{LR} N$, *then* $T_M \leq_{FR,RHR} T_N$.
iii) If U_1, U_2,... *have the* IFR *property, if* $M \leq_{MR} N$, *then* $T_M \leq_{MR} T_N$.

For analyzing the effect of unobserved heterogeneity given by random parameters, we have a random sum of mixed geometric random variables that are independent of the number of summands. The stochastic comparisons of mixed geometric random variables are studied in Ortega, Alonso and Ortega (2013).

3.4 The case of correlated inter-arrival times

Analogously, for arrival times being increasing in the ST order, the assertion in Theorem 2 holds too, and the same happens for the CX, and Lt orders. Similar results for the LR and FR orders can be given.

Theorem 4. *Let* $U_1 \sim \mathcal{G}(\alpha_1)$, $U_2 \sim \mathcal{G}(\alpha_2)$,... *be a sequence of geometric random variables. Consider* $T_M = \sum_{j=1}^{M} U_j(\alpha_j)$, $T_N = \sum_{j=1}^{N} U_j(\alpha_j)$.
i) If $U_j \leq_{CX} U_{j+1}$ *for any* $j = 1, 2, ...$ *and* $M \leq_{CX} N$, *then* $T_M \leq_{CX} T_N$.
ii) If $U_j \leq_{ST} U_{j+1}$ *for any* $j = 1, 2, ...$ *and* $M \leq_{ICX} N$, *then* $T_M \leq_{ICX} T_N$.
iii) If $U_j \leq_{Lt} U_{j+1}$ *for any* $j = 1, 2, ...$ *and* $M \leq_{Lt} N$, *then* $T_M \leq_{Lt} T_N$.

When the correlated inter-arrival times are dependent via random environments the ICX order is studied in Escudero et al. (2010). In addition, we observe that the results in Escudero et al. (2010) can be used to compare two multistate models with discrete-time pure birth process for recurrent events, with different arrival processes (i.e., different parameters for the inter-arrival time distributions) and with the same distribution of the number of experienced recurrent events. They extend the results in the literature, of stochastic comparisons for convolutions of geometric random variables, from some related majorization type orders between two parameter vectors of the geometric summands (see e.g., Boland et al. (1994)).

3.5 The case of multivariate multistate models

The earlier setting can be extended to the multivariate case in several ways. A first extension is determined by probabilities of recurrent events that depend on the state of the process apart of the number of previous events. Given that j events have occurred, then a new recurrent event happens with probability $\alpha_{j,k}$, where k represents that the process is in the state k. A second extension

comes from considering random vectors of environmental or exposure parameters for the components of the models, as in Escudero et al. (2010). Third, by taking random vectors of multistate models and using multivariate stochastic orderings, for which similar results as in Belzunce et al. (2006) can be derived. The results in this issue are omitted.

3.6 The case of discrete-time Poisson process for recurrent events

Consider a sequence of *iid* geometric random variables where $U_j \sim \mathcal{G}(\alpha)$, $j \in N$, with $0 < \alpha < 1$. Then $T_k = \sum_{j=1}^{k} U_j$ has the negative binomial distribution with parameters (k, α), with $k \in N$. Unconditioning T_M is a random sum with *iid* geometric summands, and assume that $\Pr[T_M = 0] = 0$, i.e., T_M has on values over N. For $\beta = 1 - \alpha$, the survival function of T_M is

$$\overline{H}(m) = \sum_{k=0}^{\infty} \alpha^k \beta^m k + m - 1 k \overline{P}_k, m \in N. \tag{2}$$

Next, we study the ageing properties NBU, $NBU(2)$, and $NBUC$ for the multistate model when the probability of occurring another recurrent event does not depend on the previous events, that is, in the case when there are identically distributed inter-arrival times. The dual notions arise analogously.

Theorem 5. *Consider the random sum $T_M = \sum_{j=1}^{M} U_j$ given by (2), where the summands are iid geometric random variables, that are independent of M.*
i) If M is NBU, then T_M is NBU.
ii) If M is $NBU(2)$, then T_M is $NBU(2)$.
iii) If M is $NBUC$, then T_M is $NBUC$.

The NWU notion is studied in Theorem 4.1 in Willmot and Cai (2001), and also in Li et al. (2006) and Belzunce et al. (2009) for several kind of discrete random sums, under other assumptions. Using some inequalities for these ageing notions as can be seen in Barlow and Proschan (1981), some numerical upper and lower bounds for the number of transitions of an individual can be calculated. Statistical inference can be used to test these ageing notions (see Lai and Xie (2006)). From the migration movements in demography, the previous results mean that the number of migrations to be completed by an individual in his/her life are larger, in some stochastic sense, than the number of migrations that remain to be completed by individuals who have carry out a given amount of movements. These bounds can be used to develop social and economical policies concerning with possible massive migration movements.

Proceedings, 15th Applied Stochastic Models and Data Analysis (ASMDA2013)
International Conference, Mataró (Barcelona), Spain 25 - 28 June 2013

Optimal Insurance with Investment and Loans

Darya Ostrovskaya[1]

Department of Probability Theory, Lomonosov Moscow State University, Russia
(E-mail: ostrovskaya.dar@gmail.com)

Abstract. Insurance plays the leading role in compensation for losses, and its necessity increases together with the development of the economy. Investment activity is also one of the main factors for effective operating of the insurance company. The paper under consideration is devoted to the search of the optimal investment strategy for an insurance company. Several discrete models are investigated by means of dynamic programming and Bellman equation.

1 Description of the model with equal rates for investment and borrowing

We consider the discrete-time model connected to the operating of some insurance company.
Let x be initial capital of the insurance company. In a unit interval the company earns some premia c and has to pay possible claims η_i. We let $\{\eta_i\}_{i=1}^n$ be an iid sequence with distribution function $F(t)$ and density function $f(t)$. Since claims are nonnegative, let $F(t) = 0$ and $f(t) = 0$ for $t < 0$ and suppose that $F(t)$ increases in $[0; \infty)$.
In the beginning of every period after collecting premia the company is supposed to be able to invest or to borrow some value y with some interest rate r. In the end of the period company gets claims and if it does not have enough capital to pay the claims, then it borrows lacking money immediately at a higher rate q ($q > r$). The aim of the company is to find the optimal value of investment (or borrowing) y_n^* for every $n = 1, 2, 3, ...$ in order to minimize expected costs for n periods. If y_n^* obtained is positive, then the company should borrow y_n^*, otherwise it should invest $-y_n^*$.

1.1 One-period strategy

Let us discuss optimal strategy for a company, which operates for one period only Let ξ be expected costs of the company with initial capital x, then

$$\xi = \begin{cases} yr, & \eta \le x + c + y; \\ yr + q(\eta - (x + c + y)), & \eta > x + c + y. \end{cases}$$

Denote by $P(x, y, \eta)$ capital of the company with initial capital x in the end of the first period, provided that the value y was borrowed (or $-y$ was invested).

$$P(x, y, \eta) = \begin{cases} x + c - \eta - yr, & \eta \le x + c + y; \\ -y(r + 1) - (1 + q)(\eta - (x + c + y)), & \eta > x + c + y. \end{cases}$$

Let us find the expectation of the costs for one period:

$$G(x,y) = E\xi = yr + \int_{x+c+y}^{\infty} q(s-(x+c+y))f(s)\,ds.$$

Having computed the derivative of this expression

$$G'_y(x,y) = r - q + qF(x+c+y),$$

we equate it to zero, and find the optimal solution:

$$F(x+c+y) = \frac{q-r}{q};$$

$$y_1^*(x) = F^{-1}\left(\frac{q-r}{q}\right) - x - c.$$

The second derivative of expected costs

$$G''_y(x,y) = qF'(x+c+y) = qF'\left(F^{-1}\left(\frac{q-r}{q}\right)\right) > 0,$$

is positive since $F(t)$ is increasing function. Therefore, the function of expected costs reaches its minimum in the obtained point $y_1^*(x)$

1.2 Two-period strategy

Let $f_n(x)$ be expectation of costs for n periods provided that value of y_i^* was chosen optimally in each period.
According to Bellman optimality principle we derive following equation:

$$f_n(x) = \min_y \left[G(x,y) + Ef_{n-1}\left(P(x,y,\eta)\right)\right].$$

Consider this equation for $n = 2$:

$$f_2(x) = \min_y \left[G(x,y) + Ef_1\left(P(x,y,\eta)\right)\right].$$

$f_1(x)$ may be found since we know one-period optimal solution:

$$f_1(x) = G(x, y_1^*(x)) = r\left(F^{-1}\left(\frac{q-r}{q}\right) - x - c\right) +$$

$$+ \int\limits_{F^{-1}\left(\frac{q-r}{q}\right)}^{\infty} q\left(s - F^{-1}\left(\frac{q-r}{q}\right)\right) f(s)\,ds.$$

Hence $f_1'(x) = -r$;

$$\left[f_1\left(P(x,y,\eta)\right)\right]'_y = f_1'\left(P(x,y,\eta)\right) \cdot P'_y(x,y)$$

$$P'_y(x,y,\eta) = \begin{cases} -r, & \eta \le x+c+y; \\ -(r+1)+(1+q), & \eta > x+c+y. \end{cases}$$

Having computed the derivative of this expression

$$\left[G(x,y) + Ef_1\left(P(x,y,\eta)\right)\right]'_y = (r-q)(1+r) + (1+r)qF(x+c+y).$$

we equate it to zero, and find the optimal solution:

$$F(x+c+y) = \frac{(q-r)(1+r)}{q(1+r)}.$$

$$y_2^*(x) = F^{-1}\left(\frac{q-r}{q}\right) - x - c = y_1^*(x).$$

Again the second derivative of expected costs

$$\left[G(x,y) + Ef_1\left(P(x,y,\eta)\right)\right]''_y = (r+1)qF'(x+c+y_2^*) = (r+1)qF'\left(F^{-1}\left(\frac{q-r}{q}\right)\right) > 0$$

is positive. Thus, the function of expected costs reaches its minimum in the obtained point $y_2^*(x)$

1.3 n-period strategy

Proposition 1 *$y_n^*(x) = F^{-1}\left(\frac{q-r}{q}\right) - x - c$ for every $n = 1,2,3,....$*

Proof is by induction. Suppose that for all $n \le k-1$ $y_n^*(x) = F^{-1}\left(\frac{q-r}{q}\right) - x - c$ and $f'_{n-2}(x) = 1-(1+r)^{n-2}$. We will prove that it holds for $n=k$. The recurrence equation will be as follows:

$$f_k(x) = \min_y \left[G(x,y) + Ef_{k-1}\left(P(x,y,\eta)\right)\right];$$

$$\left[f_{k-1}\left(P(x,y,\eta)\right)\right]'_y = f'_{k-1}\left(P(x,y,\eta)\right)\cdot P'_y(x,y,\eta);$$

$$f_{k-1}(x) = G(x,y_{k-1}^*(x)) + Ef_{k-2}\left(P(x,y_{k-1}^*(x),\eta)\right);$$

$$f'_{k-1}(x) = G'_x(x,y_{k-1}^*(x)) + G'_y(x,y_{k-1}^*(x))\cdot {y_{k-1}^*}'(x) + E[f_{k-2}(P(x,y_{k-1}^*(x),\eta))]'_x;$$

$$G'_y(x,y_{k-1}^*(x)) = G'_y(x,y_1^*(x)) = 0,$$

since $y_1^*(x)$ is a solution of the equation $G'_y(x,y) = 0$.

$$G'_x(x,y_{k-1}^*(x)) = G'_x(x,y_1^*(x)) = -q(1-F(x+c+y_1^*(x))) = -r;$$

$$\left[f_{k-2}(P(x,y_{k-1}^*(x),\eta))\right]'_x = f'_{k-2}(P(x,y_{k-1}^*(x),\eta))\cdot$$
$$\cdot\left(P'_x(x,y_{k-1}^*(x),\eta) + P'_y(x,y_{k-1}^*(x),\eta)\cdot {y_{k-1}^*}'(x)\right).$$

Let us find the derivatives of the capital in the end of the first period:

$$P'_x(x,y_{k-1}^*(x)) = P'_x(x,y_1^*(x),\eta) = \begin{cases} 1, & \eta \le F^{-1}\left(\frac{q-r}{q}\right); \\ 1+q, & \eta > F^{-1}\left(\frac{q-r}{q}\right). \end{cases}$$

$$P'_y(x, y^*_{k-1}(x), \eta) = P'_y(x, y^*_1(x), \eta) = \begin{cases} -r, & \eta \le F^{-1}\left(\frac{q-r}{q}\right); \\ q-r, & \eta > F^{-1}\left(\frac{q-r}{q}\right). \end{cases}$$

By the inductive assumption, ${y^*_{k-1}}'(x) = {y^*_1}'(x) = -1$.
Therefore, we find

$$E\left[f_{k-2}(P(x, y^*_{k-1}(x), \eta))\right]'_x = \left(1-(1+r)^{k-2}\right) \cdot$$

$$\cdot \left(\int\limits_0^{F^{-1}\left(\frac{q-r}{q}\right)} (1+r) f(s)\, ds + \int\limits_{F^{-1}\left(\frac{q-r}{q}\right)}^{\infty} (1+q+r-q) f(s)\, ds \right) =$$

$$= \left(1-(1+r)^{k-2}\right) \cdot \left((1+r)\frac{q-r}{q} + (1+r)\left(1-\frac{q-r}{q}\right)\right) =$$

$$= \left(1-(1+r)^{k-2}\right) \cdot (1+r);$$

$$f'_{k-1}(x) = -r + \left(1-(1+r)^{k-2}\right) \cdot (1+r) = 1-(1+r)^{k-1};$$

Using all the expressions above we may find:

$$\left[G(x,y) + E f_{k-1}\left(P(x,y,\eta)\right)\right]'_y = (r-q)(1+r)^{k-1} + qF(x+c+y)(1+r)^{k-1}.$$

By equating this derivative to zero and solving the following equation

$$F(x+c+y) = \frac{q-r}{q}.$$

we obtain $y^*_k = F^{-1}\left(\frac{q-r}{q}\right) - x - c$.
The second derivative:

$$\left[G(x,y) + E f_{k-1}\left(P(x,y,\eta)\right)\right]''_y = q(1+r)^{k-1} \cdot F'(x+c+y) > 0,$$

is positive since $F(t)$ is increasing function. Thus $y^*_k is a minimum point. Hence inductive step is done and the Propo$

2 Description of the model with different rates for investment and borrowing

In this section we assume that rates for borrowing and investment differ, namely r is rate for borrowing, v is rate for investment $(r > v)$

2.1 One-period strategy

In this model the capital of the insurance company in the end of the first period is:

$$P(x,y,\eta) = \begin{cases} x+c-\eta-yr, & \eta \le x+c+y, \quad y > 0; \\ x+c-\eta-yv, & \eta \le x+c+y, \quad y \le 0; \\ -y(r+1)-(1+q)(\eta-(x+c+y)), & \eta > x+c+y, \quad y > 0; \\ -y(v+1)-(1+q)(\eta-(x+c+y)), & \eta > x+c+y, \quad y \le 0. \end{cases} =$$

$$= \begin{cases} x+c-\eta-y(I(y>0)r+I(y\le 0)v), & \eta \le x+c+y; \\ -y(I(y>0)r+I(y\le 0)v+1)-(1+q)(\eta-(x+c+y)), & \eta > x+c+y. \end{cases}$$

The costs are as follows:

$$\xi = \begin{cases} yr, & \eta \le x+c+y, \quad y>0; \\ yv, & \eta \le x+c+y, \quad y\le 0; \\ yr+q(\eta-(x+c+y)), & \eta > x+c+y, \quad y>0; \\ yv+q(\eta-(x+c+y)), & \eta > x+c+y, \quad y\le 0. \end{cases} =$$

$$= \begin{cases} y(I(y>0)r+I(y\le 0)v), & \eta \le x+c+y; \\ y(I(y>0)r+I(y\le 0)v)+q(\eta-(x+c+y)), & \eta > x+c+y. \end{cases}$$

Let us find the expectation of the costs:

$$G(x,y) = E\xi = \int_0^{x+c+y} y\,(I(y>0)r+I(y\le 0)v)\,f(s)\,ds +$$

$$+ \int_{x+c+y}^{\infty} [y\,(I(y>0)r+I(y\le 0)v)+q(s-(x+c+y))]\,f(s)\,ds =$$

$$= y\,(I(y>0)r+I(y\le 0)v) + \int_{x+c+y}^{\infty} q(s-(x+c+y))f(s)\,ds.$$

In order to find extremums we need to find the derivative with respect to y:

$$G'_y(x,y) = (I(y>0)r+I(y\le 0)v)+q\,(F(x+c+y)-1)\,;$$

$$G''_y(x,y) = qF'(x+c+y) > 0,$$

Hence $G(x,y)$ is a convex function. Let us consider two cases:
1) $y>0$. Then, having equated derivative to zero:

$$r-q+qF(x+c+y)=0,$$

we obtain

$$y_1^* = F^{-1}\left(\frac{q-r}{q}\right) - x - c.$$

$$x < F^{-1}\left(\frac{q-r}{q}\right) - c.$$

2) $y\le 0$.

$$v-q+qF(x+c+y)=0;$$

$$y_1^* = F^{-1}\left(\frac{q-v}{q}\right) - x - c.$$

$$x \ge F^{-1}\left(\frac{q-v}{q}\right) - c.$$

Taking into account that $r > v$, notice that $F^{-1}\left(\frac{q-v}{q}\right) - c > F^{-1}\left(\frac{q-r}{q}\right) - c$. Then we need to obtain optimal value y, when $F^{-1}\left(\frac{q-v}{q}\right) - c > x \geq F^{-1}\left(\frac{q-r}{q}\right) - c$. With such initial capital the function of expected costs is decreasing for $y < 0$ and increasing for $y \geq 0$, hence function of expected costs reaches minimum at $y_1^* = 0$.
Summarizing the results we may write:

$$y_1^*(x) = \begin{cases} F^{-1}\left(\frac{q-r}{q}\right) - x - c, & x < F^{-1}\left(\frac{q-r}{q}\right) - c; \\ F^{-1}\left(\frac{q-v}{q}\right) - x - c, & x \geq F^{-1}\left(\frac{q-v}{q}\right) - c; \\ 0, \quad F^{-1}\left(\frac{q-v}{q}\right) - c > x \geq F^{-1}\left(\frac{q-r}{q}\right) - c. \end{cases}$$

2.2 Two-period strategy

In this subsection I would like to provide some graphs illustrating the behaviour of the derivative in case of exponential distribution function $F(t)$ depending on the values of premium c and initial capital x. The derivative on every interval is computed. There may be three qualitatively different situations.

1. The graph of the derivative intersects negative anxle. Thus, to reach minimal costs the company is to invest some value.

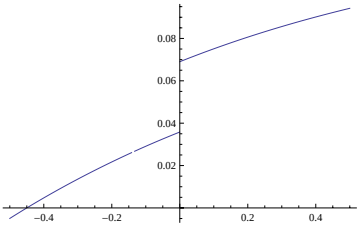

Fig. 1.

2. The graph of the derivative intersects positive anxle. Thus, to reach minimal costs company is to borrow some value.

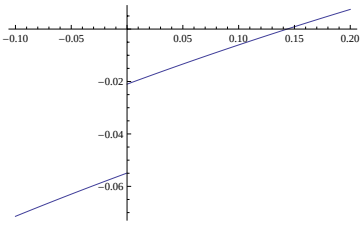

Fig. 2.

3. The graph of the derivative does not intersect anxle anywhere. In this case function of expected costs is decreasing while $y < 0$ and increasing while $y > 0$. Therefore minimum of the function of expected costs is at point $y = 0$.

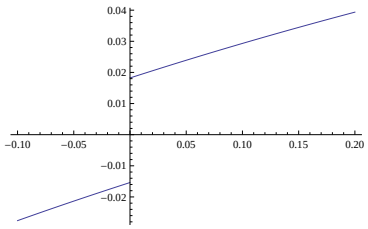

Fig. 3.

References

1.R. Bellman. *Dynamic Programming*, 1957
2.Zhongfei Li, Ken Seng Tan, Hailiang Yang. *Multiperiod Optimal Investment-Consumption Strategies with Mortality Risk and Environment Uncertainty*, 2006

Proceedings, 15th Applied Stochastic Models and Data Analysis (ASMDA2013)
International Conference, Mataró (Barcelona), Spain 25 - 28 June 2013

Estimating child mortality from information on previous birth: data from a Portuguese birth cohort.

Neir A. Paes[1]; Cristina Teixeira[2]; Henrique Barros[3]

[1] Department of Statistics of the Federal University of Paraíba, Cidade Universitária, João Pessoa, PB, Brazil (E-mail: **antunes@de.ufpb.br**)

[2,3] Institute of Public Health, University of Porto, Porto, Portugal and Department of Clinical Epidemiology, Predictive Medicine and Public Health, University of Porto Medical School, Porto, Portugal (E-mail: **cristina.teixeira@ipb.pt; hbarros@med.up.pt**).

Abstract: A whole range of techniques have been developed for estimating infant and child mortality from the information routinely recorded in maternity registers on age and reproductive history of delivering mothers. Among them, the best-known and most widely applied indirect technique was developed by William Brass. Using the baseline information from a birth cohort (Generation XXI) assembled in the period 2005-2006 in the metropolitan area of Porto, North of Portugal, we addressed in this paper the following objectives: (1) to estimate the child mortality rates based on information about previous births and their survivorship among women recruited for this birth cohort; (2) to compare these indirect estimates with direct values retrieved from Portuguese vital statistics; (3) to analyse the potential of this birth cohort to generate plausible estimates of life-table indicators. We retrieved data on mother's age, previous live births prior to the current one, and number of surviving and deceased children from a group of multiparous women (n=3521). The data was divided into seven 5-year groups by maternal age and survival and death probabilities were computed for each group. Through the Brass method, we obtained estimates of probability of dying before attaining certain exact childhood ages, $q(x)$, by using the multipliers $k(i)$ as proposed by Trussel. Then, a logit life-table system was used to derive life-table indicators. Accordingly, probabilities of dying between birth and 2, 3, 5 and 10 years were respectively: 4.1; 6.7; 9.4 and 13.1 per 1,000 children ever born, which were alocatted in time-period. These indirect estimates compared with the direct ones obtained from Portuguese vital statistics revealed that they were very similar. The life expectancy at birth was 77.6 years for both

sexes, and the implied infant mortality was 4.0 per 1000 live births for Grand Porto during the period 2005-2006. The use of indirect method to analyze the potential of the Generation XXI cohort data in provide relevant information on reproductive issues, not available in the vital statistics, seems to be an important and effective tool, and promissory for analyzing the follow-up studies of this cohort held in 2009 and 2012.

Keywords: Child mortality, Brass' Method, Preceding Birth Technique.

1 Introduction

The 5th stage of demographic transition, which many call postmodern demographic regime, already occurs in some of the more developed countries of the world where death rates, although low, begin to exceed birth rates, which results in a negative crude rate of natural increase [1]. Portugal went through all stages of the Demographic Transition Model. According to the Portuguese vital statistics [2], since 2007 the number of deaths (n=103,512) has exceeded the number of live births (n=102,492). In the recent years Portugal went into the 5th phase; the fertility rate is around 1.3 and infant mortality rate reached 3.4 per 1000 live births which are among the lowest rates in Europe [3].

Tracing the evolution of child health indicators is essential for evaluating the availability and quality of health care in a community. Infant and child mortality [4,5] have been used for this purpose. The accurate estimation of the probabilities of dying before certain age, particularly under-five years old, are largely used by international agencies to monitor development progress [6] and, is one of the principal input parameters used to develop estimates of life expectancy at birth and other summary indicators of mortality [7,8].

In the face of dramatic reduction in absolute level of infant and child mortality in developed countries, the challenge is to document disparities across groups concerning such deaths. The evaluation of potential efficacious interventions to reduce adverse neonatal and childhood outcomes should take into account a set of characteristics, namely demographic, social and obstetric factors in order to

perceive the decline of disparities rather than the decrease of crude mortality rates. The estimates of demographic and health indicators available in Portugal are based on census data and vital statistic registration [2]. From the latter the infant and child mortality rates can be directly obtained. However, Portuguese vital statistics has no information about a set of demographic characteristics such as parity, social factors as education, adverse maternal behaviours and obstetric complications; medical records are usually more detailed than vital statistics concerning such information.

A whole range of indirect techniques have been developed for estimating infant and child mortality based on the information retrieved from medical records of women delivering a child, or based on sample surveys, on age and reproductive history of delivering mothers [7-9]. These indirect estimation techniques could be useful to provide childhood mortality rates when a set of maternal characteristics is not available in vital statistics. They also offer potential estimates for continuous follow-up studies over time.

One of the largest birth cohort ever assembled in Portugal was established between 2005 and 2006 in the Porto Metropolitan Area, North of Portugal (Generation XXI). We addressed in this paper the following purposes: (1) to estimate the child mortality rates based on information about previous births and their survivorship among women recruited for this birth cohort; (2) to compare these indirect estimates with direct values retrieved from Portuguese vital statistics; (3) to analyse the potential of this birth cohort to generate plausible estimates of life-table indicators.

2 Methods

In Portugal, nearly all deliveries occur within hospitals and 90% of them occur in public hospitals free of charge for all childbearing women and their offspring. The participants of the present study were recruited in five public hospitals level III, while assembling a birth cohort in Porto Metropolitan Area, in the north of Portugal (Generation XXI). Between April 2005 and August 2006, 70% of all

pregnant women delivered at those five public hospitals were invited as participants on the basis of "first come first served" and only 8% of those invited refused to participate. This approach allowed a representative sample. The final sample comprised 8495 women who delivered live infants (>24 weeks). Information on social and demographic characteristics, obstetric and gynaecological history, lifestyles and current pregnancy events was obtained using a structured questionnaire. Individual interviews were performed 24 to 72 hours after delivery by trained interviewers. Information on pregnancy complications, delivery circumstances and data on newborn characteristics were abstracted from patient medical records.

From all mothers enrolled in this cohort only multiparous women with at least a previous child before the current delivery (n=3520) were included in the present analysis. We retrieved data on mother's age, previous live births prior to the current one and number of deceased children.

In this work we used the method developed by William Brass [7], the best-known and most widely applied indirect technique for estimating child mortality rates. Accordingly, women were stratified by five-year age groups from 15-19 to 45-49. The procedure converts proportions dead children ever born, *D(i),* reported by women's age group into estimates of the probability of dying before attaining certain exact childhood age, $q(x=1, 2, 3, 5, 10, 15$ and 20 years old), by using the multipliers *k(i)* as proposed by Palloni-Heligman, assuming that Far Eastern family in the United Nations model life tables system is an adequate representation of the pattern of mortality of Porto [7].

We computed also the reference time-period, $t(x)$, which represents an estimate of the numbers of years before the survey date to which the child mortality estimates, $q(x)$, refer. The values of the coefficients to estimate $t(x)$ were retrieved from the United Nations Report [7].

We assumed that the pattern of fertility by age of the women and the childhood mortality have remained without important changes during the recent past. Indeed, between 2000 and 2006 the total fertility rate varied from 1.36 and 1.41 live births per woman and infant mortality rate varied between 5.5 and 3.6 infant

deaths per 1000 live births. We assumed also a similar pattern of fertility by age of the multiparous in the Generation XXI and the Portuguese women as a whole. We obtained the direct estimates of child mortality from Portuguese vital statistics [2], taking into account the reference period and we compared the values of direct and indirect estimates.

Once $q(x)$ is estimated, its complement $l(x)$, the probability of surviving from birth to exact age x, is readily obtained as $l(x) = 1.0 - q(x)$, which was converted in logit function, $Y(x)$. According to the logit life-table system as proposed by Brass [7], the Portugal (2009-2011) life table was used as a standard model to derive the adjusted life table to Porto for ages under 10 [2].

3 Results and Discussion

Table 1 shows the basic data and the main results on the application of the Brass's method according to five-year age group of mother. In Portugal, increasing numbers of women are delaying childbearing into their thirties and early forties, making the consequences of older maternal age for the infant an important public health concern. Grand multiparity, by contrast, is now exceedingly rare in this country. There were 3521 multiparous women in the present analysis; only 24% (n=829) of those women reported to have 2 or more children previously to the current birth. The mean age of women was 32 years (standard deviation ±5.26). The total number of children ever born was 4651; 1.2% (n=55) of those children died.

Proportions deceased are quite instable in age group 15-19 due to the very small numbers of births. On the other hand, for the last age group, no dead was reported, and the proportion of the age group 40-44 is out of line probably due to the age composition of the sample. Therefore, mortality estimates based on the reports of women for these age groups were disregarded. Proportions deceased were also instable in age group 25-29 and 35-39, which demanded some adjustments. Since there is no evidence that the proportion of death

provided by the age group 20-24 and 30-34 are unreliable, the obtained estimates for the adjacent age groups (25-29 and 35-39) was performed by linear interpolation. As presented in Table 1, the indirect estimates of the probability of dying (mortality rates) between birth and age 2, 3, 5 and 10 years old were 4.0, 5.7, 7.3 and 9.6 per 1000 children ever born, respectively. Assuming that Porto has a little lower mortality rates compared with the country as whole, and considering the reference time-period to which child mortality $q(x)$ refer, in general the mortality rates presented similar values when indirect and direct estimates of child mortality are compared.

Calculation of logit transformation of the estimated survivorship probabilities, $l(x)$, and the corresponding logit tranformation of the standard life-table used (Portugal 2009-2010) showed a reasonable degree of coincidence between one set and the other for multiparous womem. Notably deviant points were those associated with the $l(5)$ and $l(10)$ estimate. On the basis of these observations, the level indicated to match with the standard life-table was $q(2)$, which correspond to a more recent period. In this way, the adjusted pattern was obtained by assuming an value for a level of $\alpha = 0.050$ and standard $\beta = 0.979$ according to the Brass's logit life table system.

Table 1. Data required to compute child mortality according to the Brass' method and indirect and direct estimates of mortality rates under 2, 3, 5 and 10 years old to Porto Metropolitan Area, Portugal.

Women's Age Group (years)	Average parity per women	Number of children ever born	Proportion of children dead	Index x	Generation XXI		Portuguese vital statistics	
					Prob. of dying	Reference time-period	Prob. of dying	Reference time-period
15 – 19	1,0000	35	0.0286	$q(1)$	-	-	-	-
20 – 24	1,1682	382	0.0052	$q(2)$	0,0040	2001	0,0057	2000/01
25 – 29	1,2247	894	0.0179	$q(3)$	0,0057	1999	0,0060	2000/01
30 – 34	1,2592	1681	0.0071	$q(5)$	0,0073	1997	0,0073	1999/00
35 – 39	1,4651	1279	0.0149	$q(10)$	0.0096	1997	0.0860	1999/00
40 – 44	1.7438	354	0.0141	$q(15)$	-	-	-	-
45 – 49	2,3636	26	0.0000	$q(20)$	-	-	-	-

The construction of a life table based on the estimated level (α) and pattern (α) derived from the aplication of the Brass's logit life table system, implied in a life expectancy at birth of 77.7 years and, an infant mortality of 3.7 per 1000 live births for both sexes for Grand Porto during the period 2005-2006. These life table estimates seem very plausible, since the official estimate of life expectancy at birth for the Grand Porto in the year 2005 using direct vital registration data was 78.0, and infant mortality of 3.7 per 1000 live births [2].

Conclusions

As other European countries, Portugal witnessed a dramatic decline in crude rates of child mortality [3]. The challenge nowadays is to document disparities in child mortality rates. A set of characteristics should be take into account in order to perceive the decline of these disparities. However, important demographic, social and obstetric factors are not available in the vital statistics. Thus indirect estimation of child mortality based on information about previous births retrieved from medical records of women, could be a useful tool.

We evaluated the appropriateness of the Brass' method to estimate the probability of dying of dying before attaining certain exact childhood ages based on information about previous births, and their survivorship collected in the north of Portugal from a group of multiparous women, when registering a current birth. Accordingly, we observed that the obtained indirect estimates were generally consistent with direct estimates for child mortality rate under 10 years. But don't add substantial insight beyond direct estimates when vital statistics is available. However, the use of indirect method to analyze the potential of the Generation XXI cohort data in provide relevant information on reproductive issues, not available in the vital statistics, seems to be an important and effective tool, and promissory for analyzing the follow-up studies of this cohort held in 2009 and 2012.

References

1. Rosset E. [The fifth phase of demographic transition: population regression]. *Studia Demogr.* 1980(61-62):3-27.

2. Instituto Nacional de Estatística. Available at:. http://ine.pt/. Accessed May 20, 2011.

3. World Health Organization Regional Office for Europe. European health for all database (HFA-DB). Available at. http://data.euro.who.int/hfadb/. Accessed March 14, 2012

4. EURO-PERISTAT project, with SCPE, EUROCAT, EURONEOSTAT. European Perinatal Health Report 2008. Available at:. http://www.europeristat.com. Accessed October 01, 2009.

5. Pritchard C, Williams R. Poverty and child (0-14 years) mortality in the USA and other Western countries as an indicator of "how well a country meets the needs of its children" (UNICEF). *Int J Adolesc Med Health.* 2011;23(3):251-255.

6. UNICEF. The State of the World's Children 2011. Adolescence An Age of Opportunity. 2011. Available at. 2011. http://www.unicef.org/sowc2011/pdfs/SOWC-2011-Main-Report_EN_02092011.pdf.

7. United Nations. Indirect Techniques for Demographic Estimation. Manual X. A collaboration of the Population Division of the Department of International Economic and Social Affairs of the United Nations Secretariat with the Committee on Population and Demography of the National Research Council, United States National Academy of Sciences. 1983. Available at. http://www.un.org/esa/population/publications/Manual_X/Manual_X.htm. Accessed March 21, 2013.

8. Wilmoth J, Zureick S, Canudas-Romo V, Inoue M, Sawyer C. A flexible two-dimensional mortality model for use in indirect estimation. *Popul Stud (Camb).* Mar 2012;66(1):1-28.

9. Hill AG, Aguirre A. Childhood Mortality Estimates using the Preceding Birth Technique: Some Applications and Extensions. *Population Studies.* 1990;44(2):317-340.

Proceedings, 15th Applied Stochastic Models and Data Analysis (ASMDA2013)
International Conference, Mataró (Barcelona), Spain 25 - 28 June 2013

Optimal quantization and transmission for ECG signals using genetic algorithms

Alvaro Pastor-Sanchez[1], Enrique Alexandre[1], Sancho Salcedo-Sanz[1], Daniel Gallo-Marazuela[1], and Lucas Cuadra[1]

Department of Signal Theory and Communications, University of Alcala. 28805 Alcala de Henares, Spain
(E-mail: enrique.alexandre@uah.es)

Abstract. In this paper we explore a method that, based on a particular implementation of a genetic algorithm (GA), aims to optimize the quantization of Electrocardiogram (ECG) signals to be transmitted over communication channels with low bit rate. In particular, the goal of the proposed GA is to compute the optimum number of quantization bits that minimizes the Percentage Root Mean-square-difference (PRD) between the quantized and original samples, constrained to the maximum number of available bits and the maximum distortion allowed. In this effort, we propose a novel GA-based ECG encoding approach to represent the candidate solutions or individuals, and those evolutionary algorithms that finally lead to the optimum solution. The experiments point out that, although in its preliminary steps, the method could be useful to quantize ECG signals to be transmitted over channels suffering from low bit rate.
Keywords: ECG signals, Quantization, Genetic Algorithm.

1 Introduction

Electrocardiogram (ECG) data compression is very often required because of the huge amount of information generated by this monitoring systems when applied to a patient over a long period of time. In order to store all these data, or to transmit them (for example, in telemedicine applications [1,2]), it is very important to achieve high compression ratios while maintaining an acceptable quality of the reconstructed signal in the sense that it does not interfere with the diagnostic process, or, in order words, in the effort of avoiding misdiagnosis, what is of the utmost importance.

Regarding this, there are several different approaches in the specialized literature focused on the compression of ECG data. There are important contributions, such as, for instance, [3], [4], [5] or [6], which are particular cases of either time-domain, parametric or transform-domain techniques. In [7], a different approach, consisting in the use of the JPEG2000 image compression standard to code ECG signals, has been studied.

In this paper we explore the feasibility of using Genetic Algorithms (GAs) to ECG data compression in the sense that our GA, constrained to a number of limitations (the number of available bits versus the quality of the synthesized signal), search for the optimum number of bits to quantize ECG samples.

GAs are optimization and search methods which, inspired by the principles of Genetics and Natural Selection [8], exhibit useful properties for solving

problems that, otherwise, would be intractable. Among these advantages, it is worth mentioning that GAs deal with large number of variables, provide a global solution for multilocal extrema problems, optimize functions with continuous or discrete variables, optimize variables with extremely complex cost surfaces, and do not require derivative information. In the effort of making this paper stand by itself, Section 2 focuses on summarizing the GA fundamentals that will assist us in better explaining our approach to quantize the ECG signals.

Although it will explain throughout the paper in a more detailed way, the system we propose divides the ECG signal into frames (or blocks), and computes the number of bits to properly quantize the bits of any frame. Just in this respect, Section 3 describes the proposed GA, which aims at computing the optimal number of bits to quantize the ECG that minimize the Percentage Root Mean-square-difference (PRD) of the quantized signal (when compared to the original one), constrained to the maximum number of available bits and the maximum distortion allowed.

Section 4 focuses on the experiments we have carried out in the effort of designing the GA, and discusses some preliminary results which seem to point out that the proposed GA-based approach, after some improvements, could be a feasible tool to optimally quantize ECG signals.

Finally, Section 5 summarizes our approach and the main conclusions we have found.

2 Genetic Algorithms in a nutshell

Genetic Algorithms [8] are one the most representative strategies belonging to the wide field of "Evolutionary Computation" (EC) approaches, which are inspired by the principles of Genetics and Natural Selection. In turns, EC belongs to the broader research area of "Soft-Computing" (SC). It is a key part of Artificial Intelligence (AI), and many of its methods also belong to the area of knowledge called "Natural Computing" (NC). The wider term Natural Computing refers to algorithms inspired by the way Nature solves extremely complex problems. It draws inspiration from Evolution (leading to Evolutionary Computation), Physics (Simulated Annealing), social living being networks (social insects, what leads to Ant Colony Optimization (ACO) algorithm [9], and Swarm Intelligence [10]), Neural Networks (human brain metaphor inspires Artificial Neural Networks [11,12]), Immune Systems (leading to Immunocomputing), the simulation of an orchestra composition (Harmony Search algorithm [13]), and so on.

Evolutionary Computation algorithms have been widely used for solving combinatorial optimization problems, which work primarily in intrinsically discrete search spaces. Put it very simple, these algorithms are based on an encoding of candidate solutions of the problem by using strings of numbers, and on evolving the population of candidate solutions by applying a series of evolutionary operators.

In particular, a GA is based on three key facts: 1) Encoding the candidate solution; 2) Generate an initial population of candidate solutions, and 3) Applying evolution mechanisms.

1. **Encoding candidate solutions**
   In Nature, all of the genetic information which encodes and causes the external characteristics of a living organism (or "individual") is called genotype. Any particular characteristic produced by a piece of this genetic information is encoded by a gene, the chromosome being the set of these genes. Each gene is located at a particular position on the chromosome and can have different values, called allele. Note that this strategy can be considered as transforming the real search space into another in which working is much easier. From a mathematical point of view, if F is the set containing all the candidate solutions, and G is the set of chromosomes that codifies them, this representation is equivalent of defining a bijection $\zeta : F \to G$, so that any solution is represented by an unique chromosome. Thus, roughly speaking, the terms chromosome and individual are interchangeable.
2. **Generating an initial population of candidate solutions**
   The size of the initial populations of individuals is a crucial issue for GA performance. On the one hand, a large population could cause more genetic diversity (and thus, a higher search space) and, consequently, suffer from slower convergence. On the other hand, with a very small population, only a reduced part of the search space is explored, thus increasing the risk of prematurely converging to a local extreme. Once the adequate size of the population has been explored, the second question remaining is related to the initial values its individuals should have. Usually, the values of the chromosomes representing this population are randomly initialized.
3. **Applying evolutionary mechanisms**
   In Nature, the random creation of novel genetic information may lead to the ability to survive. The better an individual is suited to an environment, the higher its probability of survival. This is the so-called *survival of the fittest* and the longer the individual's life is, the higher its chances of having descendants. In this procreation process, the parent chromosomes are combined (recombination) to provide a novel chromosome. Sporadically, and because of unavoidable errors in copying genetic information or external factors (for instance, radiation), mutations (random variations) occur. The consequence is the creation of a generation of living beings with some novel characteristic which are slightly different from those of their progenitors. If the new attribute makes the offspring better suited to the varying environment, the probabilities of survival and of having descendants also increase. Part of the offspring could inherit the modified genes and the corresponding external characteristic. In this way, the population of individuals evolves and for a number of generations the described process results in the creation of individuals better adapted to the environment, and in the extinction of those worst suited.

With these concepts in mind, we can now better understand the fundamentals of the standard genetic algorithm, proposed in [14]. This algorithm uses

operators of selection, crossover and mutation, binary encoding and selection by means of the roulette wheel method.

As motivated before, the genetic algorithm is based on a number of evolution operators, which will be detailed below, implemented in a loop process. The algorithm starts with the initialization of individuals, usually at random, and the calculation of "fitness" values associated with each individual (that is, to what extent each candidate solution solve the problem). It then enters a loop in which evolution operators are applied, until a certain stopping condition, usually, when, after a number of generations, no improvements are observed in the results. These operator work as follows:

- A selection operator aims at selecting those individuals (population components) that will be part of the population for the next generation. In the standard implementation of the algorithm, each individual has a probability of survival for the next generation proportional to its associated fitness value (objective function to optimize). This selection procedure is called the roulette method. Although the method of roulette is considered the standard algorithm, there are other well known selection methods such as the method of probabilistic tournament (widely used by its good results), the ranking selection, and so on.
- A crossover operator, whose goal consists in generating novel individuals from existing pairs of individuals. In the standard implementation, individuals are paired at random, and crossed (by exchanging parts of the binary string) with a probability called crossover probability that is usually around 60% (that is, 60% of pairs of individuals are crossed in each generation). Each pair then leads to another pair of individual offsprings, replacing parents in the next generation. There are different types of crossover methods depending on whether the parents are crossed exchanging parts in one, two or more points in the binary string.
- Mutation operator. It aims to mimic the following fact in Nature: the chromosomes (which contain genes that encode the physical characteristics of an individual −genotype−) can undergo random changes called mutations. They may be due to external causes (eg. radiation) or internal (a simple failure to copy the material). These mutations can generate individuals with novel external physical characteristics (phenotype) that may allow them (or not) adapt to the changing environment. If advantageous, the feature can be spread with a certain probability to later generations. In a Genetic Algorithm, the mutation operator generates a new individual from an existing one. This process is performed by changing certain bits chosen from 0 to 1 and vice-versa, with very low probability (usually the mutation probability for a given individual is about 1%). It differs from the previous one in that the bits change occurs within the same individual and not with another of its generation.

For non-binary implementations of algorithms, the operators of crossover and selection can be maintained as we have defined for the standard algorithm, and only the mutation operator would change, which should suit the implemented encoding selected for the specific problem.

All these concepts will assist us in explaining our approach to the problem at hand. This is just the goal of the next section.

3 The proposed GA-based quantization algorithm

Put it very simple, the ECG data stream to be quantized is divided into blocks or frames, each block containing a number of N samples. In this problem, the number of samples per block, N, and the maximum number of bits for coding the ECG signal, n_{max}, are two input parameters. For instance, the value used for n_{max} could be limited by the uplink data bit rate of the communication system in a telemedicine application.

The goal of the proposed GA-based algorithm is to find, constrained to the aforementioned limitations, the number of bits to represent the samples of each N-length block, n_i, by minimizing the overall Percentage Root Mean-square-difference (PRD) between the quantized signal and the original one. The ECG signals belong to the public MIT ECG database. This database has been divided into a training subset and a test subset to properly design the GA and test to what extent the algorithm works accurately.

The following paragraphs emphasize the key points in the design of our GA-based approach.

3.1 Encoding the candidate solution

A proper way to encode the candidate solutions or individuals is like the one illustrated by the following example. Let imagine we have only 5 blocks. The chromosome of a candidate solution could be, for example, 2 3 0 1 4, which means that each sample of the first block will be coded with 2 bits, any sample of the second block will be coded with 3 bits, and so on. To what extent this potential solution is good enough will be evaluated by the selection operator, as will be shown later on.

Once we have decided the more appropriate way of representing the candidate solution, the second key point is the design of the initial population of individuals to be evolved.

3.2 Generating the initial population of candidate solutions

The size of the initial population has been chosen to be 300 individuals, a good balance between a larger population (which could lead to slow convergence) and a smaller population (which could lead to converge to a local extreme).

The population for the problem at hand has been initialized by dividing the number of available bits, n_{max}, by all the blocks of the input signal. This division has been made randomly, ensuring that the total number of bits is equal or less than the maximum n_{max}.

Once the initial population has been initialized, the algorithm starts with the calculation of fitness values associated with each individual, and enters a loop in which evolution operators are applied until it reaches 600 generations, a stopping condition that, as will be shown in the results, keeps the PRD stable.

3.3 Applying evolutionary mechanisms

The crossover operator used is a one-point crossover operator. It randomly chooses a point on the two parent chromosomes and, by interchanging those genes before and after the point, creates the offsprings. The probability that the crossover operator is applied to each individual is called crossover probability, $p_c < 1$. In this respect, it is important to note that not all individuals are selected for crossover. After a number of experiments we have chosen $p_c = 0.9$.

The Gaussian mutation operator implemented works as follows: it selects a gene with a mutation probability p_m, adds an unit Gaussian noise (with zero mean and a standard deviation of σ chosen 0.1 times the length of the dynamic range [8,15]), and rounds it to the nearest integer. Its purpose is to maintain diversity within the population and inhibit premature convergence to local minima. Note that not all the offspring chromosomes are mutated: the probability that the mutation operator is applied to each chromosome is usually $p_m \ll 1$. Empirically, it has been observed that a value of $p_m = 0.02$ reaches good results.

Since both crossover and mutation may lead to a total number of bits higher than the maximum allowed, it is necessary to include a correction operator. This operator looks for, among all individuals, those whose number of bits is above the limit. In these cases, the number of bits is randomly reduced in steps of 1 bit until the problem is fixed.

Finally, regarding the selection, a ranking selection operator has been selected since it has been found it reaches good results.

4 Preliminary results

In this section, we present some preliminary results in the effort of checking the utility of the proposed algorithm.

Figure 1 shows the evolution of the fitness value in terms of PRD as a function of the number of generations. We have represented two PRD curves: the one corresponding to the best fitness, and another for the case in which an average of 3 bits is fixed for the genetic algorithm. As it can be observed, the convergence is fast, obtaining the best result in only around 100 generations.

While Figure 1 has shown the fast convergence of the proposed algorithm, Figure 2 represents the fitness value in terms of PRD as a function of the average number of bits per sample. As it can be observed, a fast decrease of the number of bits needed to quantify the signal is obtained when increasing the number of bits.

5 Conclusions

In this work we have explored the feasibility of using a particular implementation of genetic algorithms to optimize the quantization of electrocardiogram signals by minimizing the Percentage Root Mean-square-difference between the quantized and the original signal, constrained to the maximum number of available bits and the maximum distortion allowed. After explaning the concepts

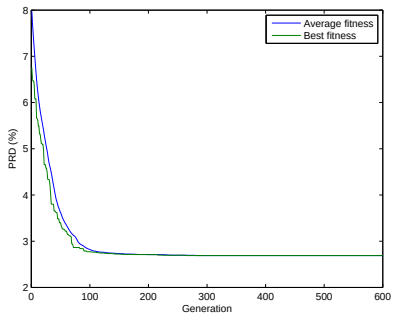

Fig. 1. Percentage Root Mean-square-difference (PRD) values (%) of the quantized signal obtained as a function of the number of generations. The blue line corresponds to the PRD results when an average of 3 bits is fixed for the genetic algorithm, while the red line corresponds to the best fitness.

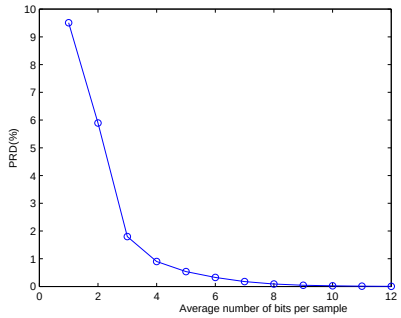

Fig. 2. Percentage Root Mean-square-difference (PRD) values (%) of the quantized signal obtained as a function of the mean number of bits per sample.

the approach is based on, we have proposed: 1) a novel encoding approach to represent the candidate chromosomes (a string of integer that labels the number of bits for each sample in a frame); and 2) some implementations of evolutionary algorithms (selection, crossover, mutation, and correction −which keeps the values of genes within the allowed dynamic margin−).

The work presented is a preliminary approach to the problem, but it is enough to show that the application of evolutionary algorithms to dynamic bit allocation problems is a promising research topic. The algorithm has proved to converge in a low number of generations, which can be reduced even more if information from one block is used to initialize the next one.

Next works will continue exploring this idea, introducing also the block length as a variable for the genetic algorithm, in the effort of improving the results.

Acknowledgements

This work has been partially supported by Spanish Ministry of Economy, under project number ECO2010-22065-C03-02.

References

1.R.S.H. Istepanian and A.A. Petrosian, Optimal zonal wavelet-based ECG data compression for a mobile telecardiology system, *IEEE Transactions on information technology in biomedicine*, 4(3) pp. 200-211, 2000.
2.A.I. Hernandez, F. Mora, M. Villegas, G. Passariello and G. Carrault, Real-time ECG transmission via Internet for nonclinical applications, *IEEE Transactions on information technology in biomedicine*, 5(3) pp. 253-257, 2001.
3.R.J. Coggins and M.A. Jabri, A low-complexity intracardiac electrogram compression algorithm, *IEEE Transactions on Biomedical Engineering*, 46(1), 1999.
4.G. Antoniol and Tonella, EEG data compression techniques, *IEEE Transactions on Biomedical Engineering*, 44(2), 1997.
5.G. Nave and A. Cohen, ECG compression using long-term prediction, *IEEE Transactions on Biomedical Engineering*, 40(9), 1993.
6.R.S.H. Istepanian, L.J. Hadjileontiadis and S.M. Panas, ECG data compression using wavelets and higher order statistics methods, *IEEE Transactions on information technology in biomedicine*, 5(2) pp. 108-115, 2001.
7.Ali Bilgin, Michael W. Marcellin and Maria I. Altbach, Compression of electrocardiogram signals using JPEG2000, *IEEE Transactions on Consumer Electronics*, 49(4) pp. 833-840, 2003.
8.A. E. Eiben and J. E. Smith, Introduction to evolutionary computing, Springer-Verlag, 2003.
9.M. Dorigo and T. Stützle, Ant Colony Optimization: Overview and Recent Advances. M. Gendreau and Y. Potvin, editors, Handbook of Metaheuristics, 2nd edition. Vol. 146 in International Series in Operations Research and Management Science, pp. 227-263. Springer, Verlag, New York, 2010.
10.R. Eberhart and Y. Shi, Particle swarm optimization: developments, applications and resources, In *Proc. IEEE Congress on Evolutionary Computation*, 2001.
11.C.M. Bishop, *Pattern Recognition and Machine Learning*, Springer 2007
12.R O. Duda, P. E. Hart , and D G. Stork, *Pattern Classification*, Wiley and Sons, 2000.
13.Z. W. Geem, J. Hoon Kim and G. V. Loganathan, A New Heuristic Optimization Algorithm: Harmony Search, *Simulation*, 76(2) (2001) 60-68.
14.D. E. Goldberg, *Genetic algorithms in search, optimization and machine learning*, Reading, MA: Addison-Wesley, 1989.
15.P.S. Andrews, An Investigation into Mutation Operators for Particle Swarm Optimization, In *Proc. 2006 IEEE Congress on Evolutionary Computation*, 2006.

Proceedings, 15th Applied Stochastic Models and Data Analysis (ASMDA2013)
International Conference, Mataró (Barcelona), Spain 25 - 28 June 2013

Multistage Non-Homogeneous Markov Chain Modeling of the Non-Homogeneous Genetic Algorithm and Convergence Results.

André G. C. Pereira[1] and Viviane S. M. Campos[2]

[1] Mathematics Department, Universidade Federal do Rio Grande do Norte, Natal/RN, Brazil
(E-mail: andre@ccet.ufrn.br)
[2] Mathematics Department, Universidade Federal do Rio Grande do Norte, Natal/RN, Brazil
(E-mail: viviane@ccet.ufrn.br)

Abstract. In this work, the results presented in the paper titled *Multistage Markov Chain Modeling of the Genetic Algorithm and Convergence Results* are extended. The size of the neighborhood in the crossover stage of the Algorithm 1, is permitted to vary throughout the evolution of the algorithm and instead of a fixed mutation probability, in mutation stage of the Algorithm 2, a sequence of mutation probabilities is introduced . Finally, numerical simulations are developed and comparisons between the original algorithms and the new versions of them are presented.

Keywords: Simulated annealing, Global optimization, Genetic Algorithms..

1 Introduction

The Canonical Genetic Algorithm (CGA), introduced in Holland[6], is a computational tool that describes the natural genetic evolutionary process of a population that undergoes three stages: selection, crossover (mating) and mutation. In the CGA, a population of N individuals or chromossomes, $(u_1, u_2, ..., u_N)$, is considered. An evaluation function $f : E \to (0, \infty)$ assigns to each individual u_i a fitness value $0 < f(u_i) < \infty$. In the selection stage, the actual population will be resampled, individuals with higher fitness are more likely to be selected and those with low fitness tends to be eliminated (elitist selection). Following the natural evolutionary process, biological reproduction (crossover) and eventual mutation occur. In the crossover stage, individuals are independently chosen for crossover with a prescribed probability p_c. Mutation also operates independently on each individual with a prescribed probability p_m. In order to be easier for implementation, each individual is represented by a binary vector of lenght l, where l depends on the desired precision. For more details as well as implementation procedures see, for example, Campos *et al.*[2], de Andrade *et al.*[3], Goldberg[5] .

In optimization context, CGAs are used to solve problems of the type $\max\{f(x), x \in E\}$ with the objective function satisfying $0 < f(x) < \infty$. The individuals represent the feasible solutions and the selection stage preserves with higher probability the best fitted/searched points. In the crossover stage,

neighboring points are searched, allowing a refined comparison in the surrounding. In the mutation stage, random points, possibly away from the preserved ones, are visited and constitute a strategy to avoid being trapped in local optimum points.

In Dorea *et al.*[4], the convergence of the genetic algorithm was proved under certain hypothesis. In particular, the Algorithm 2, which has a superindividual, was proved to converges almost surely to a set of all populations that have an optimum point as one of its elements. All algorithms presented in Dorea *et al.*[4] were modeled by an homogeneous Markov chain because theirs transition probabilities did not change through time.

The non-homogeneous Genetic Algorithms (NHGA) was introduced in Campos *et al.*[1] as an attempt of improving the eficiency of CGA, by allowing the mutation and crossover probabilities to vary under certain hypothesis. The elitist genetic algorithm (EGA), which was introduced in Rudolph[8], it was a modification in the CGA that solved the problem of eficiency of the CGAs. A non-homogeneous version of the EGA, called elitist non-homogeneous genetic algorithm (ENHGA), was introduced in Rojas Cruz and Pereira[7] in order to improve the eficiency of the EGA. Other attemptings to improve the eficiency of the CGA, without changing the mutation and crossover probabilities can be seen in Dorea *et al.*[4], some numerical comparisons between ENHGA and EGA, can be seen in Campos *et al.*[2], and the proper way of running the ENHGA can be seen in de Andrade *et al.*[3].

In this paper two different versions of each of the algorithms presented in Dorea *et al.*[4] are proposed. All algorithms presented in this paper have a superindividual as explained in Dorea *et al.*[4]. Theorical convergence results of these algorithms and numerical comparisons among these algorithms are also presented.

This paper is divided into 4 sections. In section 2, the algorithms presented in Dorea *et al.*[4], the results that guarantee their convergences as well as some other results that will be used in the rest of the paper are presented. In section 3, the changes in the algorithms presented in section 2 are introduced and convergence results are obtained. In section 4, numerical comparisons between the original algorithm and its versions are made.

2 Preliminaries

Summarizing what was said in the previous section, let $f : E \to (0, \infty)$ be a function, and genetic algorithms were set in order to find the following point

$$x^* = argmax_x\{f(x), x \in E\},$$

where E is a discretization of the domain of the function f. To proceed the following steps of the the algorithm, such points are represented as binary vectors of length l, where l depends on the desired precision. A population of size N is considered, let $Z = \{(u_1, u_2, ..., u_N); u_i \in E, i = 1, 2, ..., N\}$ be the set of all populations of size N. Z is the state space of the Markov chain that is used to prove the convergence of the algorithm, see Campos *et al.*[1], Dorea *et al.*[4],

Rojas Cruz and Pereira[7] and Rudolph[8].

In Dorea *et al.*[4], in both algorithms presented, the roulette scheme is used in the selection stage. In algorithm 1, it is proposed a different scheme for the crossover stage. In that approach, neighborhoods of the actual points of the population are used to select the next points of the population. The mutation stage is performed in a traditional way, that is, the population is considered as a binary vector and each entry can be changed independently with a fixed probability p_m . By their stages, those algorithms can be summarised in the following way:

- **Algorithm 1:** In the selection stage it is used the roulette scheme, in the crossover stage it is used neighborhoods scheme, and in the mutation scheme it is used the traditional method where each gene can be changed independently with a fix probability p_m.
- **Algorithm 2:** In the selection stage it is used the roulette scheme, there is no crossover stage, and in the mutation scheme it is used the traditional method.

The evolution of the ENHGA is different from the evolution of the EGA just by the update of the values of parameters p_m and p_c. Thus, the elitist algorithm can be summarized in the following sketch:

a)Choose randomly an initial population having N elements, each one being represented by a binary vector of length l, and create one more position, the $N+1$-th entry of the population vector, which will keep the best element from the N previous elements.

b)Repeat

1. perform selection with the first N elements
2. perform crossover with the first N elements
3. perform mutation with the first N elements
4. If the best element from this new population is better than that of the $N+1$-th position, change the $N+1$-th position by this better element, otherwise, keep the $N+1$-th position unchanged
5. perform p_c and p_m changes, as previously planned.

c) until some stopping criterion applies.

Denote this new state space by $\tilde{Z}$.

In Rojas Cruz and Pereira[7], it is shown that the ENHGA is a non-homogeneous Markov chain, with a finite state space $\tilde{Z}$, whose transition matrices are given by $P_n = SC_nM_n, \forall n \in I\!N$, where S, C_n, M_n are transition matrices which represent the selection, crossover and mutation stages respectively. Here the M_n is composed by the third and fourth steps described in sketch just presented. In the same paper it is shown that there is a sequence $\{\alpha_n\}_{n\in I\!N}$ such that

$$\inf_{i\in\tilde{Z}, j\in\tilde{Z}^*} P_n(i,j) \geq \alpha_n,$$

where $\tilde{Z}^* \subset \tilde{Z}$, which contains all populations that have the optimum point as one of its points. The following results were obtained.

Corollary 1: Let $\{X_n\}_{n\in\mathbb{N}}$ be the Markov chain which models the elitist non-homogeneous genetic algorithm, if the sequence above is such that $\sum_{k\geq 1}\alpha_k = \infty$ then

$$P(\lim_{n\to\infty} X_n \in \tilde{Z}^*) = 1. \quad (1)$$

A more simple condition, to run in simulations, that guarantee the above result is

Corollary 2: Let $\{X_n\}_{n\in\mathbb{N}}$ be the Markov chain which models the elitist non-homogeneous genetic algorithm, if the mutation probabilities $\{p_m(n)\}_{n\in\mathbb{N}}$ are such that $p_m(n) > \gamma > 0$ for all $n \in \mathbb{N}$ or $\sum_n p_m(n)^l = \infty$ then (1) holds.

3 The New Versions of the Algorithms 1 and 2

In this section, two new versions for each algorithm 1 and 2 of Dorea *et al.*[4] as well as its almost sure convergence are presented. All algorithms presented in this paper have a superindividual as explained in Dorea *et al.*[4], or in other words, the algorithms are elitists as explained in Rojas and Pereira[7].

Consider these two versions of Algorithm 1 (with a superindividual) of Dorea *et al.*[4]

- **Algorithm 1-1:** In this algorithm we perform selection and mutation as in Algorithm 1, but in crossover stage the neighborhood size is allowed to vary in a predefined way or randomly.
- **Algorithm 1-2:** In this algorithm we perform selection as in Algorithm 1, crossover as in Algorithm 1-1 and in the mutation stage, the mutation probabilities are allowed to vary throughout time. The mutation probabilities $\{p_m^{(n)}\}_{n\in\mathbb{N}}$ are such that
  $p_m^{(n)} > \gamma > 0$ for all $n \in \mathbb{N}$ or $\sum_n p_m(n)^l = \infty$.

Note that, while the algorithms 1 and 2, in their superindividual versions are EGAs, Algorithms 1-1 and 1-2, are ENHGAs, see Rojas and Pereira[7]. Thus, we have, as a consequence of corollary 2, that

Corollary 3: In a ENHGA such that its selection stage is defined as in Algorithm 1, the size of the neighborhoods are allowed to vary throughout the evolution of the algorithm and the mutation probabilities $\{p_m(n)\}_{n\in\mathbb{N}}$ are such that $p_m(n) > \gamma > 0$ for all $n \in \mathbb{N}$ or $\sum_n p_m(n)^l = \infty$ then (1) holds.

This show that algorithm 1-1 and 1-2 converge almost surely to a subset of all populations that have as one of its points, the optimum point.

Consider these two versions of Algorithm 2 of Dorea *et al.*[4]

- **Algorithm 2-1:** In this algorithm we perform selection and crossover as in Algorithm 2, but in mutation stage, the mutation probabilities $\{p_m^{(n)}\}_{n\in\mathbb{N}}$ are such that
  $p_m^{(n)} > \gamma > 0$ for all $n \in \mathbb{N}$ or $\sum_n p_m(n)^l = \infty$.

- **Algorithm 2-2:** In this algorithm the selection is performed as in Algorithm 2, crossover as in Algorithm 1-1 and in the mutation stage, a simulated annealing (SA) algorithm without a cooling schedule is performed as in example 2 of Dorea *et al.*[4]. Note that, in Dorea *et al.*[4] it is used a matrix $Q = (Q_{xy})_{x,y \in E}$ to generate the next points, and this matrix does not change through time.

Obs: The acceptance probability used in the SA is of the form (in case of maximization)

$$a_n(X_i, Y_i) = \begin{cases} 1, & \text{if } f(Y_i) \geq f(X_i) \\ e^{-\frac{f(X_i)-f(Y_i)}{T_n}}, & \text{if } f(Y_i) < f(X_i) \end{cases} i = 1, 2, ..., N$$

where $\{T_n\}_{n \in I\!N}$ is the cooling schedule. Here $a_n(x, y) = a(x, y), \forall n \in I\!N$, because the algorithm 2-2 does not have a cooling schedule, that is, $T_n = c, \forall n \in I\!N$.

When applying the SA in each entry of the population vector, in the mutation stage, $M_n(X, Y)$ is obtained as a product of terms of the form $A_i(X, Y) = Q_{X_i Y_i} a_n(X_i, Y_i)$ when $X_i \neq Y_i$ and $B_j(X, Y) = 1 - \sum_{i \neq j} Q_{X_i Y_i} a_n(X_i, Y_i)$ when $X_j = Y_j$, where X_i and Y_i are the i-th coordinate of X, the actual population vector, and the population which was generated, Y, respectively, that is, they are the i-th individuo in the actual and generated population respectively.

Theorem 1: In an ENHGA such that its selection and crossover are performed as in algorithm 1-1 and a SA is used in the mutation stage. If the SA is such that

$$Q(x, y), a(x, y) > 0, \forall x, y \in E$$

then (1) holds.

Proof: It was shown in Campos *et al.*[1] that $P_n = SC_nM_n$, where S is a stochastic matrix that describes the selection stage,C_n is a stochastic matrix that describes the crossover stage at time n and $M_n = M$ is a stochastic matrix that describes the mutation stage at time n (in that paper the selection matrix did not change as time goes by). The SA used in mutation stage is such that

$$\inf_{A \in \tilde{Z}, B \in \tilde{Z}^*} M(A, B) \geq \gamma > 0,$$

for some $\gamma \in I\!R$. That happens because Q can generate any point of the space with a positive probability, $a_n(x, y) = a(x, y) > 0, \forall x, y \in E$ and $B \in \tilde{Z}^*$ (that is essential). Observe that such constant does not exist in the case where $A \in \tilde{Z}^*$ and $B \notin \tilde{Z}^*$. Thus, for $X, Y \in \tilde{Z}$ we can write

$$P_n(X, Y) = \sum_{A,B \in \tilde{Z}} S_n(X, A) C_n(A, B) M(B, Y)$$

If $Y \in \tilde{Z}^*$,

$$P_n(X, Y) \geq \gamma \sum_{A,B \in \tilde{Z}} S_n(X, A) C_n(A, B) = \gamma > 0$$

So,

$$\inf_{X\in\tilde{Z},Y\in\tilde{Z}^*} P_n(X,Y) \geq \gamma = \delta_n > 0.$$

Hence,

$$\sum_{n=1}^{\infty} \delta_n = \infty$$

and by corollary 1, (1) holds.

4 Numerical comparisons

In this section we present numerical comparisons among algorithms 1, 1-1, 1-2 and among algorithms 2, 2-1,2-2. For these comparisons, the following two-variable functions are used:

- 1. $f : [-2,1] \times [-2,1] \to I\!R$ defined by $f(x,y) = 6 + x^2 - 3cos(2\pi x) + y^2 - 3cos(2\pi y)$.
- 2. $f : [-\frac{1280}{63}, \frac{1240}{63}] \times [-\frac{1280}{63}, \frac{1240}{63}] \to I\!R$ defined by $f(x,y) = .5 - \frac{sin^2(\sqrt{x^2+y^2})-0.5}{(1+.001*(x^2+y^2))^2}$.

These functions were chosen for having many local minimum and maximum points, which turns the convergence of optimization algorithms hard.

In the following simulations, each algorithm was run 100 times and in each repetition 1000 steps of the algorithm were performed. The graphics illustrate the results of such simulations. If (x,y) is a point of the graphic, y represents the number of repetitions in which the optimum point was found in x steps. Each interval that compounds the domain was partitioned into 2^6 points. Thus, a net of 2^{12} feasible solutions was created. Each algorithm was simulated for two different population size, namely: 5 and 15 points.

It was used $p_m = 0.01$ for those algorithms that used a fixed mutation probability. For those algorithms that uses a varying mutation probability, it was used a linear function to do this changes in the value of p_m. It begins with $p_m = 0.5$ and dimishes linearly to its final value $p_m = 0.001$ after 1000 steps.

It was used a neighborhood of size one for those algorithms which has a fixed neighborhood scheme.For those algorithms that use a varying neighborhood scheme, a linear funtion was used to change the size of the neighborhood in each step. The size of the neighborhood begins begger than half of the number of genes of the population and it diminishes linearly to its final value, which is the same of those algorithms that use a fixed neighborhood scheme.

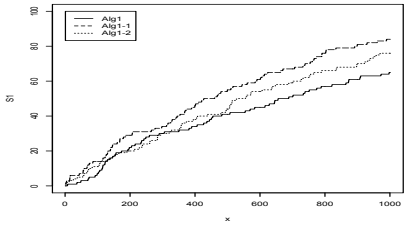

Fig. 1. Function 1, population size=5

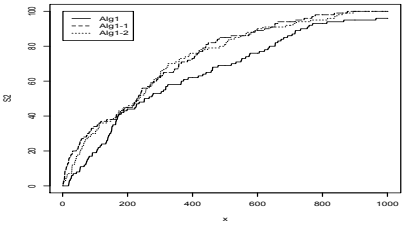

Fig. 2. Function 1, population size=15

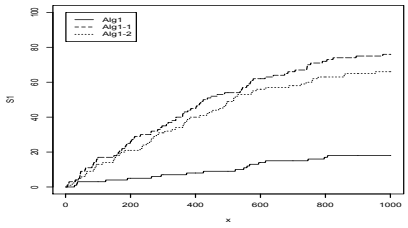

Fig. 3. Function 2, population size=5

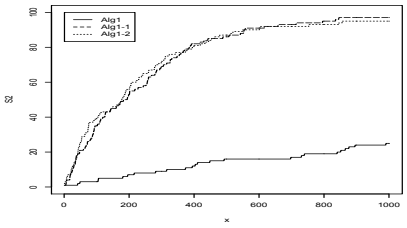

Fig. 4. Function 2, population size=15

To perform the simulations of the algorithm 2, the distribution used to generate the next point needs to be specified . In this paper a simmetric (in relation to the actual point) distribution is used. A distribution where the closer the point is from the actual point the higher is the probability of it to be chosen and its expression is given by

$$Q(x,y) = \frac{e^{-|x-y|}}{\sum_{z\in E} e^{-|x-z|}}$$

and in the acceptance probability the values of $T_n = c, \forall n \in I\!N$ that was used is $c = 10$.

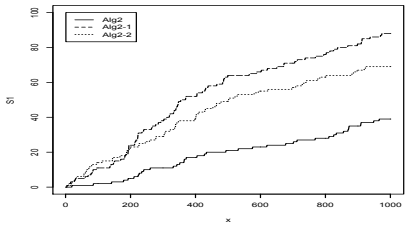

Fig. 5. Function 1, population size=5

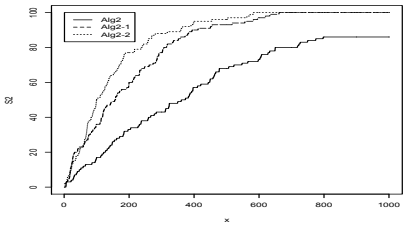

Fig. 6. Function 1, population size=15

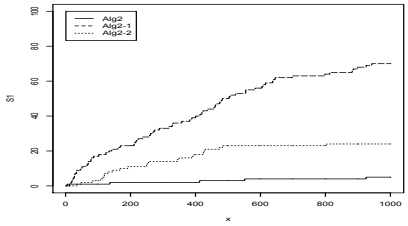

Fig. 7. Function 2, population size=5

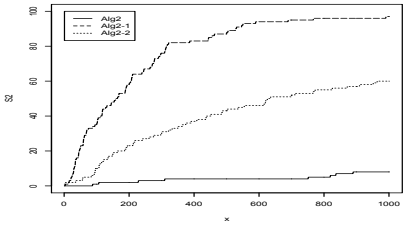

Fig. 8. Function 2, population size=15

Conclusions Changes in the algorithms 1 and 2 of [4] were proposed and sufficient conditions to guarantee its convergence almost surely to a population that has an optimum point in it were given. Examples in the previous section showed that it is possible to find a way of varying the parameters in order to obtain an improvement on the time that is spent by the algorithm for finding its optimal point. These simulations were done with the belief that higher probabilities should be used at the beginning so that the algorithm is able to search a solution in a larger region initially, and as time goes by, those probabilities should get smaller in order to do a more intense search near the population that evolves until that moment. That is just one manner to proceed, a problem that is still open is the following: How to vary the values of the parameters in order to obtain the best performance of the algorithms?

References

1.V.S.M. Campos, A.G.C. Pereira and J.A. Rojas Cruz. Modeling the Genetic Algorithm by a Non-Homogeneous Markov Chain: Weak and Strong Ergodicity. *Theory of Probability and its Applications*, v.57,Issue 1,185–192, 2012.

2.V.S.M. Campos, A.G.C. Pereira, L.A. Carlos and I.A.S. de Assis. Algoritmo Gentico por cadena de Markov homognea versus no-homognea : Un estudio comparativo. *Journal of the Chilean Institute of Operations Research*, vol 1, **1**, 2012.

3.B.B. de Andrade, A.G.C. Pereira and V.S.M. Campos. On the Convergence of Non-homogeneous Genetic Algorithms and Experimentation with Varying Mutation Rates, (submitted).

4.C.C.Yu Dorea, J.A. Guerra Jnior, R. Morgado, A.G.C. Pereira. Multistage Markov Chain Modeling of the Genetic Algorithm and Convergence Results. *Numerical Functional Analysis and Optimization*, v. 31, 164–171, 2010.

5.D.E. Goldberg. *Genetic Algorithms in Search, Optimizations and Machine Learning*, Assison Wesley, Teading, MA, 1989.

6.J.H. Holland.*Adaptation in natural and artificial systems*. Ann Arbor: The University of Michigan Press, 1975.

7.J.A. Rojas Cruz and A.G.C. Pereira. The Elitist Non-homogeneous Genetic Algorithm: Almost sure convergence. *Statistics and Probability Letters* (submitted).

8.G. Rudolph.Convergence Analysis of Canonical Genetic Algorithms. *IEEE Transactions on Neural Networks*, **5**,96–101, 1994.

Proceedings, 15th Applied Stochastic Models and Data Analysis (ASMDA2013)
International Conference, Mataró (Barcelona), Spain 25 - 28 June 2013

EXAMINING THE FACTORS OF SUCCESS OF THE FOOTBALL TEAMS IN 2011-2012 SUPER LEAGUE SEASON IN TURKEY VIA PLS PATH MODELING

Esra Polat[1], Semra Turkan[1], and Suleyman Gunay[1]

[1]Hacettepe University, Faculty of Science, Department of Statistics, 06800-Beytepe, Ankara, Turkey (E-mails: espolat@hacettepe.edu.tr, sturkan@hacettepe.edu.tr, sgunay@hacettepe.edu.tr)

Partial Least Squares (PLS) is a family of multivariate data analysis methods that allows for analyzing blocks of variables over a set of observations. The variety of PLS methods depends on the number of blocks of variables and the relationships among blocks. The common denominator of all PLS methods is the fact that they are based on an iterative algorithm in which the parameters are calculated by a series of least squares regressions. Due to the introduction of PLS, one of the main Structural Equation Modeling (SEM) techniques, by Wold in 1966, it has been received with considerable interesting among researchers. In most cases, the PLS approach to SEM is usually named as PLS Path Modeling (PLS-PM). PLS-PM is a multivariate data analysis methodology, which provides a framework for analyzing multiple relationships between a set of blocks of variables. It is supposed that the relationships among the blocks are established taking into account previous knowledge (theory) of the phenomenon under analysis. The purpose of this study is to examine the success of 18 Turkish national football teams in 2011-2012 Super League Season by using PLS-PM.

Key Words: Football Teams, Attack, Defense, Success, PLS, PLS-PM.

1. Introduction

Partial Least Squares (PLS) is a family of multivariate data analysis methods that allows for analyzing blocks of variables over a set of observations. The variety of PLS methods depends on the number of blocks of variables and the relationships among blocks. The common denominator of all PLS methods is the fact that they are based on an iterative algorithm in which the parameters are calculated by a series of Least Squares (LS) regressions. The term Partial is due to the fact that the iterative procedure involves separating the parameters instead of estimating them simultaneously (Sanchez [2]).

PLS Path Modeling (PLS-PM) is the PLS approach to Structural Equation Modeling (SEM). Although both terms are often used interchangeably, the term PLS-PM is preferred over SEM around the small but growing PLS community. PLS-PM is a multivariate data analysis methodology that provides a framework for analyzing multiple relationships between a set of blocks of variables. It is supposed that the relationships among the blocks are established taking into account previous knowledge (theory) of the phenomenon under analysis. Moreover, each block of variables is assumed to play the role of a theoretical concept represented by in the form of a latent (unobserved) variable (LV). (Sanchez [1]; Sanchez [2]).

The purpose of this study is to examine the success of 18 Turkish national football teams in 2011-2012 Super League Season by using PLS-PM. For this purpose, following the study of Sanchez (2013), a model is proposed in which the overall success of the football teams depends on the quality of the attack as well as on the quality of the defense made by them. There are three LVs which are defined as attack, defense and success. The number of won matches at home and the number of won matches away variables are taken as indicators of success, the number of goals scores at home and the number of goals scores away variables are taken as indicators of attack and the number of goals conceded at home and the number of goals conceded away are taken as indicators of defense.

2. PLS Path Modeling

Before we get involved into the details of the PLS-PM, we need to talk about a couple of things closely related to it: a) Latent Variables, b) PLS Path Model (Structural Model, Measurement Model, Weight Relations) c) Path Diagrams (Sanchez [1]; Sanchez [2]).

2.1. Latent Variables: Measuring the Immeasurable

One of the first concepts we must mention is that of LVs. The most common definition of a LV is a variable that is unobserved. More precisely, a LV is a variable that could not be measured directly. Examples of LVs abound in social sciences (e.g., psychology, sociology, economy, and politics) such as intelligence, motivation, satisfaction, socioeconomic status, economic development, social crisis, etc. (Sanchez [2]). In statistics, LVs are

widely used in several data analysis and modeling techniques with applications in many fields of knowledge. Within the literature related to LVs we can find synonymous terms like: theoretical concepts, hypothetical variables, constructs, composites, factors and intangibles (Sanchez [1]; Sanchez [2]).

In the context of PLS-PM, a LV will be obtained as a linear combination of a set of observed variables, which are also called as manifest variables (MVs), indicators or items. We assume that MVs contain information that reflect or indicate one aspect of the construct; hence we use the information contained in MVs to obtain an approximate representation of the LV. LVs can be measured in two ways: (1) through their consequences or effects reflected on their MVs and (2) through different MVs that are assumed to cause the LVs. In the first case, called reflective way, MVs are considered as being caused by the LVs. The second case is known as formative way because the MVs are forming the LVs The main difference between the reflective and formative ways has to do with the causal-effect relationships between the MVs and the LVs (Sanchez [1]; Sanchez [2]).

Let's assume that we have p variables measured on n observations (i.e. individuals, cases, samples), and that the variables can be divided in j blocks. X is the data set containing the n observations and p variables that means a matrix of dimension nxp. X can be divided in j (mutually exclusive) blocks X_1, X_2,…, X_j. Each block X_j has K variables: X_{j1}, X_{j2},…, X_{jK}. Each block X_j is assumed to be associated with a LV denoted as LVj. Keep in mind that LVj is just an abstract representation (i.e. unobserved). The estimation of a LV, also known as score, is denoted by $\hat{LV}_j = Y_j$ (Sanchez [1]).

2.2. PLS Path Model

In this section, the formalization of a PLS Path Model and its specifications are mentioned in detail.

2.2.1. Structural Model

Firstly, it could be talked about the specifications of the structural part in a PLS Path Model. A structural model, which is also called an inner model, relating some dependent LVs to other LVs (Tenenhaus *et al.* [3]).There are three things that is needed to consider about the inner relationships: Linear relationships, recursive models, regression specification.

Linear Relationships: The first aspect of an inner model is that the structural relationships are treated as linear relationships. The structural relations are expressed in mathematical notation as in Eq. (1). The subscript i of LV_i refers to all the LVs that are supposed to predict LV_j. The coeffcients β_{ji} are the path coeffients and they represent the "strength and direction" of the relations between the response LV_j and the predictors LV_i. β_0 is just the intercept term, and the $error_j$ term accounts for the residuals (Sanchez [1]).

$$LV_j = \beta_0 + \sum_{i \to j} \beta_{ji} LV_i + error_j \quad (1)$$

Recursive Models: The second aspect, which is needed to be aware of, is that the system of equations must be a recursive system. This means that the paths formed by the arrows of the inner model could not form a loop (Sanchez [1]).

Regression Specification: The third aspect about the inner relationships is something called predictor specification which is just a fancy term to express a linear regression idea. The idea behind this specification is that the linear relationships are conceived from a standard regression perspective as shown in Eq. (2) (Sanchez [1]).

$$E(LV_j | LV_i) = \beta_{0i} + \sum_{i \to j} \beta_{ji} LV_i \quad (2)$$

2.2.2. The Measurement Model

The measurement or outer model is the part of a model that has to do with the relationships between a LV and its block of MVs. The relevant aspect about the outer model is that there are two main measurement options: reflective blocks and formative blocks (Sanchez [1]; Tenenhaus *et al.* [3]).

Reflective Way: The most common type of measurement is the reflective mode. In this case, the LV is considered as the cause of the MVs. That's why it's called reflective because the MVs are "reflecting" the LV. Just like in the inner model, the outer model relationships are also considered to be linear. The outer model for reflective way is expressed in mathematical notation as in Eq. (3). The coefficients λ_{jk} are called loadings, λ_0 is the intercept term, and the error terms account for the residuals (Sanchez [1]; Tenenhaus *et al.* [3]).

$$X_{jk} = \lambda_{0jk} + \lambda_{jk} LV_j + \text{error}_{jk} \tag{3}$$

Formative Way: The other type of measurement is the formative mode. In this case, the MVs are considered to be the cause of the LV. That's why it's called formative because the MVs are "forming" the LV. The outer model for formative way is expressed in mathematical notation as in Eq. (4) (Sanchez [1]; Tenenhaus *et al.* [3]).).

$$LV_j = \lambda_{0j} + \lambda_{jk} X_{jk} + \text{error}_j \tag{4}$$

2.2.3. The Weight Relations

There's one last thing belonging to the specifications of a PLS Path Model that it is needed to mention: the weight relations. The weight relations is used to bridge the gap between the virtual LVs and the material LVs. In PLS-PM, LVs are estimated as a linear combination of their MVs. Furthermore, an estimated LV_j is called a score, denoted as Y_j as in Eq. (5). Since LVs are calculated as a weighted sum of their MVs analogously to what is done in principal component analysis, PLS-PM is referred to as a component-based approach (Sanchez [1]).

$$\hat{LV}_j = Y_j = \sum_k w_{jk} X_{jk} \tag{5}$$

2.3. Drawing Models: Arrow (Path) Diagrams

The term path modeling is a very generic term used to designate a set of different statistical techniques that seek to explain the relationships among multiple variables. The reason for the term path modeling is due to the graphical representation of structural relationships by drawing a picture of the model. Pictures of path models are called path diagrams, which are drawn according to well established conventions of terminology and symbols: Variables can be of any kind, i.e. MVs, LVs or residual variables (error terms). MVs are enclosed in boxes, LVs are enclosed in circles/ellipses and error terms are maintained unclosed. Relationships also can be of three types: causal links meaning that variable A causes variable B; correlation links indicating simply correlation between two variables A and B without implying causality; or the affection of a error term ε to some variable A. Causal relationships are assumed to be linear, and are represented by straight single-headed arrows, correlations are represented by curved two-headed arrows, and residual affection by straight lines. In addition, variables may be grouped in two classes: those that are not caused by any other variables in the diagram, and those that are caused by one or more variables. The first class of variables is called exogenous or independent variables. The second class is known as endogenous or dependent variables. The convention is to use Greek letters for the LVs, and Italic letters for the MVs. Exogenous LVs are usually represented by the Greek letter $\xi(x_i)$, while endogenous LVs are represented by $\eta(\text{eta})$. Path diagrams are very helpful because they allow for the visualization of the relations and, in terms of a causal model, its graphical display makes it possible to understand the conceptualization of the model. The visual notations of these variables and relationships in path diagrams are shown in Fig. 1 (Sanchez [2]).

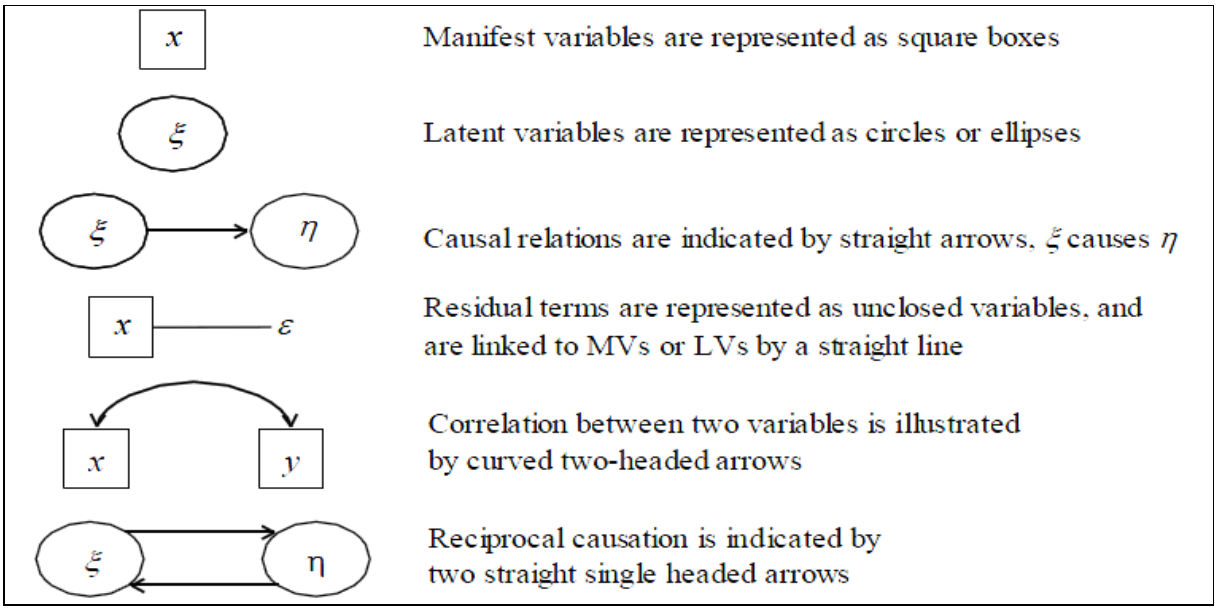

Fig. 1. Path diagram notations (Sanchez, 2009)

PLS Path Modeling follows a sequential procedure that can be divided in three major stages; Stage 1: Get the weights to compute LV scores; Stage 2: Estimating the path coefficients (inner model); Stage 3: Obtaining the loadings (outer model).

3. Application

The simple theory for examining the success of 18 Turkish national football teams in 2011-2012 Super League Season by using PLS-PM involves two hypotheses. In one of them, it is supposed that if a team improves its attack, it should be more successful, therefore, wins more matches. The other hypothesis is that if a team improves its defense, it should also be more successful or at least it should avoid losing matches. This theory could also be expressed in a more abstract form like this: $\text{Success} = f(\text{Attack}, \text{Defense})$. This is simply a conceptual way to say that Success is a function of Attack and Defense. But we could go further by specifying a linear function and expressing this theory with an equation like this one: $\text{Success} = b_1 \text{Attack} + b_2 \text{Defense}$.

3.1. Measuring Success, Attack and Defense

We have used the model proposed by Sanchez (2013) in which the Overall Success depends on the Quality of the Attack as well as on the Quality of the Defense. These are our three LVs. Now we need to establish a set of indicators for each of the three LVs. Following his study, we are going to take **GSH** and **GSA** variables as indicators of Attack; **GCH** and **GCA** variables as indicators of Defense; **WMH** and **WMA** variables as indicators of Success. These variables are defined as below:

- **GSH:** Number of goals scores at home
- **GSA:** Number of goals scores away

- **GCH:** Number of goals conceded at home
- **GCA:** Number of goals conceded away

- **WMH:** Number of won matches at home
- **WMA:** Number of won matches away

The data including these six variables, of 18 Turkish national football teams in 2011-2012 Super League Season, is given in Table 1.

Football Teams	GSH	GSA	GCH	GCA	WMH	WMA
Galatasaray	38	31	14	10	13	10
Fenerbahçe	39	22	12	22	14	6
Trabzonspor	36	24	22	17	10	5
Beşiktaş	29	21	18	21	10	5
Eskişehirspor	18	24	16	25	8	6
Büyükşehir bld	31	7	15	34	9	5
Sivaspor	25	32	20	34	7	6
Bursaspor	20	24	12	23	8	5
Gençlerbirliği	32	17	16	32	9	4
Gaziantepspor	24	15	13	20	9	4
Kayseri	28	14	19	20	8	5
Kardemir	30	14	21	35	11	2
Mersin	15	19	24	21	5	7
Ordu	17	11	13	21	7	3
Antalya	19	13	18	24	7	3
Samsun	24	12	24	23	6	3
Manisa	16	15	27	25	5	3
Ankaragücü	7	15	36	41	1	1

Table 1. The data for 18 Turkish national football teams in 2011-2012 Super League Season
(Data source: http://www.iddaliyim.org/gecmis/turkiye_superlig_gecmis/2011-2012_sup_lig_sonuc.php)

Firstly, it must be mentioned that to assess the quality of a reflective block it is need to understand the key ideas behind a reflective measurement model: it is supposed that reflective indicators are measuring the same underlying LV, hence they are reflections of the construct. On one hand, reflective indicators need to have strong mutual association. Shortly, they will be highly correlated. On the other hand, reflective indicators need to get along with its LV; they must show sings of membership and belonging to one and only one LV: they need to be loyal to its construct. If one indicator loads higher on another construct, this could be evidence of treason. **Basically, three aspects of reflective measures must be evaluated:**

1. **Unidimensionality of the indicators:** In PLS-PM there are three main indices to check unidimensionality:
a) Calculate the Cronbach's alpha**, b)** Calculate the Dillon-Goldstein's rho **c)** Check the first eigenvalue of the indicators' correlation matrix. The R output of the three indices of unidimensionality is given in Table 2. In Table 2, the first column shows the type of measurement. In our example, all the blocks are reflective. The second column indicates the number of MVs in each block (2 in our example). The third column contains the Cronbach's alpha, the fourth column is the Dillon-Goldstein's rho, the fifth and sixth columns are the first and second eignevalues, respectively. Dillon-Goldstein's rho is considered to be a better indicator than the Cronbach's alpha because it takes into account to which extent the LV explains the block of indicators. Hence, here we used this index to assess the unidimensionality. As a rule of thumb, a block is considered as unidimensional when Dillon-Goldstein's rho is larger than 0.7. As seen from Table 2, the values of Dillon-Goldstein's rho's for attack, defense and success blocks are larger than 0.7. So, these blocks are considered as unidimensional.

	Type.measure	MVs	C.alpha	DG.rho	eig.1st	eig.2nd
Attack	Reflective	2	0.4483647	0.7838111	1.288963	0.7110373
Defense	Reflective	2	0.6227777	0.8413180	1.452198	0.5478016
Success	Reflective	2	0.6940999	0.8673403	1.531511	0.4684893

Table 2. The unidimensionality metrics for each block of indicators

2. Check that indicators are well explained by its LV: Communalities represent the amount of variability explained by a LV. The loadings are correlations between a LV and its indicators. In turn, communalities are squared correlations. The R output of communalities are given in Table 3. Each element in the list is a table (a matrix) with four columns. The first column contains the outer weights. The second column are the loadings (correlations). Loadings greater than 0.7 are acceptable. In Table 3, all loadings are greater than 0.7.

Communalities are just squared loadings. They represent the amount of variablity explained by a LV. A loading grater than 0.7 means that more than $0.7^2 \approx 50\%$ of the variablity in an indicator is captured by its latent construct. As seen from third column in Table 3, the communalities of **GSA** and **GCA** are not greater than 0.7. It means that more than $0.7^2 \approx 50\%$ of the variablity in an indicator is not captured by its latent construct. But these variables are keeped in the model since loading values of these variables are greater than 0.7.

```
> data1_pls$outer.mod
$Attack
    weights std.loads communal redundan
GSH  0.7275    0.8741   0.7641        0
GSA  0.5073    0.7176   0.5149        0

$Defense
    weights std.loads communal redundan
GCH  0.6315    0.8760   0.7674        0
GCA  0.5408    0.8263   0.6828        0

$Success
    weights std.loads communal redundan
WMH  0.6122    0.8937   0.7987   0.7190
WMA  0.5296    0.8550   0.7311   0.6582
```

Table 3. The loadings and communalities

3. Assess the degree to which a given construct is different from other constructs: Besides checking the loadings of the indicators with their own LVs, the so-called cross-loadings must also be checked. That is, the loadings of an indicator with the rest of LVs. The reason for doing so is that it is needed to be sure that there are not traitor indicators. The cross-loadings are given in Table 4. It is needed to look at the list of results as if it was a super matrix. The way to read the cross-loadings is by looking at this super matrix block by block paying attention to the sections in the diagonal. These sections are the loadings of each block with its construct. A given loading in one of these sections must be greater than any other loading in its row (Sanchez [1]). For example, let's consider the first section that corresponds to the first column in the Attack block. GSH has a loading value of 0.8741. This value must be greater than any other value in that first row. The cross-loadings of **GSH** with Defense is -0.5248; the cross-loading of **GSH** with Success is 0.8127. Clearly, 0.8741 is greater than -0.5248 and 0.8127.

With the cross-loadings it is evaluated the extent to which a given construct differentiates from the others. The whole idea is to verify that the shared variance between a construct and its indicators is larger than the shared variance with other constructs. In other words, no indicator should load higher on another construct than it does on the construct it intends to measure. Otherwise, it is a traitor indicator. If an indicator loads higher with other constructs than the one it is intended to measure, its appropriateness might be considered because it is not clear which construct or constructs it is actually reflecting (Sanchez [1]).

```
> data1_pls$outer.cor
$Attack
     Attack Defense Success
GSH 0.8741 -0.5248  0.8127
GSA 0.7176 -0.2725  0.5660

$Defense
     Attack Defense Success
GCH -0.470  0.8760 -0.6974
GCA -0.413  0.8263 -0.5969

$Success
     Attack Defense Success
WMH 0.8262 -0.7076  0.8937
WMA 0.7035 -0.6230  0.8550
```

Table 4. The cross-loadings

Secondly, **the quality of the structural model is evaluated by examining three indices or quality metrics:** **a)** the R^2 determination coefficients, **b)** the redundancy index, **c)** the Goodness-of-Fit (GoF). These metrics are given in Table 5. As seen from Table 5, the inner model seems to be fine since the value of R-square, $R^2 = 0.90$,

is higher. It means that the 90% of variance in the Success explained by Attack and Defense. "Av.Redun" represents the percentage of the variance in the endogenous block that is predicted from the indepedent LVs associated to the endogenous LV. High redundancy means high ability to predict. In our model, the average redundancy for Success represents that Attack and Defense predict 68% of the variability of Success indicator. The third quality metric of model is GoF. GoF can be used as a global criterion that helps us to evaluate the performance of the model in both the inner and the outer models. Basically, GoF assess the overall prediction performance of the model. In our model, the value of GoF is 0.79 could be interpreted as if the prediction power of the model is of 79%. The naive rule of thumb is: the higher, the better. Acceptable "good" values within the PLS-PM community are GoF >0.7, as the case in our example.

```
> data1_pls$inner.sum
         LV.Type Measure MVs  R.square  Av.Commu  Av.Redun       AVE
Attack    Exogen    Rflct   2 0.0000000 0.6395011 0.0000000 0.6395011
Defense   Exogen    Rflct   2 0.0000000 0.7250808 0.0000000 0.7250808
Success Endogen    Rflct   2 0.9002366 0.7649069 0.6885972 0.7649069
```

Table 5. Quality Metrics of structural model

As PLS-PM is a soft modeling approach with no distributional assumptions, it is possible to estimate the significance of the parameters based on cross-validation methods like jack-knife and bootstrap (Trinchera and Russolillo [4]). The estimating the precision of the PLS parameter estimates is obtained by using bootstrapping which is a non-parametric approach. The bootstrap procedure is the following: M samples are created in order to obtain M estimates for each parameter in the PLS model. Each sample is obtained by sampling with replacement from the original data set, with sample size equal to the number of cases in the original data set (Sanchez [1]). The results of bootstrapping are given in Table 6. In table 6, for each of the displayed results, the bootstrap confidence interval (95%) provided by the percentiles 0.025 and 0.975 should be examined. . This is especially important for the path coefficients. When bootstrap intervals for the path coeffcients contain the zero, it means that these coefficients are not significant at a 5% confidence level. As seen from Table 6, the bootstrap confidence intervals for the Attack and Defense indicators do not contain zero. Hence, the path coefficients of these indicators are significant at a 5% confidence level.

```
BOOTSTRAP VALIDATION
weights
     Original  Mean.Boot  Std.Error  perc.025  perc.975
GSH     0.728      0.737      0.166    0.5500     0.997
GSA     0.507      0.455      0.170   -0.0584     0.626
GCH     0.631      0.644      0.181    0.3656     0.996
GCA     0.541      0.484      0.265   -0.1604     0.865
WMH     0.612      0.633      0.142    0.5154     0.926
WMA     0.530      0.479      0.179   -0.2325     0.637

loadings
     Original  Mean.Boot  Std.Error  perc.025  perc.975
GSH     0.874      0.882      0.133     0.789     0.976
GSA     0.718      0.640      0.273    -0.281     0.885
GCH     0.876      0.856      0.162     0.368     0.996
GCA     0.826      0.720      0.338    -0.255     0.952
WMH     0.894      0.899      0.130     0.782     0.973
WMA     0.855      0.776      0.298    -0.424     0.965

paths
                   Original  Mean.Boot  Std.Error  perc.025  perc.975
Attack->Success        0.66      0.655     0.1066     0.429     0.847
Defense->Success      -0.42     -0.425     0.0933    -0.614    -0.214

rsq
         Original  Mean.Boot  Std.Error  perc.025  perc.975
Success       0.9      0.908     0.0518     0.788     0.978

total.efs
                   Original  Mean.Boot  Std.Error  perc.025  perc.975
Attack->Defense        0.00      0.000     0.0000     0.000     0.000
Attack->Success        0.66      0.655     0.1066     0.429     0.847
Defense->Success      -0.42     -0.425     0.0933    -0.614    -0.214
```

Table 6. Results of Bootstrapping

In addition to expressing our model in text and mathematical format, we can also display our model in a graphical format using a path diagram as shown in Fig. 2. As mentioned before, these diagrams help us to

represent the relationships stated in our models in a visual way. In our example, the following diagram depicts the relation Success depending on the quality of the Attack as well as on the quality of the Defense. In brief, the model parameter estimates of PLS-PM of our example are shown in Fig. 2.

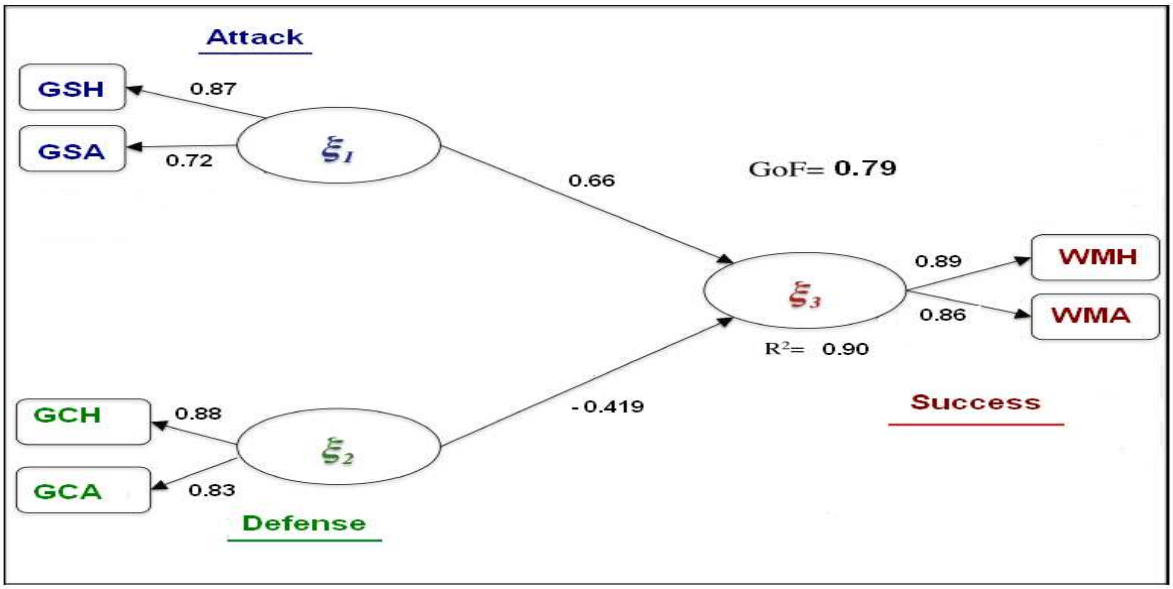

Fig. 2. PLS-PM analysis of Turkish football teams

As seen from Fig. 2, it is possible to examine the relations between Attack, Defense and Success via path coefficients: the two LVs Attack and Defense impact in opposite sense on the response Success. However, Success largely depends on Attack rather than on Defense. The higher attack causes the higher success but the higher defense causes the lower success. Because the higher defense means that the high values of GCH and GCA. Namely, teams conceded a lot of goals. Hence, the negative path coefficient related to defense refers to if the number of conceded goals of a team is increased, the success of the team is decreased. GSH, GSA, GCH, GCA, WMH, WMA are positively correlated to the LVs Attack, Defense, Success respectively.

Conclusions

In this study, we examine the success of 18 Turkish football teams using PLS Path Model. The relationship between LVs Attack, Defense and Success are examined. The LV Defense has a negative effect on the Success, however, the LV Attack is possitive effect on the Success. The Success of the Turkish teams largely depends on Attack. The better the attack, the more number of GSH and GSA, however, the better defense, the less number of GCH and GCA. Proposed a model in which the Overall Success depends on the Quality of the Attack as well as on the Quality of the Defense. Although GCH and GCA have to do with defense, they are measuring "lack" of defense. If a team has high values of GCH and GCA, they conceded a lot of goals, hence having a poor Defense quality. Briefly, GCH and GCA are pointing in the opposite direction. Hence, the better Quality of the Defense means that a team has low values of GCH and GCA.

References

1. G. Sanchez. *PLS Path Modeling with R*, http://www.gastonsanchez.com/PLS_Path_Modeling_with_R.pdf, 2013.
2. G. Sanchez. *Understanding Partial Least Squares Path Modeling (An introduction with R)*, Academic Paper, Department of Statistics and Operations Research, Universitat Politècnica de Catalunya, March, 2009.
3. M. Tenenhaus , V. Esposito Vinzi, Y.M. Chatelinc , C. Lauro. PLS path modeling. *Computational Statistics & Data Analysis*, 48, 159-205, 2005.
4. L. Trinchera and G. Russolillo. *On the use of Structural Equation Models and PLS Path Modeling to build composite indicators*, Working paper n. 30, September, 2010, http://www.unimc.it/sviluppoeconomico/wpaper/wpaper00030/filePaper .

Proceedings, 15th Applied Stochastic Models and Data Analysis (ASMDA2013)
International Conference, Mataró (Barcelona), Spain 25 - 28 June 2013

Confidence Intervals for Dynamic Concentration/Inequality Indices of Economic Systems Modeled by Birth-Death Processes

Philippe Regnault[1]

Laboratoire de Mathématiques de Reims, UFR Sciences Exactes et Naturelles,
Moulin de la Housse, BP1039, 51687 REIMS cedex 2, France
(E-mail: philippe.regnault@univ-reims.fr)

Abstract. In this paper, we are interested in estimating a dynamic index of the concentration of wealth shared by a population of economic agents – Theil's entropy. At any time, each agent produces an amount of wealth, independent of other agents. According to this wealth production, a wealth class (among predefined classes) is associated to each agent. We suppose that wealth class allocation is governed by a continuous-time birth-death process so that the repartition of total wealth's production among classes at any time is an explicit function of birth and death rates. Then, by considering Theil's entropy of wealth distribution among all classes at any time yields dynamic concentration index of wealth. If moreover, the birth-death process is ergodic, then Theil's entropy associated to the asymptotic repartition of wealth measures the concentration of wealth when agents' population reaches its equilibrium state.

When the class allocation process is observed at equidistant discrete times, it is necessary to estimate Theil's entropy index. In the same fashion as in Regnault [10], we prove the strong consistency and asymptotic normality of plug-in estimators of dynamic and asymptotic Theil's entropy, built from empirical estimators of the transition matrix of the discretized class allocation process. Confidence intervals for dynamical Theil's entropy are then derived.
Keywords: Population Dynamic, birth-death Process, Theil's Entropy, Reward, Estimation.

1 Introduction

Both inequality and wealth concentration dynamics within an economic system evolving over time have been extensively studied in the last years. In particular, D'Amico and Di Biase [1] recently proposed and studied stochastic versions of usual wealth concentration indices. They consider economic systems involving independent agents whose income evolves over time according to some discrete-time semi-Markov model. These agents are partitioned into a few number of economic classes according to their income or some other economic, social or demographic feature; concentration wealth among classes is then measured dynamically by considering its Theil's entropy at any time – the so-called dynamic Theil's entropy. The model has been successfully implemented in D'Amico *et al.* [2] for simulating an artificial economic system with immigration, and also in D'Amico *et al.* [3], applied to studying wealth concentration in several European countries whose citizen are partitioned according to their age.

The present paper aims at adapting the framework proposed by D'Amico and Di Biase [1] to estimating wealth concentration of dynamic economic systems involving a large number of independent agents, where agents' income class allocation is modeled by a continuous-time birth-death process. These assumptions are mainly motivated by the need of a simple and flexible model to be estimated and implemented for real applications. The birth-death model is also supported by previous studies; see Quah [9] and D'Amico *et al.* [3] where only transitions from one class to its neighboring classes are shown to be statistically significant. Moreover, income dynamics is usually modeled by a discrete time process because measurements of income of individuals occur at some fixed and known times, for example each year or fractions of year. On the contrary, agents' income can change at any time. One major problem is how to estimate the income inequalities from discrete observations of agents' income class allocation continuous-time process. We define and show good asymptotic properties of plug-in estimators of dynamic Theil's entropy function built from discrete observations of one or several agents' income. We then derive from these properties confidence intervals for Theil's entropy.

The paper is organized as follows: Section 2 presents the stochastic model. Section 3 introduces the dynamic version of Theil's entropy and its asymptotic value as time goes to infinity. Finally, Section 4 defines and establishes asymptotic properties of plug-in estimators of both dynamic and asymptotic Theil's entropy; confidence intervals for Theil's entropy are then derived from these properties.

2 The stochastic model

Let an economic system be composed of N economic agents, typically individuals. Each agent $i \in \{1, \ldots, N\}$ produces a quantity $X_i(t)$ of wealth – their income, changing randomly with time t so that $\mathbf{X}_i := (X_i(t))_t$ is a positive valued stochastic process.

Assume that the system evolves in a non competitive way so that wealth production of the agents do not depend on each others, that is the stochastic processes $\mathbf{X}_i$, $i \in \{1, \ldots, N\}$ are independent. The agents of the system are classified according to their income and allocated into one of K mutually exclusive and ordered classes

$$E = \{\mathcal{C}_1, \mathcal{C}_2, \ldots, \mathcal{C}_K\},$$

such that agent i belongs to $\mathcal{C}_k$ at time t if its income $X_i(t)$ belongs to $[w_k, w_{k+1}[$, where $w_1 = 0 < w_1 < \cdots < w_K < w_{K+1} = \infty$ are fixed thresholds. Then, let us introduce for any agent i, the process $\mathbf{C}_i := (C_i(t))_{t \in \mathbb{R}_+}$ that maps income $X_i(t)$ of agent i at time t into its corresponding class $\mathcal{C}_k \in E$.

The main assumptions of the present study are the following.

Assumptions 1 *1. the number of agents N tends to infinity;*
2. the processes $\mathbf{C}_i = (C_i(t))_{t \in \mathbb{R}+}$, $i \in \mathbb{N}^*$ are independent and identically distributed birth-death processes taking values in $E = \{\mathcal{C}_1, \ldots, \mathcal{C}_k\}$ with common initial distribution ν;

3. *given* $k \in \{1, \ldots, K\}$, *the conditional expectation* $W_k := \mathbb{E}(X_1(t)|C_1(t) = \mathcal{C}_k)$ *is constant over time* t.

The dynamic of the process $\mathbf{C}_i$ is completely described by its generator which is a tridiagonal matrix, say

$$\mathbf{A} := \begin{pmatrix} -\lambda_1 & \lambda_1 & & 0 \\ \mu_2 & -\lambda_2 - \mu_2 & \mu_2 & \\ & \ddots & \ddots & \ddots \\ 0 & & \mu_K & -\mu_K \end{pmatrix}. \tag{1}$$

The coefficients λ_k and μ_k are called the birth and death rates.

Finally, let us define for $\eta > 0$ and $i \in \mathbb{N}$, the sequence $\mathbf{D}_i := (C_i(\eta m))_{m \in \mathbb{N}}$ of income classes of agent i at times ηm, $m \in \mathbb{N}$ – say discretized class allocation process. It is well known that $\mathbf{D}_i$ is an homogeneous irreducible and aperiodic Markov chain with transition matrix

$$\mathbf{P}_\eta := \exp(\eta \mathbf{A});$$

see for example Bladt and Sørensen [6]. Thus, the coefficients of the matrix $\mathbf{P}_\eta$ are probabilities that an agent's income has moved from one income class to another after η units of time.

Note that η must be closed to the mean jump time of $\mathbf{C}_1$ for $\mathbf{D}_1$ to catch relevant information about $\mathbf{C}_1$; see Bladt and Sørensen [6] and references therein for more details.

Example 1 *Service providers such as retail brands constitute economic systems involving a large number of agents – the customers. Such providers offer different levels of service according to the budget (or income)* $\mathbf{X}_i$ *of customers; for example, a retail brand can sell several competitive products for a common use with a large range of prices. Customers are then partitioned into exclusive economic classes* $\mathcal{C}_1, \ldots, \mathcal{C}_K$ *at any time, according to the service level (or product) they choose. Any customer allocated to the service class* $\mathcal{C}_k$ *contributes to the provider's turnover by* W_k *units of money per unit of time, where* W_k *is the price of type* k *service.*

3 Dynamic Theil's entropy

We are interested here in quantifying the inequality of repartition of the total wealth into the different classes $\mathcal{C}_k \in E$. For this purpose, let us define the instantaneous share of produced income due to class $\mathcal{C}_k$ at time t by

$$p_k(t) := \frac{\sum_{i=1}^N X_i(t) \mathbb{1}_{\{C_i(t) = \mathcal{C}_k\}}}{\sum_{i=1}^N X_i(t)}.$$

One of the most used inequality measure is Theil's entropy proposed by Theil [13]. It derives from the mathematical theory of communication founded by Shannon [12]. As stated in Athanasopoulos and Vahid [4] or Cowell [7], it is

more sensitive to transfers of wealth in the lower tail than in the upper tail. It is also additively decomposable: for any significant grouping of agents population, Theil's entropy of the whole population can be additively decomposed to inequality between subgroups and an appropriately weighted average within each group.

A stochastic version of Theil's entropy was recently proposed in [1] by considering the process $(\mathbb{T}(t))_{t\in\mathbb{R}_+}$, where

$$\mathbb{T}(t) := \sum_{k=1}^{K} p_k(t) \log\big(K p_k(t)\big),$$

with the convention $0 \log 0 = 0$.

Assumptions 1.1 and 1.2 and the law of large numbers jointly imply that the instantaneous share of produced income of class C_k at time t is

$$\begin{aligned} p_k(t) &= \frac{\left(\int_{w_k}^{w_{k+1}} x dP_{X_1(t)}(x)\right) \mathbb{P}(C_1(t) = \mathcal{C}_k)}{\sum_{k=1}^{K} \left(\int_{w_k}^{w_{k+1}} x dP_{X_1(t)}(x)\right) \mathbb{P}(C_1(t) = \mathcal{C}_k)} \\ &= \frac{\mathbb{E}(\mathbf{X}_1(t)|C_1(t) = \mathcal{C}_k)\mathbb{P}(C_1(t) = \mathcal{C}_k)}{\sum_{k=1}^{K} \mathbb{E}(\mathbf{X}_1(t)|C_1(t) = \mathcal{C}_k)\mathbb{P}(C_1(t) = \mathcal{C}_k)}. \end{aligned}$$

Hence, the multivariate process $\mathbf{p}(t) = (p_1(t), \ldots, p_K(t))_{t\in\mathbb{R}_+}$ becomes a deterministic function of time. Assumption 1.3 yields

$$p_k(t) = \frac{W_k \mathbb{P}(C_1(t) = \mathcal{C}_k)}{\sum_{k=1}^{K} W_k \mathbb{P}(C_1(t) = \mathcal{C}_k)}.$$

Theil's entropy $\mathbb{T}(t)$ of the system at time t thus becomes an explicit function of the probability distribution of $C_1(t)$, and hence, $\mathbb{T} = (\mathbb{T}(t))_{t\in\mathbb{R}_+}$ becomes a deterministic function of time t, explicitly determined by the generator $\mathbf{A}$ and the initial distribution ν of the allocation class process $\mathbf{C}_1$. Precisely,

$$\mathbb{T}(t) = \sum_{k=1}^{K} \frac{W_k(\nu \exp(t\mathbf{A}))_k}{\sum_{j=1}^{K} W_j(\nu \exp(t\mathbf{A}))_j} \log\left(K \frac{W_k(\nu \exp(t\mathbf{A}))_k}{\sum_{j=1}^{K} W_j(\nu \exp(t\mathbf{A}))_j}\right), \quad (2)$$

where $\nu \exp(t\mathbf{A})$ denotes the product of ν and $\exp(t\mathbf{A})$, and $(\nu \exp(t\mathbf{A}))_k$ is its k-th component.

Note that the dynamic Theil's entropy $\mathbb{T}$ can be expressed as a function T of the transition matrix $\mathbf{P}_\eta$ for time values t of the form $t = m\eta$, with $m \in \mathbb{N}$. Indeed, $\exp(m\eta\mathbf{A}) = \exp(\eta\mathbf{A})^m$ gives in (2),

$$\mathbb{T}(m\eta) = T(\mathbf{P}_\eta, m) := \sum_{k=1}^{K} \frac{W_k(\nu \mathbf{P}_\eta^m)_k}{\sum_{j=1}^{K} W_j(\nu \mathbf{P}_\eta^m)_j} \log\left(K \frac{W_k(\nu \mathbf{P}_\eta^m)_k}{\sum_{j=1}^{K} W_j(\nu \mathbf{P}_\eta^m)_j}\right). \quad (3)$$

Note that T is formally defined on the set of stochastic matrices on $E = \{\mathcal{C}_1, \ldots, \mathcal{C}_K\}$, differentiable on the open set of irreducible transition matrices.

It is well known that the processes $\mathbf{C}_i$, $i \in \mathbb{N}^*$, are ergodic. Let $\pi = (\pi_1, \pi_2, ..., \pi_K)$ denote its stationary distribution; see [8] for an explicit expression. Markov chains $\mathbf{D}_i$, $i \in \mathbb{N}^*$, are also ergodic with stationary distribution π. Particularly, π satisfies $\pi \mathbf{P}_\eta = \pi$.

Consequently we can compute the asymptotic value of the dynamic Theil's entropy as follows,

$$\begin{aligned} \mathbb{T}(\infty) &:= \lim_{t\to\infty} \mathbb{T}(t) = \sum_{k=1}^{K} \frac{W_k \pi_k}{\sum_{j=1}^{K} W_j \pi_j} \log\left(K \frac{W_k \pi_k}{\sum_{j=1}^{K} W_j \pi_j} \right) \\ &= T_\infty(\pi), \end{aligned} \tag{4}$$

where T_∞ is differentiable on the set of probability measures supported by E.

4 Estimation of dynamic Theil's entropy from discrete observations

This section aims at studying sequences of plug-in estimators for both dynamic and asymptotic Theil's entropy built from discrete observations of income class allocation process of one (Section 4.1) or several (Section 4.2) agent(s).

4.1 Discrete observations of one agent's wealth

Let us suppose the income class allocation process $\mathbf{C}_1$ of one agent are observed at discrete times $m\eta$, up to time $M\eta$, where $M \in \mathbb{N}$, so that a truncated trajectory of the Markov Chain $\mathbf{D}_1$ is available. Let $\widehat{\mathbf{P}}_M$ be the empirical estimator of $\mathbf{P}_\eta$ built from $D_1(0), \ldots, D_1(M)$ as follows:

$$\widehat{\mathbf{P}}_M(k,l) := \begin{cases} \dfrac{\sum_{m=0}^{M-1} \mathbb{1}_{\{D_1(m)=\mathcal{C}_k, D_1(m+1)=\mathcal{C}_l\}}}{\sum_{m=0}^{M-1} \mathbb{1}_{\{D_1(m)=\mathcal{C}_k\}}} & \text{if } k \neq l \text{ and } \sum_{m=0}^{M-1} \mathbb{1}_{\{D_1(m)=\mathcal{C}_k\}} \neq 0, \\ 0 & \text{if } k \neq l \text{ and } \sum_{m=0}^{M-1} \mathbb{1}_{\{D_1(m)=\mathcal{C}_k\}} = 0 \\ 1 - \sum_{j\neq k} \widehat{\mathbf{P}}_M(k,j) & \text{if } k = l, \end{cases} \tag{5}$$

for $(k,l) \in \{1, \ldots, K\}^2$. It is well known (see for instance Billingsley [5]) that the sequence $(\widehat{\mathbf{P}}_M)_{M\in\mathbb{N}}$ is strongly consistent and that $(\sqrt{M}(\widehat{\mathbf{P}}_M - \mathbf{P}))_{M\in\mathbb{N}}$ is asymptotically normal, with zero mean and asymptotic variance matrix $\Sigma^2_{\mathbf{P}_\eta}$ equal to the inverse of the Fisher information of the chain $\mathbf{D}_1$.

For any $m \in \mathbb{N}$ let us define the estimator $\widehat{\mathbb{T}}_M(m\eta)$ of $\mathbb{T}(m\eta)$ built from $\widehat{\mathbf{P}}_M$ by plugging it into the function T; precisely

$$\widehat{\mathbb{T}}_M(m\eta) := T(\widehat{\mathbf{P}}_M, m).$$

Because T is differentiable on the set of stochastic matrices, the sequence $(\widehat{\mathbb{T}}_M(m\eta))_{M\in\mathbb{N}}$, for $m \in \mathbb{N}$, inherits of the good asymptotic properties of $(\widehat{\mathbf{P}}_M)_{M\in\mathbb{N}}$ – thanks to the continuous mapping theorem and the Delta method; see Van der Vaart[14] for details. Precisely, for all $m \in \mathbb{N}$,

$$\widehat{\mathbb{T}}_M(m\eta) \xrightarrow[M\to\infty]{\text{a.s.}} \mathbb{T}(m\eta),$$
$$\sqrt{M}\left(\widehat{\mathbb{T}}_M(m\eta) - \mathbb{T}(m\eta)\right) \xrightarrow[M\to\infty]{\mathcal{D}} \mathcal{N}(0, \Sigma^2_{\mathbb{T}(m\eta)}),$$

where

$$\Sigma^2_{\mathbb{T}(m\eta)} = \left(\frac{\partial}{\partial \mathbf{P}_\eta} T(\mathbf{P}_\eta, m)\right)^t \Sigma^2_{\mathbf{P}_\eta} \left(\frac{\partial}{\partial \mathbf{P}_\eta} T(\mathbf{P}_\eta, m)\right). \tag{6}$$

Similarly, for estimating the asymptotic Theil's entropy $\mathbb{T}(\infty)$, we define $\widehat{\mathbb{T}}_M(\infty)$ by plugging whether the stationary distribution $\widehat{\pi}_M$ of $\widehat{\mathbf{P}}_M$ if $\widehat{\mathbf{P}}_M$ is irreducible and aperiodic or any distribution supported by E if not, into T_∞ given by (4); precisely

$$\widehat{\mathbb{T}}_M(\infty) := \sum_{k=1}^{K} \frac{W_k \widehat{\pi}_M(\mathcal{C}_k)}{\sum_{j=1}^{K} W_j \widehat{\pi}_M(\mathcal{C}_j)} \log\left(K \frac{W_k \widehat{\pi}_M(\mathcal{C}_k)}{\sum_{j=1}^{K} W_j \widehat{\pi}_M(\mathcal{C}_j)}\right),$$

with the convention $0 \log 0 = 0$.

Again, the continuous mapping theorem and delta method ensure the strong consistency of $(\widehat{\mathbb{T}}_M(\infty))_{M\in\mathbb{N}}$ and asymptotic normality of $(\sqrt{M}(\widehat{\mathbb{T}}_M(\infty) - \mathbb{T}(\infty)))_{M\in\mathbb{N}}$, with asymptotic variance $\Sigma^2_{\mathbb{T}(\infty)} = \left(\frac{d}{d\pi} T_\infty\right)^t \Sigma^2_\pi \left(\frac{d}{d\pi} T_\infty\right)$, where Σ^2_π is explicit.

To estimate $\mathbb{T}(t)$ for $t \notin \eta\mathbb{N}$ is much more complicated. Indeed, (3) does not hold true anymore. Hence, it is required to estimate the generator of $\mathbf{C}_1$ from observations of the discretized chain $\mathbf{D}_1$ and then to plug this estimator into (2). The main mathematical obstacle is due to the non-injectivity of the exponential function for matrices : given the transition matrix $\mathbf{P}_\eta$ of $\mathbf{D}_1$, it may exists several different generators $\mathbf{A}$ such that $\exp(\eta\mathbf{A}) = \mathbf{P}_\eta$, so that the statistical model may not be identifiable. Regnault [11] shows that the model of birth-death processes with constant rates, i.e. $\lambda_k = \lambda > 0$ and $\mu_{k+1} = \mu > 0$ for all $k \in \{1, \dots, K-1\}$, is identifiable. Indeed, the generators of such processes are proven to have K distinct eigenvalues, a sufficient condition for the uniqueness of the logarithm matrix of $\mathbf{P}_\eta$. Further investigations would be necessary to extend this result to the whole family of generators given by (1).

4.2 Discrete observations of several agents' wealth

Let us now suppose that the discretized income class allocation processes $\mathbf{D}_1, \dots, \mathbf{D}_n$ of n independent agents up to time $M \in \mathbb{N}$ is observed. Let $\widehat{\mathbf{P}}^{(i)}_M$ be the maximum likelihood estimator of $\mathbf{P}_\eta$ given by (5), obtained from the trajectory $\mathbf{D}_i$, for each $i \in \{1, \dots, n\}$ and let

$$\widehat{\mathbf{P}}_{M,n} := \frac{1}{n} \sum_{i=1}^{n} \widehat{\mathbf{P}}^{(i)}_M,$$

define the estimator of $\mathbf{P}_\eta$ obtained as mean of the estimators $\widehat{\mathbf{P}}_M^{(i)}$, $i \in \{1, \ldots, n\}$.

The sequence $(\widehat{\mathbf{P}}_{M,n})_{M\in\mathbb{N}}$ is obviously strongly consistent. Moreover, observe that $\sqrt{M}(\widehat{\mathbf{P}}_{M,n} - \mathbf{P}_\eta) = \frac{1}{n}\sum_{i=1}^n \sqrt{M}(\widehat{\mathbf{P}}_M^{(i)} - \mathbf{P}_\eta)$ is the mean of n independent, asymptotically normal variables, with the same asymptotic variance $\Sigma^2_{\mathbf{P}_\eta}$, so that

$$\sqrt{Mn}\left(\widehat{\mathbf{P}}_{M,n} - \mathbf{P}_\eta\right) \xrightarrow[M\to\infty]{\mathcal{D}} \mathcal{N}(0, \Sigma^2_{\mathbf{P}_\eta}).$$

Observing n agents in the place of a unique one thus leads to improve the rate of convergence by a factor $\sqrt{n}$.

Hence, the estimators $\widehat{\mathbb{T}}_{M,n}(m\eta)$ for $m \in \mathbb{N}$, obtained by plugging $\widehat{\mathbf{P}}_{M,n}$ into T inherit this asymptotic behavior. Precisely,

$$\widehat{\mathbb{T}}_{M,n}(m\eta) \xrightarrow[M\to\infty]{\text{a.s.}} \mathbb{T}(m\eta),$$
$$\sqrt{Mn}\left(\widehat{\mathbb{T}}_{M,n}(m\eta) - \mathbb{T}(m\eta)\right) \xrightarrow[M\to\infty]{\mathcal{D}} \mathcal{N}(0, \Sigma^2_{\mathbb{T}(m\eta)}).$$

Similarly, the sequence of estimators of $\mathbb{T}(\infty)$ given by $\widehat{\mathbb{T}}_{M,n}(\infty) = T_\infty(\widehat{\pi}_{M,n})$, where $\widehat{\pi}_{M,n}$ is the stationary distribution of $\widehat{\mathbf{P}}_{M,n}$, is strongly consistent and asymptotically normally distributed, with rate of convergence $\sqrt{Mn}$.

4.3 Confidence intervals for dynamic Theil's entropy

Confidence intervals for dynamic Theil's entropy at times $m\eta$, where $m \in \mathbb{N}$, can be derived from the asymptotic distribution of estimators $\widehat{\mathbf{P}}_M$ and $\widehat{\mathbf{P}}_{M,n}$, for $n \in \mathbb{N}^*$ and M large enough. Precisely, given a confidence level α – typically, $\alpha = 0.95$, the confidence interval for $\mathbb{T}(m\eta)$ is

$$]\widehat{\mathbf{P}}_{M,n} - \frac{q_{(1+\alpha)/2}\widehat{\Sigma}_M}{\sqrt{Mn}}; \widehat{\mathbf{P}}_{M,n} + \frac{q_{(1+\alpha)/2}\widehat{\Sigma}_M}{\sqrt{Mn}}[,$$

where $q_{(1+\alpha)/2}$ is the quantile of order $(1+\alpha)/2$ of the standard normal distribution and $\widehat{\Sigma}^2_M$ is any strongly consistent estimator of $\Sigma^2_{\mathbb{T}(m\eta)}$ built from independent truncated trajectories of $\mathbf{D}_1$ up to time M. Such an estimator can be obtained by computing the inverse Fisher's information matrix $\widehat{\Sigma^2_{\mathbf{P}_\eta}}^{(1)}_M$ of the empirical transition matrix $\widehat{\mathbf{P}}_M^{(1)}$ and hence by plugging both $\widehat{\Sigma^2_{\mathbf{P}_\eta}}^{(1)}_M$ and $\widehat{\mathbf{P}}_M^{(1)}$ into (6).

Although a thinner study could refine the following limitation, we recommend to use the normal asymptotic distribution for M larger than 100 units of time when $K \leq 5$, so that truncated trajectories $\mathbf{D}_1, \ldots, \mathbf{D}_n$ catch enough information about system's dynamics.

Other applications of the central limit theorem would be of interest, such as computing the minimal number n of customers to observe to ensure a given accuracy of the estimation of Theil's entropy, for a given $M \geq 100$.

References

1.G. D'Amico and G. Di Biase. Generalized Concentration/Inequality Indices of Economic Systems Evolving in Time. *WSEAS TRANSACTIONS on MATHEMATICS*, 9, 2, 140-149, 2010.
2.G. D'Amico, G. Di Biase and R. Manca. Immigration effects on economic systems through dynamic inequality indices. *Global journal of business research*, 5, 5, 11-25, 2011.
3.G. D'Amico, G. Di Biase and R. Manca. Income Inequality Dynamic Measurement of Markov Models: Application to some European Countries. *Economic Modeling*, 29, 1598-1602, 2012.
4.G. Athanasopoulos and F. Vahid. Statistical inference on changes in income inequality in Australia. *The Economic Record*, 79, 247, 412-424, 2003.
5.P. Billingsley. *Statistical Inference for Markov Process,* The University of Chicago Press, Chicago, 1968.
6.M. Bladt and M. Sørensen. Statistical inference for discretely observed Markov jump processes. *Journal of the Royal Statistical Society*, B, 67, 395-410, 2005.
7.F. Cowell. *Measuring Inequality.* LSE handbook in Economics Series, 2nd edition, prentice Hall, London, 1995.
8.V. Girardin and A. Sesboüé. Maximizing the entropy rate of state-dependent M/M/1 queues. *Bayesian Inference and Maximum Entropy Methods in Science and Engineering, AIP Conference Proceedings*, 1073, 181-188, 2008.
9.D. Quah. Empiric for economic growth and convergence. *European Economic Review* 40, 951-958, 1996.
10.P. Regnault. Différents problèmes liés l'estimation de l'entropie de Shannon d'une loi, d'un processus de Markov. *PhD Thesis, Université de Caen – Basse Normandie*, 2011.
11.P. Regnault. Entropy estimation of M/M/1 queueing systems, *Bayesian Inference and Maximum Entropy Methods in Science and Engineering, AIP Conference Proceedings*, 1443, 330-337, 2012.
12.C.E. Shannon. A mathematical theory of communication. *Bell System Technical Journal* 27, 379-423, 1948.
13.H. Theil. *Economics and Information Theory,* North Holland, Amsterdam, 1967.
14.A.W. Van der Vaart. *Asymptotic Statistics,* Cambridge Series in Statistical an Probabilistic Mathematics, Cambridge, 1998.

Proceedings, 15th Applied Stochastic Models and Data Analysis (ASMDA2013)
International Conference, Mataró (Barcelona), Spain 25 - 28 June 2013

Longitudinal Analysis of renal function with informative observation times

Lisandra Rocha[1], Inês Sousa[1,2], and Raquel Menezes[1,2]

[1] Center of Mathematics of University of Minho, Portugal
(E-mail: ID2704@alunos.uminho.pt)
[2] Department of Mathematics and Applications of University of Minho, Portugal
(E-mail: isousa@math.uminho.pt; rmenezes@math.uminho.pt)

Abstract. In this work, we intend to analyze the progression of renal function in patients of Hope Hospital in Salford, England. The aim of this work is to model the evolution of creatinine in the blood taking into account that time measurements depend on the responses obtained. For that, we propose a model that considers dependence between the longitudinal outcome process and the follow-up time process. This model use subject-specific random effects to describe the association between the two processes of interest and a joint-likelihood-based estimation was developed for estimation. We will also analyze the same data with a standard longitudinal model which ignore the dependence assumption, aiming to compare the results of the two analyzes. The principal difference between these two models and different approaches is that, the standard longitudinal model considers the follow up time process as deterministic while the model that we propose considers the follow up time process stochastic.
Keywords: Follow up Time Process, Longitudinal Analysis, Monitoring Kidney Function.

1 Introduction

Renal failure is a disease caused by the slow and irreversible loss of renal function. It is defined by progressive loss of the ability of the kidneys to filter, responsible for eliminating toxic products to the body and producing substances essential to life. Often, the loss of renal function is silent in the absence of the manifestation of symptoms for extended periods in time. There are already some risk factors known for kidney failure such as diabetes, hypertension and patient age.
For the control of renal failure, the creatinine level in blood should be monitored. The kidneys control levels of creatinine in the blood, therefore it is an indicator for evaluating kidneys performance. High levels of creatinine in the blood warn for possible failure in the functioning of the kidneys.
The times where measurements of creatinine are observed are decided according to the patient's clinical status. For example, if the patient on the last measurement had a high value of creatinine in the blood, the patient will be measured sooner than other patient with a creatinine value within normal values. Thus, in this context, the measurement times are considered dependent of the longitudinal responses and the follow up time process can not be considered deterministic in the study design.

In standard longitudinal models (Diggle et al.[4]), the follow up time process is assumed deterministic, meaning, the follow-up time process is noninformative about the outcome longitudinal process of interest. Therefore, this type of analysis does not considered the dependence that can exist between the follow-up time process and the longitudinal outcome process. In recent years, a number of authors have considered the situation where longitudinal outcome process is correlated with the follow up time process (Sun et al.[2]; Ryu et al.[1]; Liang et al.[6]).
In this work, we intend to analyze the progression of renal function in patients of Hope Hospital in Salford, England. The aim of this work is to model the evolution of creatinine in the blood taking into account that time measurements depend on the responses obtained. For that, we propose a model that considers dependence between the longitudinal outcome process and the follow-up time process (Rocha et al.[3]). This model use subject-specific random effects to describe the association between the two processes of interest. For estimation, a joint-likelihood-based estimation was developed. We also use a standard longitudinal model which assumes follow up time process as deterministic, aiming to compare the results of the three approaches.

2 The Data Set

For study the progression of renal function in patients of Hope Hospital in Salford, England, we used two data sets: one with primary and secondary care patients and other data set with healthy patients (Hoefield et al.[5]). The response variable of interest is the indicator eGFR (estimated gromelular filtration rate). Doctors suggest that a person with an annual rate of decrease in eGFR exceeding 5% should be referred to a specialist treatment center.
Below, we show some information about the two data sets.

Healthy patients

- 162.394 patients;
- Of these 162.394 individuals, 74.222 were males and 88.172 were female;
- 9% of the patients died during the study;
- The age range 18 to 106 years, and the average is about 57 years;
- The patients follow up was maximum of 2502 days (approximately 7 years). The average length of patients follow up is 616 days (approximately 1 year and 8 months).

Primary and secondary care patients

- 18.350 patients;
- Of these 18.350 individuals, 9.457 were males and 8.893 were female;
- 25.8% of the patients died during the study;
- The age range 18 to 106 years, and the average is about 70 years;
- The patients follow up was maximum of 3066 days (approximately 8 years and half). The average length of patients follow up is 938 days (approximately 2 years and half);

- In this data set we have information about some risk factors: 45.3% of the patients have diabetes, 17.3% had a myocardial infarction, 21.9% have hypertension, 20.3% of the patients take ACE drugs and 6.4% take AT2 Blockers drugs.

Figure 1 show the logarithm of eGFR versus patient age of two databases. The solid red line in the graphs represent the mean estimate of evolution using the function smooth.spline in software R. It is known that, as will the age of patients increases, renal function worsens. It is found that, from the age of 65, measurements of the logarithm of eGFR are worse. As expected, patients in primary and secondary, on average, have values of eGFR lower than healthy patients. This means that patients in primary and secondary care are with renal function in worse condition than healthy patients.

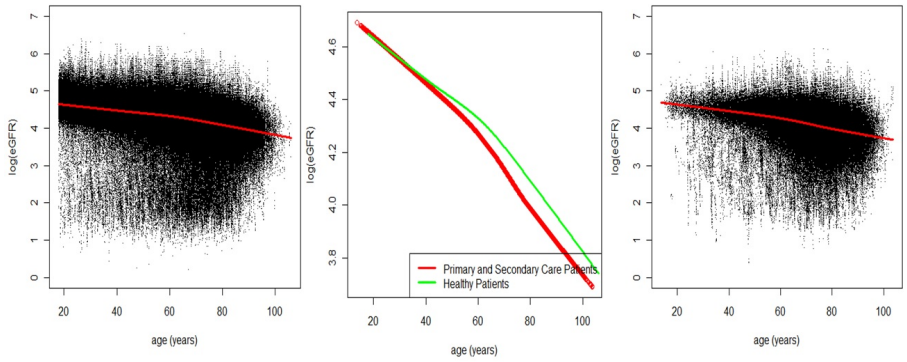

Fig. 1. Evolution of renal function in healthy patients and primary and secondary care patients

3 Notation and Model

Consider Y_{ij} the variable response observed in the individual $i = 1, , n$ at time $t_{ij} = 1, , m_i$ and X_{ij} a matrix of covariates with dimension Nxp. Consider the model defined as

$$Y_{ij} = \beta X_{ij} + W_i(t_{ij}) + U_i + \epsilon_{ij} \tag{1}$$

where β is the vector of regression parameters and ϵ_{ij} are independent realizations of a Gaussian variable with $E[\epsilon_{ij}] = 0$ and $Var[\epsilon_{ij}] = \tau^2$. Consider U_i as the random effect of individual i, where $U_i \sim Normal(0, \gamma^2)$ and $W_i(t_{ij})$ as the serial correlated variation for individual i, where $E[W_i(t_{ij})] = 0$, $Var[W_i(t_{ij})] = \sigma^2$ and $Corr[W_i(t_{ij}), W_i(t_{ij} - u)] = \rho(u)$. Also consider the follow up time process T_{ij} defined as

$$T_{ij} \sim Exp[\lambda_i(t_j)] \qquad \text{and} \qquad \lambda_i(t_j) = Exp[\alpha + \rho \int_0^{t_{i,(j-1)}} Y_i(t)dt] \tag{2}$$

where α and ρ are unknown parameters. The difference between the standard longitudinal model and our model is that, the standard longitudinal model considers the follow up time process T as deterministic while our model considers the follow up time process stochastic. The parameters are estimated by maximizing the likelihood function, using the function optim (for our model) and the function lme (for the longitudinal standard model) in software R.

4 Discussion

In this work, we propose a model for repeated measures in the presence of informative observation times. For the model adjusted to the data, the effect of age is negative. This simply means that will as, renal function decreases with age.
It was also observed that there is a changing point in age effect at 65 years of age where the decrease of renal function happens more rapidly. Is also the starting of 65 than the difference between the renal function of patients in primary and secondary and healthy patients is increased.
We believe that the model proposed is the most appropriate model to the data concerned.

5 Acknowledgements

The authors acknowledges the grant by FCT PTDC/MAT /112338/2009.
The author L. Rocha has a PhD scholarship by FCT SFRH/BD/61368/2009.
This research was financed by FEDER Funds through "Programa Operacional Factores de Competitividade COMPETE" and by Portuguese Funds through FCT - "Fundação para a Ciência e a Tecnologia", within the Project Est-C/MAT/UI0013/2011.

References

1.D. Ryu, D. Sinha, B. Mallick, S. Lipsitz and S. Lipshultz. Longitudinal studies with outcome-dependent follow-up: models and bayesian regression, *Journal of the American Statistical Association*, 102, 952-961, 2007.
2.J. Sun, D. Park, L. Sun and X. Zhao. Semiparametric regression analysis of longitudinal data with informative observation times, *Journal of the American Statistical Association*, 100, 882-890, 2005.
3.L. Rocha, I. Sousa and R. Menezes. A longitudinal model with informative observation times. (in preparation)
4.P. Diggle, K. Liang and S. Zeger. *Analysis of Longitudinal Data*, Oxford: Clarendon Press, 2002.
5.R. Hoefield, P. Kalra, P. Baker, I. Sousa, P. Diggle, M. Gibson, D. O'Donoghue, R. Middleton and J. New. The use of eGFR and ACR to predict decline in renal function in people with diabetes. *Nephrol Dial Transplant*, 1–6, 2010.
6.Y. Liang, W. Lu and Z. Ying. Joint Modeling and Analysis of Longitudinal Data with Informative Observation Times, *Biometrics*, 65, 377-384, 2009.

Proceedings, 15th Applied Stochastic Models and Data Analysis (ASMDA2013)
International Conference, Mataró (Barcelona), Spain 25 - 28 June 2013

Statistical Estimation Based on Generalized Order Statistics from Kumaraswamy Distribution

Samir K. Safi
Department of Statistics, The Islamic University of Gaza, Palestine
(E-mail: **samirsafi@gmail.com**)

Rehab H. Al Sheikh Ahmed
1Statistician Consultant, Gaza, , Palestine
(E-mail: **rehab4ps@yahoo.com**)

Abstract. The Kumaraswamy distribution is similar to the Beta distribution but has the key advantage of a closed-form cumulative distribution function. In this paper we present the estimation of Kumaraswamy distribution parameters based on Generalized Order Statistics (GOS) using Maximum Likelihood Estimators (MLE). We proved that the parameters estimation for Kumaraswamy distribution can not be obtained in explicit forms, and therefore it has been implemented using the simulated data for illustrative purposes. We compare the performances of parameters estimation through an extensive numerical simulation for different sample sizes. These simulations examine the sensitivity of estimation to different sample sizes. In particular, how do estimations perform for small, moderate and large sample sizes? The main findings are: First, the worst performance estimation for small sample size selection for different values of the parameters estimation. Secondly, as the sample size increases the MSE of the estimation decreases. Finally, the estimation accuracy reaches its superiority for large sample sizes.

Keywords: Kumaraswamy Distribution, Generalized Order Statistics, Simulation, Maximum Likelihood Estimators.

1 Introduction

Poondni Kumaraswamy was a leading Indian engineer and hydrologist. Kumaraswamy[9] introduced the distribution for variables that are lower and upper bounded. With its two non-negative shape parameters p and q, it was originally conceived to model hydrological phenomena, (See for example Mitnik[10]). The Kumaraswamy distribution is a continuous probability distribution with double-bounded support, defined on the interval [0,1] differing in the values of their two non-negative shape parameters p and q. It is similar to the Beta distribution but has the key advantage of a closed form cumulative distribution function, Carrasco *et al.*[4].

Generalized Order Statistics (GOS) concept was introduced by Kamps[8] as a unified approach to several models of ordered random variables such as upper order statistics, upper record values, sequential order statistics, ordering via truncated distributions, censoring schemes, among others. Ateya and Ahmad[3], Jaheen[7], Habibullah and Ahsanullah[6], Raqab and Ahsanullah [11]among others, utilized the GOS in their works.

Abu El-Fotouh and Nassar[1] have investigated the estimation problem for the unknown parameters of Weibull extension model based on GOS by

Maximum Likelihood Estimators (MLE). Alkasasbeh and Raqab[2] considered the MLE of the different parameters of a generalized logistic distribution and compared the performances of these procedures through an extensive numerical simulation.

This paper is organized as follows. Section 2 presents some basic definitions; Section 3 demonstrates the estimation of Kumaraswamy distribution parameters based on GOS Using MLE, the main results of this paper are stated and proved. Simulation study is shown in section 4; and Section 5 summarizes the important results.

2 Preliminaries

In this section, we introduce some basic definitions.

Definition 2.1 The random variables $X(1,n,\vec{m},k),...,X(n,n,\vec{m},k)$ are called GOS based on the Cumulative Distribution Function (*cdf*), $F(x)$, if their joint probability density function *(pdf)* is given by Kamps[8].

$$f(x_1,...,x_n)=k\left(\prod_{j=1}^{n-1}\gamma_j\right)\left[\prod_{i=1}^{n-1}(1-F(x_i))^{m_i}f(x_i)\right](1-F(x_n))^{k-1}f(x_n), \quad (2.1)$$

on the cone $F^{-1}(0)<X_1\le X_2\le ...\le X_n<F^{-1}(1)$ of $\mathbb{R}^n$, with parameters $n\in\mathbb{N}$, $n\ge 2$, $k>0$, $\vec{m}=(m_1,...,m_{n-1})\in\mathbb{R}^{n-1}$, $M_r=\sum_{j=r}^{n-1}m_j$, such that $\gamma_r=k+n-r+M_r>0$ for all $r\in\{1,...,n-1\}$, let $c_{r-1}=\prod_{j=1}^{r}\gamma_j$, $r=1,2,\mathrm{K},n-1$ and $\gamma_n=k$.

Special Case

Given Definition 2.1, let $k=1$ and $m_1=m_2=...=m_{n-1}=zero$, then the joint *pdf* of all Ordinary Order Statistics (OOS) is $f(x_1,...,x_n)=\left[\prod_{j=1}^{n-1}\gamma_j\right]\left[\prod_{i=1}^{n}f(x_i)\right]$

$\left[\prod_{j=1}^{n-1}\gamma_j\right]=\prod_{j=1}^{n-1}(k+n-j+M_j)$, $M_j=\sum_{r=j}^{n-1}m_r=zero$. Then

$\left[\prod_{j=1}^{n-1}\gamma_j\right]=\prod_{j=1}^{n-1}(1+n-j)=n(n-1)(n-2)...3\times2\times1=n!$.

Therefore, the joint *pdf* of all OOS $f(x_1,...,x_n)=n!\prod_{i=1}^{n}f(x_i)$, *which is the well known pdf of all OOS*.

Definition 2.2 The *pdf* of the Kumaraswamy distribution is given by

$$f_Z(z)=\frac{1}{(b-c)}pq\left(\frac{z-c}{b-c}\right)^{p-1}\left[1-\left(\frac{z-c}{b-c}\right)^{p}\right]^{q-1} \quad , c<z<b, \qquad (2.2)$$

with shape parameters $p>0$ and $q>0$, and boundary parameters *c* and *b*. The standard form of the Kumaraswamy density function $(c=0, b=1)$, $kum(p,q)$ is given by

$$f_X(x;p,q)=pq\,x^{p-1}\left(1-x^{p}\right)^{q-1} \qquad (2.3)$$

The closed form of the *cdf* of the Kumaraswamy distribution is given by

$$F(x;p,q)=1-\left(1-x^{p}\right)^{q} \qquad (2.4)$$

Definition 2.3 The joint *pdf* of $X(1,n,\vec{m},k)$, $X(2,n,\vec{m},k),\ldots,X(n,n,\vec{m},k)$ for Kumaraswamy distribution is

$$f(x_1,\ldots,x_n)=k\left[\prod_{j=1}^{n-1}\gamma_j\right]\prod_{i=1}^{n-1}\left[\left(1-x_i^{p}\right)^{qm_i}\,pq\,x_i^{p-1}\left(1-x_i^{p}\right)^{q-1}\right]\left(1-x_n^{p}\right)^{q(k-1)}\times$$

$$pq\,x_n^{p-1}\left(1-x_n^{p}\right)^{q-1} \qquad (2.5)$$

3. Estimation of Kumaraswamy Distribution Parameters Based on GOS Using MLE

The method of MLE is, by far, the most popular technique for deriving estimators and a reasonable choice for an estimator. The MLE is the parameter point for which the observed sample is most likely. In general, the MLE is and a good point estimator, possessing some of the optimality properties such as invariance property of MLE, Casella and Berger[5]. In this section, the estimation of Kumaraswamy distribution parameters based on GOS using MLE will be derived. Furthermore, the estimation of Kumaraswamy distribution parameters based on OOS will be derived as special case when $k=1$ and $m=0$.

Theorem 3.1 Let $X(1,n,\vec{m},k)$, $X(2,n,\vec{m},k),\ldots,X(n,n,\vec{m},k)$ be *n* GOS for Kumaraswamy with parameters *p* and *q*, i.e. *X* has *kum(p,q)*. The estimation of Kumaraswamy distribution parameters based on GOS for *p* and *q* are given by

$$\hat{p}=-n\left[\sum_{i=1}^{n-1}\left(\frac{\ln x_i\left(1-\hat{q}\left(m_i+1\right)x_i^{\hat{p}}\right)}{1-x_i^{\hat{p}}}\right)+\frac{\ln x_n\left(1-qkx_n^{\hat{p}}\right)}{1-x_n^{\hat{p}}}\right]^{-1} \qquad (3.1)$$

and

$$\hat{q} = -n\left[\sum_{i=1}^{n-1}(m_i+1)\ln\left(1-x_i^{\hat{p}}\right)+k\,\ln\left(1-x_n^{\hat{p}}\right)\right]^{-1}, \qquad (3.2)$$

respectively.

Proof. The likelihood function for GOS for *kum(p,q)* is defined by

$$L(p,q;x) = k\left[\prod_{j=1}^{n-1}\gamma_j\right]\prod_{i=1}^{n-1}\left[\left(1-x_i^{\,p}\right)^{qm_i}\,pq\,x_i^{\,p-1}\left(1-x_i^{\,p}\right)^{q-1}\right]\left(1-x_n^{\,p}\right)^{q(k-1)}\times$$

$$pq\,x_n^{\,p-1}\left(1-x_n^{\,p}\right)^{q-1}$$

Collecting terms, $L(p,q;x)$ can be written as

$$L(p,q;x) = k\left[\prod_{j=1}^{n-1}\gamma_j\right]\left[\prod_{i=1}^{n-1}(1-x_i^{\,p})^{q(m_i+1)-1}pqx_i^{\,p-1}\right](1-x_n^{\,p})^{qk-1}pqx_n^{\,p-1} \qquad (3.3)$$

While this function in (3.3) is not all that hard to differentiate, it is much easier to differentiate the log likelihood. Now take logarithm on both sides of (3.3) to get

$$ln\left[L(p,q;x)\right] =$$

$$ln\,k + \sum_{j=1}^{n-1} ln\,\gamma_j + \sum_{i=1}^{n-1}\left[\left(q(m_i+1)-1\right)ln\left(1-x_i^{\,p}\right)+ln\,p+ln\,q+(p-1)ln\,x_i\right]$$

$$+(qk-1)ln\left(1-x_n^{\,p}\right)+ln\,p+ln\,q+(p-1)ln\,x_n$$

Take the first partial derivatives, with respect to p and q, and collecting terms, we find that

$$\frac{\partial ln\left[L(p,q;x)\right]}{\partial p} = \sum_{i=1}^{n-1}\left[\frac{\ln x_i\left(1-q(m_i+1)x_i^{\,p}\right)}{1-x_i^{\,p}}\right]+\frac{\ln x_n\left(1-qkx_n^{\,p}\right)}{1-x_n^{\,p}}+\frac{n}{p},\ \text{and}$$

$$\frac{\partial ln\left[L(p,q;x)\right]}{\partial q} = \sum_{i=1}^{n-1}\left[(m_i+1)\ln\left(1-x_i^{\,p}\right)\right]+k\,\ln(1-x_n^{\,p})+\frac{n}{q},$$

respectively.

Setting these first partial derivatives equal to zero and solving for p and q, yield the solution

$$\hat{p} = -n\left[\sum_{i=1}^{n-1}\left(\frac{\ln x_i\left(1-\hat{q}(m_i+1)x_i^{\hat{p}}\right)}{1-x_i^{\hat{p}}}\right)+\frac{\ln x_n\left(1-qkx_n^{\hat{p}}\right)}{1-x_n^{\hat{p}}}\right]^{-1},\ \text{and}$$

$$\hat{q} = -n\left[\sum_{i=1}^{n-1}(m_i+1)\ln\left(1-x_i^{\hat{p}}\right)+k\,\ln\left(1-x_n^{\hat{p}}\right)\right]^{-1},$$

respectively.

Evaluating the second derivative at $p=\hat{p}$ and $q=\hat{q}$ yield $\left.\frac{\partial^2 ln\left[L(p,q;x)\right]}{\partial p^2}\right|_{p=\hat{p}} = -\frac{n}{\hat{p}^2} < 0$, and $\left.\frac{\partial^2 ln\left[L(p,q;x)\right]}{\partial q^2}\right|_{q=\hat{q}} = -\frac{n}{\hat{q}^2} < 0$, then each of $\hat{p}$ and $\hat{q}$ is the local maximum, and since they are the only values obtained when the first partial derivatives are equal to zero, then $\hat{p}$ and $\hat{q}$ are the global maximum for the likelihood function $ln\left[L\left(p,q;x\right)\right]$. This completes the proof of the Theorem. □

Corollary 3.1 The estimation of Kumaraswamy distribution parameters based on OOS for p and q are given by

$$\hat{p} = -n\left(\sum_{i=1}^{n}\left[\frac{\ln x_i\left(1-\hat{q}x_i^{\hat{p}}\right)}{1-x_i^{\hat{p}}}\right]\right)^{-1}, \qquad (3.4)$$

and

$$\hat{q} = -n\left(\sum_{i=1}^{n}\ln\left(1-x_i^{\hat{p}}\right)\right)^{-1}, \qquad (3.5)$$

respectively.

Proof. Let $m=0$ and $k=1$ in (3.1), then $\hat{p} = -n\left[\sum_{i=1}^{n-1}\left[\frac{\ln x_i\left(1-\hat{q}x_i^{\hat{p}}\right)}{1-x_i^{\hat{p}}}\right]+\frac{\ln x_n\left(1-\hat{q}x_n^{\hat{p}}\right)}{1-x_n^{\hat{p}}}\right]^{-1}$ and collecting terms, we get (3.4).

Let $m=0$ and $k=1$ in (3.2), then $\hat{q} = -n\left[\sum_{i=1}^{n-1}\ln\left(1-x_i^{p}\right)+\ln\left(1-x_n^{\hat{p}}\right)\right]^{-1}$ and collecting terms, we get (3.5). This completes the proof of the Corollary. □

Equations (3.1), (3.2), (3.4) and (3.5) are complicated and consequently computer facilities and numerical solutions are needed to compute $\hat{p}$ and $\hat{q}$.

4 Simulation Study

In this section, since there are no closed forms for the estimation of Kumaraswamy distribution parameters, we consider the simulation technique for the estimation of Kumaraswamy distribution parameters p and q for different sample sizes. These simulations examine the sensitivity of estimation to different sample sizes. In particular, how do estimations perform for small, moderate and large sample sizes?

Definition 1. The efficiency of the parameter estimation for sample size n_1 relative to that of n_2 in terms of the Mean Squared Error (MSE) of the parameter p, $RE(\hat{p})$, is given by

$$RE(\hat{p}) = \frac{n_2 \sum_{i=1}^{r} \left(\hat{p}_{i.n_1} - p_{n_1}\right)^2}{n_1 \sum_{i=1}^{r} \left(\hat{p}_{i.n_2} - p_{n_2}\right)^2}, \qquad (4.1)$$

where r represents the number of simulations. Note that, p_{n_1} and p_{n_2} are the true parameters values for the two samples sizes n_1 and n_2, respectively. A ratio greater than one indicates that the parameter estimation for the sample size n_1 is less efficient than sample size n_2 estimate, and if $RE(\hat{p})$ is close to one, then the parameter estimation for the sample size n_1 is nearly as efficient as sample size n_2 estimate. We will look for different pairs of parameters for Kumaraswamy distribution that we can use to characterize the efficiency ratio, such as $p = q = 1$, $p = 1, q = 2$, $p = 2, q = 1$ and $p = q = 2$. We will try to find an answer to the following question: How robust are Kumaraswamy parameter estimations for different sample sizes?

4.1 The Simulation Setup

Three finite sample sizes (50, 200, and 500) and four values for the parameters p and q. We also generated a simulation of length 500 observations for each of the selected parameters; (p,q): (1,1), (1,2), (2,1) and (2,2).

4.2 The Simulation Results for $RE(\hat{p})$

Table (4.1) shows the complete simulation results for all selected parameters for Kumaraswamy distribution; (p,q): (1,1), (1,2), (2,1) and (2,2) for three finite sample small, moderate and large sizes (50, 200, and 500). The estimated values of the parameters and their corresponding MSEs are given. In addition, the ratios of parameter estimation p, $RE(\hat{p})$, for sample size n_1 relative to that of n_2 in terms of the mean squared error are shown.

Looking at the Table (4.1), we see that for the parameter $p = 1$, the relative efficiency of the MSE for estimating the parameter $p = 1$ with sample size 50 with respect to 200 equals 19.3. This means the parameter estimation error for small sample size ($n = 50$) is about 19 times for moderate sample size ($n = 200$). While the relative efficiency of the MSE for estimating the parameter $p = 1$ with sample size 50 with respect to 500 equals 113.0. This means the parameter estimation error for small sample size ($n = 50$) is about 113 times for large sample size ($n = 500$). This result is the worst performance

of small sample size selection as compared to large sample size for estimating the parameter p . In addition, the relative efficiency of the MSE for estimating the parameter $p=1$ with sample size 200 with respect to 500 equals 5.9. This means the parameter estimation error for moderate sample size ($n=200$) is about 6 times for large sample size ($n=500$). This result indicates that as the sample size increases the MSE of the estimated parameters decreases. This indicates that the MLE tend to its true parameters values. In other words, the estimation accuracy reaches its superiority as the sample size gets larger and larger. Results for the other sample sizes and different parameter choices for Kumaraswamy distribution demonstrate a similar pattern as shown in Table (4.1).

Table 4.1. Estimation of the Parameters for Kumaraswamy Distribution p and q for Different Sample Sizes

Parameters	Sample Size	$\hat{p}$	$MSE(\hat{p})$	$RE(\hat{p})$	$\hat{q}$	$MSE(\hat{q})$	$RE(\hat{q})$
p = q =1	50	1.00115	0.000379	19.3*	0.988747	0.000166691	6.2*
	200	0.994804	0.000020	113.0**	0.988783	0.000027	37.4**
	500	0.994319	0.000003	5.9***	0.985543	0.000004	6.1***
p = 1 , q = 2	50	0.852075	0.002560	17.9*	1.447103	0.020512	27.2*
	200	0.945802	0.000143	387.6**	1.767986	0.000755	173.9**
	500	0.971881	0.000007	21.7***	1.877155	0.000118	6.4***
p = 2 , q =1	50	1.638147	0.005442	7.9*	0.931092	0.000379	5.1*
	200	1.660116	0.000692	29.7**	0.893285	0.000074	9.6**
	500	1.718804	0.000183	3.8***	0.91861	0.000039	1.9***
p = q =2	50	1.320175	0.019067	50.4*	1.291178	0.050228212	77.1*
	200	1.852513	0.000379	299.5**	1.829603	0.000652	462.1**
	500	1.940557	0.000064	5.9***	1.894831	0.000109	6.0***

* RE estimate of n_1=50 relative to n_2=200.
**RE estimate of n_1=50 relative to n_2=500.
*** RE estimate of n_1=200 relative to n_2=500.

5. Conclusions

This paper deals with the estimation of Kumaraswamy distribution parameters using maximum likelihood estimators. Statistical estimation of Kumaraswamy distribution parameters have been derived based on generalized order statistics. Special cases are also deduced for ordinary order statistics. The resulting

equations are complicated and numerical solutions for parameters p and q is recommended. The simulation technique is discussed.

References

1. S. Abu El-Fotouh and M. Nassar. Estimation for the Parameters of the WeibullExtension Model Based on Generalized Order Statistics. *Int. J. Contemp. Math. Sciences*, 6, 36, 1749 – 1760, 2011.
2. M. Alkasasbeh and M. Raqab. Estimation of the Generalized Logistic Distribution Parameters: Comparative Study. *Statistical Methodology*, 6, 3, 262-279, 2009.
3. S. Ateya and A. Ahmad. Inferences based on generalized order statistics under truncated type I generalized logistic distribution, *Statistics,* 45, 389-402*,* 2011.
4. J. Carrasco, S. Ferrari and G. Cordeiro. A New Generalized Kumaraswamy Distribution, 2010.
5. G. Casella and R. Berger. *Statistical Inference*, second edition, Duxbury, California, 2002.
6. M. Habibullah and M. Ahsanullah. Estimation of parameters of a Pareto distribution by generalized order statistics, *Commun. Statist.-Theor. Meth., 29, 1597-1609,* 2000.
7. Z. Jaheen. Estimation based on generalized order statistics from the Burr model, *Commun. Statist.- Theor. Meth.,* 34, 785-794, 2005.
8. U. Kamps. A Concept of Generalized Order Statistics, *ELSEVIER Journal of Statistical planning and inference,* 48, 1995.
9. P. Kumaraswamy. A generalized probability density function for double bounded random processes. *Journal of Hydrology*. 46, 79-88, 1980.
10. P. Mitnik. New Facts About Kumaraswamy Distribution. Department of Sociology, University of Wisconsin-Madison, USA, 2008.
11. M. Raqab and M. Ahsanullah. Estimation of the location and scale parameters of the generalized exponential distributions based on order statistics. *J. Statist. Comput. Simul.* 69, 109- 123, 2001.

Proceedings, 15th Applied Stochastic Models and Data Analysis (ASMDA2013)
International Conference, Mataró (Barcelona), Spain 25 - 28 June 2013

The Coral Reefs Optimization Algorithm: An Efficient Meta-heuristic for Solving Hard Optimization Problems

S. Salcedo-Sanz[1], J. Del Ser[2], I. Landa-Torres[2], S. Gil-López[2], and A. Portilla-Figueras[1]

[1] Department of Signal Processing and Communications, Universidad de Alcalá, 28805 Alcalá de Henares, Madrid, Spain.
(E-mail: sancho.salcedo@uah.es)
[2] Tecnalia Research & Innovation. Parque Tecnológico de Bizkaia, 48170 Zamudio, Bizkaia, Spain.

Abstract. This paper presents a novel bio-inspired algorithm to tackle complex optimization problems: the Coral Reefs Optimization (CRO) algorithm. The CRO algorithm artificially simulates a coral reef, where different corals (namely, solutions to the optimization problem considered) grow and reproduce in coral colonies, fighting by choking out other corals for space in the reef. This fight for space, along with the specific characteristics of the corals' reproduction, produces a robust meta-heuristic algorithm, shown to be powerful for solving hard optimization problems. In this research the CRO algorithm is detailed and tested in several continuous and discrete optimization problems, obtaining advantages over other existing meta-heuristic techniques. The obtained results confirm the excellent performance of the proposed algorithm.
Keywords: Coral Reefs Optimization algorithm, optimization problems, modern meta-heuristics, bio-inspired algorithms.

1 Introduction

In the last years, huge research efforts have been conducted towards solving hard optimization problems, by well balancing the trade-off between the complexity incurred by the utilized method and the optimality of the produced solutions. These problems, often characterized by search spaces of high dimensionality (either discrete or continuous), non-linear objective functions and/or stringent constraints, arise frequently in Science and Engineering applications. In such fields, classical optimization approaches do not provide in general good solutions to these problems, or are just not applicable, due to the unmanageable search space structure or its huge size.

In this context, modern optimization heuristics and meta-heuristics have been lately the core of research, aimed at solving the aforementioned lack of efficient methods. A good number of such algorithms are *bio-inspired* techniques such as evolutionary algorithms (EA), which includes a whole family of techniques such as Genetic Algorithms [1], Evolutionary Strategies [2], Evolutionary Programming [3], Differential Evolution [4], among others. These schemes are based on concepts borrow from natural evolution and survival of the fittest individuals in Nature. Likewise, Ant Colonies Optimization (ACO) [5] are based

on the social behavior of ants, Particle Swarm Optimization (PSO) approaches [6] are in essence elegant algorithms specially well-suited for continuous optimization problems. They imitate the behavior of birds flocks or fish schools. There have been more research activity on bio-inspired meta-heuristics, with approaches such as Artificial Bee Colony [7], the Invasive Weed Optimization Algorithm (IWO), [8], based on weed growth and their invasive properties, or the so-called Cuckoo search approach [9], built upon the reproduction and breeding of the cuckoo bird, among others.

In this paper we present a novel bio-inspired meta-heuristic for optimization problems, which will be hereafter coined as the Coral Reefs Optimization (CRO) algorithm. The CRO algorithm is based on an artificial simulation of the process of coral reefs' formation and reproduction. During this process, the CRO algorithm emulates different phases of coral reproduction and fight for space in the reef, which ultimately renders an efficient algorithm for solving difficult optimization problems. The proposed CRO approach can be regarded as a cellular-type evolutionary scheme, with superior exploration-exploitation properties thanks to the particularities of the emulated reef structure and coral reproduction. The performance of the proposed approach has been tested in different benchmark problems obtaining very good results in comparison with alternative approaches in the literature.

The rest of this article is structured as follows: for the sake of self-completeness of the manuscript, the next section provides an introduction to coral reefs and corals' structure and reproduction. Next, Section 2 presents the CRO algorithm in detail, including an analysis of similarities and differences with other existing meta-heuristics. Section 3 shows the performance of the CRO algorithm in different optimization problems. Finally, Section 4 ends the paper by giving some concluding remarks.

2 The Coral Reefs Optimization algorithm

The CRO is a novel meta-heuristic approach based on corals' reproduction and coral reefs formation. Basically, the CRO is based on the artificial modeling of a coral reef, Λ, consisting of a $N \times M$ square grid. We assume that each square (i, j) of Λ is able to allocate a coral (or colony of corals) $\Xi_{i,j}$, representing a solution to a given optimization problem, which is encoded as a string of numbers in a given alphabet $\mathcal{I}$. The CRO algorithm is first initialized at random by assigning some squares in Λ to be occupied by corals (i.e. solutions to the problem) and some other squares in the grid to be empty, i.e. holes in the reef where new corals can freely settle and grow in the future. The rate between free/occupied squares in Λ at the beginning of the algorithm is an important parameter of the CRO algorithm, which is denoted as rho, and note that $0 < \rho_0 < 1$. Each coral is labeled with an associated *health* function $f(\Xi_{ij}) : \mathcal{I} \to \mathbb{R}$, that represents the problem's objective function. The CRO is based on the fact that reef will progress, as long as healthier (stronger) corals (which represent better solutions to the problem at hand) survive, while less healthy corals perish.

After the reef initialization described above, a second phase of reef formation is artificially simulated in the CRO algorithm: a simulation of the corals' reproduction in the reef is done by sequentially applying different operators. This sequential set of operators is then applied until a given stop criteria is met. Several operators to imitate corals' reproduction are defined, among them: a modeling of corals' sexual reproduction (broadcast spawning and brooding), a model of asexual reproduction (budding), and also some catastrophic events in the reef, i.e. polyps depredation. After the sexual and asexual reproduction, the set of larvae formed (new solutions to the problem), try to locate a place to grow in the reef. It could be in a free space, or in an occupied once, by fighting against the coral actually located in that place. If larvae are not successful in locate a place to grow in a given number of attempts, they are depredated in this phase. This second phase of the CRO can be detailed as follows:

1. *Broadcast Spawning (external sexual reproduction)*: the modeling of coral reproduction by *broadcast spawning* consists of the following steps:

   1.a. In a given step k of the reef formation phase, select uniformly at random a fraction of the existing corals ρ_k in the reef to be broadcast spawners. The fraction of broadcast spawners with respect to the overall amount of existing corals in the reef will be denoted as F_b. Corals that are not selected to be broadcast spawners (i.e. $1 - F_b$) will reproduce by brooding later on, in the algorithm.

   1.b. Select couples out of the pool of broadcast spawner corals in step k. Each of such couples will form a coral larva by sexual crossover, which is then released out to the water. Note that, once two corals have been selected to be the parents of a larva, they are not chosen anymore in step k (i.e. two corals are parents only once in a given step). These couple selection can be done uniformly at random or by resorting to any fitness proportionate selection approach (e.g. roulette wheel).

2. *Brooding (internal sexual reproduction)*: as previously mentioned, at each step k of the reef formation phase in the CRO algorithm, the fraction of corals that will reproduce by brooding is $1 - F_b$. The brooding modeling consists of the formation of a coral larva by means of a random mutation of the brooding-reproductive coral (self-fertilization considering hermaphrodite corals). The produced larva is then released out to the water in a similar fashion than that of the larvae generated in step 1.b.

3. *Larvae setting*: once all the larvae are formed at step k either through broadcast spawning (1.) or by brooding (2.), they will try to set and grow in the reef. First, the health function of each coral larva is computed. Second, each larva will randomly try to set in a square (i, j) of the reef. If the square is empty (free space in the reef), the coral grows therein no matter the value of its health function. By contrast, if a coral is already occupying the square at hand, the new larva will set only if its health function is better than that of the existing coral. We define a number κ of

attempts for a larva to set in the reef: after κ unsuccessful tries, it will be depredated by animals in the reef.

4. *Asexual reproduction*: in the modeling of asexual reproduction (budding or fragmentation), the overall set of existing corals in the reef are sorted as a function of their level of healthiness (given by $f(\Xi_{ij})$), from which a fraction F_a duplicates itself and tries to settle in a different part of the reef by following the setting process described in Step 3. Note that a maximum number of identical corals (μ) are allowed in the reef.

5. *Depredation in polyp phase*: corals may die during the reef formation phase of the CRO algorithm. At the end of each reproduction step k, a small number of corals in the reef can be depredated, thus liberating space in the reef for next coral generation. The depredation operator is applied with a very small probability P_d at each step k, and exclusively to a fraction F_d of the worse health corals in Λ. For the sake of simplicity in the parameter setting of the CRO algorithm, the value of this fraction may be set to $F_d = F_a$. Any other assignment may also apply provided that $F_d + F_a \leq 1$ (i.e. no overlap between the asexually reproduced and the depredated coral sets).

3 Experiments and Numerical Results

In this paper we carry out a first performance assessment of the proposed CRO algorithm in different test problems. Specifically, different well-known continuous and discrete benchmark problems are under consideration: continuous analytical functions and several instances of the *Max-Ones* and *3-bit Deceptive*.

We have selected other meta-heuristic algorithms for comparison: Evolutionary Algorithms, Genetic Algorithms (EA and GA, [1]) and Harmony Search (HS, [10]), which have obtained excellent results in a wide range of optimization problems during the last years. Regarding the continuous benchmark problems, we have compared the results obtained by the CRO in the same problems tackled in [11].

Following this rationale, the encoding strategy used to represent the produced solutions for the aforementioned problems is set identical for all the algorithms under comparison. Specifically, real encoding has been adopted for the continuous benchmark problems, whereas the *Max Ones* and *3-bit Deceptive* problems resort to standard binary encoding. On the other hand, values of all parameters controlling the CRO approach have been set to be comparable to that of its counterparts tested in every benchmark function. Therefore we have kept the number of function evaluations constant for all the compared algorithms in *Maxones* (15000), whereas for the *3-bit Deceptive* problem the total number of function evaluations is set to 50000 for GA and HS, and 30000 for the proposed CRO. In the continuous benchmark functions, we have set the number of function evaluations to be comparable with the results in [11]. For every simulation instance, 30 executions of each algorithm have been launched so as to obtain well-sampled performance statistics (best, average and standard

deviation of the metric after all iterations are done). Note that the size of the population – $N \times M$ for CRO, population length L for the GA, and harmony memory size HM for HS – have been set equal for all the experiments for the sake of fairness in the comparison of the algorithms: in the *Max Ones* problem $N \times M = 5 \times 10$, $L = 50$ and $HM = 50$ and in the *3-bit Deceptive* problem $N \times M = 10 \times 10$, $L = 100$ and $HM = 100$. The CRO parameters F_b and ρ has been set to $F_b = 0.9$ and $\rho = 0.7$, unless otherwise stated in the discussion on the specific simulated application.

3.1 CRO Evaluation in Continuous Benchmark Problems

This first round of experiments includes four well-known benchmark functions, on which the proposed CRO is comparatively assessed with respect to different hybrid evolutionary algorithms described in [11]. In these experiments we have incorporated Gaussian and Cauchy mutations [3] in the internal reproduction (brooding) of the corals in order to accommodate the corresponding operator to the real encoding of the solutions. In the Gaussian mutation we have established a fixed standard deviation $\sigma = (max - min)/100$, where max and min are the maximum and minimum values that each component of the solution can take, whereas in the Cauchy mutation the value of the τ parameter has been fixed to 1 following the guidelines in [3]. The rest of operators in the CRO are the ones shown in Section 2.

Table 1 lists the results obtained by three different versions of the CRO (with Gaussian, Cauchy and Gaussian-Cauchy internal reproduction) in the benchmark functions tackled in this first round of experiments. Also included are the results for different versions of the hybrid evolutionary algorithm proposed in [11], labelled as Hybrid Adaptive Evolutionary Algorithm (HAEA) in what follows. It is straightforward to note that the CRO approach is able to obtain better results than the different versions of HAEA consistently – and with statistical significance positively checked through Kruskal-Wallis tests – in all the functions under consideration. The inclusion of both Gaussian and Cauchy mutations in the brooding coral reproduction (always maintaining the number of functions evaluations) appears to improve the performance of the CRO solver.

3.2 CRO Evaluation in Discrete Benchmark Problems

The first discrete benchmark problem considered is the well-known *Max Ones* problem, often used in a number of previous works aimed at evaluating different approaches of genetic algorithms (e.g. see [**?**,11] and references therein). This optimization problem is defined in a binary search space $\mathcal{S} = \{0, 1\}^n$, where n stands for the dimension of the space. The *One Max* problem is then defined as

$$\max_{\mathbf{x} \in \mathcal{S}} f(\mathbf{x}) = \frac{100}{n} \sum_{i=1}^{n} x_i \qquad [\%]. \tag{1}$$

Table 1. Results (mean/standard deviation) obtained in the different continuous benchmark functions tested.

Algorithm	Rosenbrock	Schwefel	Rastrigin	Griewank
CRO (G)	$7.0 \cdot 10^{-5}/5.0 \cdot 10^{-6}$	$1.3 \cdot 10^{-4}/2.0 \cdot 10^{-6}$	$7.1 \cdot 10^{-3}/3.0 \cdot 10^{-3}$	0.22/0.05
CRO (C)	$7.2 \cdot 10^{-5}/5.6 \cdot 10^{-6}$	$1.3 \cdot 10^{-4}/1.6 \cdot 10^{-6}$	$6.7 \cdot 10^{-3}/2.3 \cdot 10^{-3}$	0.03/0.02
CRO (G+C)	$2.3 \cdot 10^{-5}/1.0 \cdot 10^{-6}$	$1.3 \cdot 10^{-4}/1.4 \cdot 10^{-6}$	$4.3 \cdot 10^{-3}/1.5 \cdot 10^{-3}$	0.05/0.02
HAEA (XUG)	$7.0 \cdot 10^{-4}/1.0 \cdot 10^{-5}$	$5.6 \cdot 10^{-3}/0.01$	0.05/0.02	0.055/0.03
HAEA (XU)	$4.1 \cdot 10^{-3}/4.0 \cdot 10^{-3}$	1.3/0.93	0.24/0.15	0.5/0.2
HAEA (XG)	$1.3 \cdot 10^{-3}/3.6 \cdot 10^{-3}$	140.5/123.7	7.7/3.2	0.05/0.02
HAEA (GU)	$1.4 \cdot 10^{-4}/2.5 \cdot 10^{-3}$	201.9/81.2	6.3/1.4	1.6/0.38

Despite the evident simplicity of its definition, this problem is challenging for optimization algorithms when dealing with large values of the space dimensionality n.

Table 2 summarizes the results (maximum, average and standard deviation) obtained by CRO, GA and HS in *Max Ones* instances of varying size from $n = 50$ to $n = 500$. As one may expect, in the scenarios of smallest dimension all the utilized heuristic approaches are able to obtain the optimum solution (100%) in every run of the algorithm. However, when the dimensions of the simulated problem increase, the differences between the CRO and the other tested algorithms become more significant. Specially remarkable is the fact that the CRO obtains the best value in all the instances with a very high probability (over 99% of the times in which the algorithm was run). HS also obtains good solutions, but notably worse than the GA even in the smallest instances. By contrast, the CRO clearly dominates GA and HS, specially in the largest *Max Ones* instances.

Table 2. Results obtained by CRO, GA and HS in *Max Ones* problems of increasing size. The results are shown in best/average/standard deviation over 30 runs of the algorithms.

n	CRO	GA	HS
50	100/100/0	100/100/0	100/100/0
100	100/100/0	100/100/0	98/95.67/0.92
150	100/100/0	100/100/0	94.67/90.84/1.13
200	$100/99.98/9.12 \cdot 10^{-4}$	100/99.93/0.17	90/87.32/0.88
250	$100/99.97/7.3 \cdot 10^{-4}$	100/99.81/0.25	86.80/84.64/1.04
300	$100/99.96\ /8.45 \cdot 10^{-4}$	100/99.61/0.39	83.67/82.0700/0.62
350	$100/99.96/9.8 \cdot 10^{-4}$	100/99.21/0.46	81.4300/80.03/0.71
400	$100/99.95/7.3 \cdot 10^{-4}$	99.50/98.67/0.58	79.50/78.45/1.04
450	100/99.93/0.13	99.55/98.11/0.67	78.67/76.97/0.99
500	100/99.92/0.1	98.60/97.04/0.75	78/75.99/0.69

The second discrete benchmark problem addressed is the maximization of the aforementioned *3-bit Deceptive* function, which has been previously utilized to evaluate different improvements in genetic and evolutionary heuristics [11]. The 3-bit deceptive function is a binary optimization problem defined in blocks of 3 bits. Each 3-bit block is assigned a value according to Table 3. The optimization of the function is known to be computationally hard for heuristic algorithms, since the `111` block (optimum since it is assigned the highest value) is "surrounded" by low-valued blocks of two 1s (i.e. with small Hamming distance with respect to `111`). Different size functions (integer multiple of 3) are considered in this study, i.e. $n = \{15, 30, 45, 60, 75, 90, 105, 120\}$.

Table 4 shows the results obtained by the CRO in the considered 3-bit Deceptive functions, and its comparison to those of HS and GA. In this problem the CRO clearly obtains the best results among all the compared algorithms. Indeed, it is able to obtain the optimum (maximum) value in all the instances and in almost every executed run. The performance of the alternative algorithms degrades significantly in the largest instances, though in the smallest ones the GA is able to obtain the optimum value.

Table 3. Value assignment in the considered *3-bits Deceptive* function.

Groups of 3 bits	Value
1 1 1	80
0 0 0	70
0 0 1	50
0 1 0	49
1 0 0	30
1 1 0	3
1 0 1	2
0 1 1	1

Table 4. Results obtained by CRO, HS and GA in the considered *3-bit Deceptive* instances. The results are shown in best/average/standard deviation over 30 runs of the algorithms.

n	CRO	HS	GA	Upper Bound
15	400/400/0	400/399.66/1.82	400/400/0	400
30	800/800/0	800/792/8.05	800/795/6.82	800
45	1200/1200/0	1190/1159/14.93	1200/1179.3/13.37	1200
60	1600/1600/0	1560/1517.3/21.96	1590/1562.70/18.74	1600
75	2000/2000/0	1910/1882/20.97	1990/1940.30/22.04	2000
90	2400/2400/0	2280/2243/22.63	2340/2297.30/21.16	2400
105	2800/2799.70/1.82	2660/2598.80/34.20	2730/2687.70/27.75	2800
120	3200/3200/0	2990/2924.8/37.90	3090/3049/21.22	3200

4 Conclusions

In this paper we have presented a novel algorithm to solve optimization problems, inspired by the process of coral reefs formation, and guided by coral reproduction, reef expansion and fight for the space in the reef. The algorithm, named as the Coral Reef Optimization (CRO) algorithm, is a kind of cellular evolutionary algorithm rendering very good properties of convergence to global optima. In this paper we have studied the main characteristics of the proposed CRO and analyzed its comparison to other existing meta-heuristic approaches in different benchmark problems. The promising obtained results encourage the application of the proposed CRO approach to other practical optimization paradigms of high complexity.

Acknowledgements

This work has been partially supported by Spanish Ministry of Science and Innovation, under project number ECO2010-22065-C03-02.

References

1.A. E. Eiben and J. E. Smith, "Introduction to evolutionary computing," Springer-Verlag, Natural Computing Series 1st edition, 2003.
2.H. G. Beyer and H. P. Schwefel, "Evolution strategies - A comprehensive introduction," *Natural Computing*, vol. 1, no. 1, pp. 3-52, 2002.
3.X. Yao, Y. Liu and G. Lin, "Evolutionary Programming made faster," *IEEE Transactions on Evolutionary Computation*, vol. 3, no. 2, pp. 82-102, 1999.
4.R. Storn and K. Price, "Differential Evolution - A simple and efficient heuristic for global optimization over continuous spaces," *Journal of Global Optimization*, vol. 11, pp. 341-359, 1997.
5.M. Dorigo, V. Maziezzo and A. Colorni, "The ant system: optimization by a colony of cooperating ants," *IEEE Transactions on Systems, Man and Cybernetics B*, vol. 26, no. 1, pp. 29-41, 1996.
6.J. Kennedy and R. Eberhart, "Particle swarm optimization," in *Proc. of the 4th IEEE International Conference on Neural Networks*, pp. 1942-1948, 1995.
7.D. Karaboga and B. Basturk, "On the performance of the artificial bee colony (ABC) algorithm," *Applied Soft Computing*, vol. 8, pp. 687-697, 2008.
8.A. R. Mehrabian and C. Lucas, "A novel numerical optimization algorithm inspired from weed colonization," *Ecological Informatics*, vol. 1, pp. 355-366, 2006.
9.X. S. Yang and S. Deb, "Cuckoo search via Lévy flights," in *Proc. of the World Conference on Nature & Biologically Inspired Computing*, pp. 210-214, 2009.
10.Z. W. Geem, J. Hoon Kim and G. V. Loganathan, A New Heuristic Optimization Algorithm: Harmony Search, *Simulation*, vol. 76, no. 2, 2001. 60-68.
11.J. Gómez, "Self Adaptation of operator rates in evolutionary algorithms," GECCO 2004, *Lecture Notes in Computer Science*, vol. 3102, pp. 1162-1173, 2004.

Proceedings, 15th Applied Stochastic Models and Data Analysis (ASMDA2013)
International Conference, Mataró (Barcelona), Spain 25 - 28 June 2013

Estimating the Density and Hazard Rate Functions Using the Reciprocal Inverse Gaussian Kernel

Raid B. Salha
Department of Mathematics, The Islamic University, Gaza, Palestine
rbsalha@iugaza.edu.ps

Abstract. In this paper, we use the Reciprocal Inverse Gaussian (RIG) kernel to estimate nonparametrically the probability density function (pdf) and the hazard rate function for independent and identically distributed (iid) data. The estimator uses adaptive weights depending on the points at which we estimate the functions. We derive the strong consistency, the asymptotic normality and the asymptotic mean squared error (AMSE) of the proposed estimator. Also, the selection of the optimal bandwidth is investigated. The performance of the proposed estimator is compared to that of the Gaussian kernel.

Keywords: Reciprocal Inverse Gaussian kernel, hazard rate function, kernel estimation, asymptotic mean squared error, boundary bias.

2000 MSC: 62G07, 62G08

1 Introduction

Estimators of the hazard rate function based on kernel estimation have been studied extensively in literature. For example, see Watson and Leadbetter [7], Rice and Rosenblatt [2] and Salha [4, 5]. However, when the support of the curve under estimation is bounded, many nonparametric estimators appear to be biased more than the usual in regions near the endpoints. Boundary bias is due to weight allocation by the fixed symmetric kernel outside the density support when smoothing is carried out near the boundary. To solve this problem, boundary kernels are used only within the boundary region. This is an efficient way to correct boundary bias but it requires complicated adjustments to the estimator. To solve this problem, Chen [1] has replaced the symmetric kernels by asymmetric Gamma kernel which never assigns weight outside the support.

In Salha [4], the estimation of the hazard rate function using the Inverse Gaussian (IG) kernel has been considered. In this paper, we consider the RIG kernel estimation of the hazard rate function. As Gamma kernel estimator, the RIG kernel estimator is free of boundary bias, always non-negative and achieves the optimal rate of convergence for the mean integrated squared error (MISE) within the class of nonnegative kernel density estimators, see Scaillet [3].

This paper is organized as follows. In Section 2, some basic definitions and conditions are stated. In Section 3, the main results of this paper are stated and proved. The AMSE of the proposed estimator and the selection of the optimal bandwidth are investigated in Section 4. In Section 5, the performance of the proposed estimator is tested and compared to that of the Gaussian kernel estimator. Section 6, contains some concluding remarks.

2 Preliminaries

In this section, we state the conditions under which the results of this paper will be proved. Also, we introduce some basic definitions.

Conditions

1. Let $X_1, X_2, ..., X_n$ be a random sample from a distribution with an unknown probability density function f defined on $[0,\infty)$, such that f is twice continuously differentiable, and $\int_0^\infty \left(x^3 f''(x)\right)^2 dx < \infty$.
2. h is a smoothing parameter satisfying $h + \frac{1}{nh} \to 0$, and $nh^{\frac{5}{2}} \to 0$, as $n \to \infty$.

Definition 1. Scaillet [3] defined the RIG kernel estimator of the pdf $f(\cdot)$,

$$\hat{f}_{RIG}(x) = \frac{1}{n}\sum_{i=1}^{n} K_{RIG}\left(\frac{1}{x-h}, \frac{1}{h}\right)(X_i), \text{ where} \quad (1)$$

$$K_{RIG}\left(\frac{1}{x-h}, \frac{1}{h}\right)(u) = \frac{1}{\sqrt{2\pi h\, u}} \exp\left(-\frac{x-h}{2h}\left(\frac{u}{x-h} - 2 + \frac{x-h}{u}\right)\right). \quad (2)$$

Definition 2. Let X be a random variable with pdf $f(x)$ and cdf $F(x)$, the hazard rate function $r(x)$ of X is defined as

$$r(x) = \lim_{\Delta x \to 0} \frac{P(X \le x + \Delta x \mid X > x)}{\Delta x} = \frac{f(x)}{S(x)}, \; x > 0, \text{ where}$$

$S(\cdot) = 1 - F(\cdot)$ is called the survivor function.

Definition 3. The proposed kernel estimator for the hazard rate function is given by $\hat{r}_{RIG}(x) = \frac{\hat{f}_{RIG}(x)}{\hat{S}_{RIG}(x)}$, where $\hat{S}_{RIG}(x) = 1 - \int_0^x \hat{f}_{RIG}(u)\,du$.

Lemma 1. Under the conditions (1) and (2), the following hold

(i) $Bias\left(\hat{f}_{RIG}(x)\right) = \frac{1}{2} x f''(x) h + o(h)$.

(ii) $Var\left(\hat{f}_{RIG}(x)\right) = \frac{1}{2n\sqrt{\pi h}} x^{-\frac{1}{2}} f(x) + o(n^{-1}h^{-\frac{1}{2}})$.

Proof. See Proposition 1 and 2 in Scaillet [3].

3. Main Results

The asymptotic normality of the RlG kernel estimator of the pdf is given in Theorem 1.

Theorem 1. Under the conditions (1) and (2), the following holds

$$\sqrt{nh^{\frac{1}{2}}}(\hat{f}_{RIG}(x)-f(x))\xrightarrow{d}N\left(0,\frac{1}{2\sqrt{\pi}}x^{-\frac{1}{2}}f(x)\right).$$

Proof. Let $V_{ni}=K_{IG}(x,\frac{1}{h})(X_i)$, $i=1,2,...,n$, then $\hat{f}(x)=\frac{1}{n}\sum_{i=1}^{n}V_{ni}$.
Now, we show that Liapounov condition is satisfied, that is for some $\delta>0$,

$$\lim_{n\to\infty}\frac{E\,|V_n-E(V_n)|^{2+\delta}}{n^{\frac{\delta}{2}}\sigma^{2+\delta}(V_n)}=0.$$

Let η_x be a $RIG(\frac{1}{x-h},\frac{2+\delta}{h})$ distributed random variable. Hence

$$\mu_x=E(\eta_x)=x-h+\frac{h}{2+\delta}\text{ and }T_x=Var(\eta_x)=\frac{(x-h)h}{2+\delta}+\frac{2h^2}{(2+\delta)^2}.$$

$$E\,|V_n|^{2+\delta}=E\left[\left(\frac{1}{\sqrt{2\pi hy}}\right)^{2+\delta}\exp\left(-\frac{(2+\delta)(x-h)}{2h}\right)\left(\frac{y}{x-h}-2+\frac{x-h}{y}\right)\right]$$

$$=\frac{\sqrt{2\pi h}}{\sqrt{2+\delta}(2\pi h)^{1+\frac{\delta}{2}}}E\left(\eta_x^{-\frac{3}{2}(1+\delta)}f(\eta_x)\right).$$

By using the Taylor's series to expand $f(\eta_x)$ about μ_x, we obtain

$$E\left(\eta_x^{-\frac{3}{2}(1+\delta)}f(\eta_x)\right)=x^{-\frac{3}{2}(1+\delta)}f(x)+\frac{1}{2}(x^{-\frac{3}{2}(1+\delta)}f''(x)-\frac{3}{2}x^{-\frac{5}{2}(1+\delta)}f'(x)$$

$$-\frac{3}{2}x^{-\frac{5}{2}(1+\delta)}f'(x)+\frac{15}{4}x^{-\frac{7}{2}(1+\delta)}f(x))x^3h+o(h)$$

$$=x^{-\frac{3}{2}(1+\delta)}f(x)+o(h).$$

This implies that

$$\mathrm{E}|\mathrm{V_n}|^{2+\delta} = \frac{1}{\sqrt{2+\delta}\,(2\pi \mathrm{h})^{\frac{1+\delta}{2}}}\, x^{-\frac{3}{2}(1+\delta)} f(x) + o\left(h^{-\frac{(1+\delta)}{2}}\right) \to 0.$$

Lemma 2. Under the conditions (1) and (2), the following holds

$$\sqrt{nh^{\frac{1}{2}}}\,|\hat{F}(x) - F(x)| \xrightarrow{p} 0.$$

Proof. From the definition of $\hat{F}(x)$, the following Relations (3) and (4) hold.

$$E\hat{F}(x) = \int_0^{\infty}\int_0^{x} K_{RIG}\left(\frac{1}{u-h}, \frac{1}{h}\right)(y)\,du\, f(y)\,dy = \int_0^{x} E(f(\xi_u))\,du$$

$$= \int_0^{x} \left(f(u) + \frac{1}{2} u f''(u)\, h\right) du + o(h) = F(x) + o(h).$$

This implies that,

$$\sqrt{nh^{\frac{1}{2}}}\,|E\hat{F}(x) - F(x)| = o\left((nh^{\frac{5}{2}})^{\frac{1}{2}}\right) \to 0. \qquad (3)$$

Now, $\hat{F}(x)$ can be written in the following form

$$\hat{F}(x) = \frac{1}{n}\sum_{i=1}^{n}\int_0^{x} K_{RIG}\left(\frac{1}{u-h}, \frac{1}{h}\right)(X_i)\,du = \frac{1}{n}\sum_{i=1}^{n} W_i(x).$$

Let $\varepsilon > 0, \delta > 0$ be given.

$$P\left[(nh^{\frac{1}{2}})^{\frac{1}{2}}\,|\hat{F}(x) - EF(x)| > \varepsilon\right] \le \varepsilon^{-2-2\delta}(nh^{\frac{1}{2}})^{1+\delta} E\,\left|\frac{1}{n}\sum_{i=1}^{n}\left[W_i(x) - EW_i(x)\right]\right|^{2+\delta}$$

$$= \varepsilon^{-2-2\delta} h^{\frac{1+\delta}{2}} n^{-1-\delta} E\,\left|\sum_{i=1}^{n}\left[W_i(x) - EW_i(x)\right]\right|^{2+\delta} \le 2^{1+\delta}\varepsilon^{-2-2\delta}(n^{-1}h^{\frac{1}{2}})^{1+\delta}\sum_{i=1}^{n} E\,|W_i(x)|^{2+2\delta}$$

$$+2^{1+\delta}\varepsilon^{-2-2\delta}(n^{-1}h^{\frac{1}{2}})^{1+\delta}\sum_{i=1}^{n}|EW_i(x)|^{2+2\delta} \to 0.$$

This implies that,

$$\sqrt{nh^{\frac{1}{2}}}\,|\hat{F}(x) - EF(x)| \xrightarrow{p} 0. \qquad (4)$$

Now, using Relations (3), (4) and the following fact,

$|\hat{F}(x) - F(x)| \le |\hat{F}(x) - E\hat{F}(x)| + |E\hat{F}(x) - F(x)|$, we obtain that

$$\sqrt{nh^{\frac{1}{2}}}\,|\hat{F}(x) - F(x)| \le \sqrt{nh^{\frac{1}{2}}}\,|\hat{F}(x) - E\hat{F}(x)| + \sqrt{nh^{\frac{1}{2}}}\,|E\hat{F}(x) - F(x)| \xrightarrow{p} 0.$$

This completes the proof of the lemma. □

Now, the asymptotic normality of the proposed etimator is given in Theorem 2.

Theorem 2. Under the conditions (1) and (2), the following holds

$$\sqrt{nh^{\frac{1}{2}}}\left(\hat{r}(x)-r(x)\right)\xrightarrow{d}N\left(0,\frac{1}{2\sqrt{\pi}}x^{-\frac{1}{2}}\frac{r(x)}{S(x)}\right).$$

Proof.

$$\begin{aligned}\sqrt{nh^{\frac{1}{2}}}\left(\hat{r}(x)-r(x)\right)&=\sqrt{nh^{\frac{1}{2}}}\left(\frac{\hat{f}(x)}{\hat{S}(x)}-\frac{f(x)}{S(x)}\right)\\&=\sqrt{nh^{\frac{1}{2}}}\left(\frac{\hat{f}(x)}{\hat{S}(x)}-\frac{f(x)}{\hat{S}(x)}-\frac{f(x)}{S(x)}+\frac{f(x)}{\hat{S}(x)}\right)\\&=\frac{\sqrt{n\,h^{\frac{1}{2}}}}{\hat{S}(x)}\left[\hat{f}(x)-f(x)\right]+\frac{\sqrt{n\,h^{\frac{1}{2}}}f(x)}{S(x)\hat{S}(x)}\left[\hat{S}(x)-S(x)\right].\end{aligned}\quad(5)$$

The proof is completed by a combination of Theorem 1, Lemma 2 and Equation (5). Since by Theorem 1, the first term in Equation (5) is asymptotically normally distributed and the second term vanishes by Lemma 2. □

From Theorem 1 and 2, we get that

$$E\left(\hat{r}(x)\right)=\frac{E\left(\hat{f}(x)\right)}{E\left(\hat{S}(x)\right)}=\frac{f(x)+\frac{1}{2}xf''(x)h}{S(x)}+o(h)=r(x)+\frac{\frac{1}{2}xf''(x)h}{S(x)}+o(h).$$

This implies that

$$Bias\left(\hat{r}(x)\right)=\frac{\frac{1}{2}xf''(x)h}{S(x)}+o(h)\text{ and }Var\left(\hat{r}(x)\right)=\frac{1}{2n\sqrt{\pi h}}x^{-\frac{1}{2}}\frac{r(x)}{S(x)}+o(n^{-1}h^{-\frac{1}{2}}).$$

4 Bandwidth Selection

The selection of the bandwidth in kernel estimation plays an important role. It depends on choosing a value of the bandwidth that minimizes the AMSE. Using the same techniques of Scaillet [3], the AMSE is given by

$$\text{AMSE} = \left(\frac{\frac{1}{2} x f''(x) h}{S(x)} \right)^2 + \frac{1}{2n\sqrt{\pi h}} x^{-\frac{1}{2}} \frac{r(x)}{S(x)}. \qquad (6)$$

Differentiate the AMSE with respect to h, the n equating it to zero, we obtain

$$2 \left(\frac{\frac{1}{2} x f''(x)}{S(x)} \right)^2 h - \frac{1}{2n\sqrt{\pi}} x^{-\frac{1}{2}} \frac{r(x)}{S(x)} \frac{1}{2} h^{-\frac{3}{2}} = 0. \qquad (7)$$

Multiplying Equation (7) by $h^{\frac{3}{2}}$, and solving for h, we obtain

$$h = \left(\frac{1}{2\sqrt{\pi}} \frac{r(x)}{(f''(x))^2} \right)^{\frac{2}{5}} x^{-\frac{3}{5}} n^{-\frac{2}{5}}. \qquad (8)$$

5 Applications

In this section, the performance of the proposed estimator in estimating the pdf and hazard rate function is tested upon two applications. For comparison purposes we also estimate the two functions using the Gaussian kernel estimator. For the practical implementation of the RIG estimator, we used the bandwidth selection procedure described in Section 4 and for the Gaussian estimator, we used Equation (3.28) in Silverman [6].

5.1 Real Data

In this subsection, we use the suicide data given in Silverman [6], to exhibit the practical performance of the RIG estimator. The data gives the lengths of the treatment spells (in days) of control patients in suicide study. Figures 1(a) and 1(b) show the two estimators of the probability density and hazard rate functions, respectively. Although the suggested values of the density and hazard rate functions from the two estimators are different, they both suggest a similar structure for the two estimated functions. As we see, the divergence of the two estimators gets large at the boundary near the zero and becomes smaller in the interior especially from approximately $t \geq 250$.

5.2 A Simulation Study

A sample of size 200 from the exponential distribution with pdf $f(x) = e^{-x}$ is simulated. After that the density function and the hazard rate functions were estimated using the RIG and the Gaussian estimators. The estimated values and

the true functions are plotted in Figures 2(a) and 2(b), respectively. The two figures show that the performance of the RIG estimator is better than that of the Gaussian estimator at the boundary near the zero. In the interior the behavior of the two estimators becomes more similar as we get away from the zero.

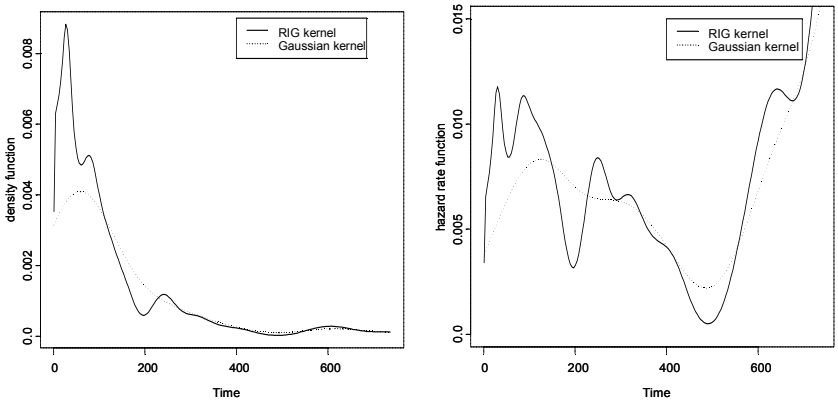

(a) (b)

Fig.1: The RIG and Gaussian kernel estimators of (a) the density function (b) the hazard rate function for the suicide data.

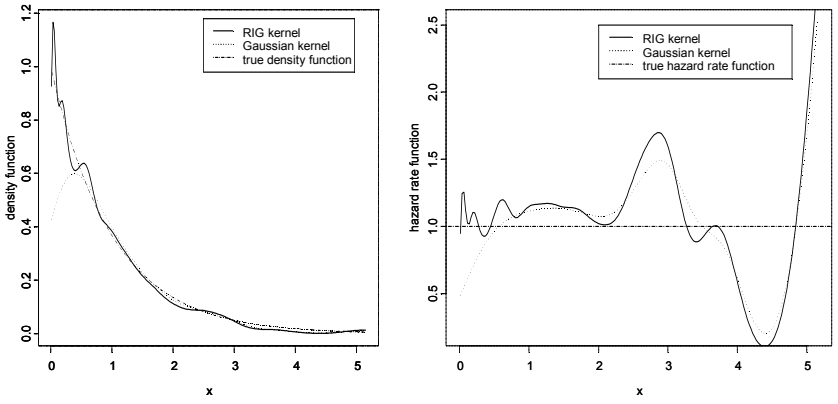

(a) (b)

Fig. 2: The RIG and Gaussian kernel estimators of (a) the density function (b) the hazard rate function for the simulated data of the exponential distribution

6. Comments and Conclusion

In this paper, we have proposed a new kernel estimator of the hazard rate function for (iid) data based on the RIG with nonnegative support which was proposed by Scaillet [3]. The proposed estimator overcomes the bias problem when the hazard rate function is estimated at the boundary region near the zero.

The asymptotic normality, the strong consistency and the AMSE of the proposed estimator were obtained. The AMSE of the new estimator is smaller than that of the Gaussian kernel near the zero.

Two applications show that the performance of the proposed estimator is better than that of the Gaussian kernel estimator at the boundary region near the zero. This is due to weight allocation by the Gaussian kernel outside the density support when smoothing is carried out at the boundary near the zero.

The new estimator can be modified by considering a new bandwidth selection technique that uses a variable bandwidth that depends on the points at which the hazard rate function is estimated rather than a constant bandwidth.

References

1. Chen, S. X. (2000). Probability density function estimation using gamma kernels. Ann. Inst. Stat. Math., 52, 471- 480.

2. J. Rice and M. Rosenblatt (1976). Estimation of the log survivor function and hazard function. Sankhya Series A 38, 60-78.

3. O. Scaillet (2004). Density estimation using inverse and reciprocal inverse Gaussian kernels. Nonparametric Statistics, 16, 217-226.

4. Salha, R. (2012). Hazard rate function estimation using inverse Gaussian kernel. The Islamic university of Gaza journal of Natural and Engineering studies, 20(1), 73-84.

5. Salha, R (2009). Adaptive kernel estimation of the hazard rate function. The Islamic university of Gaza Journal of Natural and Engineering studies,17(1), 71-81.

6. Silverman, B. W. (1986). Density estimation for statistics and data analysis. Chapman and Hall, London.

7. Watson, G. and Leadbetter, M. (1964). Hazard analysis I, Biometrika, 51, 175-184.

Proceedings, 15th Applied Stochastic Models and Data Analysis (ASMDA2013)
International Conference, Mataró (Barcelona), Spain 25 - 28 June 2013

Incorporating the Stochastic Process Setup in Parameter Estimation

Lino Sant[1] and Mark Anthony Caruana[2]

[1] Department of Statistics and Operations Research, Faculty of Science, University of Malta, Msida, Malta
(E-mail: lino.sant@um.edu.mt)
[2] Department of Statistics and Operations Research, Faculty of Science, University of Malta, Msida, Malta
(E-mail: mark.caruana@um.edu.mt)

Abstract. Estimation problems within the context of stochastic processes are usually studied with the help of statistical asymptotic theory and proposed estimators are tested with the use of simulated data. For processes with stationary increments it is customary to use differenced time series, treating them as selections from the increments' distribution. Though distributionally correct, this approach throws away most information related to the stochastic process setup. In this paper we consider the above problems with reference to parameter estimation of a gamma process. Using the derived bridge processes we propose estimators whose properties we investigate in contrast to the gamma-increments MLE. The proposed estimators have a smaller bias, comparable variance and offers a look at the time-evolution of the parameter estimation. Empirical results are presented.
Keywords: Lévy processes, gamma process, bridge process, Dirichlet distribution.

1 Introduction

The estimation of stochastic models to fit to data obtained from real systems borrows a lot from statistical estimation theory, but arguably not enough from the theory of stochastic processes. In many papers dedicated to the estimation of Lévy processes, the estimation is understandably restricted to the estimation of either the parameters of the infinitely divisible distribution of the increments or else to the Lévy measure. Clearly both characterize completely the distributional framework of the corresponding processes. However there are other static and dynamical statistical properties which are of interest to look into in practical applications.
In this paper we study the gamma process with the aim of tackling estimation issues using stochastic properties other than the stationary gamma increments. In particular, we consider the problems of estimator bias and minimization of estimator variance.
The gamma process has been much studied because of its common use in climate and hydrology related modelling exercises Thom [10] and more recently also in finance Avramidis et al. [1].
Let us denote the gamma process by $(G_t)_{t\in\mathbb{R}_+}$. The overall distributional structure of this process is underpinned by the independently gamma distributed increments with parameters α, λ. For $G_{t_1}, G_{t_2}-G_{t_1}, \ldots, G_{t_n}-G_{t_n}$ we have

the joint density function:

$$f(x_1, x_2, \ldots, x_n) = \frac{x_1^{\alpha t_1 - 1} x_2^{\alpha(t_2 - t_1)-1} \ldots x_n^{\alpha(t_n - t_{n-1})-1} \exp\left(\frac{-(x_n - x_1)}{\lambda}\right)}{\Gamma(at_1)\Gamma(a(t_2 - t_1)) \ldots \Gamma(\alpha(t_n - t_{n-1})\lambda^{\alpha(t_n - t_1)})} \quad (1)$$

So letting $Z_i = G_{t_i} - G_{t_{i-1}}$ the form above is exploited in maximum likelihood estimation applied on the increments $Z_1, Z_2, \ldots, Z_n$ which are treated as independent gamma random variables. This approach blurs out the stochastic process context.
The maximum likelihood estimator is not just a venerable tool for estimation, but a superior one on many counts. Its more important virtues are of course asymptotic normality, consistency, asymptotic efficiency and functional invariance. Nevertheless it is also known to exhibit defects, one of which is biasedness in the case of the gamma distribution. We would like to tackle this problem through the use of other estimators which make use of intrinsic properties of the gamma process.

2 The gamma bridges and their derived estimators

The gamma bridge process $(G_{tT})_{0 \leq t \leq T}$ on the time interval $[0, T]$ is derived from the gamma process by :

$$G_{tT} = \frac{G_t}{G_T} \quad (2)$$

The gamma bridge has some nice independence properties as discussed by Emery and Yor [9]. We propose the following construction of bridges. Given two time points t_1 and t_n, the time interval in between is partitioned as: $\{t_1, t_2, \ldots, t_n\}$. Now for any two intermediate time points, $0 \leq t_i < t_j \leq t_n$ the random variables $(G_{t_j} - G_{t_i})/(G_{t_n} - G_{t_1})$ and $G_{t_n} - G_{t_1}$ are independent. Furthermore standard theory as in Ferguson [8] tells us that the following random vector

$$\left(\frac{G_{t_2} - G_{t_1}}{G_{t_n} - G_{t_1}}, \frac{G_{t_3} - G_{t_2}}{G_{t_n} - G_{t_1}}, \ldots, \frac{G_{t_n} - G_{t_{n-1}}}{G_{t_n} - G_{t_1}}\right) \quad (3)$$

conditioned on the values of the bridge end-point, has a Dirichlet distribution: $f(u_1, u_2, \ldots, u_n | G_{t_1}, G_{t_n}) =$

$$\frac{\Gamma[\alpha(t_n - t_1)] u_1^{\alpha(t_2 - t_1)-1} u_2^{\alpha(t_3 - t_2)-1} \ldots u_n^{\alpha(t_n - t_{n-1})-1}}{\Gamma[\alpha(t_2 - t_1)]\Gamma[\alpha(t_3 - t_2)] \ldots \Gamma[\alpha(t_n - t_{n-1})]} \quad (4)$$

Given integer k such that $mk + 1$ takes us to the closest value to n, we take the following bridge end-points $G_{t_1}, G_{t_{k+1}}, \ldots, G_{mk+1}$. The corresponding increments are denote by $X_{(j-1)k+i}$ which is the i^{th} increment within the j^{th} bridge. We then define m Dirichlet distributed independent random vectors

$$(U_1^{k,1}, \ldots, U_k^{k,1}), \ldots, (U_1^{k,m}, \ldots, U_k^{k,m}), \quad (5)$$

defined similarly as above by

$$U_i^{k,j} = X_{(j-1)k+i} / \left(\sum_{i=1}^{k} X_{(j-1)k+i} \right)$$

These k gamma bridges thus give us an intricate construction, woven over the span of time and built from the intrinsic structure of the gamma process. It provides us with new estimation tools which we proceed to describe.
We shall assume that time increments are equal in size, say δt, and to simplify notation we drop δt which we pack in as part of α so that the joint density function will be given by $\Gamma[k\alpha](u_1 u_2 \dots u_k)^{\alpha-1})/(\Gamma[\alpha]^k)$. The log likelihood function for the j^{th} bridge is given by:

$$l_j(\alpha) = (\alpha - 1) \sum_{i=1}^{k} u_i^{k,j} + \log(\Gamma[k\alpha]) - k \log(\Gamma[\alpha]) \tag{6}$$

We quote the standard results about the Dirichlet distribution:

$$\mathbb{E}[U_j^{k,j}] = \frac{1}{k} \quad , Var[U_i^{k,j}] = \frac{(k-1)}{k^2(\alpha k + 1)}, \quad Cov[U_i^{k,j}, U_l^{k,j}] = \frac{-1}{k(\alpha k + 1)},$$

Also, $\mathbb{E}[\log U_i^{k,j}] = \psi(\alpha) - \psi(k\alpha)$, $Var[\log U_i^{k,j}] = \psi_{(1)}(\alpha) - \psi_{(1)}(k\alpha)$, and $Cov[\log U_i^{k,j}] = -\psi_{(1)}(k\alpha)$, where $\psi_{(j)}(\theta) = \partial^j \psi(\theta)/\partial\theta^j$.
The maximum likelihood equation for the j^{th} set of k readings is given by

$$\frac{1}{k} \sum_{i=1}^{k} log(U_i^{k,j}) = \psi(\hat{\alpha}_{D,j,k}) - \psi(k\hat{\alpha}_{D,j,k}), \tag{7}$$

where $\hat{\alpha}_{D,j,k}$ denotes the estimator from the j^{th} bridge using the Dirichlet model .

3 The pooled estimator $\hat{\alpha}_{D,k,n}$

Next we compare the ML estimates for α from a set of k original gamma increments with those obtained by using the Dirichlet model for the corresponding bridge increments. For the j^{th} set of k gamma distributed increments the ML equation is given by:

$$\sum_{i=1}^{k} \log(X_{(j-1)k+i}) = \psi(\hat{\alpha}_{G,j,k}) + \log \left(\frac{\sum_{i=1}^{k} X_{(j-1)k+i}}{k\hat{\alpha}_{G,j,k}} \right) \tag{8}$$

where $\hat{\alpha}_{G,j,k}$ is the corresponding ML estimator. Using equations (7) and (8) we obtain the following,

$$\begin{aligned} \psi(\hat{\alpha}_{D,j,k}) - \psi(k\hat{\alpha}_{D,j,k}) &= \sum_{i=1}^{k} \log \left(\frac{X_{(j-1)k+i}}{\sum_{l=1}^{k} X_{(j-1)k+l}} \right) \\ &= \psi(\hat{\alpha}_{G,j,k}) - \log(k\hat{\alpha}_{G,j,k}) \end{aligned} \tag{9}$$

Hence $\psi(\hat{\alpha}_{D,j,k}) - \psi(k\hat{\alpha}_{D,j,k}) < \psi(\hat{\alpha}_{G,j,k}) - \psi(k\hat{\alpha}_{G,j,k})$, and since the function $\Psi(k,x) = \psi(x) - \psi(kx)$ is a smooth, increasing function, we can conclude that $\hat{\alpha}_{D,j,k} < \hat{\alpha}_{G,j,k}$.
We are using ideas due to Berman [2] where it is also proved directly that these two estimators are both positively biased.
Using standard techniques as in Cox and Snell [6], Bowman and Shenton [3] and Cordeiro and McCullagh [5] we can obtain bias estimates for both estimators. The bias of $\hat{\alpha}_{D,j,k}$ is given by:

$$\mathbb{E}\left[\hat{\alpha}_{D,j,k}\right] - \alpha = \frac{k^2\psi_{(2)}(k\alpha) - \psi_{(2)}(\alpha)}{2k(k\psi_{(1)}(k\alpha) - \psi_{(1)}(\alpha))^2} + O\left(\frac{1}{k^2}\right), \tag{10}$$

For the gamma-based estimator, the minimal bias is attained over the whole range of readings, $k = n$, for which the bias estimate is

$$\mathbb{E}[\hat{\alpha}_{G,n}] - \alpha = \frac{\alpha\psi_{(1)}(\alpha) - \alpha^2\psi_{(2)}(\alpha) - 2}{2n(\alpha\psi_{(1)}(\alpha) - 1)^2} + O\left(\frac{1}{n^2}\right) \tag{11}$$

The results above tells us that if we increase k we will eventually have a bias which is smaller than that for $\hat{\alpha}_{G,n}$. Thus if we take $k = n-1$ so that we have one bridge with the end-points being the first and last data points, we have a guarantee that the bias of the Dirichlet estimator is smaller than the bias of the gamma estimator which uses all the data points. But we can do better since we do not have to take k too large to obtain a smaller bias. For moderate values of k , m will not be so small. So we have m Dirichlet-based estimators $\hat{\alpha}_{D,j,k}$ which we can pool together. In fact, since they are independent random variables the best thing to do is to average them as follows:

$$\hat{\alpha}_{D,k,n} = \frac{1}{m}\sum_{j=1}^{m}\hat{\alpha}_{D,j,k}. \tag{12}$$

The double-sequence of estimators $\hat{\alpha}_{D,j,k}$ offers a lot of information about the behaviour of the underlying stochastic process through its realized path. Besides testing whether the time evolution of these parameter estimators does occur in an independently random manner, we can also investigate changes as we vary the value of k. These checks would help reveal internal probabilistic structure which would go beyond the simple mechanism for the gamma process.

We now examine how the biases of the estimators $\hat{\alpha}_{D,k,n}$ and $\hat{\alpha}_{G,j,n}$ vary as we change the values of n, k, and α. Using equations 10 and 11 we first define the function $g(k,n)$ which computes their difference:

$$g(k,n) = \frac{k^2\psi_{(2)}(k\alpha) - \psi_2(\alpha)}{2k[k\psi_{(1)}(k\alpha) - \psi_{(1)}(\alpha)]^2} - \frac{\alpha[\psi_{(1)}(\alpha) - \alpha\psi_{(2)}(\alpha)] - 2}{2n(\alpha\psi_{(1)}(\alpha) - 1)^2} \tag{13}$$

Figures 1 and 2 illustrate $g(k)$ for different values of α and n. From these graphs one notices that the difference in the bias gets larger as the value of α increases for any value of k. However, as n gets larger, the difference gets smaller for any value of k. Furthermore, from some value of k, depending on n and α, onwards the bias of $\hat{\alpha}_{D,k,n}$ will be less than that of $\hat{\alpha}_{G,n}$.

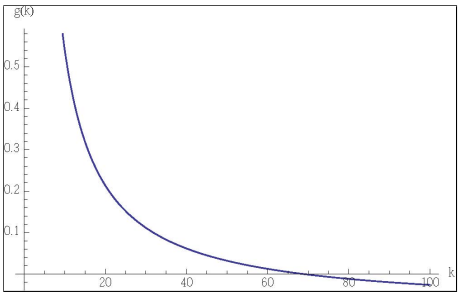

Fig. 1. $n = 100$, $\alpha = 3$

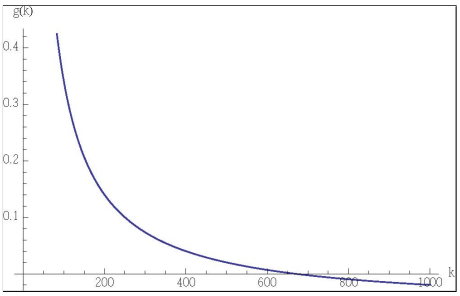

Fig. 2. $n = 1000$, $\alpha = 20$

This result is confirmed from a number of simulations the output of which is displayed in the table 1. In particular this table gives estimates of the bias of $\hat{\alpha}_{D,k,n}$ and $\hat{\alpha}_{G,n}$ as a percentage of the actual value of α. Furthermore the table gives the estimated variances of the said estimators.

k	$\widehat{\%\text{Bias}}(\hat{\alpha}_{D,k,n})$	$\widehat{\%\text{Bias}}(\hat{\alpha}_{G,n})$	$\widehat{\text{Var}}(\hat{\alpha}_{D,k,n})$	$\widehat{\text{Var}}(\hat{\alpha}_{G,n})$
50	3.9889	0.9898	0.7967	0.6650
100	1.8752	1.0049	0.6941	0.6598
250	0.7897	0.9354	0.7606	0.6507
290	0.6601	1.0468	0.7070	0.6873
n	0.5981	0.8826	0.6888	0.6934

Table 1. Simulation results using $n = 300$ and $\alpha = 10$

So the estimator we propose is one which corrects for the bias by using its estimate in the spirit of Giles and Feng [7]. This bias-corrected pooled MLE of α, which we shall denote by $\hat{\alpha}^*_{D,k,n}$, is defined by:

$$\hat{\alpha}^*_{D,k,n} = \hat{\alpha}_{D,k,n} - \frac{k^2\psi_{(2)}(k\hat{\alpha}_{D,k,n}) - \psi_{(2)}(\hat{\alpha}_{D,k,n})}{2k(k\psi_{(1)}(k\hat{\alpha}_{D,k,n}) - \psi_{(1)}(\hat{\alpha}_{D,k,n}))^2} \tag{14}$$

Note that the bias-correction procedure leaves the variance of the estimator unaltered. Table 2 illustrates the results obtained from a number of simulations during which the above bias correction technique was implemented. The said table gives the bias of $\hat{\alpha}_{D,k,n}$ and $\hat{\alpha}^*_{D,k}$ as a percentage of the true value α. Furthermore one can also observe that the estimated variances of the two estimators are comparable.

k	$\widehat{\%\text{Bias}}(\hat{\alpha}^*_{D,k,n})$	$\widehat{\%\text{Bias}}(\hat{\alpha}_{D,k,n})$	$\widehat{\text{Var}}(\hat{\alpha}^*_{D,k,n})$	$\widehat{\text{Var}}(\hat{\alpha}_{D,k,n})$
75	0.1987	2.5267	0.6781	0.7064
150	0.0872	1.2493	0.7905	0.7838
250	0.0785	0.7674	0.6435	0.6522

Table 2. Simulation results using $n = 300$ and $\alpha = 10$

4 Comparison of variances for $\hat{\alpha}_{D,k,n}$ and $\hat{\alpha}_{G,n}$

Finally we consider the variances of the above mentioned estimators. The estimator using ML on independent gamma distributed increments looks in a strong position. We know that it tends to the Cramer-Rao lower bound asymptotically. Using the usual Fisher matrix calculations an estimate for this variance is given by:

$$Var[\hat{\alpha}_{G,n}] = \frac{a}{n(a\psi_{(1)} - 1)} + O\left(\frac{1}{n^2}\right) \tag{15}$$

In the case of $\hat{\alpha}_{D,j,k}$, making suitable modifications to take the dependence between the $U_i^{k,j}$ into consideration, we apply again information matrix methodology with the Dirichlet distribution-based estimation to obtain $\mathbb{E}\left[\frac{\partial^2 l_j}{\partial \alpha^2}\right] = l_j'' = k^2\psi_{(1)} - k\psi_{(1)}(\alpha)$.
So MLE theory allows us to conclude that:

$$Var(l_j') = \mathbb{E}\left[\left(\sum_{i=1}^{k} \log\left(U_i^{k,j}\right) - k[\psi(\alpha) - \psi(k\alpha)]\right)^2\right] =$$
$$kVar\left[\log\left(U_i^{k,j}\right)\right] + k(k-1)Cov\left[U_i^{k,j}, U_l^{k,j}\right] = k\psi_{(1)}(\alpha) - k^2\psi_{(1)}(k\alpha) \tag{16}$$

Thus,

$$Var[\sqrt{k}\hat{\alpha}_{D,j,k}] = \frac{1}{\psi_{(1)} - k\psi_{(1)}(k\alpha)} + O\left(\frac{1}{k}\right).$$

It can be shown that as n and k tend to infinity, the formula for the variance of $\hat{\alpha}^*_{D,k,n}$ which is given in (17) tends from above to that of $\hat{\alpha}_{G,n}$ (15). We cannot improve on the variance-related performance of $\hat{\alpha}_{G,n}$ but we approach to it very closely with significant improvements in the bias.
Figure 3 and figure 4 shown below illustrate equations (15) and (17) with the variance of $\hat{\alpha}_{G,n}$ being indeed slightly less than that of $\hat{\alpha}_{D,k}$. As k increases the difference decreases fast to 0.

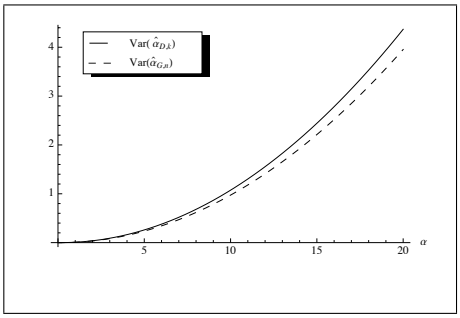

Fig. 3. $n = 200$, $k = 20$

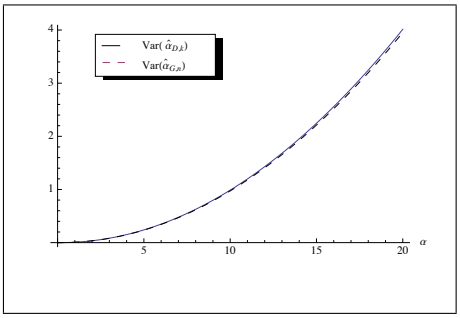

Fig. 4. $n = 200$, $k = 100$

5 Results about $\hat{\alpha}^*_{D,k,n}$

Having given all proofs and derivations above, the results are captured in the following theorem:

Theorem 1. *Estimator* $\hat{\alpha}^*_{D,k,n}$ *as defined in (14) is consistent, asymptotically unbiased with* $\mathbb{E}\left[\hat{\alpha}^*_{D,j,k}\right] - \alpha = O\left(\frac{1}{k^2}\right)$ *and*

$$Var[\hat{\alpha}^*_{D,k,n}] = \frac{1}{mk}\frac{1}{\psi_{(1)}(\alpha) - k\psi_{(1)}(k\alpha)} + O\left(\frac{1}{n^2}\right) \tag{17}$$

6 Conclusion

We started with a critique of the classical ML estimator widely used to identify gamma processes as models for given data. Arguing that the stationary increments property uses too little information about the process, we used results about the distributional evolution of the gamma process to construct a composite estimator. Over non-overlapping stretches of the data we fitted gamma-bridge-derived Dirichlet distributions to obtain a number of estimators for the same parameter. These were compared to the original one with reference to bias and variance. Using estimates for the asymptotic bias and variance we proposed the pooled estimator $\hat{\alpha}^*_{D,k,n}$ and showed it guarantees better statistical performance. It also allows modellers to see how different sections of the data behave by comparing the $\hat{\alpha}$'s from different bridges. Furthermore diagnostics can be developed to identify better anomalous sections within the data as estimates are compared with varying lengths k of the bridges. This helps build a dynamic picture of the data, which in practical applications like climate science and financial time series, can yield useful interpretations.

References

1.A. N. Avramidis, P. Lecuyer and P.A. Tremblay, Efficient Simulation of Gamma and Variance-Gamma Processes, *Proceedings of the 2003 Winter Simulation Conference*, 2003.

2.M. Berman. The maximum likelihood estimators of the parameters of the gamma distribution are always positively biased, *Communications in Statistics Theory and Methods*, 10, 7, 693-697, 1981.

3.K. O. Bowman and L.R. Shenton. Properties of estimators for the gamma distribution. *Communications in Statistics Simulation and Computation*, 11, 4, 377 519, 1982.

4.S. C. Choi and R. Wette. Maximum likelihood Estimation of the parameters of the Gamma distribution and their bias, *Technometrics*, 11, 4, 683-690, 1969

5.G. M. Cordeiro, P. McCullagh. Bias Correction in Generalized Linear Models, *Journal of the Royal Statistical Society. Series B (Methodological)*, 53, 3, 629-643.

6.D. R. Cox and E.J. Snell. A General Definition of Residuals, *Journal of the Royal Statistical Society*, 30, 2, 248-275, 1968.

7.T. S. Ferguson. A Bayesian Analysis of some nonparametric problems,*Annals of Statistics*,1, 2, 209-230, 1973.
8.D. E. Giles and H. Feng. Bias of the Maximum likelihood of the Two-Parameter Gamma Distribution Revisited, 2009.
9.M. Emery and M. Yor. A Parallel between Brownian Bridges and Gamma Bridges, *Publ. RIMS, Kyoto University*, 40, 669 688, 2004.
10.H. C. S. Thom. A Note on the Gamma Distribution, *Monthly Weather Review*, 86, 4, 117 119, 1958.

Proceedings, 15th Applied Stochastic Models and Data Analysis (ASMDA2013)
International Conference, Mataró (Barcelona), Spain 25 - 28 June 2013

Identification of a Simple Homeostasis Stochastic Model Based on Active Principle of Adaptation

Innokentiy V. Semushin[1], Julia V. Tsyganova[2], and Anatoli G. Skovikov[3]

[1] Ulyanovsk State University, 42 Leo Tolstoy Str., Ulyanovsk, Russia
(E-mail: i2nokvsem@gmail.com)
[2] Ulyanovsk State University, 42 Leo Tolstoy Str., Ulyanovsk, Russia
(E-mail: tsyganovajv@gmail.com)
[3] Ulyanovsk State University, 42 Leo Tolstoy Str., Ulyanovsk, Russia
(E-mail: Transferfaculty@gmail.com)

Abstract. The Active Principle of Adaptation for linear time-invariant state-space stochastic MIMO filter systems is applied to human body temperature daily variation adaptive stochastic modeling.
Keywords: Adaptation, active principle, homeostasis, parameter estimation, stochastic modeling, thermoregulation.

1 Introduction

Stochasticity is a form of uncertainty among those discussed in general by Wolkenhauer[1]. As stated by Liao *et al.*[2] and many others in recent times, stochasticity is increasingly appreciated to play fundamental roles in systemic biology and bioinformatics especially when biological and clinical processes are studied at the cellular level. However, the reality in this life-critical area of research is such that the uncertainty of models is twofold: (1) models are stochastic in nature, id est, they are represented by stochastic differential equations, and (2) they are full of unknown parameters. Even if the stochastic models are linear in state, they are complex in the sense that many parameters need to be estimated from the data that are usually noisy and incomplete.

This is a traditional situation of uncertainty in many engineering problems where also emerges the question as to adaptive system modeling. Adaptation of models treated as *fitting models for data* is intended to eliminate or, at the very least, to reduce uncertainty. In Gibson's view, as cited in Semushin[3] the following three functions are considered as the determinant attributes of each adaptive system: (1) quickest Change Point Detection or more generally, Model Classification, (2) reliable Model Identification, and (3) adequate System Modification (or Change Parring). For engineering applications, there exist well-established mathematical methods for solving above three problems.

In systemic biology or medicine, systems are much more complicated than engineering ones because they include a living being, a human. This notwithstanding, it is yet very interesting to extend the approaches developed for engineering systems to biological or clinical processes.

Our work is aimed at such an extension. As a trial, benchmark task, we take a stochastic model of human body temperature. In so doing, we keep in mind three goals of research:

1. The *basic goal* is to extend the range of applicability of our active principle of adaptation (APA, Semushin[3]) to systemic biology, bioinformatics and medicine.
2. The *applied goal* is to implement the APA in some biomedical monitoring.
3. The *basic and applied goal* is to establish an all-purpose Computational Lab for Adaptive Stochastic Systems Modeling (CLASS-M).

The paper paves the way to the first goal only. Its outline is as follows. In Section 2, we start from a baseline model (BM) written as a system of stochastic differential equations for human body temperature daily variation. Section 3 shows what transformations are to be made towards the Discrete-time Standard Observable Model in order to build the Discrete Time Adaptive Kalman Filter in Section 4. Computational experiments with the filter are made in Section 5. We conclude the paper in Section 6.

2 Baseline model

Human body temperature regulation is a great example of how the homeostatic mechanism works. Let us consider human body temperature daily variation as it can be seen in many sources, for instance, in ANTRANIK.org (Fig. 1).

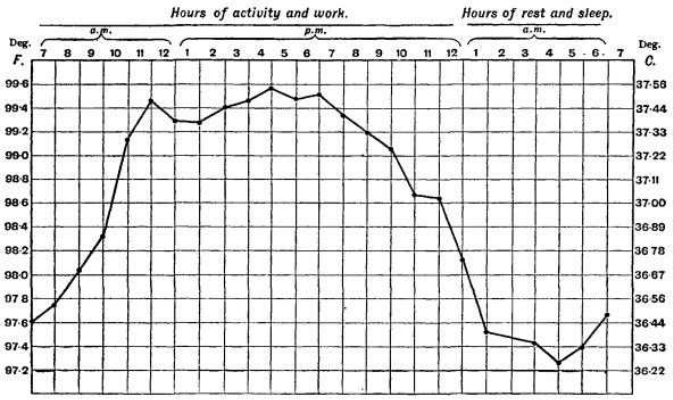

Fig. 1. Human body temperature daily variation (HBTDV). (Courtesy of ANTRANIK.org http://antranik.org/regulation-of-body-temperature/)

Consider the experimental data similar to Fig. 1 as a sample from a continuous-time stochastic process. Decompose it into the following additive components:

- $\bar{\theta}_t$, a mathematical expectation of temperature variation relative to daily mean temperature $\theta^\star$, for example, $\theta^\star = 36.7\ ^\circ C$,

- $\mathring{\theta}_t \triangleq \{\mathring{\theta}_t(\omega)\}$ represents a zero-mean stochastic process with $\omega \in \Omega$ being a point of a fundamental sample space Ω,
- $\tilde{\theta}_t = \mathring{\theta}_t + \theta^\star$, for which $\mathrm{d}\tilde{\theta}_t = \mathrm{d}\mathring{\theta}_t$ because $\theta^\star = \text{const}$.
- $\theta_t \triangleq \bar{\theta}_t + \tilde{\theta}_t$, the sum process modeling experimental data similar to those of Fig. 1.

For simplicity, in what follows we assume that $\bar{\theta}(t)$ is modeled by a A° C harmonic oscillator whose equation is well known:

$$\begin{bmatrix}\dot{x}_1\\ \dot{x}_2\end{bmatrix}_t = \begin{bmatrix}0 & 1\\ -\omega_\mathrm{n}^2 & 0\end{bmatrix}\begin{bmatrix}x_1\\ x_2\end{bmatrix}_t, \qquad \begin{bmatrix}x_1\\ x_2\end{bmatrix}_0 = \begin{bmatrix}\theta_0{}^\circ\, C\\ \omega_0\,\mathrm{min}^{-1}\end{bmatrix} \tag{1}$$

$$y_t = \begin{bmatrix}1 & 0\end{bmatrix} x_t, \qquad t \in [0,\infty) \tag{2}$$

The solution to (1) is

$$\bar{\theta}_t \triangleq x_{1t} = A\sin(\omega_\mathrm{n} t + \varphi)\,, \quad A = \sqrt{\theta_0^2 + \left(\frac{\omega_0}{\omega_\mathrm{n}}\right)^2}\,, \quad \bar{\omega}_t \triangleq x_{2t}$$

$$\sin\varphi = \theta_0/A\,, \quad \cos\varphi = \left(\frac{\omega_0}{\omega_\mathrm{n}}\right)\Big/ A\,, \quad \tan\varphi = \theta_0 \Big/ \left(\frac{\omega_0}{\omega_\mathrm{n}}\right)$$

To obtain $A = 1^\circ\, C$ and $\varphi = 0$, the following initial condition must be assigned: $\begin{bmatrix}x_1\\ x_2\end{bmatrix}_0 = \begin{bmatrix}\theta_0 := 0^\circ\, C\\ \omega_0 := \omega_\mathrm{n}\,\mathrm{min}^{-1}\end{bmatrix}$. Obviously, to obtain $A = 0.65^\circ\, C$ and $\varphi = 0$, the initial condition are to be: $\begin{bmatrix}x_1\\ x_2\end{bmatrix}_0 = \begin{bmatrix}\theta_0 := 0^\circ\, C\\ \omega_0 := 0.65\,\omega_\mathrm{n}\,\mathrm{min}^{-1}\end{bmatrix}$, and so on.

To represent $\mathring{\theta}_t$, we introduce a Gaussian first order Markov process so as to write

$$\mathrm{d}\mathring{\theta}_t = -(1/T)\mathring{\theta}_t\,\mathrm{d}t + \mathrm{d}\beta_t\,, \qquad \lim_{t_0\to-\infty}\beta_{t_0} = 0 \text{ (a.s.)} \tag{3}$$

where β_t represents the scalar-valued Brownian motion (Wiener process, WP) with its constant diffusion $Q = 2\sigma^2/T$, or, in other words, the zero-mean process $\mathring{\theta}_t$ with mean squared value $\sigma^2 \triangleq \mathbf{E}\left\{\mathring{\theta}_t^2\right\} = QT/2$ and correlation time T. Here $\mathbf{E}\{\cdot\}$ denotes the expectation operator on Ω and $t_0 \to -\infty$ to provide wide-sense stationarity for $\mathring{\theta}_t$. Equation (3) is assumed to obtain the process $\mathring{\theta}_t$ with autocorrelation $\Psi_{\mathring{\theta}\mathring{\theta}}(\tau) \triangleq \mathbf{E}\left\{\mathring{\theta}_t\mathring{\theta}_{t+\tau}\right\} = \sigma^2\mathrm{e}^{-|\tau|/T}$. As a result, $\tilde{\theta}_t$ satisfies the following equation

$$\mathrm{d}\tilde{\theta}_t = -(1/T)(\tilde{\theta}_t - \theta^\star)\,\mathrm{d}t + \sigma\sqrt{2/T}\,\mathrm{d}\mathring{\beta}_t \tag{4}$$

where $\mathring{\beta}_t$ is the *standard* WP, that is, the unit diffusion Wiener process defined from $\beta_t \triangleq \sigma\sqrt{2/T}\mathring{\beta}_t = \eta\mathring{\beta}_t$, $\eta \triangleq \sigma\sqrt{2\lambda}$, $\lambda \triangleq 1/T$.

Having introduced $\tilde{\theta}_t$ as the third component into (1)–(2), we obtain

$$\begin{bmatrix}\dot{x}_1\\ \dot{x}_2\\ \dot{x}_3\end{bmatrix}_t = \begin{bmatrix}0 & 1 & 0\\ -\omega_\mathrm{n}^2 & 0 & 0\\ 0 & 0 & -\lambda\end{bmatrix}\begin{bmatrix}x_1\\ x_2\\ x_3\end{bmatrix}_t + \begin{bmatrix}0\\ 0\\ \lambda\end{bmatrix}u_t + \begin{bmatrix}0\\ 0\\ \eta\end{bmatrix}\mathring{w}_t \tag{5}$$

$$y_t = \begin{bmatrix}1 & 0 & 1\end{bmatrix}x_t + v_t, \quad \begin{bmatrix}x_1\\ x_2\\ x_3\end{bmatrix}_0 = \begin{bmatrix}\theta_0{}^\circ\, C\\ \omega_0\,\mathrm{min}^{-1}\\ 0\end{bmatrix}, \; t \in [0,\infty) \tag{6}$$

There in the above equations $u_t \triangleq \theta^\star$, $\theta^\star$ is considered known, and $\mathring{w}_t$ is the *standard* Gaussian white noise defined by formally writing $\mathring{w}_t \triangleq \mathrm{d}\mathring{\beta}_t / \mathrm{d}t$, as it is usual in control literature. Thus, the baseline model (5), (6) has been built. In (6), a random measure error v_t has been introduced.

3 Towards the discrete-time standard observable model

Our sequence of model transformations is as follows.

3dCRPhM = 3-dimension Continuous-time Real-valued "Physical" Model is given by (5), (6). Assuming there $\begin{bmatrix} x_1 \\ x_2 \\ x_3 \end{bmatrix}_0 = \begin{bmatrix} 0^\circ C \\ \omega_\mathrm{n} \\ 0 \end{bmatrix}$, we have a $1^\circ C$ harmonic oscillator with $x_{1,t} = (1^\circ C)\sin\omega_\mathrm{n} t$, $x_{2,t} = (1^\circ C/\mathrm{min})\cos\omega_\mathrm{n} t$ with $\omega_\mathrm{n} = 2\pi/1440\ \mathrm{min}^{-1}$. Considering transformation $x = T_1 x^\star$ with

$$T_1 = \left[\begin{array}{c|c|c} 1 & 1 & 0 \\ \omega_\mathrm{n} & -\omega_\mathrm{n} & 0 \\ 0 & 0 & 1 \end{array}\right], \quad T_1^{-1} = \frac{1}{2}\left[\begin{array}{c|c|c} 1 & \omega_\mathrm{n}^{-1} & 0 \\ 1 & -\omega_\mathrm{n}^{-1} & 0 \\ 0 & 0 & 2 \end{array}\right]$$

we change to the next model.

3dCRCM = 3-dimension Continuous-time Real-valued Canonical Model

$$\begin{bmatrix} \dot{x}_1^\star \\ \dot{x}_2^\star \\ \dot{x}_3^\star \end{bmatrix}_t = \begin{bmatrix} 0 & -\omega_\mathrm{n} & 0 \\ \omega_\mathrm{n} & 0 & 0 \\ 0 & 0 & -\lambda \end{bmatrix} \begin{bmatrix} x_1^\star \\ x_2^\star \\ x_3^\star \end{bmatrix}_t + \begin{bmatrix} 0 \\ 0 \\ \lambda \end{bmatrix} \theta^\star + \begin{bmatrix} 0 \\ 0 \\ \sigma\sqrt{2\lambda} \end{bmatrix} \mathring{w}_t \tag{7}$$

$$y_t = \begin{bmatrix} 1 & 1 & 1 \end{bmatrix} x_t^\star + v_t, \quad \begin{bmatrix} x_1^\star \\ x_2^\star \\ x_3^\star \end{bmatrix}_0 = \begin{bmatrix} 1/2 \\ -1/2 \\ 0 \end{bmatrix} \tag{8}$$

To make possible further using the active principle of filter adaptation in order to estimate the unknown parameters λ and σ, we need to have the discrete-time standard observable model. Getting ready to this final step, we construct two more models as follows.

3dDRCM = 3-dimension Discrete-time Real-valued Canonical Model. Here we omit the $_\star$s and *s for variables and matrices and denote the sampling interval $\tau \triangleq \Delta t \triangleq t_{i+1} - t_i = \mathrm{const}$:

$$\begin{bmatrix} x_1 \\ x_2 \\ x_3 \end{bmatrix}_{t+1} = \underbrace{\begin{bmatrix} c & -s & 0 \\ s & c & 0 \\ 0 & 0 & d \end{bmatrix}}_{\Phi} \begin{bmatrix} x_1 \\ x_2 \\ x_3 \end{bmatrix}_t + \underbrace{\begin{bmatrix} 0 \\ 0 \\ a \end{bmatrix}}_{\Psi} u_t + \underbrace{\begin{bmatrix} 0 \\ 0 \\ b \end{bmatrix}}_{\Gamma} \mathring{w}_{\mathrm{d}t} \tag{9}$$

$$y_t = \underbrace{\begin{bmatrix} 1 & 1 & 1 \end{bmatrix}}_{H} x_t + v_t, \quad \begin{bmatrix} x_1 \\ x_2 \\ x_3 \end{bmatrix}_0 = \begin{bmatrix} 1/2 \\ -1/2 \\ 0 \end{bmatrix} \tag{10}$$

$$c \triangleq \cos\omega_\mathrm{n}\tau,\ s \triangleq \sin\omega_\mathrm{n}\tau,\ d \triangleq e^{-\lambda\tau}$$

$$a \triangleq 1 - d,\ b \triangleq \sigma\sqrt{1 - d^2}$$

where $\mathring{w}_{\mathrm{d}t}$ is a *discrete* standard (that is, with unit covariance $\mathring{Q}_{\mathrm{d}} = 1$) Gaussian white noise.

3dDSOM = 3-dimension Discrete-time Standard Observable Model. Entering upon the construction of this final model, we determine the observability matrix

$$W_\star \triangleq \left[\, H^T \,\middle|\, (H\Phi)^T \,\middle|\, (H\Phi^2)^T \,\right]^T \tag{11}$$

This matrix can be calculated either by hand or with Maple. Below are the results of our by-hand calculations:

$$W_\star = \left[\begin{array}{c|c|c} 1 & 1 & 1 \\ c+s & c-s & d \\ f+g & f-g & d^2 \end{array}\right], \quad f \triangleq \cos 2\omega_{\mathrm{n}}\tau,\ g \triangleq \sin 2\omega_{\mathrm{n}}\tau, \tag{12}$$

$$\det W_\star = 2(-d^2 s + dg + sf - cg) = 2(dg - s(1+d^2))$$

The sought 3dDSOM is obtained as a result of transform $x^\star = W_\star x$ in the following equations:

$$\begin{bmatrix} x_1^\star \\ x_2^\star \\ x_3^\star \end{bmatrix}_{t+1} = \underbrace{\begin{bmatrix} 0 & 1 & 0 \\ 0 & 0 & 1 \\ -a_3 & -a_2 & -a_1 \end{bmatrix}}_{\Phi_\star} \begin{bmatrix} x_1^\star \\ x_2^\star \\ x_3^\star \end{bmatrix}_t + \underbrace{\begin{bmatrix} 1 \\ d \\ d^2 \end{bmatrix}}_{\Psi_\star} (1-d)\,\theta^\star + \underbrace{\begin{bmatrix} 1 \\ d \\ d^2 \end{bmatrix}}_{\Gamma_\star} \sigma\sqrt{1-d^2}\,\mathring{w}_{\mathrm{d}t} \tag{13}$$

$$y_t = \underbrace{\begin{bmatrix} 1 & 0 & 0 \end{bmatrix}}_{H_\star} x_t + v_t, \quad \begin{bmatrix} x_1^\star \\ x_2^\star \\ x_3^\star \end{bmatrix}_0 = \begin{bmatrix} 0 \\ s \\ g \end{bmatrix} \tag{14}$$

$$\begin{aligned} -a_3 &= d\,, \\ -a_2 &= -1 - 2d\cos\omega_{\mathrm{n}}\tau\,, \\ -a_1 &= d + 2\cos\omega_{\mathrm{n}}\tau \end{aligned}$$

An effective way to check the constructed 3dDSOM is to compare it with the same result produced by Maple™.

In the case when the daily average temperature $\theta^\star$ is considered unknown and so is to be also estimated, we infer usage of Maple the only reasonable way to change from the following 4dDRCM

$$\begin{aligned} x_{t+1} &= \begin{bmatrix} \cos\omega_{\mathrm{n}}\tau & -\sin\omega_{\mathrm{n}}\tau & 0 & 0 \\ \sin\omega_{\mathrm{n}}\tau & \cos\omega_{\mathrm{n}}\tau & 0 & 0 \\ 0 & 0 & d & 0 \\ 0 & 0 & 0 & 1 \end{bmatrix} x_t + \begin{bmatrix} 0 \\ 0 \\ \sigma\sqrt{1-d^2} \\ 0 \end{bmatrix} \mathring{w}_{\mathrm{d}t} \\ y_t &= \begin{bmatrix} 1 & 1 & 1 & 1 \end{bmatrix} x_t + v_t \end{aligned}$$

to the 4dDSOM (this case is omitted here for saving room).

4 Discrete-time adaptive Kalman filter

Our benchmark point for constructing the APA-b-AKF should be the Discrete-time Standard Observable Model (DSOM) written, according to Semushin[3], in the general case as follows:

$$\mathcal{D}^{\star}(\theta):\ \begin{array}{l} x^{\star}_{t+1} = \Phi_{\star}x^{\star}_{t} + \Psi_{\star}u_t + \Gamma_{\star}\mathring{w}_{\mathrm{d}t}\,,\ t\in\mathbb{Z}_{+}\,,\ x^{\star}\in\mathbb{R}^{n} \\ y_t = H_{\star}x^{\star}_{t} + v_t\,,\ t\in\mathbb{Z}_{1}\,,\ y\in\mathbb{R}^{m} \end{array} \tag{15}$$

Omitting details from the general theory by Semushin[3], recall that $W_{\star}$, the observability matrix, in our case is given by (11) and (12).

If we work in the context of DSOM, the set

$$\mathcal{A}^{\star} = \left\{ \mathfrak{M}^{\star}(\widehat{\theta}\,) \,\middle|\, \widehat{\theta}\in\Theta\subset\mathbb{R}^{l} \right\} \tag{16}$$

of adaptive models $\mathfrak{M}^{\star}(\widehat{\theta}\,)$ should be used with $\widehat{\theta}$ denoting an estimate of $\theta\in\mathbb{R}^{l}$. Reasoning from the Kalman (optimal) filter $\mathfrak{M}^{\star}(\theta\,)$, we build the adaptive model

$$\mathfrak{M}^{\star}(\widehat{\theta}\,):\ \begin{array}{l} \widehat{g}_{t+1|t} = A\widehat{g}_{t|t-1} + \Psi_{*}u_t + C\eta_{t|t-1} \\ y_t = H_{\star}\widehat{g}_{t|t-1} + \eta_{t|t-1} \end{array} \tag{17}$$

or equivalently (due to $C=AD$) the model

$$\mathfrak{M}^{\star}(\widehat{\theta}\,):\ \begin{array}{l} \widehat{g}_{t+1|t} = A\widehat{g}_{t|t} + \Psi_{*}u_t \\ \widehat{g}_{t|t} = \widehat{g}_{t|t-1} + D\eta_{t|t-1} \\ y_t = H_{\star}\widehat{g}_{t|t-1} + \eta_{t|t-1} \end{array} \tag{18}$$

with $H_{\star}$ and $A=A_{\star}$ taken in the form of (13) and (14).

With the understanding that errors

$$\begin{array}{ll} e_{t+1|t} \triangleq x^{\star}_{t+1} - \widehat{g}_{t+1|t}\,, & e_{t|t} \triangleq x^{\star}_{t} - \widehat{g}_{t|t} \\ r_{t+1|t} \triangleq x^{\star}_{t+1|t} - \widehat{g}_{t+1|t}\,, & r_{t|t} \triangleq x^{\star}_{t|t} - \widehat{g}_{t|t} \end{array} \tag{19}$$

are fundamentally unmeasurable, we construct the auxiliary performance index $\mathcal{J}^{\mathrm{a}}_{t}(\widehat{\theta}\,)$ which guarantees (proofs are done in Semushin[3]):

True (Unbiased) System Identifiability

$$\min_{\widehat{\theta}} \mathcal{J}^{\mathrm{a}}_{t}(\widehat{\theta}\,) \iff \mathfrak{M}^{\star}(\widehat{\theta}\,) \equiv \mathfrak{M}^{\star}(\theta^{\dagger})$$

5 Computational experiments made with MATLAB®

From now on, let $\rho\in\mathbb{R}^{l}$ be the vector of unknown parameters. Consider cases:

1. Parameter λ is unknown, parameter σ is known, i. e. $\rho=\lambda$.
2. Parameter σ is unknown, parameter λ is known, i. e. $\rho=\sigma$.
3. Parameters λ and σ are unknown, i. e. $\rho=[\lambda\,\big|\,\sigma]^{T}$.

To measure the quality of estimates compute three values (Table 1). Experimental conditions are shown in Table 2. The APA-b-AKF has been implemented in a robust square-root form developed by Tsyganova[4]. Results obtained are as shown in Tables 3 through 5.

1. The estimation sample mean	$\text{MEAN} = \frac{1}{N_{EXP}} \sum_{j=1}^{N_{EXP}} \hat{\rho}_j$
2. The root-mean-square error	$\text{RMSE} = \sqrt{\frac{\sum_{j=1}^{N_{EXP}} \|\|\hat{\rho}_j - \rho_*\|\|^2}{N_{EXP}}}$
3. The mean absolute percentage error	$\text{MAPE} = \frac{100\%}{N_{EXP}} \sum_{j=1}^{N_{EXP}} \frac{\|\|\hat{\rho}_j - \rho_*\|\|}{\|\|\rho_*\|\|},$
$\hat{\rho}_j$ is the parameter estimation obtained in the j-th experiment run, ρ_* is the true value of model parameter.	

Table 1. Values to measure the quality of parameter estimates

Number of experiments	$N_{EXP} = 100$
Sampling interval (min)	$\tau = 5$
True model noise parameter	$\sigma_* = 0.3$
Model noise correlation time (min)	$T_{\text{n}} = 24 \cdot 60$, $\omega_{\text{n}} = 2\pi/T_{\text{n}}$
Average daily temperature	$\theta^* = 36.85\ ^\circ C$
Covariance of measurement noise	$R = 0.1$
Initial values	$x_0^* = [0,\ 0.65\sin(\omega_{\text{n}}\tau),\ 0.65\sin(2\omega_{\text{n}}\tau)]$
True parameter values λ	$\lambda_* = 1/T = 0.01(6)$, $T = 60$
Initial value for estimate of λ	$\lambda_0 = 1/(2T)$
Initial value for estimate of σ	$\sigma_0 = 1.$

Table 2. Experimental conditions for estimating parameters λ and σ.

N	MEAN	RMSE	MAPE
0.5	0.01673842	0.00176175	8.53495848
1	0.01668899	0.00128099	6.00706384
3	0.01677946	0.00007005	3.24514550
6	0.01669467	0.00005602	2.80900894
12	0.01665221	0.00004990	2.37861756
24	0.01670608	0.00004936	2.40873864
48	0.01664612	0.00004899	2.43864040
72	0.01669707	0.00004534	2.20453053

Table 3. Experimental results for estimating parameter λ (N stands for hours of measurements collection).

6 Conclusion

In this paper, The Active Principle of Adaptation for linear time-invariant state-space stochastic MIMO systems is applied to human body temperature daily variation adaptive stochastic modeling.

The baseline HBTDV model has been patterned after the physical data available. The adaptive model $\mathfrak{M}^\star(\widehat{\theta})$, a replica of the Kalman filter for the standard observable data model, has been specified.

Computational experiments have been made to demonstrate the applicability of our Active Principle of Adaptation to bioinformatics problems.

N	MEAN	RMSE	MAPE
0.5	0.32169022	0.34800311	96.09089193
1	0.31693915	0.30205901	81.97886696
3	0.30406180	0.18993025	49.42388770
6	0.27961800	0.12641243	32.91595681
12	0.29865439	0.08187854	22.40155093
24	0.29767603	0.06173083	16.00851023
48	0.29723777	0.03914056	10.35061636
72	0.29601063	0.03366058	9.09541878

Table 4. Experimental results for estimating parameter σ (N stands for hours of measurements collection).

N	MEAN	RMSE	MAPE
0.5	$\bar{\rho} = \begin{bmatrix} 0.01659436 \\ 0.10575119 \end{bmatrix}$	0.28056287	85.14674225
1	$\bar{\rho} = \begin{bmatrix} 0.01669789 \\ 0.11527021 \end{bmatrix}$	0.27826336	84.28790200
3	$\bar{\rho} = \begin{bmatrix} 0.01658014 \\ 0.16829851 \end{bmatrix}$	0.22572891	65.65149641
6	$\bar{\rho} = \begin{bmatrix} 0.01669664 \\ 0.23287266 \end{bmatrix}$	0.16211670	44.23780054
12	$\bar{\rho} = \begin{bmatrix} 0.01666193 \\ 0.27265297 \end{bmatrix}$	0.08541397	22.48302905
24	$\bar{\rho} = \begin{bmatrix} 0.01672629 \\ 0.28222717 \end{bmatrix}$	0.06480563	17.75995499
48	$\bar{\rho} = \begin{bmatrix} 0.01668300 \\ 0.29025029 \end{bmatrix}$	0.03909148	10.45862558
72	$\bar{\rho} = \begin{bmatrix} 0.01666895 \\ 0.29820202 \end{bmatrix}$	0.03539374	9.21590355

Table 5. Experimental results for estimating parameters ρ (N stands for hours of measurements collection).

7 Acknowledgments

This paper was partly supported by the RFBR grant No. 13-01-97035.

References

1.O. Wolkenhauer. *Data engineering: Fuzzy mathematics in system theory and data analysis*, John Wiley & Sons, Inc., New York, 2001.

2.D. Liao, L. Estévez-Salmerón and Th. D. Tlsty. Generalized principles of stochasticity can be used to control dynamic heterogeneity. *Physical Biology*, 9, 6, 065006, 2012. http://iopscience.iop.org/1478-3975/9/6/065006/. doi:10.1088/1478-3975/9/6/065006.

3.I. V. Semushin, Adaptation in stochastic dynamic systems—survey and new results II, *Int. J. Communications, Network and System Sciences*, 4, 4, 266–285, 2011. http://www.SciRP.org/journal/ijcns. doi:10.4236/ijcns.2011.44032.

4.Yu. V. Tsyganova, Computing the gradient of the auxiliary quality functional in the parametric identification problem for stochastic systems, *Automation and Remote Control*, 72, 9, 1925–1940, 2011.

Proceedings, 15th Applied Stochastic Models and Data Analysis (ASMDA2013)
International Conference, Mataró (Barcelona), Spain 25 - 28 June 2013

Optimal control of systems with several replenishment sources

Ksenia Shakhgildyan

Department of Mathematics and Mechanics, Lomonosov Moscow State University,
GSP-1, Leninskie Gory, Moscow, 119991, Russia
(E-mail: ksy-shakhgildyan@yandex.ru)

Abstract The aim of the paper is to investigate a model of inventory management with several sources of replenishment. There is a possibility of sending orders to either of two suppliers or both of them. It is supposed that the first supplier delivers orders immediately, while the other one is unreliable delivering the orders immediately only with probability $p \in (0,1)$. The optimal strategy of the company can be determined, namely, the values of orders at any step of the multi-step model for various values of the parameters are obtained. However, the information about the parameters as well as about distribution functions is often incomplete. This is the reason why we examine the sensitivity of solutions to small changes in parameters.
Keywords: Periodic-review inventory system, Optimal control, Unreliable suppliers, Sensitivity.

1 Introduction and model description

The development of a vast body of knowledge known as modern inventory theory is rapid nowadays and has a range of applications to practical situations. Modern information technology has created new possibilities for more sophisticated and efficient control of supply chains. Most organizations can substantially reduce their costs associated with the flow of materials. Inventory control techniques are crucial components in this development process.

A model of inventory management with the participation of several sources of replenishment is examined.

Let c_1 be the unit price with the first supplier and we assume that delivery is made immediately. In its turn, the second supplier makes delivery immediately with probability p and at the beginning of the next period with probability $q = 1 - p$. Denote by c_2 the corresponding unit price. At the beginning of each period (a day, a week, a month, etc.) the decision to order a certain amount of goods from the first and second supplier is made, namely $z_1 \geq 0$ and $z_2 \geq 0$ respectively. We also consider the storage cost h and deficiency payment for unit price r. Suppose x is the initial stock, from this moment onwards claims are received periodically, namely the amount ξ_i is demanded during the i-th period, $i \geq 1$. We assume that $\{\xi_i\}_{i\geq 0}$ form a sequence of mutually independent random variables with a common distribution function $F(\cdot)$ having density $\varphi(s) > 0$ for $s \in [a,b]$, where $a \geq 0$.

Denote by $f_n(x)$ minimum average discounted costs over n periods.
Estimated costs for one period are equal to

$$L(v) = E[r(\xi_1 - v)^+ + h(v - \xi_1)^+], \quad v = x + z_1, \; u = v + z_2.$$

By definition, put

$$G_n(u,v) = (c_1 - c_2)v + c_2 u + pL(u) + qL(v) + \alpha E f_{n-1}(u - \xi_1),$$

where α is the discount factor.
In this case, according to the Bellman's Principle of Optimality for $n \geq 1$ we obtain the following recurrence relations:

$$f_n(x) = -c_1 x + \min_{x \leq v \leq u} G_n(u,v), \quad f_0(x) = 0.$$

Note that the parameters of the model u and v corresponding to the minimum costs mean that it is optimal to order the amount $v - x$ of goods from the first supplier and the amount $u - v$ from the second.

2 Notations and preliminary results

Let us introduce the partial derivative of a function $G_n(u,v)$ with respect to the variables v and u:

$$A(v) = \frac{\partial G_1(u,v)}{\partial v} = c_1 - c_2 + qL'(v),$$

$$B_n(u) = \frac{\partial G_1(u,v)}{\partial u} = c_2 + pL'(u) + \alpha \int_0^\infty f'_{n-1}(u-t)\varphi(t)dt,$$

As well as a function

$$C_n(v) = \frac{\partial G_1(v,v)}{\partial v} = A(v) + B_n(v) = c_1 + L'(v) + \alpha \int_0^\infty f'_{n-1}(v-t)\varphi(t)dt.$$

It can be shown in the usual way that all the functions above are nondecreasing.

Critical levels v^*, u_n и v_n, in case of the existence, are defined as the solutions of the equations

$A(v^*) = 0$, $B_n(u_n) = 0$ and $C_n(v_n) = 0$ respectively.

In case of the nonexistence set them equal to $-\infty$ by definition. That is natural by the monotonicity of functions.
At each step we need to find the value of $\min\limits_{x \leq v \leq u} G_n(u,v)$

First let us obtain the values of $u_n(x)$ and $v_n(x)$ corresponding to the minimum costs depending on the relation of critical levels.

Lemma 1. *Let us consider 2 cases:*
1) If $u_n \geq v^*$, *the argument of* $\min\limits_{x \leq v \leq u} G_n(u,v)$ *is* $\begin{cases} v_n(x) = max(x, v^*) \\ u_n(x) = max(x, u_n). \end{cases}$
2) If $u_n < v^*$, *the argument of* $\min\limits_{x \leq v \leq u} G_n(u,v)$ *is* $v_n(x) = u_n(x) = max(x, v_n)$.

The proof follows directly from the analysis of partial derivatives of the function $G_n(u,v)$.
The next Lemma is needed for the sequel.

Lemma 2. *Suppose* $B_n(v^*) \geq 0$ *then* $u_n \leq v_n \leq v^*$, *whereas for* $B_n(v^*) < 0$ *we have* $v^* < v_n < u_n$.

Proof. Since $A(v^*) = C(v^*) - B(v^*) = 0$, we see that $C(v^*) = B(v^*)$.
It now follows from the monotonicity of functions that for $v < v^*$ we have $A(v) = C(v) - B(v) < 0 \Leftrightarrow C(v) < B(v)$, whereas for $v \geq v^*$
$A(v) = C(v) - B(v) \geq 0 \Leftrightarrow C(v) \geq B(v)$. Clearly, the Lemma statement is true.□

3 Optimal control for $n = 1$

In this case $A(v) = c_1 - c_2 + qL'(v) = 0$, $B_1(u) = c_2 + pL'(u) = 0$,
$C_1(v) = c_1 + L'(v) = 0$. From the explicit form of functions, taking into account $0 \leq F(x) \leq 1$, it can easily be checked that:

$$\begin{cases} v^* = F^{-1}\left(\frac{qr+c_2-c_1}{q(h+r)}\right) & \text{for } (c_1, c_2) \text{ such that } c_2 \geq c_1 - qr; \\ v^* = -\infty & \text{in the converse case;} \end{cases}$$

$$\begin{cases} u_1 = F^{-1}\left(\frac{pr-c_2}{p(h+r)}\right) & \text{for } (c_1, c_2) \text{ such that } c_2 \geq pr; \\ u_1 = -\infty & \text{in the converse case;} \end{cases}$$

$$\begin{cases} v_1 = F^{-1}\left(\frac{r-c_1}{h+r}\right) & \text{for } (c_1, c_2) \text{ such that } c_1 \leq r; \\ v_1 = -\infty & \text{in the converse case.} \end{cases}$$

According to Lemma 1, we need to compare u_1 and v^*, in order to find the optimal control. First note that $F(u) \geq F(v) \Leftrightarrow u \geq v$. Consequently,
$u_1 \geq v^* \Leftrightarrow \frac{pr-c_2}{p(h+r)} \geq \frac{qr+c_2-c_1}{q(h+r)} \Leftrightarrow prq - c_2 q \geq prq + pc_2 - pc_1$
$\Leftrightarrow -c_2(1-p) \geq pc_2 - pc_1 \Leftrightarrow c_2 \leq pc_1$. Therefore, we have

Theorem 1. *The optimal values of orders are the following:*
For $\{(c_1, c_2) : \ c_2 \geq pr, \ c_1 \geq r\}$ *we obtain that* $v_1(x) = u_1(x) = x$.
Whereas for $\{(c_1, c_2) : \ c_2 \leq c_1 - qr, \ c_2 \leq pr\}$ *the optimal orders are* $v_1(x) = x$, $u_1(x) = \max(x, u_1)$.
In turn, for $\{(c_1, c_2) : \ c_1 - qr \leq c_2 \leq pc_1\}$ *we have* $v_1(x) = \max(x, v^*)$, $u_1(x) = \max(x, u_1)$.
The remaining $\{(c_1, c_2) : \ c_2 \geq c_1 - qr, \ c_1 \leq r\}$ *coincides with* $v_1(x) = u_1(x) = \max(x, v_1)$.

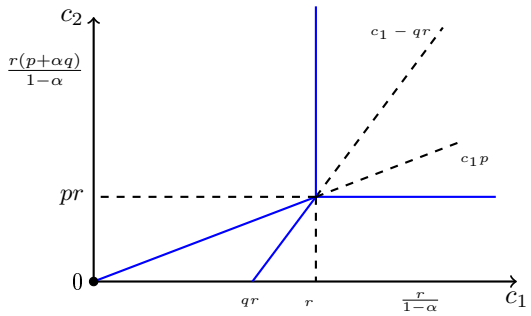

Proof. 1) Let us consider $\{(c_1, c_2) : \ c_2 \geq pr, \ c_1 \geq r\}$.
By Lemma 1 we have that $v_1(x) = u_1(x) = max(x, v_1)$ in the area above the line $c_2 = c_1 p$. Moreover, $v_1 = -\infty$ in the given area, hence $v_1(x) = u_1(x) = x$.
On the other hand $v_1(x) = max(x, v^*), \ u_1(x) = max(x, u_1)$ in the area below the line $c_2 = c_1 p$. However $v^* = u_1 = -\infty$ in this case, thus $v_1(x) = u_1(x) = x$.
2) As far as $\{(c_1, c_2) : \ c_2 \leq c_1 - qr, \ c_2 \leq pr\}$ is concerned
$v_1(x) = max(x, v^*), \ u_1(x) = max(x, u_1)$ by Lemma 1. Note that $v^* = -\infty$ in the considered area, so we obtain $v_1(x) = x, \ u_1(x) = max(x, u_1)$.
3) When it comes to $\{(c_1, c_2) : \ c_1 - qr \leq {}_2 \leq pc_1\}$ neither v^* nor u_1 are equal to $-\infty$. Consequently, $v_1(x) = \max(x, v^*)$, $u_1(x) = \max(x, u_1)$.
4) In the latter case, namely $\{(c_1, c_2) : \ c_2 \geq c_1 - qr, \ c_1 \leq r\}$, v_1 is not equal to $-\infty$. It now follows from Lemma 1 that $v_1(x) = u_1(x) = \max(x, v_1)$.□

4 Optimal control for $n = 2$

In order to discover optimal orders it is necessary to examine ranges of values of (c_1, c_2): D_I, D_{II}, D_{III} and D_{IV}.

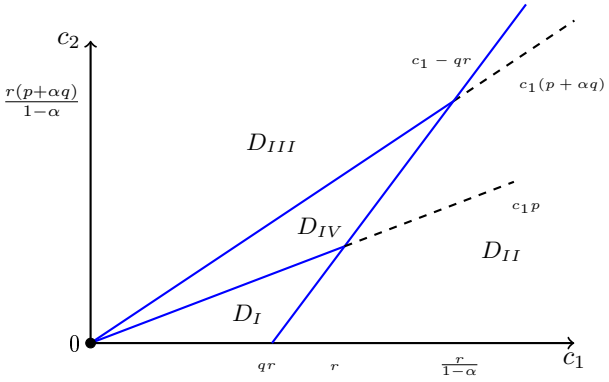

1) Let us look first of all at D_I.
First note that $v^* \leq v_1 \leq u_1$ in this area. What we need is to get an equation for $u_2(x)$.

Lemma 3.

$$f_1'(x) = \begin{cases} -c_1, \ x < v^* \\ -c_2 + qL'(x), \ v^* \leq x < u_1 \\ L'(x), \ x \geq u_1 \end{cases} = -c_1 + \begin{cases} 0, \ x < v^*; \\ A(x), \ v^* \leq x < u_1; \\ A(x) + B_1(x), \ x \geq u_1. \end{cases}$$

Proof. This proposition can be proved by direct calculations. It now follows that $B_2(u) = B_1(u) + \alpha E f_1'(u - \xi_1) = c_2 - \alpha c_1 - pr + p(h + r)F(u) + \alpha F(u - - u_1)(c_2 - rp) + \alpha F(u - v^*)(c_1 - c_2 - qr) + \alpha(h + r)(p \int_0^{u-u_1} F(u - t)\varphi(t)dt + + q \int_0^{u-v^*} F(u - t)\varphi(t)dt)$, where u_2 is the root of the equation.
It can be easily seen that $B_2(v^*) = \frac{c_2 - c_1(p+\alpha q)}{q} < 0$ since $c_2 < c_1(p + \alpha q)$ in the considered area. So we can conclude that $v^* \leq u_2$ by Lemma2.
Finally, by Lemma 1 we obtain $v_2(x) = max(x, v^*), \ u_2(x) = max(x, u_2)$.□

Lemma 4. $u_2 \geq u_1$.

Proof. Consider the difference $B_2(u)-B_1(u) = -c_1\alpha+\alpha\int_0^{u-u_1} B_1(u-t)\varphi(t)dt+ \alpha\int_0^{u-v^*} A(u-t)\varphi(t)dt$. Substituting u_1 in the equation, we get:
$B_2(u_1) = -c_1\alpha + \alpha\int_0^{u_1-v^*} A(u_1-t)\varphi(t)dt =$
$= -c_1\alpha + c_1\alpha F(u_1-v^*) - c_2\alpha F(u_1-v^*) + q\alpha\int_0^{u_1-v^*} L'(u_1-t)\varphi(t)dt \leq$
$-c_2\alpha F(u_1-v^*) + q\alpha\int_0^{u_1-v^*} L'(u_1-t)\varphi(t)dt < 0$, since $L'(u_1-t) < 0$ over the region of integration. Thus we have $u_1 \leq u_2$ by the monotonicity of $B_2(u)$.□

2) Now let us turn to D_{II}.
To begin with, $v^* = -\infty$ in this area, therefore $u_2 \geq v^*$. Now if we recall Lemma 1, we get $v_2(x) = max(x, v^*) = x,\ u_2(x) = max(x, u_2)$.
As before, the aim is to obtain an equation for $u_2(x)$.

Lemma 5.
$$f_1'(x) = \begin{cases} -c_2 + qL'(x), & x < u_1 \\ L'(x), & x \geq u_1 \end{cases} = -c_1 + \begin{cases} A(x), & x < u_1; \\ A(x) + B_1(x), & x \geq u_1. \end{cases}$$

Consequently, $B_2(u) = B_1(u) + \alpha E f_1'(u-\xi_1) =$
$= c_2(1-\alpha) - r(p+\alpha q) + p(h+r)F(u) + \alpha F(u-u_1)(c_2-rp) +$
$+ \alpha(h+r)(\int_0^{u-u_1} F(u-t)\varphi(t)dt + q\int_{u-u_1}^{\infty} F(u-t)\varphi(t)dt)$,
where u_2 is the root.

Interestingly, $f_1' = L'(x)$ for $c_2 \geq pr$. In its turn,
$B_2(u) = c_2 - r(p+\alpha) + (h+r)(pF(u) + \alpha F^{*2}(u))$. Therefore
$F(u_2) + \frac{\alpha}{p}F^{*2}(u_2) = \frac{r(p+\alpha)-c_2}{p(h+r)}$. Since $F(u) + \frac{\alpha}{p}F^{*2}(u) \geq 0$, we see that
$u_2 = -\infty$ for $c_2 \geq r(p+\alpha)$.

Lemma 6. $u_2 \geq u_1$.

Proof. Consider the difference $B_2(u) - B_1(u) =$
$= -c_1\alpha + \alpha\int_0^{u-u_1} B_1(u-t)\varphi(t)dt + \alpha\int_0^{\infty} A(u-t)\varphi(t)dt$
Substituting u_1 in the equation, we get: $B_2(u_1) = -c_1\alpha+\alpha\int_0^{\infty} A(u-t)\varphi(t)dt =$
$-c_2\alpha - qr\alpha + \alpha q(h+r)F^{*2}(u_1) \leq -_2\alpha - qr\alpha + q\alpha(h+r)F(u_1) = -\frac{c_2\alpha}{p} < 0$
As a result we have $u_1 \leq u_2$ by the monotonicity of $B_2(u)$.□

The results for D_{III} and D_{IV} can be acquired in the same way.

It should be mentioned that optimal orders are $v_2(x) = u_2(x) = max(x, v_2)$ for D_{III}, $v_2 \geq v_1$. Whenever $c_1 \geq r$, it follows that $f_1' = L'(x)$ and
$C_2(v) = c_1 - r(1+\alpha) + (h+r)(F(v) + \alpha F^{*2}(v))$. Arguing as above, we see that: $F(v_2) + \alpha F^{*2}(v_2) = \frac{r(1+\alpha)-c_1}{h+r}$.
Let us also remark that $F(v) + \alpha F^{*2}(v) \geq 0$, hence $v_2 = -\infty$ for $c_2 \geq r(1+\alpha)$.

5 Optimal control for any step n.

Denote by $v_n(x)$ and $u_n(x)$ optimal values of orders at the $n-$th step, meaning that we need to purchase the amount $v_n(x) - x$ of goods from the first supplier

and the amount $u_n(x) - v_n(x)$ from the second.

Our main results are the following:

Theorem 2. *For $(c_1, c_2) \in D_I$ we have:*

$$f_n'(x) = -c_1 + \begin{cases} 0, & x < v^*; \\ A(x), & v^* \le x < u_n; \\ A(x) + B_n(x), & x \ge u_n. \end{cases}$$

The corresponding values of orders are $v_n(x) = \max(x, v^*)$ and $u_n(x) = \max(x, u_n)$. Moreover, the sequence u_n is nondecreasing.

Proof. The proof is by induction on n from $n = 1$. The basis has already been proved in the 3th and 4th sections. Now let us assume that conditions of the Theorem are true for $f_m'(x)$, $m \le n-1$.

By direct calculations, using $u_{n-2} \le u_{n-1}$, we obtain: $B_n(u) - B_{n-1}(u) =$
$= \alpha Q_{n-1}(u)$, where $Q_{n-1}(u) = \int\limits_0^{u-u_{n-1}} (B_{n-1}(u-t) - B_{n-2}(u-t))\varphi(t)dt -$
$- \int\limits_{u-u_{n-1}}^{u-u_{n-2}} B_{n-2}(u-t)\varphi(t)dt$. Substituting u_{n-1}, we get:

$$B_n(u_{n-1}) = -\alpha \int\limits_0^{u_{n-1}-u_{n-2}} B_{n-2}(u_{n-1} - t)\varphi(t)dt < 0.$$

Therefore, by the monotonicity of B_n and by Lemma 2, it is true that $u_{n-1} \le u_n$ and $v^* < v_n < u_n$.□

The following theorems can be proved in the same way.

Theorem 3. *For $(c_1, c_2) \in D_{II}$ it is true that:*

$$f_n'(x) = -c_1 + \begin{cases} A(x), & x < u_n; \\ A(x) + B_n(x), & x \ge u_n. \end{cases}$$

*We obtain $v_n(x) = x$ u $u_n(x) = \max(x, u_n)$. In addition, the sequence u_n nondecreasing. At the same time for all (c_1, c_2) such that $(c_1, c_2) \in \{r(p +$
$+ \sum\limits_{i=1}^{m-1} \alpha^i) \le c_2 \le r(p + \sum\limits_{i=1}^{m} \alpha^i)\}$ it follows that $u_n = -\infty \; \forall n \le m$, whereas u_{m+1} is defined by the equation $\alpha F(u_{m+1}) + \sum\limits_{i=1}^{m} \alpha^i F^{*(i+1)}(u_{m+1}) = \frac{r(p + \sum_{i=1}^{m} \alpha^i) - c_2}{h+r}$.*

Theorem 4. *For $(c_1, c_2) \in D_{III}$ we have:*

$$f_n'(x) = -c_1 + \begin{cases} 0, & x < v_n; \\ C_n(x), & x \ge v_n. \end{cases}$$

*Optimal values of orders are $v_n(x) = u_n(x) = \max(x, v_n)$. Besides, the sequence v_n is nondecreasing. Furthermore, assume that $(c_1, c_2) \in \{r(1 + \sum\limits_{i=1}^{m-1} \alpha^i) \le$
$c_1 \le r(1 + \sum\limits_{i=1}^{m} \alpha^i)\}$. In this case, $v_n = -\infty \; \forall n \le m$, and for v_{m+1} we get an equation $F(v_{m+1}) + \sum\limits_{i=1}^{m} \alpha^i F^{*(i+1)}(v_{m+1}) = \frac{r(1 + \sum_{i=1}^{m} \alpha^i) - c_1}{h+r}$.*

Theorem 5. *For* $(c_1, c_2) \in D_{IV}$ *it is true that:*
$f_n'(x) = -c_1 + \begin{cases} 0, & x < v_n; \\ C_n(x), & x \geq v_n. \end{cases}$
There exists $k(c_1, c_2)$ *such that for any* $n < k$ *we obtain* $v_n(x) = u_n(x) = \max(x, v_n)$, *whereas for any* $n \geq k$ *we get* $v_n(x) = \max(x, v^*)$ *and* $u_n(x) = \max(x, u_n)$.

In order to analyze the sensitivity of the obtained results let us introduce Sobol's decomposition. Assume that $A = (A_1, ..., A_n)$ is uniformly distributed in $K^n = [0,1]^n$ and the function $g(a), a \in K^n$, is integrable. Put $g_0 = \mathbb{E}R = \int\limits_{K^n} g(a)da$, $g_i(a_i) = \int\limits_0^1 ... \int\limits_0^1 g(a) \prod\limits_{k \neq i} da_k - g_0$, $g_{i,j}(a_i, a_j) = \int\limits_0^1 ... \int\limits_0^1 g(a) \prod\limits_{k \neq i,j} da_k - (g_0 + g_i(a_i) + g_j(a_j))$,...
Then the following decomposition of variance holds for a square integrable random variable $R = g(A)$:

$$V[R] = \sum_{i=1}^{n} V_i + \sum_{i<j} V_{i,j} + \sum_{i<j<k} V_{i,j,k} + ... + V_{1,2,...,n},$$

where $V[R] = \int\limits_{K^n} g^2(a)da - g_0^2$ and partial variances are calculated by way of $V_{i_1,...,i_s} = \int\limits_0^1 ... \int\limits_0^1 g^2_{i_1,...,i_s}(a_{i_1}, ..., a_{i_s}) \prod\limits_{k=i_1,...,i_s} da_k$. Assuming $V[R] \neq 0$ we can formulate the following definition:
Sensitivity index $S_{i_1,...,i_s}$ for a group of parameters $(a_{i_1}, ..., a_{i_s}), 1 \leq i_1 < ... < i_s \leq n$, is given by $V_{i_1,...,i_s}/V[R]$, whereas the sensitivity index of order s is $\sum_{1 \leq i_1 < ... < i_s \leq n} S_{i_1,...,i_s}$. Moreover, global sensitivity index $GI(a_i)$ of parameter a_i is the sum os all indices $S_{i_1,...,i_s}, s \geq 1$, containing i

$$GI(a_i) = (V_i + \sum_{i \neq j} V_{i,j} + ... + V_{1,2,...,n})/V[R]$$

Thus, $GI(a_i)$ represents the total contribution of parameter a_i to the variance of output.
Applying this approach in Wolfram Mathematica we examined the sensitivity of the obtained solutions to small changes in parameters.

References

1.Bellman, R. (1957). *Dynamic Programming*, Princeton, New York: Princeton University Press.
2.Bulinskaya, E. (2007). Some aspects of decision making under uncertainty. Journal of Statistical Planning and Inference 137:2613–2632.
3.Bulinskaya, E. (2012). Optimal and asymptotically optimal control for some inventory models. In: A.N.Shiryaev et al. eds. *Prokhorov and Contemporary Probability Theory*, Springer Proceedings in Mathematics and Statistics, 33, chapter 8, Berlin: Springer-Verlag.

4.Caliskan-Demirag, O., Chen, Y. and Yang, Yi. (2012). Ordering policies for periodic-review inventory systems with quantity-dependent fixed costs. Operations Research 60:785–796.
5.Fox, E.J., Metters, R. and Semple, J. (2006). Optimal inventory policy with two suppliers. Operations Research 54:389–393.
6.Huggins, E.L., Olsen, T-L. (2010). Inventory control with generalized expediting. Operations Research 58:1414–1426.
7.Li, Q., Wu, X., Cheung, K.L. (2009). Optimal policies for inventory systems with separate delivery request and order-quantity decision. Operations Research 57:626–636.
8.Papachristos, S., Katsaros, A. (2008). A periodic-review inventory model in a fluctuating environment. IIE Transactions 40:356–366.
9.Sobol',I., (1990). Sensitivity estimayes for nonlinear mathematical models. Matematicheskoe Modelirovanie 2:112-118(in Russian).

Proceedings, 15th Applied Stochastic Models and Data Analysis (ASMDA2013)
International Conference, Mataró (Barcelona), Spain 25 - 28 June 2013

Stability Selection and Randomization in L_1 Quantile Regression

Sidi Zakari Ibrahim[1], Mkhadri Abdallah[2], and N'Guessan Assi[3]

[1] Department of Mathematics, Faculty of Sciences Semlalia ,Cadi Ayyad University, 40000, Marrakech, Morocco
(E-mail: i.sidizakari@uca.ma)
[2] Department of Mathematics, Faculty of Sciences Semlalia ,Cadi Ayyad University, 40000, Marrakech, Morocco
(E-mail: mkhadri@uca.ma)
[3] Department of Mathematics
University of Sciences and Technologies of Lille, 59650, Villeneuve d'Ascq, France
(E-mail: assi.nguessan@polytech-lille.fr)

Abstract Statistical models in linear regression generally focus on estimation and interpretation of conditional mean effects. However, in some situations considering mean effects could be not appropriate when for example we have great variations in response variable percentiles or when we have outliers. We here propose the Stability Selection method for variables selection in high dimension penalized linear Quantile Regression. This approach combines subsampling and variable selection algorithms adapted to the case of high dimension. Particularly, we apply Stability Selection with Lasso and Randomized Lasso Quantile Regression. Finally, the proposed method is compared with its competitors on simulated and real data sets.
Keywords: Quantile Regression, High Dimension, Resampling, Stability Selection.

1 Introduction

Meinshausen and Bühlmann[7] advocate that subsampling can be used for Stability Selection in penalized linear regression models to determine the amount of regularization such that a certain family type I error rate in multiple testing can be conservatively controlled for finite sample size. Particularly for complex and high dimensional problems, a finite sample control is much more valuable than an asymptotic statement with the number of observations tending to ∞. Moreover, the previous authors also prove that subsampling in conjunction with L_1-penalized estimation requires much weaker assumptions on the design matrix for asymptotically consistent variable selection than what is needed for the non-subsampled L_1-penalty scheme. Furthermore they show that additional improvements can be achieved by randomizing not only via subsampling but also in the selection process for the variables. Recently a variant approach called Complementary Pairs Stability Selection (CPSS) has been also proposed by Shah and Sameworth[2]. Beinrucker et al.[1] also propose a simple extension of the original stability feature selection approach used in Meinshausen and Bühlmann[7]. We can mention here that variable selection approaches based on bootstrap, Random Lasso[5] and Bolasso[10], have been proposed in linear regression case.

In the lines below, we will focus on the adaptation of Stability Selection[7] and bootstrap based approaches to Quantile Regression[17]. As a motivation of this work we have a dataset on volatile compounds previously used in Duflos et al.[6]. The classical approach based on penalized mean regression is not adapted for this setting since the response variable presents many variations. On the other hand, we want to select the set of stable variables among the volatile compounds which represent the predictors.

The second section of this paper is devoted to the adaptation of Stability Selection to Quantile Regression(QR). Moreover, an illustration on a real dataset is presented and the selection of the tuning parameter based on Belloni and Chernozhukov[3] idea is discussed in the same section. Finally, last section is devoted to numerical experiments including simulations and real data set applications.

2 Linear Quantile Regression Stability Selection

2.1 Variable selection in Quantile Regression

We consider a size n i.i.d sample $\{(\mathbf{x}_i, y_i), i = 1, ..., n\}$ from some unknown population, where $\mathbf{x}_i \in \mathbb{R}^p$ and $y_i \in \mathbb{R}$. Linear quantile regression solves the following optimization problem for $0 < \tau < 1$:

$$(\hat{\beta}_0(\tau), \hat{\beta}(\tau)) = \text{argmin}_{(\beta_0,\beta)\in\mathbb{R}^{p+1}} \left\{ \sum_{i=1}^{n} \rho_\tau(y_i - \beta_0 - \mathbf{x}_i^t\beta) \right\}. \quad (1)$$

The function $\rho_\tau(.)$ is called the check function and is defined by $\rho_\tau(u) = \tau u I_{u>0} + (\tau - 1)u I_{u\leq 0}$, where $I(.)$ is the indicator function which takes value 0 or 1. Since we are interested on variable selection, which is a common practice because in major studies, the main objective is to have a set of relevant variables in a set of predictors used to explain the response variable y.

The following penalized problem is considered:

$$(\hat{\beta}_0(\tau), \hat{\beta}(\tau)) = \text{argmin}_{(\beta_0,\beta)\in\mathbb{R}^{p+1}} \left\{ \sum_{i=1}^{n} \rho_\tau(y_i - \beta_0 - \mathbf{x}_i^t\beta) + \lambda P(\beta) \right\}, \quad (2)$$

where $P(.)$ is the penalty function and the tuning parameter $\lambda > 0$ controls the sparsity of the model. As a survey on frequently used penalty functions in the field of quantile regression we can cite the excellent references of Zou and Yuan [11], Wu and Liu [9] and Slawski [8]. Since the idea of our proposed methods are based on Lasso penalty[14], in all the lines below, we will only focus on the following problem defined by:

$$\min_{(\beta_0,\beta)\in\mathbb{R}^{p+1}} \left\{ \sum_{i=1}^{n} \rho_\tau(y_i - \beta_0 - \mathbf{x}_i^t\beta) + \lambda \parallel \beta \parallel_1 \right\}. \quad (3)$$

All of the methods in this paper are based on the previous formulation except the Randomized Lasso[7] for quantile regression with weakness $\alpha \in (0, 1]$ which

takes the following form:

$$\min_{(\beta_0,\beta)\in\mathbb{R}^{p+1}} \left\{ \sum_{i=1}^{n} \rho_\tau(y_i - \beta_0 - \mathbf{x}_i^t\beta) + \lambda \sum_{k=1}^{p} \frac{\mid \beta_k \mid}{W_k} \right\}, \tag{4}$$

where W_k are iid random variables in $[\alpha, 1]$ for $k = 1, ...p$.

2.2 Stability Selection and pointwise control

This part is a slightly modified part of Meinshausen and Bühlmann[7] approach. Since stability paths are derived from the concept of regularization paths, we recall that for each quantile τ, $0 < \tau < 1$ a regularization path is given by the coefficient value of each variable over all regularization parameters

$$\{\hat{\beta}_k^\lambda(\tau); \lambda \in \Lambda, k = 1, ..., p\}.$$

Stability paths are the probability for each variable to be selected when randomly resampling from the data. For any given regularization parameter $\lambda \in \Lambda$, the selected set $\hat{S}_\tau^\lambda$ is implicitly a function of the samples $I = \{1, ..., n\}$.

Definition 1(selection probabilities): *Let I be a random subsample of $\{1, ..., n\}$ of size $\lfloor n/2 \rfloor$, drawn without replacement. For every set $K \subseteq \{1, ..., p\}$, the probability of being in the selected set $\hat{S}_\tau^\lambda(I)$ is*

$$\hat{\Pi}_K^\lambda(\tau) = P^*\{K \subseteq \hat{S}_\tau^\lambda(I)\}. \tag{5}$$

For every variable $k = 1, ..., p$, the stability path is given by the selection probabilities $\hat{\Pi}_K^\lambda(\tau)$, $\lambda \in \Lambda$.

In the remainder of the paper, we look at the selection probabilities of individual variables. Generally, for each quantile of interest variable selection is concerned by the choice of one element in the set of models

$$\{\hat{S}_\tau^\lambda; \lambda \in \Lambda\}, \tag{6}$$

where Λ is again the set of regularization parameters considered, which can be either continuous or discrete. There are typically two problems: first, the correct model S_τ might not be a member of set (6). Second, even if it is a member it is typically very difficult for high dimensional data to determine the right amount of regularization λ to select exactly S_τ, or at least a close approximation. With Stability Selection, we do not simply select one model in the list (6), instead the data are perturbed (e.g by subsampling) many times and we choose all variables that occur in a large fraction of the resulting selection sets.

Definition 2(stable variables). *For a cut-off π_{thr} with $0 < \pi_{thr} < 1$ and a set of regularization parameters Λ, the set of stable variables for a quantile τ is defined as*

$$\hat{S}_\tau^{stable} = \{k : max_{\lambda\in\Lambda}(\hat{\Pi}_k^\lambda(\tau)) \geq \pi_{thr}\}. \tag{7}$$

We keep variables with a high selection probability and discard those with low selection probabilities.

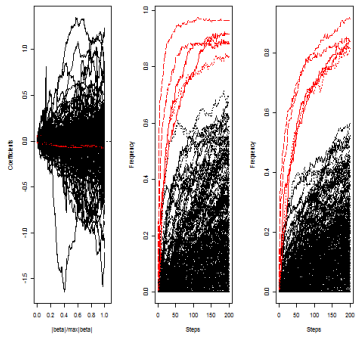

Figure1. From left to right: comparison between L_1 median regression regularization paths, QR Stability Selection without randomization and QR Randomized Stability Selection with $\alpha = 0.1$ on PAC dataset for log(y).

2.3 Illustration on PAC dataset

In Figure1, we illustrate the advantage of using Stability Selection with or without Randomization. We use PAC data available under R software about GC-retention indices of polycyclic aromatic compounds(y) which have been modeled by molecular descriptors(X). The data set contains n=209 observations and p=467 predictors. We first take the 50 variables with the highest marginal correlation with log(y) and randomly select five predictors. These five predictors are kept unpermuted and the remaining 462 are permuted across the samples, using the same permutation that keeps the dependence structure between the permuted observations intact. The left plot, corresponding to L_1 penalized median regression shows that it is very difficult to isolate the five unpermuted variables paths with noise variables paths. For Stability Selection, a threshold of $\pi_{thr} = 0.6$ includes all of the five unpermuted variables with some noise variables. When using Stability Selection with randomization parameter $\alpha = 0.1$, we can see that with the same threshold $\pi_{thr} = 0.6$ all of the five unpermuted variables are selected without any noise variable.

2.4 Tuning parameter selection

Among many alternatives on the choice of the tuning parameter we can cite (see Li and Zhu[12]) the Schwarz Information Criterion (Schwarz[16]; Koenker, Ng, and Portnoy[15]) (SIC) and the generalized approximate cross-validation criterion (Yuan[13]). The SIC is defined by

$$SIC(\lambda) = log(\frac{1}{n}\sum_{i=1}^{n}\rho_\tau(y_i - f(\mathbf{x_i}))) + \frac{log(n)}{2n}df,$$

where df is a measure of the effective dimensionality of the fitted model. In our case, $f(\mathbf{x_i}) = \beta_0 + \mathbf{x}_i^t\beta$. However, recently Koenker[4] claims that using the SIC optimization method often produced insufficient shrinkage and the optimization

process was quite slow. He also claims that when simulating realizations of the random vector $S_n = \sum_{i=1}^{n}(\tau - I(U_i \leq \tau))\mathbf{x_i}$, one can assert that the event $\|S_n\|_\infty \leq \lambda$ should hold with high probability, provided of course that λ is chosen sensibly so that $\hat{\beta}$ is close to the true parameter $\beta(\tau)$. Following this idea, Belloni and Chernozukov[3] suggested choosing $\hat{\lambda}$ as a $(1-\alpha)$ quantile of the simulated distribution of $\|S_n\|_\infty$, or perhaps a constant multiple of such a quantile for some $c \in (1, 2]$. This extremely simple approach was used in our simulations for $\alpha = 0.1$ and $c = 1$.

3 Numerical results

3.1 Simulations settings

For our simulations, we consider the following model $Y = X\beta(0.5) + \epsilon$, where Y is the n dimensional response vector, X is the $n \times p$ predictors matrix, $\beta(\tau)$ is the true p dimensional parameter vector and ϵ is the n dimensional vector of errors. In the lines below, we consider $p = 200$-dimensional predictor variables follow an $N(0, \Sigma)$ distribution, where $\Sigma_{ij} = \rho^{|i-j|}$ and $\rho \in \{0, 0.5, 0.75, 0.9\}$. The sample size is fixed to $n = 100$ and the Signal to Noise Ratio $SNR = Var(X\beta(\tau))/Var(\epsilon)$ considered takes values in {0.5,2,4}. The error vector $\epsilon \sim N(0, 1)$ and $\beta(\tau)$ vector has s nonzero components chosen as uniforms on $[0, 1]$. The s value considered here is $s \in \{4, 8, 12, 20\}$.

Simulations are performed 100 times and median of False positive, False negative and the mean probability to select $0.1s$ and $0.4s$ correct variables without any noise variable are given on Figure 2 and Figure 3.
Each plot gives the performances of the following five methods "QR Stability Selection","QR Randomized Stability Selection", "QR Lasso", "QR Bolasso" and "QR Random Lasso".

Results for n=50 seems to be similar. For Stability Selection based approaches, the threshold is fixed to $\pi_{thr} = 0.6$ and $\alpha = 0.5$ for Randomized Stability Selection . We use fixed value of the tuning parameter(pointwise control) as previously advocated. Nevertheless we can use R software "lpRegPath" package which generates the entire solution path as a function of the tuning parameter. Taking into account the limited size for papers, we only present results for $s \in \{4, 8\}$.

For $s = 4$ and $\rho = 0$, stability selection based methods and QR Bolasso do not introduce FP ($SNR \in \{0.5, 2, 4\}$). QR Lasso FP selection is around 14 FP which represents the median about 100 bootstrap ($SNR \in \{0.5, 2, 4\}$). QR Random Lasso seems to introduce more FP variables for $SNR = 0.5$ than for $SNR \in \{2, 4\}$. In terms of FN, QR Randomized Stability Selection and QR Bolasso seems to delete more true regression coefficients than other methods with decreasing number of median FN when SNR increases. In terms of P($0.1s$ correct), QR Randomized Stability Selection and QR Bolasso give very good result (probability=1), QR Stability Selection corresponding probability increases when the SNR increases (0.73,0.77,0.78). Since QR Lasso introduces too many variables, the corresponding probability is zero. QR Random Lasso also have increasing probability with increasing SNR (0.02,0.27,0.41).

For P($0.4s$ correct) and $SNR = 0.5$, QR Stability Selection gives great probability(0.68) followed by QR Randomized Stability Selection (probability=0.46) and QR Bolasso (0.18). QR Lasso and QR Random Lasso give zero probability. For $SNR \in \{2, 4\}$, QR Randomized Lasso and QR Bolasso give great similar probability (0.99 and 1 respectively) and we have probability values of 0.01 and 0.1 for the QR Random Lasso. QR Stability selection gives probability of 0.89 and 0.86. The previous comments and for other values of ρ can be seen on Figure 2 and Figure 3.
When $s = 8$ and $\rho \in \{0, 0.5\}$ we have the same remarks as previous (s=4) for the median number of FP and FN. For P($0.1s$ correct), QR Randomized Stability and QR Bolasso have higher performances followed by QR Stability Selection and QR Random Lasso. For P($0.4s$ correct), QR Stability Selection has the highest performances due to the fact that it has the best trade off between FP and FN, followed by Randomized Stability Selection. We remark that QR Bolasso has the higher performance for P($0.1s$ correct) when $\rho = 0.75$ followed by QR Randomized Stability Selection and QR Stability Selection without Randomization. QR Random Lasso has very low selection probability. For P($0.4s$ correct) and SNR=0.5, all methods fail to select 40% of correct variables without introducing any noise variables, due to the fact that QR Lasso and QR Random Lasso introduce noise variables, and other methods delete some correct variables. Results for other values of SNR and for $\rho = 0.9$ can be seen on Figure2 and Figure3.

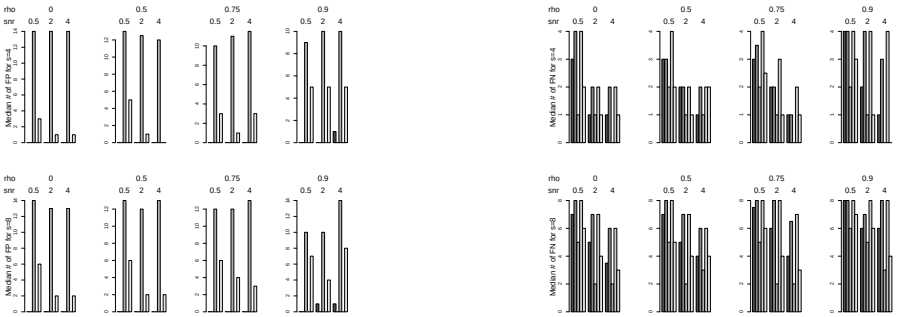

Figure2. Median number of False Positive and False Negative selection among 100 replications for s=4(top row) and s=8(bottom row). For each SNR value we have from left to right "QR Stability Selection","QR Randomized Stability Selection", "QR Lasso", "QR Bolasso" and "QR Random Lasso".

3.2 Real data application

We consider the data set on volatile compounds previously used in Duflos et al.[6]. The sample considered consists of $n = 37$ observations and $p = 49$ predictors(X) used to model Freshness index and Quality scores (y). A direct use of methods on the full data gives results only for L_1 median regression and QR Bolasso. For Stability Selection and bootstrap based methods, we have no results due to the fact that subsampling of size $n/2$ leads in some cases

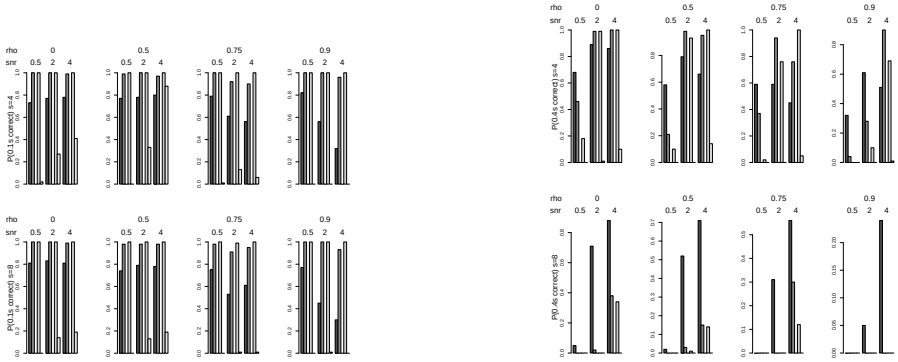

Figure3. Probability of selection of 0.1s and 0.4s of relevant variables without selection any noise variables among 100 replications for s=4(top row) and s=8(bottom row). For each SNR value we have from left to right "QR Stability Selection","QR Randomized Stability Selection", "QR Lasso", "QR Bolasso" and "QR Random Lasso".

to singular design sub matrixes and we cannot compute the tuning parameter $\lambda = c\Lambda(1-\alpha|X)$ since the matrix of predictors X is very sparse with many zero entries. On another hand, QR Bolasso with 100 bootstrap selects no variables for many values of λ, so we consider QR Soft Bolasso (QR SBolasso) which selects at least 60% of variables which are selected for all bootstrap samples. In the line below we only consider compounds with at least $n/2$ nonzero observations which lead to a predictors matrix with sizes $n = 37$ and $p = 37$. Selection results are summarized below where for the tuning parameter λ, $c = 2$ and $\alpha = 0.1$. For stability selection methods, the threshold is fixed to $\pi_{thr} = 0.6$. According to selection results in Table1, we see that for $\lambda = 25.253$ no variable is selected by all of the methods. Selection results for $\lambda/5$ and $\lambda/10$ are given in Table1 with selected volatiles names given in Table2. As expected, subsampling improves important variables selection and additional randomization prevents against noise variables selection. The selected compounds by Stability Selection approach also have been found by Duflos et al.[6] to be related to fish spoilage during storage. This important compounds are Ethanol(d), Ethyl acetate(o), 3-Methyl butanal(r) and 3-Methyl-1-butanol(ag) where more stable compounds seem to be Ethanol(d) and 3-Methyl-1-butanol(ag).

Methods	Selected Compounds	
λ=25.253	Freshness index	Quality scores
All methods	-	-
$\lambda/5$		
QR Lasso	a,d,l,o,q,r,aa,ag	b,d,r,aa,ag,ah
QR SBolasso	d,r,ag	d,ag,ah
QR Stability Selection	d,r,ag	d,ag
QR Randomized Stability Selection $\alpha = 0.2$	-	-
QR Randomized Stability Selection $\alpha = 0.5$	d,ag	ag
QR Randomized Stability Selection $\alpha = 0.8$	d,r,ag	d,ag
$\lambda/10$		
QR Lasso	b,d,j,l,o,r,aa,ag,aq,ar,bh	b,d,l,aa,ag,ah,aq,bh
QR SBolasso	d,o,r,ag,bh	d,r,ag
QR Stability Selection	d,o,r,ag	d,ag
QR Randomized Stability Selection $\alpha = 0.2$	d	d,ag
QR Randomized Stability Selection $\alpha = 0.5$	d,r,ag	d,ag
QR Randomized Stability Selection $\alpha = 0.8$	d,r,ag	d,ag

Table1. Selected volatiles for penalized median regression.

Compounds	Names	Compounds	Names
a	Acetaldehyde	r	3-Methyl butanal
b	Methanethiol	aa	2,3-Pentanedione
d	Ethanol	ag	3-Methyl-1-butanol
j	2,3-Butanedione	ah	2-Methyl-1-butanol
l	2-Butanone	aq	1-Hexanol
o	Ethyl acetate	ar	3-Heptanone
q	2-Methyl-1-propanol	bh	Nonanal

Table2. Selected volatiles names.

References

1.A. Beinrucker, U. Dogan, and G. Blanchard. A Simple Extension of Stability Feature Selection.*Pattern Recognition Lecture Notes in Computer Science*, 7476, 256-265, 2012.

2.R. Shah and R. Samworth. Variable selection with error control: Another look at stability selection. *J. Roy. Statist. Soc., Ser. B* (to appear), 2012.

3.A. Belloni and V. Chernozhukov. L_1-penalized quantile regression in high-dimensional sparse models. *Annals of Statistics*, 39, 1, 82-130, 2011.

4.R. Koenker. Additive models for quantile regression: Model selection and confidence bandaids. *Brazilian Journal of Probability and Statistics*, 25, 3, 239-262, 2011.

5.S. Wang, B. Nan, S. Rosset and J. Zhu. Random Lasso. *Annals of Applied Statistics*, 5, 1, 468-485, 2011.

6.G. Duflos, F. Leduc, A. N'Guessan, F. Krezewinski, K. Ossarath and P. Malle. Freshness characterisation of whiting (Merlangius merlangus) using an SPME/GC/PM method and a statistical multivariate approach. *J Sci Food Agric*, 90, 2568-2575, 2010.

7.N. Meinshausen and P. Buhlmann. Stability selection. *Journal of the Royal statistical Society, B.*, 72, 4, 417-473, 2010.

8.M. Slawski. The structured elastic net for quantile regression and support vector classification. *Statistics and Computing*, (to appear), 2010.

9.Y. Wu and Y. Liu. Variable selection in quantile regression. *Statistica Sinica*, 19, 801-817, 2009.

10.F. R. Bach. Bolasso: Model Consistent Lasso Estimation through the Bootstrap. *Proceedings of the 25 th International Conference on Machine Learning, Helsinki, Finland*, 2008.

11.H. Zou and M. Yuan. Regularized simultaneous model selection in multiple quantiles regression. *Computational Statistics and Data Analysis*, 52, 5296-5304, 2008.

12.Y. Li and J. Zhu. L_1-Norm Quantile Regression. Journal of Computational and Graphical Statistics, 17, 1, 1-23, 2008.

13.M. Yuan. GACV for Quantile Smoothing Splines. *Computational Statistics and Data Analysis*, 5, 813-829, 2006.

14.R. Tibshirani. Regression shrinkage and selection via the Lasso. *journal of the Royal statistical Society, B.*, 58, 267-288, 1996.

15.R. Koenker, P. Ng and S. Portnoy. Quantiles smoothing splines.*Biometrika*, 81, 4, 673-80, 1994.

16.G.Schwarz. Estimating the Dimension of a Model. *The annals of Statistics*, 6, 461-464, 1978.

17.R. Koenker and G. Bassett. Regression Quantiles. *Econometrica*, Econometric Society, 46, 1, 33-50, 1978.

Proceedings, 15th Applied Stochastic Models and Data Analysis (ASMDA2013)
International Conference, Mataró (Barcelona), Spain 25 - 28 June 2013

Alternative Assessments of the Probability of Death with a Case Study for Persons with Celiac Disease in Selected East European Countries

Simpach Ondrej

Department of Demography, Faculty of Informatics and Statistics, University of Economics in Prague, Winston Churchill sq. 4, 130 67, Prague, Czech Republic (E-mail: ondrej.simpach@vse.cz)

Abstract. The probability of death depended in the past to a considerable extent on the level of advancement of the health service, the medical findings acquired and knowledge of the appropriate treatment processes. In the case of persons with Celiac Disease, which is a disease involving gluten intolerance, the hope of survival in the majority of countries was slim until the eighties of last century. These people died at a very young age thanks to ignorance of the diagnosis of their disease. However, as soon as it was possible to determine the diagnosis of Celiac Disease correctly there was a considerable breakthrough and progress rapidly changed the hope of survival for these people. This breakthrough occurred earlier in some countries and later in others. In this way treatment procedures were found for hitherto unknown diseases, or at least there was information on reducing the consequences of these diseases. The submitted study will provide a look at the alternative assessment of the probability of death of persons with Celiac Disease and the probability of death in general. The modelling of the probability of death is possible with the use of the LOGIT model. On the basis of supplementary information about the population it is then possible to construct various probability scenarios with the utilisation of alternative variables.
Keywords: Probability of Death, Celiac Disease, LOGIT, Alternative Assessment.

1 Introduction

In spite of the fact that medicine is constantly bringing people new information and the diagnosis of new diseases, there were and still are diseases for which the existing diagnosis is only partial and thus insufficient for the complete cure of the patients (Logan et al. [4]). In the second half of last century the diagnosis began to appear in some countries of a disease involving gluten intolerance, later described as Celiac Disease. This diagnosis, however, only spread to certain countries. There were countries not only in Europe, but also throughout the world, which did not have all the necessary information from science and research published abroad (Rubio-Tapia et al. [5]). This caused various information delays and the consequences of insufficient information about the diagnoses of certain diseases had an impact on the life expectancy of these people. The probability of the death of persons with specific diseases was thus raised in comparison with the probability of death of persons in the general population not burdened by any of the diseases with a still insufficient diagnosis.

2 Methodology and Model

The dependence on age of the probability of death of a person x years old can be explained with the use of further variables, both discrete and also categorical (Freese and Long [1]). The LOGIT models are capable of estimating, with the use of the distribution function of logistic distribution, the value of the probability of death of a person x years old, where further supplementary information may create various forms of the probability function. In the presented model the probability of death of a person x years old will be estimated for the course of the next k years after the medical examination (where k is any whole number) in the case where the person has some diagnosed disease, or in the case where the person is completely healthy. In the illustration case study the analysis will be used of the probability of death of persons with Celiac Disease in comparison with the probability of death for the population as a whole. The explained variables of Y will be alternative. When the value of variable Y equals 1, then the person will die within k years, and on the contrary when the value of variable Y equals 0, the person will survive k years. So that it would be possible also to determine the values of the probability of the occurrence of this phenomenon between the two extremes, the LOGIT model of discrete selection will be applied, when the explained variables acquire values from the interval <0 ; 1> (Hoyos et al. [2]). The following variables may be used for the model:
- AGE is the precise current age of the person invited for a health check,
- CIRD is the Constant of Increased Risk of Death, which acquires values from the interval $< l ; h >$, where l and h are whole numbers. The calculation of this constant arises for the i^{th} patient from Table 1, which is created during the medical examination and where instead of the verbal replies given there were recorded $w_{i,j}$, acquiring the values 0 and 1, where 0 = patient's reply does not coincide with the word given in the appropriate square and 1 = patient's reply coincides with the word given in the appropriate square.

	$\mathbf{V}_1$	$\mathbf{V}_2$	$\mathbf{V}_3$	$\mathbf{V}_1$	$\mathbf{V}_2$	$\mathbf{V}_3$
Smoker	no	occasionally	regularly	$v_{i,j} = 0/1$	...	...
Black Coffee	no	occasionally	regularly	...		
Alcohol	no	occasionally	regularly	...		
Sleep	regular	irregular	poor	...		
Nutrition	regular	irregular	poor	...		

Table 1. Replies of patients to doctor's questions during general examination (left) and 0/1 matrix replies (right)

From Table 1, in which the replies are recorded in the 0/1 format, emerges the CIRD for the i^{th} patient from the formula (1),

$$CIRD = (w_1 \times \sum_{i=1}^{5} v_{i,1}) + (w_2 \times \sum_{i=1}^{5} v_{i,2}) + (w_3 \times \sum_{i=1}^{5} v_{i,3}) \qquad (1)$$

where w_1, w_2 and w_3 are the weights recommended on the basis of the doctor's opinion, who provided data matrices for analysis. (We can use $w_1 = 1$, $w_2 = 3.5$ and $w_3 = 7$). The general rule, arising from the literature, is not here. This Constant can take values from interval <5 ; 35>, where the extreme value of 5 means, that the patient does not increase the risk of death because of its poor lifestyle and extreme value of 35 means, that the patient increases the risk of death in the worst way possible.
- ILL is a binary variable, acquiring the values 0 = the person does not have a diagnosed illness, or 1 = the person has a diagnosed illness. In the model with Celiac Disease the variable CEL will be used.
- DEATH_K is a binary variable, acquiring the values 0 = the person did not die within k years after the medical examination, or 1 = the person died within k years after the medical examination.

The probability function for the LOGIT model (Christensen [3]) is

$$P_i = E(Y = 1|\mathbf{X}_i) = \frac{1}{1 + e^{-(b_0 + \mathbf{b}^{'}\mathbf{x}_i)}} \tag{2}$$

modified for this study in the form

$$P_i = E(Y = 1|\mathbf{X}_i) = \frac{1}{1 + e^{-(b_0 + b_1 AGE_i + b_2 CIRD_i + b_3 CEL_i)}}, \tag{3}$$

where i is the i^{th} patient. Let us set

$$Z_i = b_0 + \mathbf{b}^{'}\mathbf{x}_i \tag{4}$$

and let us insert it for the purposes of this study

$$Z_i = b_0 + b_1 AGE_i + b_2 CIRD_i + b_3 CEL_i. \tag{5}$$

The subsequent expression

$$P_i = \frac{1}{1 + e^{-Z_i}} = \frac{e^{Z_i}}{1 + e^{Z_i}} = F(Z_i) \tag{6}$$

is the distribution function of the logistic distribution. The probability that a person aged x-years will not die within k years after the moment of the medical examination is

$$1 - P_i = \frac{1}{1 + e^{Z_i}} \tag{7}$$

and therefore

$$\frac{P_i}{1 - P_i} = e^{Z_i}. \tag{8}$$

By calculating the logarithm we obtain LOGIT

$$ln(\frac{P_i}{1 - P_i}) = Z_i = b_0 + \mathbf{b}^{'}\mathbf{x}_i, \tag{9}$$

which is transferred for the purposes of this study into the form

$$ln(\frac{P_i}{1 - P_i}) = Z_i = b_0 + b_1 AGE_i + b_2 CIRD_i + b_3 CEL_i. \tag{10}$$

From the general assumptions, the logarithm of the credibility function

$$lnL(b_0, \mathbf{b}) = \sum_{i=1}^{N} [Y_i ln(\frac{e^{Z_i}}{1+e^{Z_i}}) + (1-Y_i) ln(1 - \frac{e^{Z_i}}{1+e^{Z_i}})] \tag{11}$$

there arises after the substitution

$$lnL(b_0, \mathbf{b}) = \sum_{i=1}^{N} [Y_i ln(\frac{e^{b_0+\mathbf{b}'\mathbf{x}_i}}{1+e^{b_0+\mathbf{b}'\mathbf{x}_i}}) + (1-Y_i) ln(1 - \frac{e^{b_0+\mathbf{b}'\mathbf{x}_i}}{1+e^{b_0+\mathbf{b}'\mathbf{x}_i}})] \tag{12}$$

and for the purposes of this study is

$$lnL(b_0, b_1, b_2, b_3,) = \sum_{i=1}^{N} [Y_i ln(\frac{e^{b_0+b_1 AGE_i+b_2 CIRD_i+b_3 CEL_i}}{1+e^{b_0+b_1 AGE_i+b_2 CIRD_i+b_3 CEL_i}}) +$$

$$+(1-Y_i) ln(1 - \frac{e^{b_0+b_1 AGE_i+b_2 CIRD_i+b_3 CEL_i}}{1+e^{b_0+b_1 AGE_i+b_2 CIRD_i+b_3 CEL_i}})]. \tag{13}$$

3 Data, Material and Case Study

For the study mentioned it is possible to use data from the databases of health insurance companies and medical statistics. There are few health insurance companies which record events to the necessary extent. Practical analysis will be carried out for selected periods of the nineties in the Czech Republic, Slovakia and Poland. The analysis will be restricted to persons with Celiac Disease and persons with no health complications and the results will be published separately for the male and the female gender. For the experiment of non-linear regression (Spector and Mazzeo [6] or Yang and Raehsler [7]), applied in the first part of this study about 200 observations of variables consisting of two samples were obtained for each country - Czech Rep., Slovakia and Poland. It is important to note, that this is not a representative selection for the application of standard methods of mathematical statistics. The selection was not taken at random. This is the data matrix, obtained by tentative minor research. Selection consists all individual invited in 1990 to general medical examination and their health status was checked in the future. For consecutive experiment of non-linear regression, applied in the second part of the study, approximately other 200 observations of patients, consisting of two samples were obtained for each country. It is a selection of patients invited in 1995 to the overall medical examination and their health status was checked in the future (but obtained from other sources than the first selection). We hope that there is minimum probability that some patients from the first sample are contained in the second sample. Estimating the unknown parameters of non-linear regression models is no problem today. To estimate the parameters of LOGIT model Statgraphics Centurion XVI version 16.1.11 and Gretl 1.8.7 build 2010-01-24 were used.
Based on the methodology showed above the estimates of unknown parameters of LOGIT models for males in 1990 and 1995 as well as for females in 1990 and

1995 were calculated for Czech Rep., Slovakia and Poland. Table 2 shows the results for the Czech Republic (top), for Slovakia (middle) and Poland (bottom). The first model for each country is always for males in 1990, the second model always for females in 1990, a third model always for males in 1995 and the fourth model always for females in 1995. Of the estimated models were constructed graphs showing the development of the probability of death of x-years old person. (See Figure 1 for Czech Rep., Figure 2 for Slovakia and finally Figure 3 for Poland.

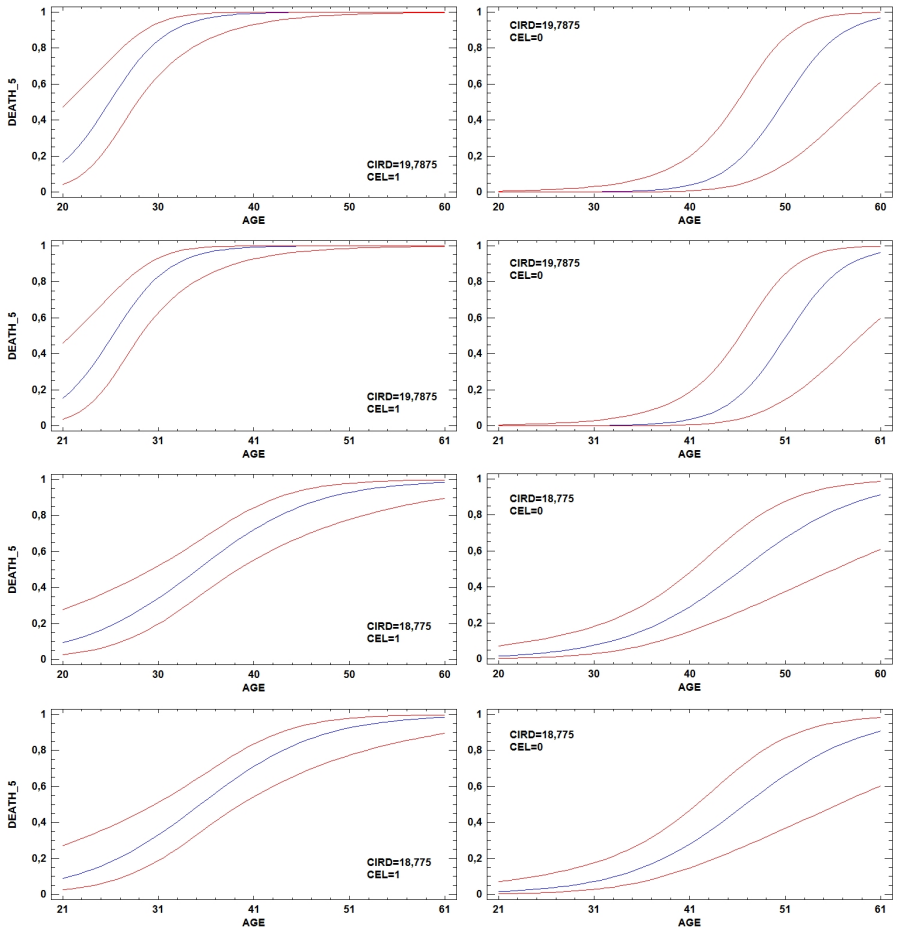

Fig. 1. Probability of death of x-years old person in the Czech Republic (males 1990 with CEL - 1^{st} row left, males 1990 without CEL - 1^{st} row right, females 1990 with CEL - 2^{nd} row left, females 1990 without CEL - 2^{nd} row right, males 1995 with CEL - 3^{rd} row left, males 1995 without CEL - 3^{rd} row right, females 1995 with CEL - 4^{th} row left and females 1995 without CEL - 4^{th} row right.)

Parameter	Estimate	St. Error	Odds Ratio	Factor	Chi-Sq.	DF	P-Value
Constant	-15,6423	3,71635					
AGE	0,333211	0,09654	1,40052	AGE	31,3889	1	0,0000
CIRD	0,370041	0,08211	1,40563	CIRD	39,0002	1	0,0000
CEL-0	-8,23231	1,90601	0,00029	CEL	78,8484	1	0,0000
Constant	-15,7816	3,71599					
AGE	0,329121	0,08534	1,38975	AGE	31,2349	1	0,0000
CIRD	0,361625	0,08578	1,43566	CIRD	38,8651	1	0,0000
CEL-0	-8,19201	1,89216	0,00027	CEL	78,8339	1	0,0000
Constant	-9,17489	1,90414					
AGE	0,161341	0,03913	1,17509	AGE	21,591	1	0,0000
CIRD	0,195672	0,04715	1,21613	CIRD	22,1363	1	0,0000
CEL-0	-1,84446	0,52223	0,15811	CEL	14,2464	1	0,0002
Constant	-9,26566	1,91888					
AGE	0,189633	0,04001	1,18655	AGE	22,0001	1	0,0000
CIRD	0,201122	0,04023	1,22366	CIRD	22,1963	1	0,0000
CEL-0	-1,83663	0,52889	0,16889	CEL	14,6398	1	0,0001
Constant	-14,771	3,61432					
AGE	0,319513	0,08661	1,37646	AGE	29,5255	1	0,0000
CIRD	0,337395	0,08146	1,40129	CIRD	36,9356	1	0,0000
CEL-0	-7,98723	1,89016	0,00033	CEL	76,0443	1	0,0000
Constant	-11,177	2,47924					
AGE	0,221478	0,05806	1,24792	AGE	22,5223	1	0,0000
CIRD	0,27303	0,06150	1,31394	CIRD	33,842	1	0,0000
CEL-0	-5,64065	1,16173	0,00355	CEL	64,0071	1	0,0000
Constant	-7,16711	1,60754					
AGE	0,133789	0,03569	1,14315	AGE	16,7686	1	0,0000
CIRD	0,146313	0,04042	1,15756	CIRD	15,711	1	0,0001
CEL-0	-1,90989	0,50245	0,14809	CEL	16,8345	1	0,0000
Constant	-7,05805	1,62331					
AGE	0,119955	0,03438	1,12745	AGE	14,1924	1	0,0002
CIRD	0,15557	0,04191	1,16832	CIRD	16,4657	1	0,0000
CEL-0	-1,87092	0,49519	0,15398	CEL	16,4205	1	0,0001
Constant	-10,565	2,35537					
AGE	0,23943	0,05954	1,27053	AGE	28,3616	1	0,0000
CIRD	0,2161	0,05382	1,24123	CIRD	24,6238	1	0,0000
CEL-0	-5,30962	1,12046	0,00494	CEL	59,8911	1	0,0000
Constant	-8,55789	1,92926					
AGE	0,163137	0,04635	1,1772	AGE	16,7961	1	0,0000
CIRD	0,217977	0,04990	1,24356	CIRD	28,4366	1	0,0000
CEL-0	-4,27303	0,84652	0,01393	CEL	51,4505	1	0,0000
Constant	-5,64467	1,42814					
AGE	0,103277	0,03250	1,1088	AGE	11,2856	1	0,0008
CIRD	0,122385	0,03745	1,13019	CIRD	12,1086	1	0,0005
CEL-0	-1,80914	0,47412	0,16379	CEL	16,6206	1	0,0000
Constant	-7,11323	1,63255					
AGE	0,123955	0,04111	1,13222	AGE	14,2396	1	0,0000
CIRD	0,23357	0,04263	1,17888	CIRD	16,4756	1	0,0000
CEL-0	-1,89992	0,50122	0,14536	CEL	16,4322	1	0,0000

Table 2. Estimations of unknown LOGIT models parameters

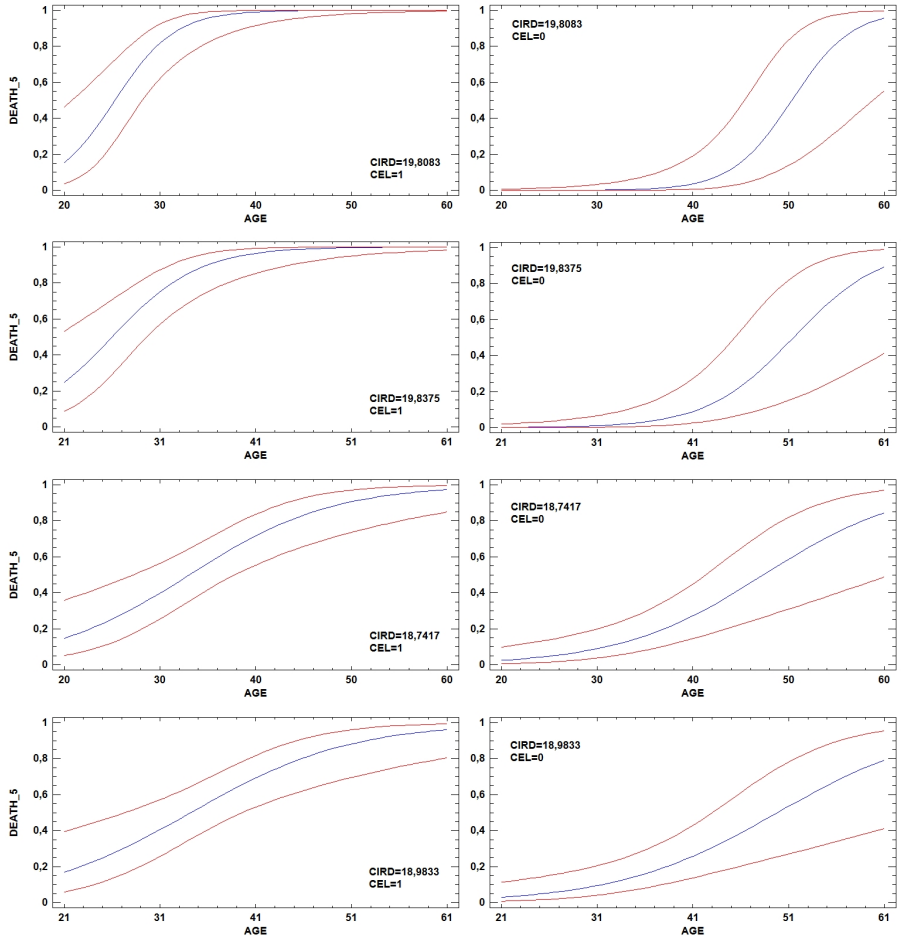

Fig. 2. Probability of death of x-years old person in Slovakia (see legend in FIG. 1.)

4 Conclusion

The aim of this study was to analyse the probability of death of x-year old persons in Czech Rep., Slovakia and Poland during next five years ($k = 5$) after the general medical examination in 1990 and 1995. The analyses were solved using LOGIT models and tried to confirm the hypothesis claiming, that the probability of death of x-year old person suffering from celiac disease decreased few years after the gaining of another medical knowledge from other countries. Even if some assumptions for the application of methods of mathematical statistics are broken, it is possible to say, that the key hypothesis was confirmed. Looking at Fig. 1, 2 and 3 we can see only slight differences between the presented countries. Their development of the compared statistics in the past should be similar.

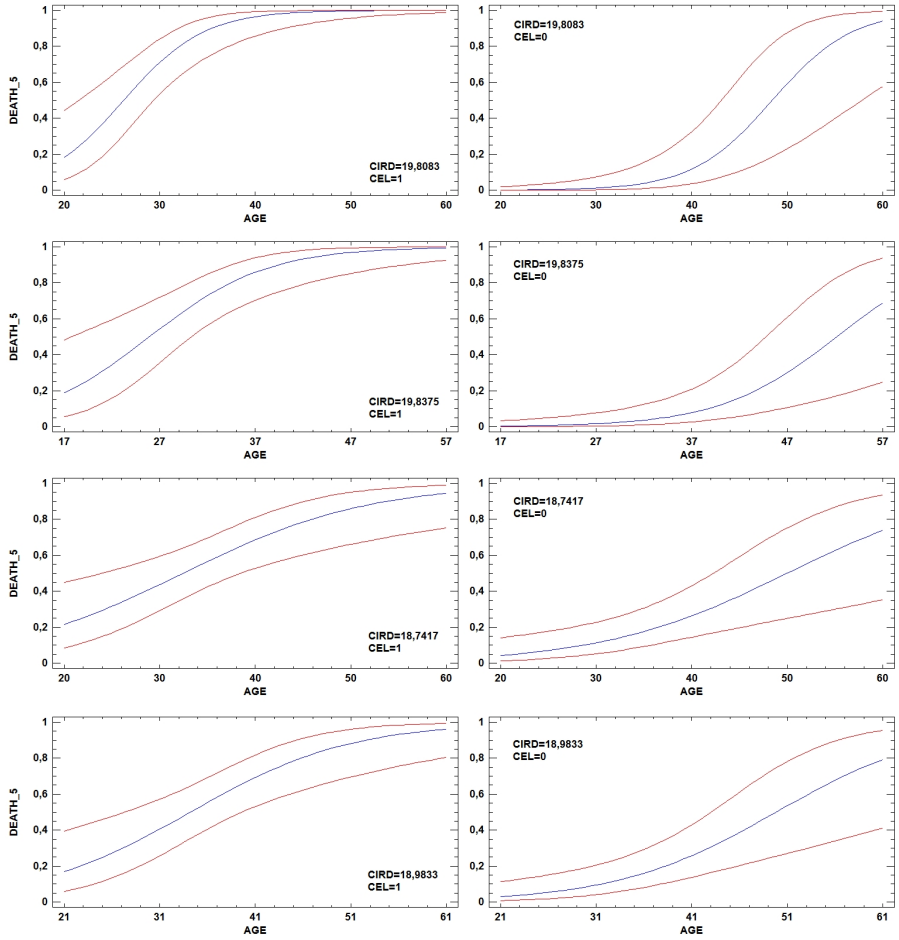

Fig. 3. Probability of death of x-years old person in Poland (see legend in FIG. 1.)

References

1.J. Freese and J. S. Long. Regression Models for Categorical Dependent Variables Using Stata, *College Station: Stata Press,* 2006.
2.D. Hoyos, P. Mariel and J. Meyerhoff. Comparing the performance of different approaches to deal with attribute non-attendance in discrete choice experiments: a simulation experiment, *BILTOKI 201001*, Universidad del Pais Vasco, 2010.
3.R. Christensen. Log-Linear Models *Springer-Verlag*, New York, 1990.
4.R. F. Logan, E. A. Rifkind, I.D. Turner and A. Ferguson. Mortality in celiac disease. *Gastroenterology*, 97(2), 265–271, 1989.
5.A. Rubio-Tapia et al. Increased Prevalence and Mortality in Undiagnosed Celiac Disease. *Gastroenterology*; 137 : 88–93. 2009.
6.L. C. Spector and M. Mazzeo. Probit Analysis and Economic Education, *Journal of Economic Education*. Spring, 11, pp. 37-44. 1980.
7.CH. W. Yang and R. D. Raehsler. An Economic Analysis on Intermediate Microeconomics: An Ordered PROBIT Model, *Journal for Economic Educators*, Volume 5, No. 3, Fall. 2005.

Proceedings, 15th Applied Stochastic Models and Data Analysis (ASMDA2013)
International Conference, Mataró (Barcelona), Spain 25 - 28 June 2013

High frequency trading with Hidden Markov Models by using clustering and PPCA algorithms

I. Róbert Sipos[1], János Levendovszky[2]

[1] Department of Networked Systems and Services, Budapest University of Technology and Economics, Budapest, Hungary (e-mail: siposr@hit.bme.hu)
[2] Department of Networked Systems and Services, Budapest University of Technology and Economics, Budapest, Hungary (e-mail: levendov@hit.bme.hu)

Abstract. In this paper a Hidden Markov Model (HMM) based prediction algorithm will be introduced for algorithmic trading, the performance of which is enhanced by clustering and PPCA algorithms. The performance of the new method is tested on different financial assets and instruments. We use various training methods (e.g. Baum-Welch expectation maximization, simulated annealing and hybrid methods) for optimizing the parameters of HMM in order to capture the underlying characteristics of the financial time series. The new hybrid algorithm combines simulated annealing (SA) with the Baum Welch algorithm (used as a local search after each step of SA) and can provide relatively fast and good quality solutions. The real time nature of learning can be guaranteed by running SA only for a limited number steps determined by a predefined time interval. To cope with the underlying complexity and perform high frequency trading we apply clustering for reducing the number of data and PPCA for dimension reduction as preprocessings. The algorithms are tested on US SWAP rates and FOREX series. The results demonstrate that a good average return can be obtained by HMM based prediction and the applied preprocessings. It is noteworthy that the continuous model gives better result, however it requires more complex training.

Keywords: Hidden Markov Models, financial time series, algorithmic trading

1 Introduction

In this paper we investigate the performance of prediction based trading on financial time series by Hidden Markov Models (HMM). HMMs are widely used for predictions (Mamon and Elliott[15], Durbin *et al.*[5], Jurafsky and Martin[13], Hassan and Nath[7]), however there are no efficient algorithms have yet been developed for real-time training of the free parameters for the purpose of high-frequency algorithmic trading (Hassan *et al.*[8]). The trading action is based on the probabilities of the predicted future values. For minimizing the risk, the highest probability future value is selected and depending its increasing (or decreasing) nature a buying (or short-selling) action is taken. In order to optimize the parameters of the HMM, different training methods are used: Baum-Welch expectation maximization (Baum *et al.*[3]), simulated annealing (Kirkpatrick *et al.*[14]) and hybrid methods proposed by the present paper. In the hybrid method, after accepting a new state by SA the Baum-Welch algorithm is used as a local search method. After the convergence of the Baum-Welch algorithm to a state in the parameter space, SA adopts it as the new state and calculates its next step from there. The real-time nature of this

algorithm can be ensured by limiting the number of steps of SA making it fit into a predefined time interval. In this way, good quality solutions can be achieved in relatively short time.
Unfortunately, the algorithms in the present form are very exhaustive computationally. Thus, to ease the complexity, we introduce clustering to limit the number of data and PPCA to reduce the dimension.
The HMM based predictor is tested on US SWAP rates and FOREX series. The results demonstrate that a good average return can be obtained. It is noteworthy that the continuous model gives better result, however it requires more complex training.
The material is treated in the following order:

- in section 2, the discrete and continuous HMM is briefly summarized;
- in section 3, the computational model is mapped out;
- in section 4, we delve into the different learning algorithms;
- in section 5 and 6 we explain the preprocessing with clustering and PPCA, respectively;
- in section 7 the trading method is outlined;
- in section 8, the numerical results are given;
- finally, in section 9, some conclusions are drawn.

2 The model

A Hidden Markov Model (HMM) (Baum and Petrie[2]) is a statistical model which is an extension of Markov chains. In this model, the current state is no longer directly visible to the observer, but each state emits an observable output quantity denoted by

$$\mathbf{X} = \{o_1, o_2, ..., o_T\}, \tag{2.1}$$

and each emission depends only on the hidden state

$$\mathbf{Q} = \{q_1, q_2, ..., q_T\}. \tag{2.2}$$

The probability of an emitting a specific output is determined by the conditional probabilities $P(o_t \mid \mathbf{Q}) = P(o_t \mid q(t) = q_t)$, while the transition probabilities of the underlying Markov chain, describing the jumping probabilities from one state to another is given by the transition probability matrix $A_{ij} = P\left(q(t+1) = q_i \,\middle|\, q(t) = q_j\right)$. $\boldsymbol{\pi}_N$ denotes the initial distribution vector.

HMMs are commonly used in various fields, for instance in bioinformatics (Durbin *et al.*[5]) or speech recognition (Jurafsky and Martin[13], Rabiner[17]). In our case we use them to predict future values of financial time series.

2.1 Description of a discrete HMM

If we treat the observations having discrete values over a given alphabet

$$o_t \in \{k_1, k_2, ..., k_M\}, \tag{2.3}$$

then the observation probability matrix, $\mathbf{B}_{NxM}$ describes the probability distribution over the possible values for each state. For continuous data, pre-processing is needed to quantize the data to the discrete alphabet. The easiest

alphabet has a three-element code indicating that the asset price is {increasing, stagnating, decreasing}. In the discrete case, HMM is described by

$$\Theta = \{\boldsymbol{\pi}, \mathbf{A}, \mathbf{B}\}. \quad (2.4)$$

Vector valued observations can be coded as n-tuples, note that in this case the alphabet size will grow according to $O(M^n)$.

2.2 Description of a continuous HMM

When the observable output is continuous, the observation probabilities are described by a probability density function, instead of a probability matrix. For this purpose a multivariate Gaussian mixture model (Dasgupta[4]) was used, in which the density function is composed as a weighted sum (according to the $\boldsymbol{W}$ weight matrix) of M independent Gaussian functions:

$$P(o_t \mid q(t) = q_j) = \sum_{k=1}^{M} w_{jk} b_{jk}(o_t), \quad (2.5)$$

where $b_{jk}(o_t) \sim N(\boldsymbol{\mu}_{jk}, \boldsymbol{\Sigma}_{jk})$. Note that this approach can handle multivariate observations as well. In the continuous case, HMM is then described as

$$\Theta = \{\boldsymbol{\pi}, \mathbf{A}, \mathbf{W}, \boldsymbol{\mu}, \boldsymbol{\Sigma}\}. \quad (2.6)$$

3 The computational approach to trading

The model parameters of HMM are identified during the training phase based on a set of observations in historical data sequences. After learning, the HMM can predict the values of the newly observed sequence, and then the predicted distribution is converted to a trading signal for taking the appropriate trading actions.

Our computational framework is shown on the following structural block diagram (Fig. 1) and detailed as follows:

- Training phase: HMM model fitting (by using one of the learning algorithms described in section 4) based on a training set;
- Prediction: using the identified model and a newly observed sequence of the time series, in this step the most likely prediction for the future asset prices is calculated (see chapter 7);
- Trading strategy forming the trading signal: mapping the prediction into a trading action (also detailed in chapter 7);
- Performance analysis: a framework for trading and testing and evaluating various numerical indicators for the sake of comparison of the profitability of different methods (chapter 8 contains further details).

This framework will be extended in chapter 6 with dimensional reduction.

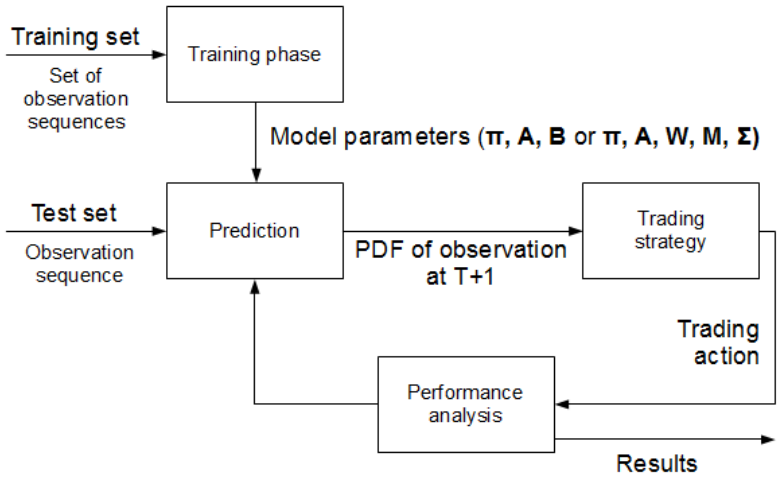

Fig. 1. Computational approach

4 Training for predicting future values of financial time series

The model parameter estimation (learning) is a key aspect when we are using HMMs for prediction. First, the construction of a training set is needed. This is carried out by sampling the input time series with a sliding window of length *T*:

$$\mathbf{X} = \{\mathbf{X}_1, \mathbf{X}_2, ..., \mathbf{X}_K\}, \tag{4.1}$$

where $\mathbf{X}_t = \{\mathbf{r}_{t-T+1}, ..., \mathbf{r}_t\}$ and $\mathbf{r}_t$ is the daily return at the *t*th time instance:

$$r_{t,i} = \frac{p_{t,i} - p_{t-1,i}}{p_{t-1,i}}; \mathbf{r}_t = \{r_{t,i}, i = 1, ..., n\}, \tag{4.2}$$

where $p_{t,i}$ denotes the price of the *i*th asset in the *t*th time instance.

In the discrete case, the daily returns were partitioned into *M* equal sized subsets. While handling the daily returns as a continuous value required a normalization step:

$$r^*_{t,i} = \frac{r_{t,i} - \bar{\mathbf{r}}^{(i)}}{std(\mathbf{r}^{(i)})}. \tag{4.3}$$

During training, the likelihood of the model is maximized based on the given observations (Rabiner and Juang[16]):

$$\Theta_{opt} = \arg\max_{\Theta} P(\mathbf{X} \mid \Theta). \tag{4.4}$$

To avoid numerical instabilities due to the small order of magnitude of such probabilities, it is better to calculate the logarithm of the likelihood:

$$L(\Theta) = \log P(\mathbf{X} \mid \Theta). \tag{4.5}$$

The optimization problem described in (4.4) can be solved in multiple ways.

4.1 Baum-Welch expectation maximization

The Baum-Welch expectation maximization (EM) algorithm (Baum *et al.*[3]) is a mechanism to iteratively update the model ((2.4) or (2.6)) starting from an arbitrary initial value and iterating until the likelihood of the model converges to a certain value. Since this is an iterative method, which can use the forward-backward algorithm, implemented in an efficient way by dynamic programming (Rabiner[17]), this algorithm is relatively fast.
On the other hand, it may get stuck in one of the local minima making the final result highly dependent on the initialization. In our implementation, these matrices were initialized randomly.

4.2 Simulated annealing

In the absence of analytical solutions for finding the global optimum of the likelihood of model parameters, one can use simulated annealing (SA) to obtain good quality heuristic solutions. Simulated annealing (Kirkpatrick *et al.*[14]) is a stochastic search method for finding the global optimum in a large search space. In this context the energy function $J(\Theta)$ is the log-likelihood of the selected model:

$$J(\Theta) = L(\Theta). \tag{4.6}$$

Let Θ be an arbitrarily initialized model, and then by calling random number generation a model Θ' is generated subject to its constraints. The neighbor function on each iteration modifies one of the probability vectors or matrices with an amount according the current temperature (*T*). Accept the new model if $J(\Theta') > J(\Theta)$, or otherwise with $e^{-\frac{J(\Theta)-J(\Theta')}{T}}$ probability. Continue the sampling while decreasing the *T* until zero. The last state is now describes the identified model.
This method, in theory, can provide us the best fitting model. It is a rather slow method due to the large dimension of the search space.

4.3 Hybrid solution

Having the Baum-Welch EM algorithm and the SA at hand, one can construct a hybrid solution. In this case, after a new state was accepted during the annealing process, we ran the Baum-Welch as a local optimization algorithm to speed up the convergence. After the Baum-Welch algorithm converged to a state in the parameter space, SA adopts it as the new initial state and calculates its next move from there. The real-time nature of this algorithm can be ensured by limiting the number of steps of SA. In this way, good quality solutions can be achieved in relatively short time. This approach can bring more reliable results, which are less dependent on the initialization.

5 Clustering algorithms

As we have seen, optimizing model likelihood in the full space of Θ including every available observation is computationally exhausting. To ease the underlying computational complexity, one can pre-process the training set and

form clusters out of the observations. Having the clusters at hand and assigning them to the corresponding hidden states, the p.d.f. describing the observation probabilities can be estimated for each cluster, separately. (Note that the obtained model parameters could also be used as an initial estimate for the previously shown methods.)
Rabiner addressed this topic in his work (Rabiner[17]) suggesting the following algorithm in continuous case:

Algorithm 1.:

1. Arbitrary initialization of model parameters.
2. Segment the observations in the training set based on the optimal state sequence (Viterbi path) calculated by the Viterbi algorithm (Viterbi[20], Forney[6]) and assign each data point to the corresponding maximum likelihood hidden states.
3. Perform k-means clustering over the observation vectors within each state resulting *M* clusters per state.
4. Re-estimate the model parameters in a standard manner (calculate the relative frequency of observations in each state and the relative frequency of transitions, estimate sample mean and covariance for each cluster).
5. Calculate statistical similarity with the previous model, if we can assume convergence then stop, continue from step 2 otherwise.

It has been demonstrated in (Rabiner[17]) that the algorithm above performs well in the field of speech recognition, giving essentially identical likelihood values in an order of magnitude faster than the model obtained by the Baum-Welch algorithm. However, attempts of application for financial time series shown in (Idvall and Jonsson[11]) has yielded much more moderate performance, although the importance of a proper clustering mechanism is emphasized. This gives the motivation for our new approach to obtain HMM model parameters by clustering.
The main idea was to avoid a separate and linear clustering phase if a non-linear GMM is used to describe the observation p.d.f. for the hidden states. This leads to the following algorithm:

Algorithm 2.:

1. Fit a Gaussian mixture distribution using every data point in the training set.
2. Assign each mixture component to a corresponding hidden state, index the price vectors accordingly.
3. Calculate the transition probabilities and the initial distribution vector from relative frequencies (note that the remaining model parameters, namely the p.d.f. of the observations, are already estimated during the first step).

One may note, that in the proposed algorithm only one single Gaussian component will belong to each state. This will not restrict generality, as a model having *N* hidden states with *M* mixture components can be rewritten in the form of *N* times *M* states with only one component. Clearly, a grouping step could take place in the algorithm forming two phase clustering similar to the previous one. However, if the model parameter estimation is not used for further iteration in the EM or SA algorithm, then the increased state space does not cause difficulties in terms of computational resources. Using only one component per state also gives us the advantage to control the model degree by tuning only one free parameter.

The performance of the algorithm can be further enhanced by also taking into consideration the price vector in the next time instance besides the current one during clustering, as data points having similar distribution can differ in this aspect. In this case we need to perform the Gaussian mixture estimation (step 1.) on the following data set:

$$\boldsymbol{\tau} = \left\{ \left\{ \mathbf{r}_i, \mathbf{r}_{i+1} \right\}, 0 \le i < K \right\}, \tag{5.1}$$

which embed the return vectors into a *2n* dimensional space. After the clustering is done, in step 2, we need to consider only the top-left quarter of the matrices describing the p.d.f., which belongs to the first *n* dimensions.

6 Dimension reduction

Transforming the data from a higher dimensional space into a space of fewer dimensions as a pre-processing step for the HMM can also yield certain advantages:

- a smaller dimensional space requires much less computational time, which enables us to do higher frequency trading, or to involve a larger number of assets, which was not feasible formerly;
- allows us to control the model degree in order to avoid overfitting.

Deploying a feature extraction algorithm into to computational framework introduced in chapter 3 can be done in a straightforward manner.

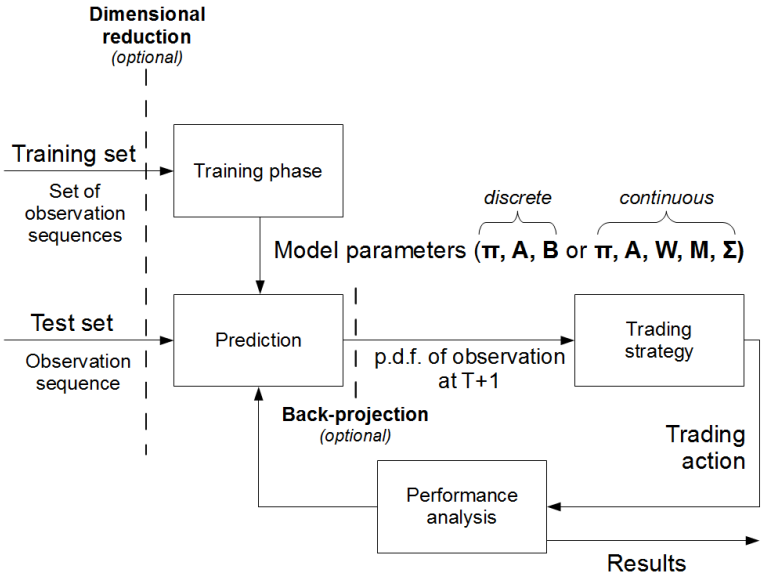

Fig. 2. Extended computational approach

As it is shown in figure 2, the dimensional reduction (as in (6.2)) and the back-projection to the original space (will be given in (6.1)) is simply precedes and follows the training and prediction modules, while the trading strategy is the same as before.

The goal of dimension reduction is to relate a *d*-dimensional return vector ($\mathbf{r}$) into a *q*-dimensional ($q < d$) latent vector denoted by $\mathbf{x}$. If we assume a linear relationship with non-zero mean, we get the basic model of factor analysis (Bartholomew[1]):

$$\mathbf{r} = \mathbf{W}\mathbf{x} + \boldsymbol{\mu} + \boldsymbol{\varepsilon}, \tag{6.1}$$

where matrix $\mathbf{W}_{d\times q}$ describes the transformation between the two spaces, $\boldsymbol{\mu}$ is the mean and $\boldsymbol{\varepsilon}$ represents the noise in the model. Having the mapping matrix and the mean of the data, the reduction can be formulated as

$$\mathbf{x} = (\mathbf{r} - \boldsymbol{\mu})\left(\mathbf{W}^T\right)^{-1}. \tag{6.2}$$

6.1 Probabilistic principal component analysis

Principal component analysis (PCA) is a well-known technique for dimension reduction in various applications (Jolliffe[12]), however, the lack of associated probabilistic model called for a derivation, called probabilistic PCA (PPCA), having a proper density-estimation framework (Tipping and Bishop[18]).

If we assume isotropic Gaussian noise in (6.1) with $\boldsymbol{\varepsilon} \sim N\left(0, \sigma^2\mathbf{I}\right)$, that leads us to the following conditional probability distribution (Tipping and Bishop[18]):

$$\mathbf{r} \mid \mathbf{x} \sim N\left(\mathbf{W}\mathbf{x}+\boldsymbol{\mu}, \sigma^2\mathbf{I}\right). \tag{6.3}$$

By convention, the marginal distribution for the latent variables is Gaussian with

$$\mathbf{x} \sim N\left(0, \mathbf{I}\right), \tag{6.4}$$

causing the marginal distribution for the observed data to be

$$\mathbf{r} \sim N\left(\boldsymbol{\mu}, \mathbf{W}\mathbf{W}^T+\sigma^2\mathbf{I}\right). \tag{6.5}$$

To obtain the maximum-likelihood estimator for $\mathbf{W}$ and σ^2, in the lack of a closed-form solution, we used an iterative expectation-maximization (EM) algorithm to estimate their values (Tipping and Bishop[18]). The EM algorithm consists of the following two steps:

$$\tilde{\mathbf{W}} = \mathbf{S}\mathbf{W}\left(\sigma^2\mathbf{I}+\mathbf{M}^{-1}\mathbf{W}^T\mathbf{S}\mathbf{W}\right)^{-1} \tag{6.6}$$

and

$$\tilde{\sigma}^2 = \frac{1}{d} tr\left(\mathbf{S} - \mathbf{S}\mathbf{W}\mathbf{M}^{-1}\tilde{\mathbf{W}}^T\right), \tag{6.7}$$

where $\mathbf{M} = \mathbf{W}^T\mathbf{W}+\sigma^2\mathbf{I}$, $\mathbf{S}$ is the covariance matrix

$$\mathbf{S} = \frac{1}{K}\sum_{i=1}^{K}\left(\mathbf{r}_i-\boldsymbol{\mu}\right)\left(\mathbf{r}_i-\boldsymbol{\mu}\right)^T, \tag{6.8}$$

while $\tilde{\mathbf{W}}$ and $\tilde{\sigma}$ denote the new value of the related parameters. When the iteration judged to have converged, one should perform an orthogonalization on the matrix $\mathbf{W}$ as well.

7 Prediction based trading

After the training phase has been done, the model is able to predict future stock prices based on a window of observed previous data denoted by ***X***. The forward algorithm (Rabiner[17]) can be used to calculate the forward values, the conditional probabilities being in each hidden state:

$$\alpha_t\left(i\right) = P\left(\mathbf{X} \mid \Theta, q(t) = q_i\right). \tag{7.1}$$

The forward algorithm calculates these values in a memory- and running time efficient manner by using a dynamic programming table. In our case, we are interested only in the probability vector belonging to the last state: $\boldsymbol{\alpha} = \left\{\alpha_T\left(i\right), i = 1, ..., N\right\}$. Having this at hand, one can formulate the probability density functions belonging to observations in the next step as follows:

- discrete case: $\boldsymbol{\omega} = \boldsymbol{\alpha}\mathbf{A}\mathbf{B}$, where $\omega_i = P\left(o_{T+1} = k_i\right)$;
- continuous case:

$$\xi \sim N\left(\sum_{i=1}^{N}\left(\boldsymbol{\alpha}\mathbf{A}\right)_i\sum_{j=1}^{M}w_{ij}\boldsymbol{\mu}_{ij}, \sum_{i=1}^{N}\left(\boldsymbol{\alpha}\mathbf{A}\right)_i\sum_{j=1}^{M}w_{ij}\boldsymbol{\Sigma}_{ij}\right), \tag{7.2}$$

and $P\left(\xi = \mathbf{y}\right) = P\left(\mathbf{o}_{T+1} = \mathbf{y}\right)$.

These p.d.f.-s are our predictions for the future asset prices. In each step, the asset with the highest probability of increasing (or decreasing) is selected which determines the trading action, whether to buy or shortsell for the sake of maximizing the profit. In the discrete case, the trading action is determined by the movement coded by different states, we can de-quantize it as $E(\xi) = \boldsymbol{\omega}^T \mathbf{v}$ accordingly, where $\boldsymbol{v}$ denotes the quantization vector used to map the alphabet (in the case of vector data, represented as n-tuples, an additional decoding step is needed to sum up the probabilities belonging to each asset). While, in the continuous case, a de-normalization step is needed as per (4.3). Thus, the trading signal is described as:

$$i := \arg\max_i \left| E(\xi_i) \right|; \begin{matrix} E(\xi_i) > 0 \rightarrow buy \\ E(\xi_i) < 0 \rightarrow shortsell \end{matrix}. \qquad (7.3)$$

8 Simulation results and performance analysis

An extensive back-testing framework was created to handle trading actions on various input data sets and provide numerical results for comparison of different methods on different financial data series. In this section we show the numerical results obtained on SWAP and FOREX mid-prices.

For performance analysis we used the following data sets:

- U.S. SWAP rates (between August 2008 and August 2010 in daily resolution);
- FOREX rates (EUR/USD, GBP/USD, AUD/USD, NZD/USD, USD/CHF, USD/CAD between December 2009 and 2011 in daily resolution).

The training set consisted of the first one year long period of daily returns, while the tests were performed on the second year of data.

For the sake of comparison the following performance measures were calculated for each simulation, where c_t denotes the sum of owned cash and the market value of the owned portfolio at time instance t, while c_0 denotes the initial cash (in each case the agent started with \$10,000): (i) minimal value $G_{\min} = \frac{1}{c_0} \min_{0 \le t \le T} c_t$; (ii) final value $G_{final} = \frac{c_T}{c_0}$; (iii) maximal value $G_{\max} = \frac{1}{c_0} \max_{0 \le t \le T} c_t$; (iv) average value $G_{avg} = \frac{1}{c_0} \frac{1}{T} \sum_{t=1}^{T} c_t$.

8.1 Comparison of different training methods

Both in the training set and during the test phase a sliding window of 8 days were used (T=8). In the continuous case, 3 hidden states (N=3) were used with the mixture of 3 uncorrelated Gaussian functions (M=3). Unfortunately, there is no analytical method known to find the optimal value for these parameters (Hassan *et al.*[8]). During the simulations, using the discrete representation of

observations, it turned out that trading SWAP rates is more profitable with a larger number of hidden states and a smaller alphabet size (during the simulations N=4 and M=2 were used), while on FOREX data a longer alphabet size together with less hidden states proved to be more favorable (we used N=2 and M=5 respectively).
In this period, the U.S. SWAP rates had a decreasing tendency, at the end of the year they are worth only 60.73% of their initial prices on average. The bar charts (Fig. 3 and Fig. 4) show that all of the introduced methods beat this tendency, and in the scenario when SA was used to train the continuous mode HMM the trading was profitable with a 108.52% yearly profit.
The FOREX rates in this period showed only a slight increase during the year (0.45%), our methods achieved up to 26.62% profit (Fig. 4).

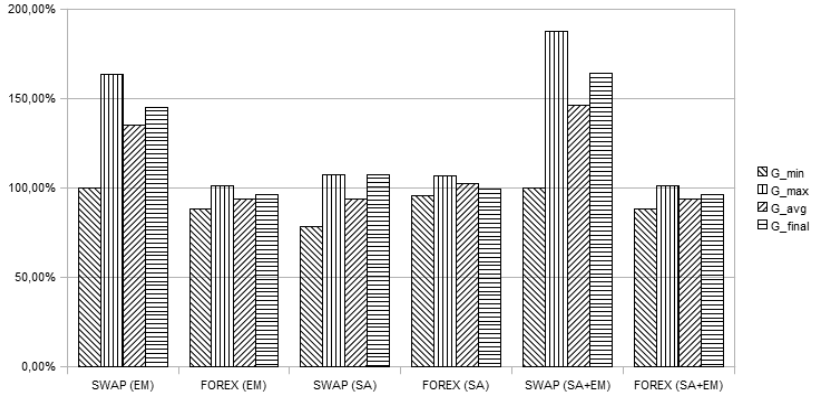

Fig. 3. Trading results in discrete case

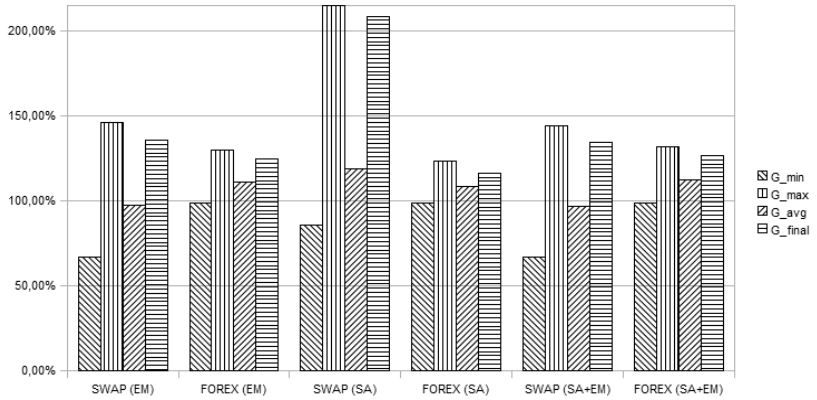

Fig. 4. Trading results in continuous case

As one can see, the novel HMM optimization methods outperform the traditional EM algorithm in most scenarios.

During the training phase, an EM step takes around *900ms*, while one step of SA consumes *250ms* using the continuous training sets on an Intel M330@2.13GHz processor. The prediction based trading step is quasi real-time. The hybrid approach speeds up the convergence with one order of magnitude.

8.2 Results obtained with clustering and PPCA

During clustering 8 clusters were formed in each case (N=8, M=1) with a shared covariance matrix. On the following bar charts `CLUST` denotes the case when clustering were applied as described in algorithm 2, while `CLUST (2)` refers to its enhanced version, where the next states are also taken into consideration. In the case of SWAP data, we investigated the event when the number of dimensions were reduced to 3 by PPCA from the original 8 assets. Similarly, the dimensions of FOREX data were reduced to 4 from 6.

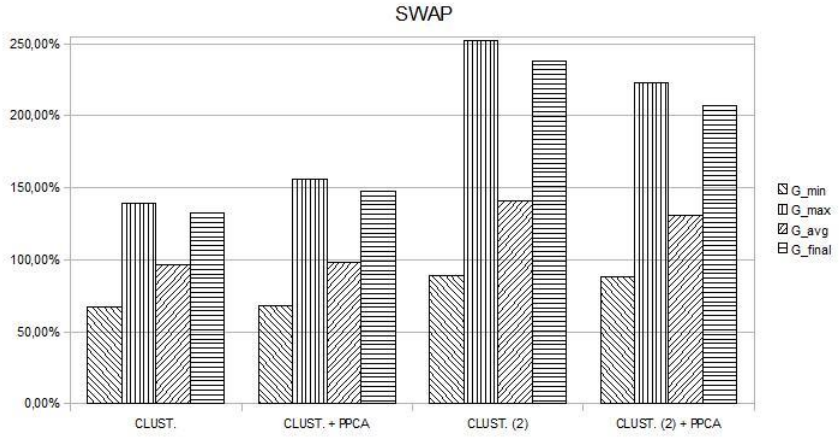

Fig. 5. Trading results on SWAP using clustering and PPCA

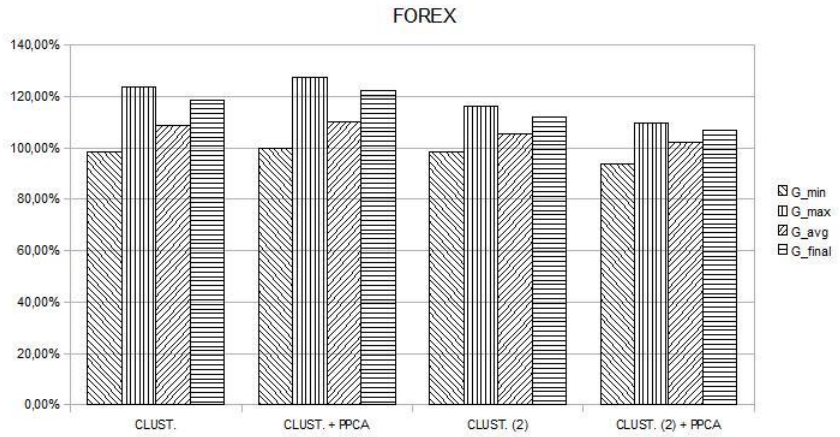

Fig. 6. Trading results on FOREX using clustering and PPCA

As it is shown in figure 5 and 6, these methods were also proven to be profitable on the tested time series, outperforming the market tendencies. The numerical results show that applying PPCA is beneficial with normal clustering, and less profitable with the enhanced version.
In comparison with the results shown in section 8.1, the range of the realized profits are comparable, reaching up to total 138.28% yearly profit on SWAP. The applied preprocessing steps yielded over one order of magnitude speed up compared to the previous methods.

9 Conclusion

In this paper we have proposed novel approaches for training HMMs and using them for predicting future values of financial time series. The proposed trading algorithms proved to be profitable in real scenarios. Using the continuous representation yields better trading results, however, its training time is substantially longer than the discrete case. We used three learning methods: (i) Baum-Welch EM; (ii) SA; and (iii) a hybrid solution. The performance analysis demonstrated that a better learning algorithm could increase trading efficiency and profit compared to the traditional learning strategies. The newly introduced clustering and PPCA methods can further speed up the algorithms giving rise to high frequency trading applications.
As a direction for future research, besides single asset price prediction, HMMs could be used for portfolios, obtained from an arbitrary portfolio optimization method, as well.

Acknowledgement

This work was partially supported by the European Union and the European Social Fund through project FuturICT.hu (grant no.: TAMOP-4.2.2.C-11/1/KONV-2012-0013).

References

1. D. J. Bartholomew. Latent variable models and factor analysis. Charles Griffin & Co. Ltd., London, 1987.
2. L. E. Baum and T. Petrie. Statistical Inference for Probabilistic Functions of Finite State Markov Chains. The Annals of Mathematical Statistics 37 (6): 1554–1563, 1966.
3. L. E. Baum, T. Petrie, G. Soules and N. Weiss. A maximization technique occurring in the statistical analysis of probabilistic functions of Markov chains. Ann. Math. Statist., vol. 41, no. 1, pp. 164–171, 1970.
4. S. Dasgupta. Learning Mixtures of Gaussians. Proceedings of Symposium on Foundations of Computer Science (FOCS), 1999.
5. R. Durbin, S. R. Eddy, A. Krogh and G. Mitchison. Biological sequence analysis, Cambridge University Press, 1998.
6. G. D. Forney. The Viterbi algorithm. Proc. IEEE, vol. 61, pp. 268-278, Mar. 1973.
7. R. Hassan and B. Nath. Stock Market Forecasting Using Hidden Markov Model: A New Approach. Proceedings of the 2005 5th International Conference on Intelligent Systems Design and Applications.

8. R. Hassan, B. Nath and M. Kirley. A fusion model of HMM, ANN and GA for stock market forecasting. Expert Systems with Applications 33 (2007) 171–180.
9. M. Hassoun. Fundamentals of artificial neural networks. MIT Press, 1995.
10. S. Haykin. Neural Networks a comprehensive foundation. MacMillan 2004.
11. P. Idvall and C. Jonsson. Algorithmic Trading - Hidden Markov Models on Foreign Exchange Data. Master's Thesis, Department of Mathematics, Linköpings Universitet, 2008.
12. I. T. Jolliffe. Principal Component Analysis. Springer-Verlag, New York, 1986.
13. D. Jurafsky and J. H. Martin. Speech and Language Processing: An Introduction to Natural Language Processing. Computational Linguistics, and Speech Recognition, 2nd Edition, Pearson Prentice Hall, London, 2006.
14. S. Kirkpatrick, C. D. Gelatt and M. P. Vecchi. Optimization by Simulated Annealing. Science, 220, pp. 671-680, 1983.
15. R. S. Mamon and R. J. Elliott. Hidden Markov Models in Finance, Springer Science Business Media, 2007.
16. L. R. Rabiner and B. H. Juang. An introduction to hidden Markov models. IEEE ASSP Magazine 3:4-16, 1986.
17. L. R. Rabiner. A Tutorial on Hidden Markov Models and Selected Applications in Speech Recognition. Proceedings of the IEEE, 77 (2), p. 257–286, February 1989.
18. M. Tipping, and C. Bishop. Probabilistic principal component analysis. Journal of the Royal Statistical Society: Series B, 61, part 3, pp. 611-622, 1999.
19. T. L. Tri, H. N. Van, N. T. Thi, V. P. Quoc and K. D. Xuan. A Normal - Hidden Markov Model in forecasting stock prices, 2011.
20. A. J. Viterbi. Error bounds for convolutional codes and an asymptotically optimal decoding algorithm. IEEE Trans. Informat. Theroy, vol. IT-13, pp. 260-269, Apr. 1967.
21. K. F. C. Yiu, Y. Liu and K. L. Teo. A Hybrid Descent Method for Global Optimization. Journal of Global Optimization 28: 229–238, 2004.

Proceedings, 15th Applied Stochastic Models and Data Analysis (ASMDA2013)
International Conference, Mataró (Barcelona), Spain 25 - 28 June 2013

Numerical approximation of solutions of stochastic differential equations driven by multifractional Brownian motion

Anna Soós[1]

Faculty of Mathematics and Computer Science, Babes-Bolyai University, Cluj Napoca, Romania
(E-mail: asoos@math.ubbcluj.ro)

Abstract. We study the numerical approximation of Ito stochastic differential equations driven by multifractional Brownian motion.

We consider the following stochastic differential equation driven by multifractional Brownian motion

$$X(t) = X_0 + \int_0^t F(X(s), s)ds + \int_0^t G(X(s), s)dB(s),\ t \in [0, T]. \tag{1}$$

We assume that with probability 1 we have $F \in C(\mathbb{R}^n \times [0,T], \mathbb{R}^n), G \in C^1(\mathbb{R}^n \times [0,T], \mathbb{R}^n)$ and for each $t \in [0,T]$ the functions $F(\cdot, t), \frac{\partial G(\cdot,t)}{\partial x}, \frac{\partial G(\cdot,t)}{\partial t}$ are locally Lipschitz. B is a multifractional Brownian motion.

The equation (1) will be approximated for each $N \in \mathbb{N}$ through

$$X_N(t) = X_0 + \int_0^t F(X_N(s), s)ds + \int_0^t G(X_N(s), s)dB_N(s). \tag{2}$$

We will show that the equation (2) has a local solution, which converges in probability to the solution of (1) in the interval, where the solutions exist. We use power series expansions for multifractional Brownian motion.
Keywords: multifractional Brownian motion, stochastic differential equations, series expansion.

1 Introduction

The notion of fractional Brownian motion (fBm) was introduced by Kolmogorov in 1940. Self-similarity, long-range dependence, and smoothness of the sample paths make fBm a useful tool in modelling natural phenomena. A constant Hurst parameter is too rigid for some applications, for example in finance and turbulence. Therefore different generalizations of fBm have been introduced. The multifractional Brownian motion (mfBm) was proposed in [11] and [2] replacing the Hurst parameter H of fBm by a scaling function $t \to H(t)$.

The fractional Brownian motion (fBm) with Hurst index $H \in (0,1)$ is a zero mean Gaussian random process $\Big(B(t)\Big)_{t\geq 0}$ with continuous sample paths and with covariance function

$$E\Big(B(s)B(t)\Big) = \frac{1}{2}\Big(t^{2H} + s^{2H} - |s-t|^{2H}\Big).$$

For $H = \frac{1}{2}$ the fractional Brownian motion is the ordinary standard Brownian motion.

The fractional Brownian motion B has on any finite interval $[0, T]$ Hölder continuous paths with exponent $\gamma \in (0, H)$ (see [5]). Moreover, the quadratic variation on $[a, b] \subseteq [0, T]$ is

$$\lim_{|\Delta_n| \to 0} \sum_{i=1}^{n} \left(B(t_i^n) - B(t_{i-1}^n) \right)^2 = \begin{cases} \infty & \text{if } H < \frac{1}{2}, \\ b - a & \text{if } H = \frac{1}{2}, \\ 0 & \text{if } H > \frac{1}{2}, \end{cases} \tag{3}$$

where $\Delta_n = (a = t_0^n < \ldots < t_n^n = b)$ is a partition of $[a, b]$ with $|\Delta_n| = \max_{1 \le i \le n} (t_i^n - t_{i-1}^n)$.

The multifractional Brownian motion (mfBm) is obtained by replacing the constant parameter H of the fractional Brownian motion by a smooth enough functional parameter $H(\cdot)$. We denote by H a function defined on the real line and with values in a fixed interval $[a, b] \subset (0, 1)$. We assume that it is uniformly Hölder continuous of order $\beta > b$ on each compact subset of $\mathbb{R}$. For example let H piecewise constant function $H : R \to]0, 1[$

$$H(t) = \sum_{i=0}^{k} a_i \mathbf{1}_{[\tau_i, \tau_{i+1}[}(t)$$

where $\tau_0 = -\infty, \tau_{k+1} = \infty$ and $\tau_1, \tau_2, \ldots \tau_k$ is an increasing finite sequence of real numbers.

Investigations concerning stochastic differential equations driven by a fractional Brownian motion or a more general fractional process have been done by L. Coutin and L. Decreusefond [3], L. Coutin and Z. Qian [4], M.L. Kleptsyna, P.E. Kloeden and V.V. Anh [7], F. Klingenhöfer and M. Zähle [8], M. Zähle [16], [17] and many others. These studies were motivated by the problems in mathematical finance, internet traffic, biology, hydrology etc. The main difficulty raised by the fractional Brownian motion and the processes related to it, is that they are not Markovian, even more, they are not even semimartingales. Hence a new approach to stochastic fractional calculus was developed. There exist several ways to define the stochastic integral pathwise and related techniques, Dirichlet forms, anticipating techniques using Malliavin calculus and Skorohod integration (e.g. [15], [5]). In this paper we use the approach of M. Zähle [15], based on the ideas of Lebesgue-Stieltjes integrals and fractional calculus [12] for fractional Brownian motion.

The multifractional Brownian motion $\Big(B(t)\Big)_{t \in [0,1]}$ with Hurst index H can be approximated using the series expansion given in [13].

For $\nu \neq -1, -2, \ldots$ **the Bessel function J_ν of the first type of order** ν is defined on the region $\{z \in \mathbb{C} : |\arg z| < \pi\}$ as the absolutely convergent sum

$$J_\nu(z) = \sum_{k=0}^{\infty} \frac{(-1)^k}{\Gamma(k+1)\Gamma(\nu + k + 1)} \left(\frac{z}{2} \right)^{\nu + 2k}.$$

It is known that for $\nu > -1$ the function J_ν has a countable number of real, positive simple zeros (see [14]). Let $x_1(t) < x_2(t) < \dots$ be the positive, real zeros of $J_{-H(t)}$ and let $y_1(t) < y_2(t) < \dots$ be the positive, real zeros of $J_{1-H(t)}$.

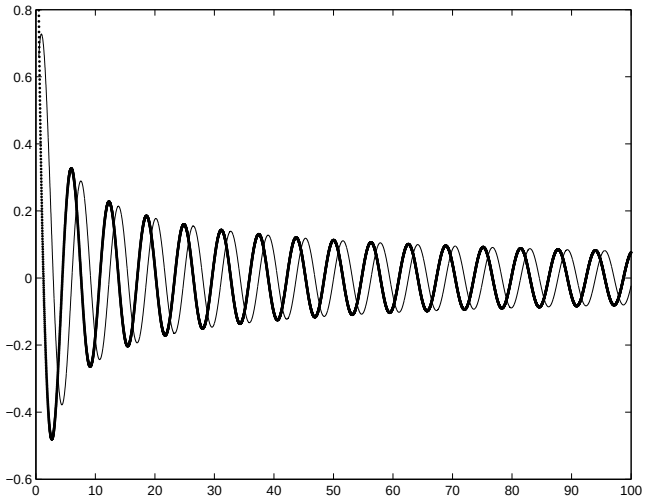

Fig. 1. Bessel functions: J_{-H} (with '·'), J_{1-H} (with '-'), $H = 0.65$

Let $(X_n)_{n\in\mathbb{N}}$ and $(Y_n)_{n\in\mathbb{N}}$ be two independent sequences of independent Gaussian random variables such that for each $n \in \mathbb{N}$ we have

$$E(X_n) = E(Y_n) = 0$$

and

$$\mathrm{Var}X_n = \frac{2c^2_{H(t)}}{x_n^{2H(t)} J^2_{1-H(t)}(x_n)}, \quad \mathrm{Var}Y_n = \frac{2c^2_{H(t)}}{y_n^{2H(t)} J^2_{-H(t)}(y_n)},$$

where

$$c^2_{H(t)} = \frac{\sin(\pi H(t))}{\pi} \Gamma(1 + 2H(t)).$$

It is proved in [13] that the random process $\Big(B(t)\Big)_{t\in[0,1]}$ given by

$$B(t) = \sum_{n=1}^{\infty} \frac{\sin(x_n t)}{x_n} X_n + \sum_{n=1}^{\infty} \frac{1 - \cos(y_n t)}{y_n} Y_n, \quad t \in [0, 1]$$

is well defined and both series converge absolutely and uniformly in $t \in [0, 1]$with probability 1. The process B is a mfBm with Hurst index H.

For each $N \in \mathbb{N}$ we define the process

$$B_N(t) = \sum_{n=1}^{N} \frac{\sin(x_n t)}{x_n} X_n + \sum_{n=1}^{N} \frac{1 - \cos(y_n t)}{y_n} Y_n, \quad t \in [0, 1]. \tag{4}$$

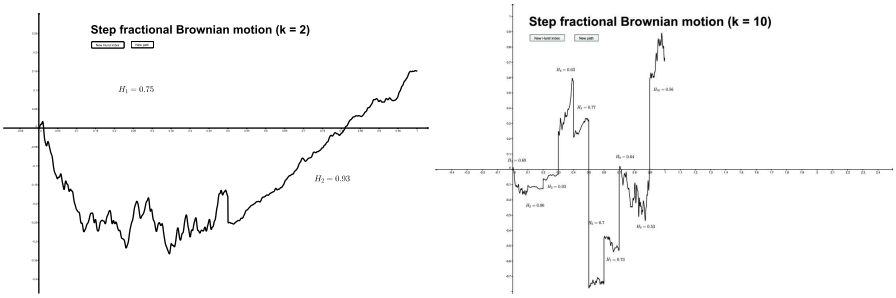

a) $K = 2$ b) $K = 10$

Fig. 2. Approximation B_N of multifractional Brownian motion

Then using the above mentioned result from [6] we have

$$P(\lim_{N\to\infty} \sup_{t\in[0,1]} |B(t) - B_N(t)| = 0) = 1. \tag{5}$$

We will use the following result:

Theorem 1. *For all $N \in \mathbb{N}$ the approximating processes $(B_N(t))_{t\in[0,1]}$ are Lipschitz continuous with probability* 1 .

Proof. Let $N \in \mathbb{N}$ be fixed. We write

$$|B_N(t) - B_N(s)| \le \sum_{n=1}^{N} \left| \frac{\sin(x_n t) - \sin(x_n s)}{x_n} X_n \right| + \sum_{n=1}^{N} \left| \frac{\cos(y_n s) - \cos(y_n t)}{y_n} Y_n \right|.$$

But the functions sin and cos are Lipschitz continuous, therefore

$$|B_N(t) - B_N(s)| \le |t-s| \sum_{n=1}^{N} \Big(|X_n| + |Y_n| \Big) = C_N |t-s| \text{ for all } s,t \in [0,1],$$

where $C_N = \sum_{n=1}^{N} \Big(|X_n| + |Y_n| \Big) < \infty$ is a random variable.

2 Fractional Integrals and Derivatives

Let $a, b \in \mathbb{R}$, $a < b$ and $f, g : \mathbb{R} \to \mathbb{R}$. We use notions and results about fractional calculus from [12] and [15]:

$$f(a+) := \lim_{\delta \searrow 0} f(a+\delta), \quad f(b-) := \lim_{\delta \searrow 0} f(b-\delta),$$

$$f_{a+}(x) = \mathbb{I}_{(a,b)}(x)(f(x) - f(a+)), \quad g_{b-}(x) = \mathbb{I}_{(a,b)}(x)(g(x) - g(b-)).$$

Note that for $\alpha > 0$ we have $(-1)^\alpha = e^{i\pi\alpha}$.

For $f \in L_1(a,b)$ and $\alpha > 0$ the **left-** and **right-sided fractional Rieman-Liouville integral of f of order** α on (a,b) is given for a.e. x by

$$I_{a+}^{\alpha} f(x) = \frac{1}{\Gamma(\alpha)} \int_a^x (x-y)^{\alpha-1} f(y) dy$$

and

$$I_{b-}^{\alpha} f(x) = \frac{(-1)^{-\alpha}}{\Gamma(\alpha)} \int_x^b (y-x)^{\alpha-1} f(y) dy.$$

For $p > 1$ let $I_{a+}^{\alpha}(L_p(a,b))$, be the class of functions f which have the representation $f = I_{a+}^{\alpha} \Phi$, where $\Phi \in L_p(a,b)$, and let $I_{b-}^{\alpha}(L_p(a,b))$ be the class of functions g which have the representation $g = I_{b-}^{\alpha} \varphi$, where $\varphi \in L_p(a,b)$. If $0 < \alpha < 1$, then the functions Φ, respectively φ, in the above representations agree a.s. with the **left-sided** and respectively **right-sided fractional derivative of f of order** α (in the Weyl representation)

$$\Phi(x) = D_{a+}^{\alpha} f(x) = \frac{1}{\Gamma(1-\alpha)} \left(\frac{f(x)}{(x-a)^{\alpha}} + \alpha \int_a^x \frac{f(x)-f(y)}{(x-y)^{\alpha+1}} dy \right) \mathbb{I}_{(a,b)}(x)$$

and

$$\varphi(x) = D_{b-}^{\alpha} g(x) = \frac{(-1)^{\alpha}}{\Gamma(1-\alpha)} \left(\frac{g(x)}{(b-x)^{\alpha}} + \alpha \int_x^b \frac{g(x)-g(y)}{(y-x)^{\alpha+1}} dy \right) \mathbb{I}_{(a,b)}(x).$$

The convergence at the singularity $y = x$ holds in the L_p-sense. Recall that

$$I_{a+}^{\alpha}(D_{a+}^{\alpha} f) = f \text{ for } f \in I_{a+}^{\alpha}(L_p(a,b)), \quad I_{b-}^{\alpha}(D_{b-}^{\alpha} g) = g \text{ for } g \in I_{b-}^{\alpha}(L_p(a,b))$$

and

$$D_{a+}^{\alpha}(I_{a+}^{\alpha} f) = f, \quad D_{b-}^{\alpha}(I_{b-}^{\alpha} g) = g \text{ for } f, g \in L_1(a,b).$$

For completeness we denote

$$D_{a+}^{0} f(x) = f(x), D_{b-}^{0} g(x) = g(x), D_{a+}^{1} f(x) = f'(x), D_{b-}^{1} g(x) = g'(x).$$

Let $0 \le \alpha \le 1$. The **fractional integral** of f with respect to g is defined as

$$\int_a^b f(x) dg(x) = (-1)^{\alpha} \int_a^b D_{a+}^{\alpha} f_{a+}(x) D_{b-}^{1-\alpha} g_{b-}(x) dx + \\ + f(a+)(g(b-) - g(a+)) \tag{6}$$

if $f_{a+} \in I_{a+}^{\alpha}(L_p(a,b)), g_{b-} \in I_{b-}^{1-\alpha}(L_q(a,b))$ for $\frac{1}{p} + \frac{1}{q} \le 1$.

In our investigations we will take $p = q = 2$. If $0 \le \alpha < \frac{1}{2}$, then the integral in (6) can be written as

$$\int_a^b f(x) dg(x) = (-1)^{\alpha} \int_a^b D_{a+}^{\alpha} f(x) D_{b-}^{1-\alpha} g_{b-}(x) dx \tag{7}$$

if $f \in I_{a+}^{\alpha}(L_2(a,b))$, $f(a+)$ exists, $g_{b-} \in I_{b-}^{1-\alpha}(L_2(a,b))$ (see [15]).

3 The Stochastic Integral

Without loss of generality we consider $0 < T \leq 1$, because for arbitrary $T > 0$ we can rescale the time variable using the H-self-similar property of the mfBm meaning that $\Big(B(ct)\Big)_{t\geq 0}$ and $\Big(c^H(t)B(t)\Big)_{t\geq 0}$ are equal in distribution for every $c > 0$.

We will define the Itô integral $\int\limits_0^T G(u)dB(u)$ instead of $\int\limits_0^t G(u)dB(u)$ and use

$$\int\limits_0^t G(u)dB(u) = \int\limits_0^T \mathbb{I}_{[0,t]}(u)G(u)dB(u) \text{ for } t \in [0,T]$$

(see [15]).

We consider $\alpha > 1 - H$. It follows by (7) that

$$\int\limits_0^T G(u)dB(u) = (-1)^\alpha \int\limits_0^T D^\alpha_{0+}G(u)D^{1-\alpha}_{T-}B_{T-}(u)du \tag{8}$$

for $G \in I^\alpha_{0+}(L_2(0,T))$, where $G(0+)$ exists and $B_{T-} \in I^{1-\alpha}_{T-}(L_2(0,T))$.

The condition $G \in I^\alpha_{0+}(L_2(0,T))$ (with probability 1) means that $G \in L_2(0,T)$ and

$$\mathcal{I}_\varepsilon(x) = \int\limits_0^{x-\varepsilon} \frac{G(x) - G(y)}{(x-y)^{\alpha+1}}dy \text{ for } x \in (0,T)$$

converges in $L^2(0,T)$ as $\varepsilon \searrow 0$.

The condition $B_{T-} \in I^{1-\alpha}_{T-}(L_2(0,T))$ means $B_{T-} \in L_2(0,T)$ and

$$\mathcal{J}_\varepsilon(x) = \int\limits_{x+\varepsilon}^T \frac{B(x) - B(y)}{(y-x)^{2-\alpha}}dy \text{ for } x \in (0,T)$$

converges in $L_2(0,T)$ as $\varepsilon \searrow 0$ This condition for B is fulfilled for $\alpha > 1 - H$, since the fractional Brownian motion B is a.s. Hölder continuous with exponent $\gamma \in (0,H)$ (see [5]).

We will use (7) for the integrals with respect to the approximating processes $\Big(B_N(t)\Big)_{t\in[0,T]}$. Observe that $B_{N,T-} \in I^{1-\alpha}_{T-}(L_2(0,T))$, which follows from the Lipschitz continuity property in Theorem 1. We have

$$\int\limits_0^T G(u)dB_N(u) = (-1)^\alpha \int\limits_0^T D^\alpha_{0+}G(u)D^{1-\alpha}_{T-}B_{N,T-}(u)du \tag{9}$$

for $G \in I^\alpha_{0+}(L_2(0,T))$, where $G(0+)$ exists.

Let $\Big(Z(t)\Big)_{t\in[0,T]}$ be a cádlág process. Its **generalized quadratic variation process** $\Big([Z](t)\Big)_{t\in[0,T]}$ is defined as

$$[Z](t) = \lim_{\varepsilon\searrow 0} \varepsilon \int_0^1 u^{\varepsilon-1} \int_0^t \frac{1}{u}(Z_{t-}(s+u) - Z_{t-}(s))^2 dsdu + (Z(t) - Z(t-))^2,$$

if the limit exists uniformly in probability (see [17]).

In particular, if B is a fractional Brownian motion with Hurst index $H \in (\frac{1}{2}, 1)$ and B_N is an approximation of B as given in (4), it is easy to verify that

$$[B](t) = 0 \quad \text{and} \quad [B_N](t) = 0 \quad \text{for each} \ \ t \in [0,T], \tag{10}$$

because B is locally Hölder continuous with exponent $> \frac{1}{2}$ and B_N is Lipschitz continuous. The **Ito formula** for change of variable for fractional integrals is given in the next theorem.

Theorem 2 ([17]). *Let $\Big(Z(t)\Big)_{t\in[0,T]}$ be a continuous process with generalized quadratic variation $[Z]$. Let $Q : \mathbb{R}\times[0,T] \to \mathbb{R}$ be a random function such that a.s. we have $Q \in \mathcal{C}^1(\mathbb{R}\times[0,T])$ and $\frac{\partial^2 Q}{\partial x^2} \in \mathcal{C}(\mathbb{R}\times[0,T])$. Then, for $t_0, t \in [0,T]$ we have*

$$Q(Z(t),t) - Q(Z(t_0),t_0) = \int_{t_0}^t \frac{\partial Q}{\partial x}(Z(s),s)dZ(s) + \int_{t_0}^t \frac{\partial Q}{\partial t}(Z(s),s)ds + \frac{1}{2}\int_{t_0}^t \frac{\partial^2 Q}{\partial^2 x}(Z(s),s)d[Z]s.$$

Let $1 - H < \alpha < \frac{1}{2}$ and let $G \in I^{\alpha}_{0+}(L_2(0,T))$ such that $G(0+)$ exists. We define the processes

$$Z(t) = \int_0^t G(s)dB(s) \text{ and } Z_N(t) = \int_0^t G(s)dB_N(s), \quad t \in]0,T].$$

Then by [17] it follows that

$$[Z](t) = 0 \text{ and } [Z_N](t) = 0.$$

So,if $Q : \mathbb{R}\times[0,T] \to \mathbb{R}$ is a random function such that a.s. we have $Q \in \mathcal{C}^1(\mathbb{R}\times[0,T])$ and $\frac{\partial^2 Q}{\partial x^2} \in \mathcal{C}(\mathbb{R}\times[0,T])$, then for $t_0, t \in [0,T]$ we have

$$Q(Z(t),t) - Q(Z(t_0),t_0) = \int_{t_0}^t \frac{\partial Q}{\partial x}(Z(s),s)G(s)dB(s) + \int_{t_0}^t \frac{\partial Q}{\partial t}(Z(s),s)ds \tag{11}$$

and

$$Q(Z_N(t),t) - Q(Z_N(t_0),t_0) = \int_{t_0}^{t} \frac{\partial Q}{\partial x}(Z_N(s),s)G(s)dB_N(s) + \int_{t_0}^{t} \frac{\partial Q}{\partial t}(Z_N(s),s)ds. \tag{12}$$

4 Stochastic Differential Equations Driven by MultiFractional Brownian Motion

Let $\Big(B(t)\Big)_{t\geq 0}$ be a mfBm with Hurst parameter H such that $H(t) > \frac{1}{2}$. We investigate stochastic differential equations of the form

$$\begin{aligned} dX(t) &= F(X(t),t)dt + G(X(t),t)dB(t), \\ X(t_0) &= X_0, \end{aligned} \tag{13}$$

where $t_0 \in]0,T]$, X_0 is a random vector in $\mathbb{R}^n$ and the random functions F and G satisfy with probability 1 the following conditions:

(C1) $F \in C(\mathbb{R}^n \times [0,T], \mathbb{R}^n), G \in C^1(\mathbb{R}^n \times [0,T], \mathbb{R}^n)$;

(C2) for each $t \in [0,T]$ the functions $F(\cdot,t), \dfrac{\partial G(\cdot,t)}{\partial x^i}, \dfrac{\partial G(\cdot,t)}{\partial t}$ are locally Lipschitz for each $i \in \{1,\ldots,n\}$.

We consider the pathwise auxiliary partial differential equation on $\mathbb{R}^n \times \mathbb{R} \times [0,T]$

$$\begin{aligned} \frac{\partial K}{\partial z}(y,z,t) &= G(K(y,z,t),t), \\ K(Y_0,Z_0,t_0) &= X_0, \end{aligned} \tag{14}$$

where Y_0 is an arbitrary random vector in $\mathbb{R}^n$ and Z_0 an arbitrary random variable in $\mathbb{R}$. From the theory of differential equations it follows that with probability 1 there exists a local solution $K \in C^1(\mathbb{R}^n \times \mathbb{R} \times [0,T], \mathbb{R}^n)$ in a neighbourhood V of (Y_0,Z_0,t_0) with partial derivatives being Lipschitz in the variable y and

$$\det\left(\frac{\partial K^i}{\partial y^j}(y,z,t)\right)_{1\leq i,j\leq n} \neq 0.$$

For $(x,y,t) \in V$ we have

$$\frac{\partial^2 K}{\partial z^2}(y,z,t) = \sum_{j=1}^{n} \frac{\partial G}{\partial x^j}(K(y,z,t),t)G^j(K(y,z,t),t).$$

We also consider the pathwise differential equation (in matrix representation) on $[0,T]$

$$\frac{\partial K}{\partial y}(Y(t),B(t),t)dY(t)+\frac{\partial K}{\partial t}(Y(t),B(t),t)dt=F(K(Y(t),B(t),t),t)dt \quad (15)$$

$$Y(t_0)=Y_0, \quad (16)$$

or

$$dY(t)=\left(\frac{\partial K}{\partial y}(Y(t),B(t),t)\right)^{-1}\left[F(K(Y(t),B(t),t),t)-\frac{\partial K}{\partial t}(Y(t),B(t),t)\right]dt$$
$$Y(t_0)=Y_0,$$

which has a unique local solution on a maximal interval $]t_0^1,t_0^2[\subseteq[0,T]$ with $t_0\in]t_0^1,t_0^2[$ (see [9]).

Applying the Ito formula, and relation (11), to the random function $Q(z,t)=K(Y(t),z,t)$ (in fact, successively for $K^1,\ldots,K^n$) and the step fractional Brownian motion B we obtain

$$\begin{aligned}
&K(Y(t),B(t),t)-K(Y(t_0),B(t_0),t_0)\\
&=\sum_{j=1}^{n}\int_{t_0}^{t}\frac{\partial K}{\partial y^j}(Y(s),B(s),s)dY^j(s)+\int_{t_0}^{t}\frac{\partial K}{\partial z}(Y(s),B(s),s)dB(s)\\
&\quad+\int_{t_0}^{t}\frac{\partial K}{\partial t}(Y(s),B(s),s)ds\\
&=\sum_{j=1}^{n}\int_{t_0}^{t}\frac{\partial K}{\partial y^j}(Y(s),B(s),s)dY^j(s)+\int_{t_0}^{t}G(K(Y(s),B(s),s),s)dB(s)\\
&\quad+\int_{t_0}^{t}\frac{\partial K}{\partial t}(Y(s),B(s),s)ds\\
&=\int_{t_0}^{t}F(K(Y(s),B(s),s),s)ds+\int_{t_0}^{t}G(K(Y(s),B(s),s),s)dB(s).
\end{aligned}$$

Therefore,

$$X(t):=K(Y(t),B(t),t)$$

satisfies

$$X(t)=X_0+\int_{t_0}^{t}F(X(s),s)ds+\int_{t_0}^{t}G(X(s),s)dB(s).$$

Instead of the process $\Big(B(t)\Big)_{t\in[0,1]}$ we consider its approximations $\Big(B_N(t)\Big)_{t\in[0,1]}$ given in (4). For each $N\in\mathbb{N}$ we consider the pathwise differential equation (in

matrix representation)

$$dY_N(t) = \left(\frac{\partial K}{\partial y}(Y_N(t), B_N(t), t)\right)^{-1} \Big[F(K(Y_N(t), B_N(t), t), t) - \frac{\partial K}{\partial t}(Y_N(t), B_N(t), t)\Big]dt$$
$$Y_N(t_0) = Y_0,$$

which has a unique local solution Y_N on a maximal interval $(t^1, t^2) \subset (t_0^1, t_0^2)$ of existence which contains t_0 ([13]). Applying the Ito formula to the random function $Q(z,t) = K(Y_N(t), z, t)$ (in fact, successively for $K^1, \ldots, K^n$) and the process B_N we obtain

$$\begin{aligned}
&K(Y_N(t), B_N(t), t) - K(Y_N(t_0), B_N(t_0), t_0) \\
&= \sum_{j=1}^{n} \int_{t_0}^{t} \frac{\partial K}{\partial y^j}(Y_N(s), B_N(s), s) dY_N^j(s) + \int_{t_0}^{t} \frac{\partial K}{\partial z}(Y_N(s), B_N(s), s) dB_N(s) \\
&\quad + \int_{t_0}^{t} \frac{\partial K}{\partial t}(Y_N(s), B_N(s), s) ds \\
&= \sum_{j=1}^{n} \int_{t_0}^{t} \frac{\partial K}{\partial y^j}(Y_N(s), B_N(s), s) dY_N^j(s) + \int_{t_0}^{t} G(K(Y_N(s), B_N(s), s), s) dB_N(s) \\
&\quad + \int_{t_0}^{t} \frac{\partial K}{\partial t}(Y_N(s), B_N(s), s) ds \\
&= \int_{t_0}^{t} F(K(Y_N(s), B_N(s), s), s) ds + \int_{t_0}^{t} G(K(Y_N(s), B_N(s), s), s) dB_N(s).
\end{aligned}$$

Therefore,

$$X_N(t) := K(Y_N(t), B_N(t), t)$$

satisfies

$$X_N(t) = X_0 + \int_{t_0}^{t} F(X_N(s), s) ds + \int_{t_0}^{t} G(X_N(s), s) dB_N(s), \quad t \in]t_1, t_2[.$$

So we have the following pathwise property

$$\lim_{N \to \infty} \sup_{t \in]t_1, t_2[} \|Y_N(t) - Y(t)\| = 0.$$

Then the continuity properties of K and (5) imply that for a.e. $\omega \in \Omega$ it holds

$$\lim_{N \to \infty} \sup_{t \in]t_1, t_2[} \|X_N(t) - X(t)\| = 0.$$

By this we have proved the main result of our paper:

Theorem 3. *Let B be a mfBm approximated by the processes B_N given in* (4) *and* (5). *Let $F, G : \mathbb{R}^n \times [0,T] \to \mathbb{R}^n$ be random functions satisfying conditions* (C1) *and* (C2) *with probability* 1. *Let $t_0 \in]0,T]$ be fixed. Then each of the stochastic equations*

$$X(t) = X_0 + \int_{t_0}^{t} F(X(s),s)ds + \int_{t_0}^{t} G(X(s),s)dB(s),$$

$$X_N(t) = X_0 + \int_{t_0}^{t} F(X_N(s),s)ds + \int_{t_0}^{t} G(X_N(s),s)dB_N(s), \quad N \in \mathbb{N}$$

admits almost surely a unique local solution on a common interval $]t_1,t_2)[$ (which is independent of N and contains t_0). Moreover, we have the following approximation result

$$P(\lim_{N\to\infty} \sup_{t\in]t_1,t_2[} \|X_N(t) - X(t)\| = 0) = 1.$$

5 Application

We consider the one dimensional stochastic linear equation from financial mathematics, modeling the price S of a stock

$$S(t) = S_0 + \int_0^t \mu(s)S(s)ds + \int_0^t \sigma(s)S(s)dB(s),$$

where $(B(t))_{t\in[0,T]}$ is a mfBm with Hurst index $H(t) > \frac{1}{2}$, μ is the interest rate and σ the volatility function.

It is known (see [8]) that this equation has the following unique solution

$$S(t) = S_0 \exp\left\{\int_0^t \mu(u)du + \int_0^t \sigma(u)dB(u)\right\} \text{ for all } t \in [0,T].$$

By the methods of the above section we approximate B through the processes B_N, via (4) and (5) and consider

$$S_N(t) = S_0 \exp\left\{\int_0^t \mu(u)du + \int_0^t \sigma(u)dB_N(u)\right\} \text{ for all } t \in [0,T].$$

Using Theorem 3 it follows that

$$P(\lim_{N\to\infty} \sup_{t\in[0,T]} \|S_N(t) - S(t)\| = 0) = 1.$$

In the special case when μ and σ are constants, we obtain that the price of a stock is

$$S(t) = S_0 e^{\mu t + \sigma B(t)}$$

and we can simulate it by computer using

$$S_N(t) = S_0 e^{\mu t + \sigma B_N(t)}$$

as given in Figure 3, where K is the number of constant pieces of H.

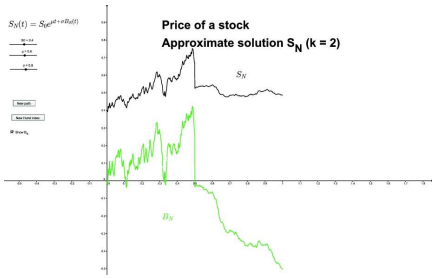

$K = 2$

Fig. 3. Approximated solution S_N

References

1.A. Ayache and M. S. Taqqu. Rate optimality of wavelet series approximations of fractional Brownian motion. *Jour. Fourier Anal. Appl.* **9**, 451-471, 2003.
2.A. Benassi, S. Jaffard and D. Roux. Elliptic Gaussian random processes, *Rev. Mathematica Iberoamericana,* **13**, no.1, 19–90, 1997.
3.L. Coutin and L. *Decreusefond. Stochastic Differential Equations Driven by a Fractional Brownian Motion*, Tech. Report 97C004, ENST Paris 1997.
4.L. Coutin and Z. Qian. Stochastic Differential Equations for Fractional Brownian Motions, *C. R. Acad. SCI. Paris,* **331**, Srie I, 75–80, 2000.
5.L. Decreusefond and A.S. Üstünel. Stochastic Analysis of the Fractional Brownian Motion. *Potential Analysis,* **10**, 177–214, 1999.
6.D. Dzhaparidze and H. van Zanten. A Series Expansion of Fractional Brownian Motion, *Probab. Theory Relat. Fields,* **130**, 39–55, 2004.
7.M.L. Kleptsyna, P.E. Kloeden and V.V. Anh. Existence and Uniqueness Theorems for FBM Stochastic Differential Equations, *Information Transmission Problems,* **34**, 41–51, 1998.
8.F. Klingenhöfer and M. Zähle. Ordinary Differential Equations with Fractal Noise, *Proc. Amer. Math. Soc.* **127**, 1021–1028, 1999.
9.H. Lisei, and A. Soós. Approximation of Stochastic Differential Equations Driven by Fractional Brownian Motion, in *Seminar on stochastic analysis, random fields and applications V, Progress in Probability,* **59**, Birkhuser Verlag, 229-244, 2007.
10.B. Mandelbrot, and Van Ness. Fractional Brownian motion, fractional noises and applications, *SIAM Rev.,* **10**, 422-437, 1968.
11.R. Peltier and J. Lévy Vehel. *Multifractional Brownian Motion: definition and preliminary results*, Rapport technique INRIA, 1996.

12.S. G. Samko, A. A. Kilbas, and O. I. Marichev. *Fractional Integrals and Derivatives. Theory and Applications,* Gordon and Breach, 1993.
13.A. Soós. Series expansion of multifractional Brownian motion,(to appear).
14.G. N. Watson. *A Treatise on the Theory of Bessel Functions,* Cambridge University Press, 1944.
15.M. Zähle. Integration with respect to Fractal Functions and Stochastic Calculus I., *Probab.Theory Relat. Fields,* **111**, 333–374, 1998.
16.M. Zähle. Ordinary Differential Equations with Fractal Noise. *Proc. Am. Math. Soc.,* **127**, 333–374, 1999.
17.M. Zähle. Integration with respect to Fractal Functions and Stochastic Calculus II. *Math. Nachr.,* **225**, 145–183, 2001.

Proceedings, 15th Applied Stochastic Models and Data Analysis (ASMDA2013)
International Conference, Mataró (Barcelona), Spain 25 - 28 June 2013

Interpolation methods for internet traffic

Soós Anna Somogyi Ildikó

Abstract

The classical methods of data interpolation can be generalized with fractal interpolation. Our aim is to maid some comparison of the fractal and numerical analysis interpolation methods. The experimental data regarding the internet traffic were processed using fractal interpolation and also spline and some Shepard type interpolation.

1 Spline interpolation

Let $H^{m,2}[a,b]$, $m \in \mathbb{N}^*$ be the set of functions $f \in C^{m-1}[a,b]$ with $f^{(m-1)}$ absolutely continuous on $[a,b]$ and $f^{(m)} \in L^2[a,b]$, $\Lambda = \{\lambda_i | \lambda_i : H^{m,2}[a,b] \to \mathbb{R}, i = 1...,n\}$ a set of linear functionals, $yin\mathbb{R}^n$ and

$$U_y = \{f \in H^{m,2}[a,b] | \lambda_i(f) = y_i, i = 1,...,n\}.$$

Definition 1 *The problem that consists of determining the elements $s \in U$ such that*

$$\left\| s^{(m)} \right\|_2 = \inf_{u \in U} \left\| u^{(m)} \right\|_2$$

is called polinomial spline interpolation problem.

For the solution of a spline interpolation problem we can give the following structural characterization theorem ([4]):

Theorem 2 *Let Λ be a set of Birkhoff type functionals and let U be the corresponding interpolatory set. The functions $s \in U$ is a solution of the spline interpolation problem if and only if:*

1. $s^{(2m)}(x) = 0, \quad x \in [x_1, x_k]$
   $\{x_1, ...x_k\}$,
2. $s^{(m)}(x) = 0, \quad x \in (a, x_1) \cup (x_k, b)$,
3. $s^{(2m-\mu-1)}(x_i - 0) = s^{(2m-\mu-1)}(x_i + 0), \quad \mu\{0, 1, ..., m-1\}$
   I_i *for* $i = 1, ..., k$.

The caracterization theorem states that the solution s of the polynomial spline interpolation problem is a polynomial of $2m-1$ degree on each interior interval (x_i, x_{i+1}) and it is a polynomial of $m-1$ degree on the intervals $[a, x_1)$ and $(x_k, b]$. Furthermore, the derivative of order $2m-\mu-1$ is continuous in x_i if the value of the νth ordin derivative in x_i does not belong to Λ.

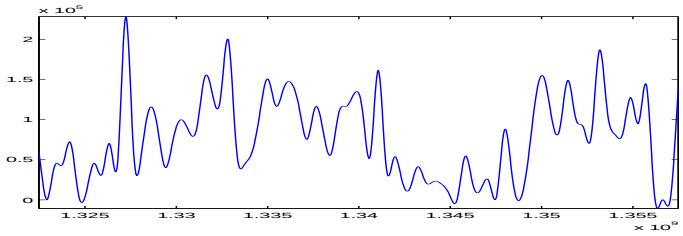

Figure 1: Spline interpolation: for internet traffic data

Definition 3 *The solution s of the polynomial spline interpolation problem is called a natural spline function of order $2m-1$.*

When $\Lambda = \{\lambda_i | \lambda_i(f) = f(x_i), i = 1, ..., n\}$, with $x_i \in [a, b], i = 1, ..., n$ and $n \geq m$, then for every $f \in H^{m,2}[a, b]$ the interpolation spline function $S_L f$ exists, is unique and the corresponding operator is called the spline operator of Lagrange type.
The function $S_L f$ may be written in the form

$$S_L f = \sum_{k=1}^{n} s_k f(c_k),$$

where $s_k k = 1, .., n$ are the fundamental interpolation spline functions. To determine these functions we use the caracterization theorem and we have

$$s_k(x) = \sum_{i=0}^{m-1} a_i^k x_i + \sum_{j=1}^{n} b_j^k (x - x_j)_+^{2m-1}, k = 1, ..., n,$$

whith $a_i^k, i = 0, ..., m-1$ and $b_j^k, j = 1, ..., n$ obtained as the solution of the following systems:

$$\begin{aligned} s_k^p(\alpha) &= 0, \ p = m, ..., 2m-1, \ \texttt{and} \ \alpha > x_n \\ s_k(x_\nu) &= \delta_{k\nu}, \ \nu = 1, ..., n \end{aligned}$$

for $k = 1, ..., n$.
We will use the third degree Lagrange type spline interpolation operator on internet traffic datas.

2 The Shepard operator

Our next approximation method is the Shepard method, introduced in 1968, which is a well suited method for interpolation of very large scattered data sets. It has the advantages of a small storage requirement and an easy generalization to additional independent variables.

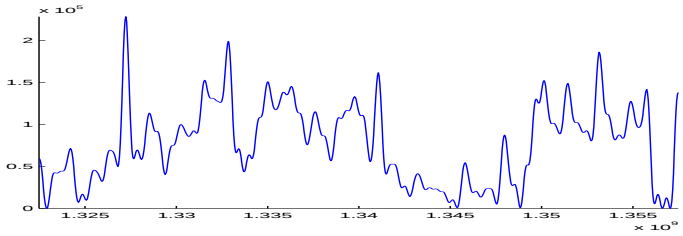

Figure 2: Shepard interpolation: for internet traffic data

Considering the interpolation points $(x_i, f(x_i))$, $i = 0, ..., N$, Shepard introduced in [5] the linear interpolation operator

$$(S_0 f)(x) = \sum_{i=0}^{N} A_{i,\mu}(x) f(x_i), \qquad \mu > 0,$$

with

$$A_{i,\mu}(x) := \frac{\|x - x_i\|^{-\mu}}{\sum_{k=0}^{N} \|x - x_k\|^{-\mu}}, \qquad i = 0, ..., N.$$

S_0 reproduces exactly only the constant functions. To avoid this, several authors, starting with Shepard himself, have suggested to apply S_0 not directly to $f(x_i)$, but to some interpolation operators $P[f, x_i](x)$ at x_i by considering the so-called combined operator:

$$(S_P f)(x) = \sum_{i=0}^{N} A_{i,\mu}(x) P[f, x_i](x), \qquad \mu > 0. \tag{1}$$

The operator S_P still interpolates f at x_i, $i = 0, ..., N$ but the algebraic degree of exactness is $\max_{i=0,...,N} \text{dex}(P[f, x_i])$.

The combined Shepard-Lagrange operator S_{L_m} is given by [3], [2]:

$$(S_{L_m} f)(x) = \sum_{i=0}^{N} A_i(x) (L_m^i f)(x),$$

where

$$(L_m^i f)(x) = \sum_{\nu=0}^{m} \frac{u_i(x)}{(x - x_{i+\nu}) u_i'(x_{i+\nu})} f(x_{i+\nu})$$

is the Lagrange polynomial corresponding to the set $\Lambda_i(f) = f(x_{i+\nu}) : \nu = 0, 1, \ldots, m\}$, $i = 0, \ldots, N$, with $x_{N+\nu} = x_{N-\nu}$.

In our next Figure we plot the graphics of $S_0 f$ considering $\mu = 2$ and the same datas.

3 Fractal functions

The tird interpolation will be the fractal interpolation on internet traffic datas.

Let (X, d) be a complete metric space, let $D(X)$ the class of all non-empty closed bounded subsets of X. Then $(D(X), h)$ is a complete metric space with the Hausdorff metric: $h : D(X) \times D(X) \to R$

$$h(A, B) := \sup\{\sup_{a\in A} \inf_{b\in B} d(a, b), \sup_{b\in B} \inf_{a\in A} d(a, b)\}$$

Let $E \subset X$, $p \geq 0$, $\epsilon > 0$, and define the Hausdorff p-dimensional measure of E:

$$\mathcal{H}^p(E) := \lim_{\epsilon\to 0} \mathcal{H}^p_\epsilon(E) = \sup_{\epsilon>0} \mathcal{H}^p_\epsilon(E),$$

where

$$\mathcal{H}^p_\epsilon(E) := \inf\{\sum_{i=1}^{\infty} |E_i|^p, E \subset \cup_{i=1}^{\infty} E_i, |E_i| < \epsilon\}$$

For each E there is a unique real number q,named the Hausdorff dimension of E, such that

$$\mathcal{H}^p(E) = \begin{cases} +\infty & if \quad 0 \leq p < q \\ 0 & if \quad q < p < \infty \end{cases}$$

B. Mandelbrot define fractal as the set of which Hausdorff dimension is noninteger.

The functions $f : I \to \mathbf{R}$, where I is a real closed interval, is named by M. F. Barnsley *fractal function* if the Hausdorff dimensions of their graphs are noninterger.

Let N a natural number, $N > 1$, and let $w_i : \ X \to X : \ i \in \{1, ..., N\}$ be continuous. Then we call $\{X, w_i : i = 1, ..., N\}$ an *iterated function sistem (IFS).*

If, for some $0 \leq k < 1$ and all $i \in \{1, ..., N\}$,

$$d(w_i(x), w_i(x')) \leq kd(x, x'), \forall\, x, x' \in X,$$

then the IFS is named *hyperbolic.*

Define $W : \mathcal{D}(X) \to \mathcal{D}(X)$ by

$$W(A) := \cup_{i=1}^{N} w_i(A),$$

where $w_i(A) = \{w_i(x) : x \in A\}$.

W is a contraction mapping if the IFS is hyperbolic:

$$h(W(A), W(B)) \leq kh(A, B) \,\forall\, A, B \in \mathcal{D}(X).$$

Any set $G \in D(X)$ such that $W(G) = G$ is called an *attractor* for the IFS.

Theorem 4 *(Hutchinson) Let $\{X, w_i\, i = 1, ..., N\}$ an hyperbolic IFS. There is a unique compact set $G \subset X$, such that $W(G) = G$, and*

$$G := \lim_{n\to\infty} W^n(E), \ E \in \mathcal{D}(X), W^0$$

Let $\{(x_i, y_i) \in R^2, i = 0, 1, \cdots, N\}$ be given, and $I = [x_0, x_N]$. The functions $f : I \to R$, which interpolate the data according to $f(x_i) = y_i$, $i = 0, 1, ..., N$, and whose graphs are attractors of IFS are *fractal interpolation functions*

Let $X = I \times [a, b]$ with Euclidean metric d, $I_n = [x_{n-1}, x_n]$ $u_n : I \to I_n$, $n \in \{1, 2, ..., N\}$, contractiv homeomorphism such that

$$u_n(x_0) := x_{n-1},\ u_n(x_N) := x_n,\ \forall n \in \{1, \cdots, N\}.$$

$$|u_n(c_1) - u_n(c_2)| \leq l|c_1 - c_2|,\ c_1, c_2 \in I,\ 0 \leq l < 1$$

$v_n : X \to [a, b]$ continuous, with

$$v_n(x_0, y_0) := y_{n-1},\ v_n(x_N, y_N) := y_n,\ \forall n \in \{1, \cdots, N\}.$$

$$|v_n(c, d_1) - v_n(c, d_2)| \leq q|d_1 - d_2|,\ c \in I,\ d_1, d_2 \in [a, b], 0 \leq q < 1.$$

Let $w_n : X \to X$, $n \in \{1, 2, ..., N\}$

$$w_n(x, y) = (u_n(x), v_n(x, y)).$$

$\{X, w_n : n = 1, 2, ..., N\}$ is an IFS but may not be hyperbolic.

Theorem 5 *(Barnsley) For the IFS $\{X, w_n : n = 1, 2, ..., N\}$ defined above, there is a metric d equivalent to the Euclidean metric, such that the IFS is hyperbolic with respect to d. The unique attractor G of the IFS is the graph of a continuous function $f : I \to R$ which interpolates the date set $\{(x_i, y_i) \in R^2, i = 0, 1, \cdots, N\}$*

Example: Let $\{(x_i, y_i) \in R^2, i = 0, 1, \cdots, N\}$, $N > 1$

$$w_n(x, y) = \begin{pmatrix} a_n & 0 \\ c_n & d_n \end{pmatrix} \begin{pmatrix} x \\ y \end{pmatrix} + \begin{pmatrix} e_n \\ f_n \end{pmatrix},$$

where $|d_n| < 1$ is given, a_n, c_n, e_n, f_n are real number such that

$$w_n(x_0, y_0) := (x_{n-1}, y_{n-1}),\ w_n(x_N, y_N) := (x_n, y_n)$$

We can solve the above equations for a_n, c_n, e_n, f_n

$$a_n = \frac{x_n - x_{n-1}}{x_N - x_0},$$

$$c_n = \frac{y_n - y_{n-1}}{x_N - x_0} - \frac{d_n(y_N - y_0)}{x_N - x_0},$$

$$e_n = \frac{x_N x_{n-1} - x_0 x_n}{x_N - x_0}$$

$$f_n = \frac{x_N y_{n-1} - x_0 y_n}{x_N - x_0} - \frac{d_n(x_N y_0 - x_0 y_N)}{x_N - x_0}.$$

w_n is a shear transformation: it maps lines parallel to the y-axis into the lines parallel to the y-axis. d_n is the vertical scaling factor.

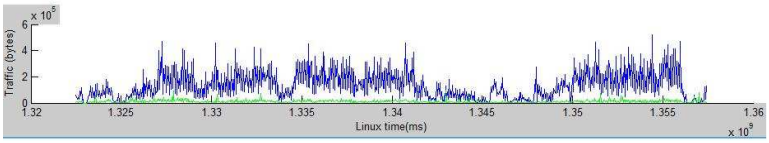

Figure 3: Fractal interpolation: for internet traffic data

References

[1] Barnsley M.F., *Fractals everywhere*, Academic Press, Orlando, Florida, 1988.

[2] Cătinaş, T., *Interpolation of scattered data*, Ed. "Casa Cărţii de Ştiinţă", Cluj-Napoca, 2007

[3] Coman Gh., Trîmbiţaş, R., *Combined Shepard univariate operators*, East Jurnal on Approximations **7** (2001), pp. 471–483

[4] Coman Gh., Birou M., Oşan C., Somogyi I., Cătinaş T., Oprişan A., Pop I., Todea I., *Interpolation operators*, Ed. "Casa Cărţii de Ştiinţă", Cluj, 2004.

[5] Shepard, D., *A two dimensional interpolation function for irregularly spaced data*, Proc. 23rd Nat. Conf. ACM, 1968, pp. 517–523.

[6] Somogyi I., András Sz., *Numerikus Analízis*, Ed. "Presa Universitară Clujeană", Cluj, 2009.

[7] Ruoyu Yan, Yingfeng Wang, *Hurst Parameter for Security Evaluation of LAN Traffic*, Information Technology Journal, 2-12, 11: 269 − 275. ($http://scialert.net/fulltext/?doi = itj.2012.269.275\&org = 11$)

Proceedings, 15th Applied Stochastic Models and Data Analysis (ASMDA2013)
International Conference, Mataró (Barcelona), Spain 25 - 28 June 2013

Intergenerational transmission of education in Greece: evidence from the European Social Survey 2002–2010

G. Stamatopoulou, M. Symeonaki, K. Michalopoulou

Department of Social Policy, Panteion University of Social and Political Sciences,
136 Syggrou Av., 176 71, Athens, Greece
(E-mail: gl.stamat@gmail.com, msimeon@panteion.gr, kmichal@panteion.gr)

Abstract. The present paper explores the patterns of intergenerational educational mobility in Greece and its changes for different birth cohorts born between 1930 and 1976. More specifically, we investigate the transmission of educational attainments from both father and mother through generations and over time. The main purpose is to trace the transitions of individuals between educational categories and to determine the relationship between an individual's education class and the class of his or her parents. Based on data drawn from ESS (2002–2010), our analysis provides Markov transition probability matrices and the absolute and relative mobility rates, by comparing the different rounds of the survey.
Keywords: Transmission of education, intergenerational mobility, transition probability matrices, mobility indices, cohort analysis, ESS.

1 Introduction

Intergenerational mobility can be defined as the trajectories observed from one generation to another and between different social classes. The term indicates whether and to what extent the socio-economic status of origins (measured here in terms of parental education) transmit from parents to children and has been used as a measurement of equality of opportunities.

Among other factors, education has played an important role in the study of social mobility, as it can mediate between the class of origins and the class of destination, by forming the individuals' social status. In this respect and driven by the principles of human capital theory, in the middle '60s, the Greek educational system has undergone major reforms, in order to provide more equal opportunities in education and to promote greater social mobility and fairness. As a result, an explosion of education and an improvement in individuals' educational outcomes were observed and the number of higher education graduates has rapidly increased in recent decades [4,9].

Empirical evidence illustrates that despite the expansion of education, Greece as well as other Mediterranean countries are the most immobile across Europe, as there is a linkage between paternal education and individuals outcomes [2,3,12]. However, an increase in the mobility rates is observed over time and the individuals seem to move upwards, attaining a higher educational level [4,15].

In the present paper, we investigate the intergenerational transmission of education in Greece. The main aim is to capture the extent of educational mobility through generations and to provide further evidence on the movements of individuals within the Greek educational system. Two specific research questions are examined: (i) To what degree does the educational status of both parents pass on to their children? (ii) How have the mobility rates changed over time and among different birth cohorts? Our analysis is based on data drawn from all rounds of ESS (2002–2010), except for the third one (2006) in which Greece did not participate.

The paper is organised as follows. Section 2 deals with the data and the methodology used in the analysis of intergenerational mobility. Section 3 presents the findings of the analysis, the relationship between origins and individuals' education and the respective patterns of educational mobility, while Section 4 provides the conclusions regarding the finding of Section 3.

2 Data and methods

The European Social Survey (ESS)[1] is a long-term comparative research project designed to record and document the attitudes, beliefs and behavioural patterns of the European populations. Funding via the European Commission's Framework programmes, the European Science Foundation and national academic funding agencies, the survey aims to produce comparable social indicators to be used for the European social policy. Started in 2002, the ESS is conducted every two years in more than 20 European countries. It involves national probability samples, a minimum target response rate of 70% and rigorous methodological criteria. The survey population is defined as all individuals aged 15 years and more, regardless of their nationality, citizenship or legal status. The 'homeless' and people living in collective dwellings are excluded.[8]

The ESS is one of the very few free access databases in Greece which provides the opportunity to investigate the trends of intergenerational social mobility, as it provides data on social status of both parents and individuals, even if they do not live in the same residence. In particular, we focus on raw data relating to the highest educational attainment of both parents and individuals, which were harmonised according to the latest version of International Standard Classification of Education (ISCED11).

For analytical purposes, the educational attainment has been recoded into four educational states, as indicated in Table 1.[2] Moreover, the data was weighted by applying the design weight ('dweight'), as is required by probability sampling theory.

In contrast to the economic trandition, where a regression approach is usually adopted, we base our analysis on a more sociological descriptive perspective. Thus, as in Symeonaki *et al* [14–16], we constructed Markov transition

[1] For more information on ESS visit http://www.europeansocialsurvey.org/.

[2] Since 1974 both primary and lower secondary education are compulsory, while attendance in the upper secondary schools is optional. According to OECD, the advanced vocational training or post-secondary can be allocated to tertiary education in a broader way, even if it is not tertiary level.[3]

ISCED	Educational categories	Description	States
0-1	Less than lower secondary	Primary education (un)completed	1
2	First stage of secondary completed	3-year lower secondary education	2
3	Second stage of secondary completed	3-year upper secondary education	3
4-6	Advanced education	Post-secondary or tertiary education	4

Table 1. Educational categories according to ISCED11 classification used by ESS.

probability matrices, the elements of which show the transitions that take place between educational categories. Each element $p_{ij}, \forall i, j = 1, 2, ..., n$ of a Markov matrix $\mathbf{P}$ describes the probability of an individual to move from state i (educational level of origins) to state j (individual's educational level). The elements found off the main diagonal of matrix $\mathbf{P}$ give the movements of individuals, while p_{ii} denotes the probabilities of individuals, $\forall i, j = 1, 2, ..., n$ being immobile.

Two types of indices are calculated to show the movements of individuals within the educational system: (i) relative indices such as the Prais-Shorrocks index, which indicate the rate of social fluidity and (ii) absolute mobility indices, which reflect the direction of the movements.[3] More specifically, we have computed the following indices:

The Prais-Shorrocks index [11,13] given by Equation (1):

$$M_{PS} = \left(\frac{1}{n-1}\right)(n - tr(\mathbf{P})) \tag{1}$$

where $tr(\mathbf{P})$ represents the sum of the diagonal elements of a transition matrix $\mathbf{P}$, n is the number of states and $M_{PS} \in [0, 1]$.
$M_{PS} = 1$ indicates perfect mobility and $M_{PS} = 0$ implies perfect immobility.

The Bartholomew Index[1] defined by Equation (2):

$$M_B = \frac{1}{k}\sum_{i=1}^{k}\sum_{j=1}^{k} p_{ij}|i - j| \tag{2}$$

where p_{ij} as mentioned above denotes the probability of an individual to move from state i (social status of origins) to state j (individual's social status) and k is the number of states. The minimum value of the index is zero, which indicates perfect immobility.

The immobility ratio[7] is given by:

$$IM = \left(\frac{tr(\mathbf{P})}{n}\right) \tag{3}$$

and provides individual's rate of remaining to the social state of their origin, as well the degree of educational transmission through generations.

[3] Absolute mobility indices refer to the absolute number of individuals moving from one state to another, while the relative mobility rates are referring to the probabilities that individuals have to move upwards or downwards.[10]

Finally, Equations (4) and (5) define an upward and downward mobility index, respectively, based on the absolute number of individuals [10]:

$$u = \frac{1}{N} \sum_{j>i} n_{ij} \tag{4}$$

$$d = \frac{1}{N} \sum_{j<i} n_{ij}. \tag{5}$$

Additionally, in order to show how the mobility patterns have changed through generations, a synchronic cohort analysis was carried out. Three birth cohorts were defined (1930–1945, 1946–1960, 1961–1976) to ensure sufficiently large number of cases in each cell. Individuals aged 25 and less were not included in the analysis, as they have not in theory completed their education.[5]

3 Empirical results

In this section, we proceed with the presentation of the results of our analysis. In Table 2, the Markov transition probability matrices and the mobility indices according to father's educational profile are provided for all rounds of ESS.

ESS	**Father's state**	**Individual's state**				**Mobility indices**	
		1	2	3	4	M_{PS}	M_B
2002	1	0.492	0.189	0.239	0.080	0.734	0.758
	2	0.131	0.270	0.401	0.197		
	3	0.042	0.130	0.568	0.260		
	4	0.017	0.160	0.354	0.470		
2004	1	0.483	0.168	0.246	0.104	0.803	0.857
	2	0.126	0.126	0.437	0.311		
	3	0.030	0.131	0.475	0.364		
	4	0.018	0.188	0.288	0.506		
2008	1	0.265	0.210	0.355	0.171	0.870	0.943
	2	0.057	0.205	0.405	0.333		
	3	0.011	0.165	0.414	0.410		
	4	0.007	0.108	0.378	0.507		
2010	1	0.374	0.127	0.369	0.128	0.794	0.887
	2	0.085	0.144	0.520	0.251		
	3	0.046	0.108	0.551	0.295		
	4	0.014	0.061	0.376	0.549		

Table 2. The transition probabilities and the estimated mobility indices according to father's educational state (European Social Survey 2002–2010)

As shown, the transmission of paternal educational disadvantages to individuals attainments is obvious in the first two rounds of ESS, as children of less

educated fathers have high chances to remain to the first educational category in accordance with their origins', while those of more educated fathers are more likely to attain a higher educational level. The picture is somewhat different in the last two rounds, as more upward movements are observed. As a result, both M_{PS} and M_B are quite high for the whole surveyed population and they seem to slightly increase across the ESS rounds, indicating that father's educational profile affects the individuals' educational attainments to a lesser extent over time.

A similar pattern is detected when we examine the transition probability matrices and the extracted mobility indices according to mother's educational background (Table 3). Note that the mother's education and the individual's educational attainment are related in different rounds of ESS. However, an increasing trend of mobility rates over time is also observed.

ESS	**Mother's state**	**Individual's state**				**Mobility indices**	
		1	2	3	4	M_{PS}	M_B
2002	1	0.467	0.192	0.246	0.095	0.809	0.807
	2	0.056	0.240	0.497	0.207		
	3	0.016	0.141	0.471	0.372		
	4	0.000	0.143	0.462	0.396		
2004	1	0.462	0.163	0.255	0.120	0.838	0.945
	2	0.028	0.159	0.434	0.379		
	3	0.027	0.153	0.448	0.372		
	4	0.092	0.183	0.308	0.417		
2008	1	0.253	0.203	0.358	0.186	0.870	0.943
	2	0.010	0.161	0.389	0.440		
	3	0.011	0.207	0.428	0.355		
	4	0.000	0.141	0.329	0.529		
2010	1	0.357	0.124	0.370	0.150	0.826	0.887
	2	0.035	0.106	0.603	0.255		
	3	0.024	0.123	0.541	0.312		
	4	0.013	0.094	0.375	0.519		

Table 3. The transition probabilities and the estimated mobility indices according to mother's educational state (European Social Survey 2002–2010)

A more illustrative representation of the above results is given in Figure 1, where the progress of both mobility rates across the different rounds of the survey is provided. The increasing trend of the mobility rates based on both parents' profile over time is notable. Additionally, although the mobility rates seem to follow the same patterns for both parents, it is remarkable that the transmission of father's educational status to individuals attainments is more evident than that of mother's.

The comparison between birth cohorts gives also interesting results (Tables 4–5), as it reveals an increasing trend in mobility rates over time.

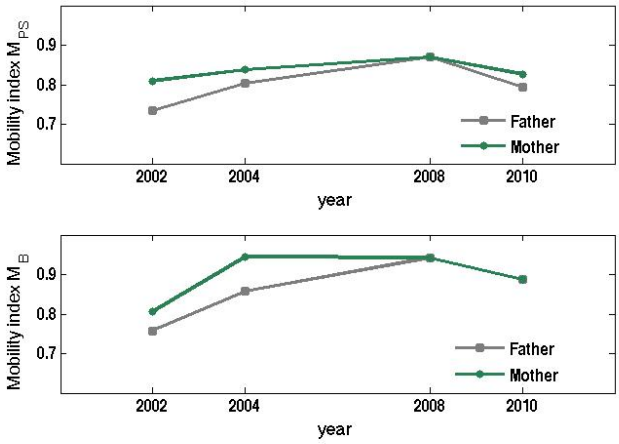

Fig. 1. The mobility rates across the European Social Survey

Birth cohorts	M_{PS}	M_B	IM	UM	DM
ESS Round 1, 2002					
1930 – 1945	0.717	0.744	0.462	0.242	0.061
1946 – 1960	0.755	0.810	0.434	0.531	0.038
1961 – 1976	0.792	0.836	0.406	0.655	0.045
ESS Round 2, 2004					
1930 – 1945	0.710	0.785	0.467	0.241	0.034
1946 – 1960	0.736	0.794	0.448	0.494	0.022
1961 – 1976	0.812	0.892	0.391	0.717	0.022
ESS Round 4, 2006					
1930 – 1945	0.528	0.487	0.604	0.336	0.022
1946 – 1960	0.900	0.935	0.325	0.626	0.036
1961 – 1976	0.825	0.960	0.381	0.781	0.026
ESS Round 5, 2008					
1930 – 1945	0.636	0.685	0.523	0.233	0.040
1946 – 1960	0.706	0.761	0.470	0.533	0.039
1961 – 1976	0.834	0.932	0.375	0.721	0.035

Table 4. Intergenerational mobility based on father's education, by birth cohorts and ESS rounds

More particularly, although both the M_{PS} and M_B differ between the rounds of ESS, the indices seem to increase through generations, indicating that both paternal and maternal educational profile affects to a lesser extent the individuals' educational attainments. The most illustrative example is provided in the fourth round of ESS (Table 5), while the Bartholomew mobility index with respect to mother's educational profile has substantially changed through generations, taking values between 0.463 (for the oldest birth cohort) and 1.004 (for the youngest birth cohort).

Birth cohorts	M_{PS}	M_B	IM	UM	DM
ESS Round 1, 2002					
1930 – 1945	0.687	0.653	0.484	0.269	0.010
1946 – 1960	0.890	0.881	0.333	0.584	0.017
1961 – 1976	0.857	0.889	0.357	0.740	0.020
ESS Round 2, 2004					
1930 – 1945	0.846	1.203	0.365	0.264	0.018
1946 – 1960	0.844	0.906	0.367	0.540	0.013
1961 – 1976	0.869	0.968	0.348	0.748	0.020
ESS Round 4, 2006					
1930 – 1945	0.533	0.463	0.600	0.346	0.009
1946 – 1960	0.805	0.838	0.396	0.656	0.004
1961 – 1976	0.885	1.004	0.336	0.852	0.012
ESS Round 5, 2008					
1930 – 1945	0.571	0.524	0.571	0.275	0.005
1946 – 1960	0.729	0.767	0.454	0.582	0.007
1961 – 1976	0.830	0.937	0.377	0.780	0.017

Table 5. Intergenerational mobility based on mother's education, by birth cohorts and ESS rounds

Consequently, the immobility ratio appears to decrease through generations, indicating that the transmission of parental background to their children's education seems to be weakened.

Regarding the directions of the movements, it is worth noting that very low rates of upward mobility for the oldest birth cohort (1930–1945) exist in all rounds but increase considerably over time. Nevertheless, the upward movements are more perceptible than the downward transitions.

4 Concluding remarks

In the present paper we attempted to provide further analysis on the relationship between parental education and individuals educational outcomes, based

on data drawn from ESS. Focusing on the method of Markov transition probability matrices and by estimating widely used mobility indices, our analysis revealed that mobility patterns have substantially changed through generations and an increase in the chances of individuals to attain a higher educational level has been noted over time. Additionally, it seems that the effect of paternal educational background on individuals' attainments is stronger, as the mobility rates appear higher with respect to mother's profile. However, in terms of social policy, there is a further need of actions to consider in order to weaken the intergenerational transmission of educational disadvantades.

References

1.D.J. Bartholomew. *Stochastic Models for social processes*, London, 1982. Wiley.
2.O. Causa and A. Johansson. Intergenerational social mobility in OECD countries. *OECD Journal: Economic Studies*, 2010:1-44, 2010.
3.S. Comi. Intergenerational mobility in Europe: Evidence from ECHP. *Universita di Milano*, 2004.
4.J. Daouli, M. Demousis, N. Giannakopoulos. Mothers, fathers and daughters: Intergenerational transmision of education in Greece. *Economics of Education Review*, 29:83-93, 2010.
5.M. van Doorn, I. Pop, M. Wolbers. Intergenerational Transmission of Education across European countries and cohorts. *European Societies*, 13:93-117, 2011
6.R. Erikson and J.H. Goldthorpe. *The Constant Flux: The Study of Class Mobility in Industrial Society*, Oxford, 1992. Clareston Press.
7.G. Heineck and R. Riphahn. Intergenerational transmission of educational attainment in Germany - the last five decades. *Journal of Economic and Statistics*, 229:36-60, 2007.
8.R. Jowel and the Central Co-ordination Team. *European Social Survey 2004/2005: Technical Report*. Centre for Comparative Social Surveys, City University. London, 2005.
9.H. Lambropoulos, G. Psacharopoulos. Educational expansion and earnings differentials in Greece. *Comparative Education Review*, 36:52-70, 1992.
10.M. Papadakis. *Techniques of Social Mobility Analysis*, Athens, 1993. In Greek, Vita.
11.S. Prais. Measuring social mobility. *Journal of the Royal Statistical Society*, Series A, 118:56-66, 1955.
12.H. Patrinos. Socioeconomic background schooling, experience, ability and monetary rewards in Greece. *Economics of Education Review*, 14:85-91, 1995.
13.A. Shorrocks. The measurement of social mobility. *Econometrica*, 46:1013-1024, 1978.
14.M. Symeonaki and G. Stamatopoulou. Exploring intergenerational educational mobility in Greece with data drawn from EU-SILC.*International Sociological Association RC04 & RC10 Conference: Social Justice and Participation. The Role of Higher Education*, Cyprus, 2011.
15.M. Symeonaki, G. Stamatopoulou. Exploring the transitions to Higher Education in Greece: issues of intergenerational educational mobility. *Policy Futures in Education* (to appear).
16.M. Symeonaki, G. Stamatopoulou, C. Michalopoulou. Intergenerational Occupational Mobility in Greece: Evidence from EU-SILC. *Proceedings of Demografics Conference*, Crete, Greece, 2012.

Proceedings, 15th Applied Stochastic Models and Data Analysis (ASMDA2013)
International Conference, Mataró (Barcelona), Spain 25 - 28 June 2013

Delayed Heston Model: Improvement of the Volatility Surface Fitting and Pricing & Hedging of Volatility Swaps

Anatoliy Swishchuk[1] and Nelson Vadori[2]

[1] Corresponding author. University of Calgary, Department of Mathematics, 2500 University Drive NW, Calgary, AB, Canada T2N 1N4;e-mail: aswish@ucalgary.ca; Tel.: 1(403)220-3274; Fax: 1(403) 282-5150.
[2] University of Calgary, Department of Mathematics, e-mail: nvadori@ucalgary.ca.

Abstract. We present a variance drift adjusted version of the Heston model which leads to significant improvement of the market volatility surface fitting (compared to Heston). The numerical example we performed with recent market data shows a significant (44%) reduction of the average absolute calibration error [1] (calibration on Sep. 30^{th} 2011 for underlying EURUSD). Our model has two additional parameters compared to the Heston model, can be implemented very easily and was initially introduced for volatility derivatives pricing purpose. The main idea behind our model is to take into account some past history of the variance process in its (risk-neutral) diffusion. Using change of time method for continuous local martingales, we derive a closed formula for the Brockhaus&Long approximation of the volatility swap price in this model. We also consider dynamic hedging of volatility swaps using a portfolio of variance swaps.

Keywords: variance swap; volatility swap; stochastic volatility with delay; Heston model with delayed stochastic volatility, change of time; dynamic hedging.

1 Introduction

The volatility process is an important concept in financial modeling as it quantifies at each time t how likely the modeled asset log-return is to vary significantly over some short immediate time period $[t, t+\epsilon]$. This process can be stochastic or deterministic, e.g. local volatility models in which the (deterministic) volatility depends on time and spot price level. In quantitative finance, we often consider the volatility process $\sqrt{V_t}$ (where V_t is the variance process) to be stochastic as it allows to fit the observed vanilla option market prices with an acceptable bias as well as to model the risk linked with the future evolution of the volatility smile (which deterministic model cannot), namely the forward smile. Many derivatives are known to be very sensitive the forward smile, one of the most popular example being the cliquet options (options on future asset performance).

Heston model (Heston [6]; Heston and Nandi [7]) is one of the most popular stochastic volatility models in the industry as semi-closed formulas for vanilla

[1] average of the absolute differences between market and model implied BS volatilities

option prices are available, few (five) parameters need to be calibrated, and it accounts for the mean-reverting feature of the volatility.

One might be willing, in the variance diffusion, to take into account not only its current state but also its past history over some interval $[t-\tau, t]$, where $\tau > 0$ is a constant and is called the delay. Starting from the discrete-time GARCH(1,1) model (Bollerslev [1]), a first attempt was made in this direction in Kazmerchuk et al. [8], where a non-Markov delayed continuous-time GARCH model was proposed (S_t being the asset price at time t, γ, θ, α some positive constants):

$$\frac{dV_t}{dt} = \gamma\theta^2 + \frac{\alpha}{\tau}\ln^2\left(\frac{S_t}{S_{t-\tau}}\right) - (\alpha+\gamma)V_t, \tag{1}$$

this model being inherited from its discrete-time analogue:

$$\sigma_n^2 = \tilde{\gamma}\tilde{\theta}^2 + \frac{\tilde{\alpha}}{L}\ln^2\left(\frac{S_{n-1}}{S_{n-1-L}}\right) + (1-\tilde{\alpha}+\tilde{\gamma})\sigma_{n-1}^2 \tag{2}$$

The parameter θ^2 (resp. γ) can be interpreted as the value of the long-range variance (resp. variance mean-reversion speed) when the delay is equal to 0 (we will see that introducing delay modifies the value of these two model features), and α a continuous-time equivalent of the variance ARCH(1,1) autoregressive coefficient. In fact, we can interpret the right-hand side of previous diffusion equation as the sum of two terms:

- the delay-free term $\gamma(\theta^2 - V_t)$ which accounts for the mean-reverting feature of the variance process
- $\alpha\left(\frac{1}{\tau}\ln^2\left(\frac{S_t}{S_{t-\tau}}\right) - V_t\right)$ which is a pure (noisy) delay term, i.e. that vanishes when $\tau \to 0$ and takes into account the past history of the variance (via the term $\ln\left(\frac{S_t}{S_{t-\tau}}\right)$). The autoregressive coefficient α can be seen as the amplitude of this pure delay term.

J.C. Duan remarked the importance to incorporate the real world $\mathbb{P}-$drift $d_{\mathbb{P}}(t,\tau) := \int_{t-\tau}^{t}(\mu - \frac{1}{2}V_u)du$ of $\ln\left(\frac{S_t}{S_{t-\tau}}\right)$ in the model (where μ stands for the real world $\mathbb{P}-$drift of the stock price S_t), transforming the variance dynamics into:

$$\frac{dV_t}{dt} = \gamma\theta^2 + \frac{\alpha}{\tau}\left[\ln\left(\frac{S_t}{S_{t-\tau}}\right) - d_{\mathbb{P}}(t,\tau)\right]^2 - (\alpha+\gamma)V_t \tag{3}$$

The latter diffusion (3) was introduced in Swishchuk [12] and Kazmerchuk et al. [9], and the proposed model was proved to be complete and to account for the mean-reverting feature of the volatility process. This model is also non Markov as the past history $(V_u)_{u\in[t-\tau,t]}$ of the variance appears in its diffusion equation via the term $\ln\left(\frac{S_t}{S_{t-\tau}}\right)$, as it is shown in Swishchuk [12].

In the continuity of this approach, pricing of variance swaps for one-factor stochastic volatility with delay has been presented in Swishchuk [12], for multi-factor stochastic volatility in Swishchuk [13] and for one-factor stochastic volatility with delay and jumps in Swishchuk and Li [10]. Variance swap for local

Levy-based stochastic volatility with delay has been calculated in Swishchuk and Malenfant [15].

Unfortunately, the model (3) doesn't lead to (semi-)closed formulas for the vanilla options, making it difficult to use for practitioners willing to calibrate on vanilla market prices. Nevertheless, one can notice that the Heston model and the delayed continuous-time GARCH model (3) are very similar in the sense that the expected values of the variances are the same - when we make the delay tend to 0 in (3). As mentioned before, the Heston framework is very convenient, and therefore it is naturally tempting to adjust the Heston dynamics in order to incorporate the delay introduced in (3). In this way, we considered in a first approach adjusting the Heston drift by a deterministic function of time so that the expected value of the variance under the delayed Heston model is equal to the one under the delayed GARCH model (3). In addition to making our delayed Heston framework coherent with (3), this construction makes the variance process diffusion dependent not on its past history $(V_u)_{u\in[t-\tau,t]}$, but on the past history of its risk-neutral expectation $(\mathbb{E}_0^{\mathbb{Q}}(V_u))_{u\in[t-\tau,t]}$, preserving the Markov feature of the Heston model (where we denote $\mathbb{E}_t^{\mathbb{Q}}(\cdot) := \mathbb{E}^{\mathbb{Q}}(\cdot|\mathcal{F}_t)$). The purpose of sections 2 and 3 is to present the Delayed Heston model as well as some calibration results on call option prices, with a comparison to the Heston model. In sections 4 and 5, we will consider the pricing and hedging of volatility and variance swaps in this model.

Volatility and variance swaps are contracts whose payoff depend (respectively convexly and linearly) on the realized variance of the underlying asset over some specified time interval. They provide pure exposure to volatility, and therefore make it a tradable market instrument. Variance Swaps are even considered by some practitioners to be vanilla derivatives. The most commonly traded variance swaps are discretely sampled and have a payoff $P_n^V(T)$ at maturity T of the form:

$$P_n^V(T) = N\left[\frac{252}{n}\sum_{i=0}^{n}\ln^2\left(\frac{S_{i+1}}{S_i}\right) - K_{var}\right]$$

, where S_i is the asset spot price on fixing time $t_i \in [0,T]$ (usually there is one fixing time each day, but there could be more, or less), N the notional amount of the contract (in currency per unit of variance) and K_{var} the strike specified in the contract. The corresponding volatility swap payoff $P_n^v(T)$ is given by:

$$P_n^v(T) = N\left[\sqrt{\frac{252}{n}\sum_{i=0}^{n}\ln^2\left(\frac{S_{i+1}}{S_i}\right)} - K_{vol}\right]$$

One can also consider continuously sampled volatility and variance swaps (on which we will focus in this article), which payoffs are respectively defined as the limit when $n \to +\infty$ of their discretely sampled versions. Formally, if we denote $(V_t)_{t\geq 0}$ the stochastic volatility process of our asset, adapted to some brownian filtration $(\mathcal{F}_t)_{t\geq 0}$, then the continuously-sampled realized variance

V_R from initiation date of the contract $t = 0$ to maturity date $t = T$ is given by $V_R = \frac{1}{T}\int_0^T V_s ds$. The fair variance strike K_{var} is calculated such that the initial value of the contract is 0, and therefore is given by:

$$\mathbb{E}_0^{\mathbb{Q}}\left[e^{-rT}(V_R - K_{var})\right] = 0 \Rightarrow K_{var} = \mathbb{E}_0^{\mathbb{Q}}(V_R)$$

In the same way, the fair volatility strike K_{vol} is given by:

$$\mathbb{E}_0^{\mathbb{Q}}\left[e^{-rT}(\sqrt{V_R} - K_{var})\right] = 0 \Rightarrow K_{vol} = \mathbb{E}_0^{\mathbb{Q}}(\sqrt{V_R})$$

The volatility swap fair strike might be difficult to compute explicitly as we have to compute the expectation of a square-root. In Brockhaus and Long [4], the following approximation - based on Taylor expansion - was proposed to compute the expected value of the square-root of an almost surely non negative random variable Z:

$$\mathbb{E}(\sqrt{Z}) \approx \sqrt{\mathbb{E}(Z)} - \frac{Var(Z)}{8\mathbb{E}(Z)^{\frac{3}{2}}} \tag{4}$$

We will refer to this approximation in our paper as the Brockhaus&Long approximation.

Carr and Lee [5] provides an overview of the current market for volatility derivatives. They survey the early literature on the subject. They also provide relatively simple proofs of some fundamental results related to variance swaps and volatility swaps. Pricing of variance swaps for one-factor stochastic volatility with delay has been presented in Swishchuk [11], for multi-factor stochastic volatility in Swishchuk [13] and for one-factor stochastic volatility with delay and jumps in Swishchuk and Li [10]. Variance swap for local Levy-based stochastic volatility with delay has been calculated in Swishchuk and Malenfant [15]. Variance and volatility swaps in energy markets have been considered in Swishchuk [14]. Broadie and Jain [3] covers pricing and dynamic hedging of volatility derivatives in the Heston model.

The paper is organized as follows: in section 2, we present the Delayed Heston model; in section 3, we present calibration results (for underlying EURUSD on September 30th 2011) as well as a comparison with the Heston model. In section 4, we compute the price process $X_t(T) := \mathbb{E}_t^{\mathbb{Q}}(V_R)$ of the floating leg of the variance swap of maturity T, as well as the Brockhaus&Long approximation of the price process $Y_t(T) := \mathbb{E}_t^{\mathbb{Q}}(\sqrt{V_R})$ of the floating leg of the volatility swap of maturity T. This leads in particular to closed formulas for the fair volatility and variance strikes. In section 5, we consider - in this model - dynamic hedging of volatility swaps using variance swaps.

2 Presentation of the Delayed Heston model

Throughout this paper, we will assume constant risk-free rate r, dividend yield q and finite time-horizon T. We will also denote $\mathbb{E}_t^{\mathbb{Q}}(\cdot) := \mathbb{E}^{\mathbb{Q}}(\cdot|\mathcal{F}_t)$ and

$Var_t^{\mathbb{Q}}(\cdot) := Var^{\mathbb{Q}}(\cdot|\mathcal{F}_t)$

Assume the following risk-neutral $\mathbb{Q}-$ stock price dynamics ($Z_t^{\mathbb{Q}}$ and $W_t^{\mathbb{Q}}$ being two correlated standard brownian motions):

$$dS_t = (r-q)S_t dt + S_t\sqrt{V_t}dZ_t^{\mathbb{Q}}. \tag{5}$$

The well-known Heston model has the following $\mathbb{Q}-$dynamics for the variance V_t:

$$dV_t = \gamma(\theta^2 - V_t)dt + \delta\sqrt{V_t}dW_t^{\mathbb{Q}}, \tag{6}$$

where θ^2 is the long-range variance, γ the variance mean-reversion speed, δ the volatility of the variance and ρ the brownian correlation coefficient ($\left\langle W^{\mathbb{Q}}, Z^{\mathbb{Q}}\right\rangle_t = \rho t$). We also assume $S_0 = s_0$ a.e. and $V_0 = v_0$ a.e., for some positive constants v_0, s_0.

As explained in the introduction, the following delayed continuous-time GARCH dynamics have been introduced for the variance in Swishchuk [12]:

$$\frac{dV_t}{dt} = \gamma\theta^2 + \frac{\alpha}{\tau}\left[\int_{t-\tau}^{t}\sqrt{V_s}dZ_s^{\mathbb{Q}} - (\mu - r)\tau\right]^2 - (\alpha+\gamma)V_t, \tag{7}$$

where μ stands for the real world $\mathbb{P}-$drift of the stock price S_t. We can interpret the right-hand side of previous diffusion equation [2] as the sum of two terms:

- the delay-free term $\gamma(\theta^2 - V_t)$ which accounts for the mean-reverting feature of the variance process
- $\alpha\left(\frac{1}{\tau}\left[\int_{t-\tau}^{t}\sqrt{V_s}dZ_s^{\mathbb{Q}} - (\mu-r)\tau\right]^2 - V_t\right)$ which is a pure (noisy) delay term of amplitude α, i.e. that vanishes when $\tau \to 0$ and takes into account the past history of the variance via the integral $\int_{t-\tau}^{t}\sqrt{V_s}dZ_s^{\mathbb{Q}}$. As we will see below, the introduction of this pure delay term modifies the value of both the long-range variance and variance mean-reversion speed of the model.

We can see that the two models are very similar. Indeed, they both give the same expected value for V_t as the delay goes to 0 in (7), namely $\theta^2 + (V_0 - \theta^2)e^{-\gamma t}$. The idea here is to adjust the Heston dynamics (6) in order to account for the delay introduced in (7). Our approach is to adjust the drift by a deterministic function of time so that the expected value of V_t under the adjusted Heston model is the same as under (7). This approach can be seen as a correction by a pure delay term of amplitude α (in the sense of (15)) of the Heston drift by a deterministic function in order to account for the delay.

[2] note that θ^2 (resp. γ) has been defined in introduction for the delayed continuous-time GARCH model as the value of the long-range variance (resp. variance mean-reversion speed) when $\tau = 0$, therefore it has the same meaning as the Heston long-range variance (resp. variance mean-reversion speed). That is why we use the same notations in both models.

Namely, we assume the adjusted Heston dynamics:

$$dV_t = \left[\gamma(\theta^2 - V_t) + \epsilon_\tau(t)\right] dt + \delta\sqrt{V_t} dW_t^{\mathbb{Q}}, \tag{8}$$

$$\epsilon_\tau(t) := \alpha\tau(\mu - r)^2 + \frac{\alpha}{\tau}\int_{t-\tau}^{t} v_s ds - \alpha v_t, \tag{9}$$

with $v_t := \mathbb{E}_0^{\mathbb{Q}}(V_t)$. It was shown in Swishchuk [12] that v_t solves the following:

$$\frac{dv_t}{dt} = \gamma\theta^2 + \alpha\tau(\mu - r)^2 + \frac{\alpha}{\tau}\int_{t-\tau}^{t} v_s ds - (\alpha + \gamma)v_t. \tag{10}$$

And we have the following expression for v_t:

$$v_t = \theta_\tau^2 + (V_0 - \theta_\tau^2)e^{-\gamma_\tau t}, \tag{11}$$

with:

$$\theta_\tau^2 := \theta^2 + \frac{\alpha\tau(\mu - r)^2}{\gamma}, \tag{12}$$

The parameter θ_τ^2 can be interpreted as the adjusted long-range variance - that has been (positively) shifted from its original value θ^2 because of the introduction of delay. We have $\theta_\tau^2 \to \theta^2$ when $\tau \to 0$, which is coherent. We will see below that we can interpret the parameter $\gamma_\tau > 0$ as the adjusted mean-reversion speed. This parameter is given in Swishchuk [12] by a (nonzero) solution to the following equation:

$$\gamma_\tau = \alpha + \gamma + \frac{\alpha}{\gamma_\tau\tau}(1 - e^{\gamma_\tau\tau}). \tag{13}$$

By (9), (11) and (13) we get an explicit expression for the drift adjustment:

$$\epsilon_\tau(t) = \alpha\tau(\mu - r)^2 + (V_0 - \theta_\tau^2)(\gamma - \gamma_\tau)e^{-\gamma_\tau t} \tag{14}$$

The following simple property gives us some information about the correction term $\epsilon_\tau(t)$ and γ_τ, that will be useful for interpretation purpose and in the derivation of the semi-closed formulas for call options in the next section. Indeed, given (15) and (11), the parameter γ_τ can be interpreted as the adjusted variance mean-reversion speed, and we have by (13) that $\gamma_\tau \to \gamma$ when $\tau \to 0$, which is coherent.

Property 1: γ_τ is the unique solution to (13) and:

$$0 < \gamma_\tau < \gamma, \quad \lim_{\tau\to 0}\sup_{t\in\mathbb{R}^+} |\epsilon_\tau(t)| = 0 \tag{15}$$

Proof: Let's show $\gamma_\tau \geq 0$. If $\gamma_\tau < 0$ then by (13) we have $\alpha+\gamma+\frac{\alpha}{\gamma_\tau\tau}(1-e^{\gamma_\tau\tau}) < 0$, i.e. $1-e^{\gamma_\tau\tau}+\gamma_\tau\tau > -\frac{\gamma}{\alpha}\gamma_\tau\tau$. But $\tau > 0$ so $\exists x_0 > 0$ s.t. $1-e^{-x_0}-x_0 > \frac{\gamma}{\alpha}x_0$. A simple study shows that is impossible whenever $\frac{\gamma}{\alpha} \geq 0$, which is what we have by assumption. Therefore $\gamma_\tau \geq 0$, and in fact $\gamma_\tau > 0$ since it is a nonzero

solution of (13). If $\gamma \leq \gamma_\tau$ then by (13) $\gamma_\tau \tau + 1 - e^{\gamma_\tau \tau} \geq 0$. But $\gamma_\tau \tau > 0$ therefore $\exists x_0 > 0$ s.t. $x_0 + 1 - e^{x0} \geq 0$. A simple study shows that is impossible. The uniqueness comes from a similar simple study. Now, because $\gamma_\tau > 0$, we have $\sup_{t \in \mathbb{R}^+} |\epsilon_\tau(t)| \leq \alpha\tau(\mu - r)^2 + |(V_0 - \theta_\tau^2)(\gamma - \gamma_\tau)|$ and $(V_0 - \theta_\tau^2)(\gamma - \gamma_\tau) = \circ(1)$ by (13). So $\lim_{\tau \to 0} \alpha\tau(\mu - r)^2 + |(V_0 - \theta_\tau^2)(\gamma - \gamma_\tau)| = 0$. $\triangle$

3 Calibration on call option prices and comparison to the Heston model

It is possible to get semi-closed formulas for call options in our delayed Heston model. Indeed, our model is a time-dependent Heston model with time-dependent long-range variance $\tilde{\theta}^2(t) := \theta_\tau^2 + (V_0 - \theta_\tau^2)\frac{(\gamma - \gamma_\tau)}{\gamma} e^{-\gamma_\tau t}$. We perform our calibration on September 30^{th} 2011 for underlying EURUSD on the whole volatility surface (maturities from 1M to 10Y, strikes ATM, 25D Call/Put, 10D Call/Put). The implied volatility surface, the Zero Coupon curves EUR Vs. Euribor 6M and USD Vs. Libor 3M and the spot price are taken from Bloomberg (mid prices). The drift $\mu = 0.0188$ is estimated from 7.5Y of daily close prices (source: www.forexrate.co.uk).

The calibrated parameters for delayed Heston are:

$$(V_0, \gamma, \theta^2, \delta, \rho, \alpha, \tau) = (0.0343, 3.9037, 10^{-8}, 0.808, -0.5057, 71.35, 0.7821)$$

and for Heston:

$$(V_0, \gamma, \theta^2, \delta, \rho) = (0.0328, 0.5829, 0.0256, 0.3672, -0.4824)$$

The absolute calibration error (in bp of the BS volatility) for Heston model and our delayed Heston model are given below. The results show a 44% reduction of the average absolute calibration error (46bp for delayed Heston, 81bp for Heston).

	ATM	25D Call	25D Put	10D Call	10D Put
1M	152	192	41	193	67
2M	114	139	15	136	81
3M	89	109	3	110	92
4M	48	61	17	67	101
6M	5	15	34	29	85
9M	59	42	63	2	85
1Y	107	83	102	31	96
1.5Y	141	116	111	42	73
2Y	166	137	127	54	68
3Y	145	124	77	52	0
4Y	96	95	18	37	66
5Y	29	47	52	7	138
7Y	39	10	112	28	186
10Y	100	67	168	58	225

***Table 1**: Heston Absolute Calibration Error (in bp of the BS volatility)*

	ATM	25D Call	25D Put	10D Call	10D Put
1M	116	91	109	128	115
2M	44	24	59	54	88
3M	14	3	32	36	60
4M	18	28	1	5	29
6M	31	37	23	19	3
9M	45	45	56	37	57
1Y	51	47	82	50	104
1.5Y	29	30	79	49	129
2Y	24	23	83	47	139
3Y	11	9	29	30	90
4Y	41	28	14	17	38
5Y	76	55	59	5	16
7Y	71	49	58	1	14
10Y	26	8	18	47	24

Table 2: *Delayed Heston Absolute Calibration Error (in bp of the BS volatility)*

4 Pricing Variance and Volatility Swaps

In this section, we derive a closed formula for the Brockhaus&Long approximation of the volatility swap price using change of time method introduced in Swishchuk [11], as well as the price of the variance swap. Precisely, in Brockhaus and Long [4], the following approximation was presented to compute the expected value of the square-root of an almost surely non negative random variable Z: $\mathbb{E}(\sqrt{Z}) \approx \sqrt{\mathbb{E}(Z)} - \frac{Var(Z)}{8\mathbb{E}(Z)^{\frac{3}{2}}}$. We denote $V_R := \frac{1}{T}\int_0^T V_s ds$ the realized variance on $[0,T]$.

We let $X_t(T) := \mathbb{E}_t^{\mathbb{Q}}(V_R)$ (resp. $Y_t(T) := \mathbb{E}_t^{\mathbb{Q}}(\sqrt{V_R})$) the price process of the floating leg of the variance swap (resp. volatility swap) of maturity T.

Theorem 1: The price process $X_t(T)$ of the floating leg of the variance swap of maturity T in the delayed Heston model (5)-(8) is given by:

$$\begin{aligned} X_t(T) = \frac{1}{T}\int_0^t V_s ds + \frac{T-t}{T}\theta_\tau^2 + (V_t - \theta_\tau^2)\left(\frac{1-e^{-\gamma(T-t)}}{\gamma T}\right) \\ +(V_0 - \theta_\tau^2)e^{-\gamma_\tau t}\left(\frac{1-e^{-\gamma_\tau(T-t)}}{\gamma_\tau T} - \frac{1-e^{-\gamma(T-t)}}{\gamma T}\right) \end{aligned} \tag{16}$$

Proof: By definition, $X_t(T) = \mathbb{E}_t^{\mathbb{Q}}(\frac{1}{T}\int_0^T V_s ds) = \frac{1}{T}\int_0^t V_s ds + \frac{1}{T}\int_t^T \mathbb{E}_t^{\mathbb{Q}}(V_s)ds$. Let $s \geq t$. Then we have by (8) that $\mathbb{E}_t^{\mathbb{Q}}(V_s - V_t) = \mathbb{E}_t^{\mathbb{Q}}(V_s) - V_t = \int_t^s \gamma(\theta^2 - \mathbb{E}_t^{\mathbb{Q}}(V_u)) + \epsilon_\tau(u)du + \mathbb{E}_t^{\mathbb{Q}}(\int_t^s \sqrt{V_u}dW_u^{\mathbb{Q}})$. But $(\sqrt{V_t})_{t\geq 0}$ is an adapted process s.t. $\mathbb{E}^{\mathbb{Q}}(\int_0^T V_u du) < +\infty$, therefore $\int_0^t \sqrt{V_u}dW_u^{\mathbb{Q}}$ is a martingale and we have $\mathbb{E}_t^{\mathbb{Q}}(\int_t^s \sqrt{V_u}dW_u^{\mathbb{Q}}) = 0$. Therefore $\forall s \geq t \geq 0$, the function $s \to \mathbb{E}_t^{\mathbb{Q}}(V_s)$ is a solution of $y_s' = \gamma(\theta^2 - y_s) + \epsilon_\tau(s)$ with initial condition $y_t = V_t$. Simple calculations give us $\mathbb{E}_t^{\mathbb{Q}}(V_s) = \theta_\tau^2 + (V_t - \theta_\tau^2)e^{-\gamma(s-t)} + (V_0 - \theta_\tau^2)e^{-\gamma_\tau t}(e^{-\gamma_\tau(s-t)} - e^{-\gamma(s-t)})$. A calculation of $\int_t^T \mathbb{E}_t^{\mathbb{Q}}(V_s)ds$ completes the proof.

Corollary 1: The price K_{var} of the variance swap of maturity T at initiation of the contract $t = 0$ in the delayed Heston model (5)-(8) is given by:

$$K_{var} = \theta_\tau^2 + (V_0 - \theta_\tau^2)\frac{1-e^{-\gamma_\tau T}}{\gamma_\tau T} \tag{17}$$

Proof: By definition, $K_{var} = X_0(T)$.

Now, let $x_t := -(V_0 - \theta_\tau^2)e^{(\gamma-\gamma_\tau)t} + e^{\gamma t}(V_t - \theta_\tau^2)$. Then by Ito's Lemma we get:

$$dx_t = \delta e^{\gamma t}\sqrt{(x_t + (V_0 - \theta_\tau^2)e^{(\gamma-\gamma_\tau)t})e^{-\gamma t} + \theta_\tau^2}dW_t^{\mathbb{Q}}. \tag{18}$$

Which is of the form $dx_t = f(t, x_t)dW_t^{\mathbb{Q}}$ with:

$$f(t,x) := \delta e^{\gamma t}\sqrt{(x + (V_0 - \theta_\tau^2)e^{(\gamma-\gamma_\tau)t})e^{-\gamma t} + \theta_\tau^2}$$

The process $(x_t)_{t\geq 0}$ is therefore a continuous local martingale, and even a true martingale since $\mathbb{E}^{\mathbb{Q}}(\int_0^T f^2(s, x_s)ds) < \infty$. We can use the change of time method introduced in Swishchuk [11] and we get $x_t = \tilde{W}_{\phi_t}$, where $\tilde{W}_t$ is a $\mathcal{F}_{\phi_t^{-1}}-$ adapted $\mathbb{Q}-$Brownian motion, which is based on the fact that every continuous local martingale can be represented as a time-changed brownian motion. The process $(\phi_t)_{t\geq 0}$ is a.e. increasing, non negative, $\mathcal{F}_t-$ adapted and is called the change of time process. This process is also equal to the quadratic variation $\langle x\rangle_t$ of the (square-integrable) continuous martingale x_t.

Expressions of ϕ_t, ϕ_t^{-1} and $\tilde{W}_t$ are given by:

$$\phi_t = \langle x\rangle_t = \int_0^t f^2(s, x_s)\, ds \tag{19}$$

$$\tilde{W}_t = \int_0^{\phi_t^{-1}} f(s, x_s)dW_s^{\mathbb{Q}} \tag{20}$$

$$\phi_t^{-1} = \int_0^t f^{-2}\left(\phi_s^{-1}, x_{\phi_s^{-1}}\right) ds. \tag{21}$$

This immediately yields:

$$V_t = \theta_\tau^2 + (V_0 - \theta_\tau^2)e^{-\gamma_\tau t} + e^{-\gamma t}\tilde{W}_{\phi_t} \tag{22}$$

Lemma 1:

$$\mathbb{E}_t^{\mathbb{Q}}(\tilde{W}_{\phi_s}) = \tilde{W}_{\phi_{t\wedge s}} \tag{23}$$

And for $s, u \geq t$:

$$\begin{aligned}\mathbb{E}_t^{\mathbb{Q}}(\tilde{W}_{\phi_s}\tilde{W}_{\phi_u}) = x_t^2 + \delta^2 \Bigg[&\theta_\tau^2\left(\frac{e^{2\gamma(s\wedge u)} - e^{2\gamma t}}{2\gamma}\right) \\ &+(V_0 - \theta_\tau^2)\left(\frac{e^{(2\gamma-\gamma_\tau)(s\wedge u)} - e^{(2\gamma-\gamma_\tau)t}}{2\gamma - \gamma_\tau}\right) + x_t\left(\frac{e^{\gamma(s\wedge u)} - e^{\gamma t}}{\gamma}\right)\Bigg]\end{aligned} \tag{24}$$

Proof: (23) comes from the fact that $x_t = \tilde{W}_{\phi_t}$ is a martingale. Let $s \geq u \geq t$. Then by iterated conditioning: $\mathbb{E}_t^{\mathbb{Q}}(\tilde{W}_{\phi_s}\tilde{W}_{\phi_u}) = \mathbb{E}_t^{\mathbb{Q}}(\mathbb{E}_u^{\mathbb{Q}}(\tilde{W}_{\phi_s}\tilde{W}_{\phi_u})) = \mathbb{E}_t^{\mathbb{Q}}(\tilde{W}_{\phi_u}\mathbb{E}_u^{\mathbb{Q}}(\tilde{W}_{\phi_s})) = \mathbb{E}_t^{\mathbb{Q}}(\tilde{W}_{\phi_u}^2)$, because $x_t = \tilde{W}_{\phi_t}$ is a martingale. Now, by definition of the quadratic variation, $x_u^2 - \langle x \rangle_u$ is a martingale and therefore $\mathbb{E}_t^{\mathbb{Q}}(\tilde{W}_{\phi_u}^2) = x_t^2 - \langle x \rangle_t + \mathbb{E}_t^{\mathbb{Q}}(\langle x \rangle_u) = x_t^2 - \phi_t + \mathbb{E}_t^{\mathbb{Q}}(\phi_u) = x_t^2 - \phi_t + \phi_t + \mathbb{E}_t^{\mathbb{Q}}(\int_t^u f^2(s, x_s)\, ds)$. By definiton of $f^2(s, x_s)$ and since x_t martingale, then we have (for $s \geq t$) $\mathbb{E}_t^{\mathbb{Q}}(f^2(s, x_s)) = f^2(s, x_t)$, and so that $\mathbb{E}_t^{\mathbb{Q}}(\tilde{W}_{\phi_s}\tilde{W}_{\phi_u}) = x_t^2 + \int_t^u f^2(s, x_t)\, ds$. A simple integration completes the proof.

The following theorem gives the expression of the Brockhaus&Long approximation of the volatility swap floating leg price process $Y_t(T)$.

Theorem 2: The Brockhaus&Long approximation of the price process $Y_t(T)$ of the floating leg of the volatility swap of maturity T in the delayed Heston model (5)-(8) is given by:

$$Y_t(T) \approx \sqrt{X_t(T)} - \frac{Var_t^{\mathbb{Q}}(V_R)}{8X_t(T)^{\frac{3}{2}}} \tag{25}$$

where $X_t(T)$ is given by Theorem 1 and:

$$\begin{aligned} Var_t^{\mathbb{Q}}(V_R) = {} & \frac{x_t\delta^2}{\gamma^3 T^2}\left[e^{-\gamma t}\left(1 - e^{-2\gamma(T-t)}\right) - 2(T-t)\gamma e^{-\gamma T}\right] \\ & + \frac{\delta^2}{2\gamma^3 T^2}\left[2\theta_\tau^2\gamma(T-t) + 2(V_0 - \theta_\tau^2)\frac{\gamma}{\gamma_\tau}e^{-\gamma_\tau t} + 4\theta_\tau^2 e^{-\gamma(T-t)} - \theta_\tau^2 e^{-2\gamma(T-t)} - 3\theta_\tau^2\right] \\ & - \frac{\delta^2(V_0 - \theta_\tau^2)}{\gamma^2 T^2(\gamma_\tau^2 + 2\gamma^2 - 3\gamma\gamma_\tau)}\left[2(\gamma_\tau - 2\gamma)e^{-\gamma(T-t)-\gamma_\tau t}\right. \\ & \left. + (\gamma - \gamma_\tau)e^{-2\gamma(T-t)-\gamma_\tau t} + 2\frac{\gamma^2}{\gamma_\tau}e^{-\gamma_\tau T}\right] \end{aligned} \tag{26}$$

Proof: The (conditioned) Brockhaus&Long approximation gives us:

$$Y_t(T) = \mathbb{E}_t^{\mathbb{Q}}(\sqrt{V_R}) \approx \sqrt{\mathbb{E}_t^{\mathbb{Q}}(V_R)} - \frac{Var_t^{\mathbb{Q}}(V_R)}{8\mathbb{E}_t^{\mathbb{Q}}(V_R)^{\frac{3}{2}}} = \sqrt{X_t(T)} - \frac{Var_t^{\mathbb{Q}}(V_R)}{8X_t(T)^{\frac{3}{2}}}$$

Furthermore:

$$\begin{aligned} Var_t^{\mathbb{Q}}(V_R) &= \mathbb{E}_t^{\mathbb{Q}}((V_R - \mathbb{E}_t^{\mathbb{Q}}(V_R))^2) \\ &= \frac{1}{T^2}\mathbb{E}_t^{\mathbb{Q}}\left(\left(\int_0^T (V_s - \mathbb{E}_t^{\mathbb{Q}}(V_s))ds\right)^2\right) \end{aligned} \tag{27}$$

From (22) we have $V_t = \theta_\tau^2 + (V_0 - \theta_\tau^2)e^{-\gamma_\tau t} + e^{-\gamma t}\tilde{W}_{\phi_t}$, and since $\tilde{W}_{\phi_t}$ is a martingale, $V_s - \mathbb{E}_t^{\mathbb{Q}}(V_s) = 0$ if $s \leq t$, and $V_s - \mathbb{E}_t^{\mathbb{Q}}(V_s) = e^{-\gamma s}(\tilde{W}_{\phi_s} - x_t)$ if $s > t$.

Therefore

$$\begin{aligned} Var_t^{\mathbb{Q}}(V_R) &= \frac{1}{T^2}\mathbb{E}_t^{\mathbb{Q}}\left(\left(\int_t^T e^{-\gamma s}(\tilde{W}_{\phi_s} - x_t)ds\right)^2\right) \\ &= \frac{1}{T^2}x_t^2\left(\int_t^T e^{-\gamma s}ds\right)^2 + \frac{1}{T^2}\mathbb{E}_t^{\mathbb{Q}}\left(\left(\int_t^T e^{-\gamma s}\tilde{W}_{\phi_s}ds\right)^2\right) \\ &- \frac{2}{T^2}x_t\left(\int_t^T e^{-\gamma s}\mathbb{E}_t^{\mathbb{Q}}(\tilde{W}_{\phi_s})ds\right)\left(\int_t^T e^{-\gamma s}ds\right) \\ &= -\frac{1}{T^2}x_t^2\left(\int_t^T e^{-\gamma s}ds\right)^2 + \frac{1}{T^2}\mathbb{E}_t^{\mathbb{Q}}\left(\left(\int_t^T e^{-\gamma s}\tilde{W}_{\phi_s}ds\right)^2\right) \\ &= \frac{1}{T^2}\int_t^T\int_t^T e^{-\gamma(s+u)}\mathbb{E}_t^{\mathbb{Q}}(\tilde{W}_{\phi_s}\tilde{W}_{\phi_u})dsdu - \frac{1}{T^2}x_t^2e^{-2\gamma t}\left(\frac{1-e^{-\gamma(T-t)}}{\gamma}\right)^2 \end{aligned} \tag{28}$$

Lemma 1 and some straightforward computations complete the proof.

Corollary 2: The Brockhaus&Long approximation of the volatility swap price K_{vol} of maturity T at initiation of the contract $t = 0$ in the delayed Heston model (5)-(8) is given by:

$$K_{vol} \approx \sqrt{K_{var}} - \frac{Var^{\mathbb{Q}}(V_R)}{8K_{var}^{\frac{3}{2}}} \tag{29}$$

where K_{var} is given by Corollary 1 and:

$$\begin{aligned} Var^{\mathbb{Q}}(V_R) = \frac{\delta^2 e^{-2\gamma T}}{2T^2\gamma^3}\Big[\theta_\tau^2\left(2\gamma T e^{2\gamma T} + 4e^{\gamma T} - 3e^{2\gamma T} - 1\right) + \frac{\gamma}{2\gamma - \gamma_\tau}(V_0 - \theta_\tau^2) \\ \left(2e^{2\gamma T}\left(2\frac{\gamma}{\gamma_\tau} - 1\right) - 4\gamma e^{\gamma T}\left(\frac{e^{(\gamma-\gamma_\tau)T} - 1}{\gamma - \gamma_\tau}\right) + 4e^{\gamma T}\left(1 - \frac{\gamma}{\gamma_\tau}e^{(\gamma-\gamma_\tau)T}\right) - 2\right)\Big] \end{aligned} \tag{30}$$

We notice that letting $\tau \to 0$ (and therefore $\gamma_\tau \to \gamma$) we get the formula of Swishchuk [11].

Proof: We have by definition $K_{vol} = Y_0(T)$, and straightforward computations using theorem 2 finish the proof.

5 Volatility Swap Hedging

In this section, we consider dynamic hedging of volatility swaps using variances swap. In the spirit of Broadie and Jain [3], we consider a portfolio containing at time t one unit of volatility swap and β_t units of variance swaps, both of maturity T. Therefore the value Π_t of the portfolio at time t is:

$$\Pi_t = e^{-r(T-t)}\left[Y_t(T) - K_{vol} + \beta_t(X_t(T) - K_{var})\right] \tag{31}$$

The portfolio is self-financing, therefore:

$$d\Pi_t = r\Pi_t dt + e^{-r(T-t)}\left[dY_t(T) + \beta_t dX_t(T)\right] \tag{32}$$

The price processes $X_t(T)$ and $Y_t(T)$ can be expressed, denoting $I_t := \int_0^t V_s ds$ the accumulated variance at time t (known at this time):

$$X_t(T) = \mathbb{E}_t^{\mathbb{Q}}\left[\frac{1}{T}I_t + \frac{1}{T}\int_t^T V_s ds\right] = g(t, I_t, V_t) \tag{33}$$

$$Y_t(T) = \mathbb{E}_t^{\mathbb{Q}}\left[\sqrt{\frac{1}{T}I_t + \frac{1}{T}\int_t^T V_s ds}\right] = h(t, I_t, V_t) \tag{34}$$

Letting $\tilde{\theta}_t^2 := \theta_\tau^2 + (V_0 - \theta_\tau^2)\frac{(\gamma-\gamma_\tau)}{\gamma}e^{-\gamma_\tau t}$ and noticing that $dI_t = V_t dt$, by Ito's lemma we get:

$$dX_t(T) = \left[\frac{\partial g}{\partial t} + \frac{\partial g}{\partial I_t}V_t + \frac{\partial g}{\partial V_t}\gamma(\tilde{\theta}_t^2 - V_t) + \frac{1}{2}\frac{\partial^2 g}{\partial V_t^2}\delta^2 V_t\right]dt + \frac{\partial g}{\partial V_t}\delta\sqrt{V_t}dW_t^{\mathbb{Q}} \tag{35}$$

$$dY_t(T) = \left[\frac{\partial h}{\partial t} + \frac{\partial h}{\partial I_t}V_t + \frac{\partial h}{\partial V_t}\gamma(\tilde{\theta}_t^2 - V_t) + \frac{1}{2}\frac{\partial^2 h}{\partial V_t^2}\delta^2 V_t\right]dt + \frac{\partial h}{\partial V_t}\delta\sqrt{V_t}dW_t^{\mathbb{Q}} \tag{36}$$

As conditional expectations of cashflows at maturity of the contract, the price processes $X_t(T)$ and $Y_t(T)$ are by construction martingales, and therefore we should have:

$$\frac{\partial g}{\partial t} + \frac{\partial g}{\partial I_t}V_t + \frac{\partial g}{\partial V_t}\gamma(\tilde{\theta}_t^2 - V_t) + \frac{1}{2}\frac{\partial^2 g}{\partial V_t^2}\delta^2 V_t = 0 \tag{37}$$

$$\frac{\partial h}{\partial t} + \frac{\partial h}{\partial I_t}V_t + \frac{\partial h}{\partial V_t}\gamma(\tilde{\theta}_t^2 - V_t) + \frac{1}{2}\frac{\partial^2 h}{\partial V_t^2}\delta^2 V_t = 0 \tag{38}$$

The second equation, combined with some appropriate boundary conditions, was used in Broadie and Jain [3] to compute the value of the price process $Y_t(T)$, whereas we focus on its Brockhaus&Long approximation.

Therefore we get:

$$dX_t(T) = \frac{\partial g}{\partial V_t}\delta\sqrt{V_t}dW_t^{\mathbb{Q}} \tag{39}$$

$$dY_t(T) = \frac{\partial h}{\partial V_t}\delta\sqrt{V_t}dW_t^{\mathbb{Q}} \tag{40}$$

and so:

$$d\Pi_t = r\Pi_t dt + e^{-r(T-t)}\left[\frac{\partial h}{\partial V_t}\delta\sqrt{V_t}dW_t^{\mathbb{Q}} + \beta_t\frac{\partial g}{\partial V_t}\delta\sqrt{V_t}dW_t^{\mathbb{Q}}\right] \tag{41}$$

In order to dynamically hedge a volatility swap of maturity T, one should therefore hold β_t units of variance swap of maturity T, with:

$$\beta_t = -\frac{\frac{\partial h}{\partial V_t}}{\frac{\partial g}{\partial V_t}} = -\frac{\frac{\partial Y_t(T)}{\partial V_t}}{\frac{\partial X_t(T)}{\partial V_t}} \tag{42}$$

The initial hedge ratio β_0 is given by ($Var^{\mathbb{Q}}(V_R)$, K_{var} being given resp. in Corollary 2 and 1):

$$\beta_0 = -\frac{\frac{\partial Y_0(T)}{\partial V_0}}{\frac{\partial X_0(T)}{\partial V_0}} \tag{43}$$

$$\frac{\partial X_0(T)}{\partial V_0} = \frac{1-e^{-\gamma_\tau T}}{\gamma_\tau T} \tag{44}$$

$$\frac{\partial Y_0(T)}{\partial V_0} \approx \frac{\frac{\partial X_0(T)}{\partial V_0}}{2\sqrt{K_{var}}} - \frac{K_{var}\frac{\partial Var^{\mathbb{Q}}(V_R)}{\partial V_0} - \frac{3}{2}\frac{\partial X_0(T)}{\partial V_0}Var^{\mathbb{Q}}(V_R)}{8K_{var}^{\frac{5}{2}}} \tag{45}$$

$$\begin{aligned}\frac{\partial Var^{\mathbb{Q}}(V_R)}{\partial V_0} = \frac{\delta^2 e^{-2\gamma T}}{T^2\gamma^3}\frac{\gamma}{2\gamma-\gamma_\tau}\left[e^{2\gamma T}\left(2\frac{\gamma}{\gamma_\tau}-1\right)\right.\\ \left.-2\gamma e^{\gamma T}\left(\frac{e^{(\gamma-\gamma_\tau)T}-1}{\gamma-\gamma_\tau}\right)+2e^{\gamma T}\left(1-\frac{\gamma}{\gamma_\tau}e^{(\gamma-\gamma_\tau)T}\right)-1\right]\end{aligned} \tag{46}$$

The hedge ratio β_t for $t>0$ is given by ($Var_t^{\mathbb{Q}}(V_R)$, $X_t(T)$ being given resp. in Theorem 2 and 1):

$$\beta_t = -\frac{\frac{\partial Y_t(T)}{\partial V_t}}{\frac{\partial X_t(T)}{\partial V_t}} \tag{47}$$

$$\frac{\partial X_t(T)}{\partial V_t} = \frac{1-e^{-\gamma(T-t)}}{\gamma T} \tag{48}$$

$$\frac{\partial Y_t(T)}{\partial V_t} \approx \frac{\frac{\partial X_t(T)}{\partial V_t}}{2\sqrt{X_t(T)}} - \frac{X_t(T)\frac{\partial Var_t^{\mathbb{Q}}(V_R)}{\partial V_t} - \frac{3}{2}\frac{\partial X_t(T)}{\partial V_t}Var_t^{\mathbb{Q}}(V_R)}{8X_t(T)^{\frac{5}{2}}} \tag{49}$$

$$\frac{\partial Var_t^{\mathbb{Q}}(V_R)}{\partial V_t} = \frac{\delta^2}{\gamma^3 T^2}\left[1-e^{-2\gamma(T-t)}-2(T-t)\gamma e^{-\gamma(T-t)}\right] \tag{50}$$

We take the parameters that have been calibrated in section 3 and we plot the naive Volatility Swap strike $\sqrt{K_{var}}$ and the adjusted Volatility Swap strike $\sqrt{K_{var}} - \frac{Var^{\mathbb{Q}}(V_R)}{8K_{var}^{\frac{3}{2}}}$ along the maturity dimension, as well as the convexity adjustment $\frac{Var^{\mathbb{Q}}(V_R)}{8K_{var}^{\frac{3}{2}}}$:

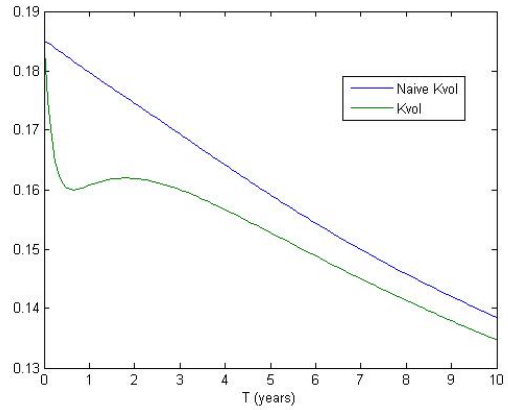

Figure 1: *Naive Volatility Swap Strike Vs. Adjusted Volatility Swap Strike*

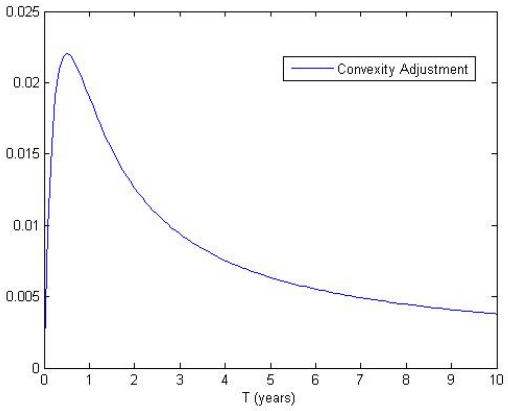

Figure 2: *Convexity Adjustment*

We also plot the initial hedge ratio β_0 along the maturity dimension.

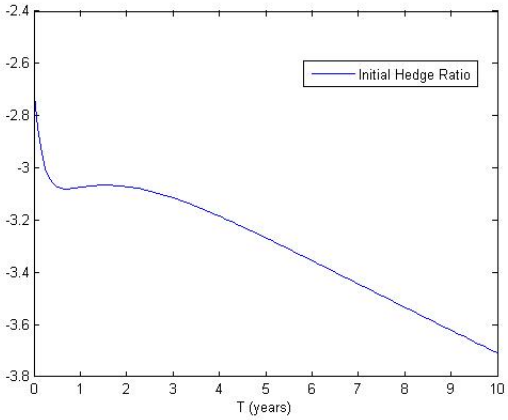

Figure 3: *Initial Hedge Ratio*

References

1.Bollerslev, T. Generalized autoregressive conditional heteroscedasticity. *J. Economics* 31, 307-27, 1986.
2.Broadie, M. and Jain, A. The effect of jumps and discrete sampling on volatility and variance swaps. *Intern. J. Theor. Appl. Finance*, vol. 11, no. 8, pp. 761-797, 2008.
3.Broadie, M and Jain, A. Pricing and Hedging Volatility Derivatives. *Journal of Derivatives*, Vol.15, No.3, 7-24, 2008.
4.Brockhaus, O. and Long, D. Volatility swaps made simple. *Risk*, January, 92-96, 2000.
5.Carr, P. and Lee, R. Volatility Derivatives. *Annu. Rev, Financ. Econ.*, 1:1-21 (doi:10.1146/annurev.financial.050808.114304), 2009.
6.Heston, S. A closed-form solution for options with stochastic volatility with applications to bond and currency options. *Review of Financial Studies*, 6, 327-343, 1993.
7.Heston, S. and Nandi, S. Derivatives on volatility: some simple solutions based on observables. *Federal Reserve Bank of Atlanta*, working paper 2000-20, November, 2000.
8.Kazmerchuk, Y., Swishchuk, A. and Wu, J. The pricing of options for security markets with delayed response. *Mathematics and Computers in Simulation* 75 6979, 2007.
9.Kazmerchuk, Y., Swishchuk, A. and Wu, J. A continuous-time GARCH model for stochastic volatility with delay. *Candian Appl. Math. Quart.*, v. 13, No. 2, 2005.
10.Swishchuk, A. and Li, X. Pricing variance swaps for stochastic volatilities with delay and jumps, *Intern. J. Stoch. Anal.*, vol. 2011 (2011), Article ID 435145, 2011.
11.Swishchuk, A. Modeling of variance and volatility swaps for financial markets with Stochastic volatilities. *Wilmott Magazine*, September issue, No. 2, pp. 64-72, 2004.
12.Swishchuk, A. Modeling and pricing of variance swaps for stochastic volatilities with delay. *Wilmott Magazine*, September, No. 19, pp. 63-73, 2005.
13.Swishchuk, A. Modeling and Pricing of Variance Swaps for Multi-Factor Stochastic Volatilities with Delay. *Canad. Appl. Math. Quart.*, Volume 14, Number 4, Winter 2006.
14.Swishchuk, A. Variance and volatility swaps in energy markets. *J. Energy Markets*, Volume 6/Number 1, Spring 2013 (3349), 2013.
15.Swishchuk, A and Malenfant, K. Variance swap for local Levy based stochastic volatility with delay. *Intern. Rev. Appl. Fin. Iss. Econ. (IRAFIE)*, Vol. 3, No. 2, 2011, pp. 432-441, 2011.

Proceedings, 15th Applied Stochastic Models and Data Analysis (ASMDA2013)
International Conference, Mataró (Barcelona), Spain 25 - 28 June 2013

Intergenerational mobility as a distance measure between probability distribution functions

M. Symeonaki and G. Stamatopoulou

Department of Social Policy, Panteion University of Social and Political Sciences,
136 Syggrou Av., 176 71, Athens, Greece
(E-mail: msymeonaki@me.com, gl.stamat@gmail.com)

Abstract. This paper presents a methodology of estimating social intergenerational mobility as a distance or similarity measure between the parent's probability distribution function and the sibling's. Several distance and similarity measures are provided and their properties are discussed. An illustration of the methodology is presented providing the measurement of the intergenerational occupational mobility with evidence drawn from the Survey of Health, Ageing and Retirement in Europe (SHARE project), and more specifically from SHARELIFE release 1.0, concerning Greece[1].
Keywords: Intergenerational mobility, distance and similarity measures, SHARE project, occupational intergenerational mobility.

1 Introduction

The measurement of intergenerational mobility is of utmost important for the Social and Economical Sciences as it reveals information about the existence of social inequalities, the intergenerational transmission of poverty, social inclusion etc providing a measurement of the extent to which positions, social status or socio-economical thesis change from one generation to another.

There are many approaches to the measurement of intergenerational social mobility. The statistical approach (see for example Bartholomew [3], Bartholomew *et al.* [2] and Boudon [5] among others), where the concept of transition matrices is used and social mobility is studied by examining the

[1] This paper uses data from SHARE wave 4 release 1, as of November 30th 2012. The SHARE data collection has been primarily funded by the European Commission through the 5th Framework Programme (project QLK6-CT-2001-00360 in the thematic programme Quality of Life), through the 6th Framework Programme (projects SHARE-I3, RII-CT-2006-062193, COMPARE, CIT5- CT-2005-028857, and SHARELIFE, CIT4-CT-2006-028812) and through the 7th Framework Programme (SHARE-PREP, No 211909, SHARE-LEAP, No 227822 and SHARE M4, No 261982). Additional funding from the U.S. National Institute on Aging (U01 AG09740-13S2, P01 AG005842, P01 AG08291, P30 AG12815, R21 AG025169, Y1-AG-4553-01, IAG BSR06-11 and OGHA 04-064) and the German Ministry of Education and Research as well as from various national sources is gratefully acknowledged (see www.share-project.org for a full list of funding institutions).
This study was supported in part by a grand from THALIS-Panteion University-Investigating Crucial Interdisciplinary Linkages in Ageing Societies

mathematical properties of these transition matrices. A number of mobility indices based on the elements of the transition probabilities are proposed in the context of the transition matrix approach [13,11,3]. Other approaches based on the estimation of transition probabilities and on empirical data can be found in Symeonaki *et al.* [14–16].

On the other hand, there is the distance approach (see for example Cowell [6] and Fields and Ok [7]). The concepts of distance and similarity are essential in both abstract and applied sciences and consequently distance measures have become an important tool in many areas including Probability and Statistics, Computer Science, Social Sciences, Pattern Recognition, Image Processing, etc. In the literature, distances, dissimilarity and similarity measures, or similarity coefficients are used to express quantitatively the similarity or dissimilarity of two data points, objects, clusters, distributions, samples, etc. Similarity measures and similarity coefficients are used to describe how similar two data points (clusters, objects, samples, distributions, etc) are, whereas distance measures or dissimilarity measures are used to examine how dissimilar two data points (clusters, objects, samples, distributions, etc) are ([9]). Many measures of similarity or dissimilarity have been proposed in the literature. Understanding the relationship between different distance measures is helpful in choosing a proper one for a particular application.

In the study of social mobility, the distance approach covers only the income intergenerational mobility, where the continuous variable of income is taken into account. Therefore, this leaves out the comparison of discrete probability distribution functions and moreover it uses income as the means of stratification. This is not always the best way, since in most cases we cannot have access to valid income data. In the present paper, we propose alternatively the measurement of intergenerational occupational mobility and provide a methodology of measuring mobility with the aid of distance or similarity measures. More specifically, we provide distance and similarity measures that can account for the dissimilarity between the parent's occupational distribution and the respective distribution of the sibling. In this case, we are actually looking for a distance or similarity measure, between two discrete probability distributions. In order to illustrate the methodology, we use data drawn from the Survey of Health, Ageing and Retirement in Europe (SHARE project) and more specifically data drawn from SHARELIFE release 1.0, concerning Greece in respect to the respondent's occupation and the occupation of main breadwinner.

The paper has been organised in the following way. Section 2 provides the preliminaries and the notation employed in the paper, whereas Section 3, presents the distance and similarity measures of occupational intergenerational mobility. Having presented the measures the similarity and distance measures between the respondent and main breadwinner in respect to their occupation are estimated for Greece, with data drawn from SHARELIFE release 1.0, in order to facilitate the theoretical aspects of Section 3. Section 5 summarises the conclusions of our analysis.

2 Preliminaries and notation

The mathematical notion of (metric) distance introduced in Frechet [8] and Hausdorff [10] is given by the following Definitions.

Definition 1. Let X be a set. A distance on X is a function $d : X \times X \to R$, where R is the set of real numbers, if and only if it satisfies the following conditions, $\forall x, y \in X$:

1. $d(x, y) \geq 0$, (non-negativity or positivity axiom),
2. $d(x, y) = 0$, if and only if $x = y$, (reflexivity axiom), and
3. $d(x, y) = d(y, x)$, (symmetry axiom).

Definition 2. Let X be a set. A metric distance on X is a function $d : X \times X \to R$, where R is the set of real numbers, if and only if it satisfies the following conditions, $\forall x, y \in X$:

1. $d(x, y) \geq 0$, (non-negativity or positivity axiom),
2. $d(x, y) = 0$, if and only if $x = y$, (identity axiom),
3. $d(x, y) = d(y, x)$, (symmetry axiom), and
4. $d(x, z) \leq d(x, y) + d(y, z)$ (triangle inequality).

Table 1 provides a summary of the basic notation used in the remaining of the paper.

Table 1. Summary of the notation used

Notation	Description
d	denotes the number of occupational classes, i.e. the occupational space, denoted by S is equal to $S = \{1, 2, ..., d\}$,
x_i	is the number of respondents in the $i-th$ occupational class,
f_i	is the number of main breadwinners in the $i-th$ occupational class,
x	is the total number of respondents, i.e. $x = \sum_{i=1}^{d} x_i$,
f	is the total number of main breadwinners, i.e. $f = \sum_{i=1}^{d} f_i$,
p_i^x	denotes the proportion of respondents in $i-th$ occupational level, i.e. $p_i^x = \frac{x_i}{x}$,
p_i^f	denotes the proportion of fathers in $i-th$ occupational level, i.e. $p_i^f = \frac{f_i}{f}$,
$\mathbf{p}_x$	denotes the vector $\mathbf{p}_x = [p_1^x, p_2^x, ..., p_d^x]$, and
$\mathbf{p}_f$	denotes the vector $\mathbf{p}_f = [p_1^f, p_2^f, ..., p_d^f]$.

3 Intergenerational mobility based on distance and similarity measures

In the present section, following the notation introduced in Section 2 we provide a number of distance and similarity measures, which will be used in the measurement of intergenerational mobility of occupation. The most widely known distance between two points (clusters, objects, etc) is the Euclidean distance. The Euclidean distance between the vectors $\mathbf{p}_f$ and $\mathbf{p}_x$ is given by Equation (1):

$$d_{Euc} = \sqrt{\sum_{i=1}^{d} |p_i^f - p_i^x|^2}. \tag{1}$$

In Manhattan distance (Equation (2)) the distance between two points is calculated as the sum of the absolute differences of their coordinates. Its true meaning, therefore, lies in the fact that it represents the total proportional variation of parents and siblings when their distribution to occupational classes is considered.

$$d_{Man} = \sum_{i=1}^{d} |p_i^f - p_i^x|. \tag{2}$$

The Minkowski distance (Equation (3)), or L_p, is a metric on Euclidean space which can be considered as a generalization of both the Euclidean distance and the Manhattan distance. It is also true that the higher the value of p, the greater the importance given to large differences. Therefore, deciding upon an appropriate value of p, comes to the emphasis that one would like to give to the larger differences of proportions to the occupational classes between siblings and parents.

$$d_{Mk} = \sqrt[p]{\sum_{i=1}^{d} |p_i^f - p_i^x|^p}. \tag{3}$$

The Sorensen index (Equation (4)), also known as Sorensen's similarity coefficient, is a statistical index used for comparing the similarity of two samples.

$$d_{Sor} = \frac{\sum_{i=1}^{d} |p_i^f - p_i^x|}{\sum_{i=1}^{d} (p_i^f + p_i^x)} = \frac{\sum_{i=1}^{d} |p_i^f - p_i^x|}{2}. \tag{4}$$

It is obvious from Equation (2) that $d_{Sor} = \frac{d_{Man}}{2}$ and is usually used as a measure for gender segregation.

Gower's similarity index is given by Equation (5).

$$d_{Gow} = \frac{\sum_{i=1}^{d} |p_i^f - p_i^x|}{d}. \tag{5}$$

Chebyshev distance, or L^∞ metric is a metric on a vector space where the distance between two vectors is the greatest of their differences along any

coordinate dimension. Chebychev distance considers only the part for which the difference is maximum, while Manhattan distance gives equal importance to all differences. Therefore, we could assume that Chebychev distance represents the maximum proportional variation of the occupational distribution between parents and siblings.

$$d_{Cheb} = \max_i |p_i^f - p_i^m|. \quad (6)$$

4 Distance and similarity measures of intergenerational mobility with evidence from the SHARELIFE release 1.0.

The SHARE project[1,4] is a multidisciplinary, longitudinal and cross-national panel database, developed to understand the relations between health, labour force participation and institutional context of old people support in Europe. Funding mainly via the European Commission, as well as the US National Institute on Ageing and national sources, it is designed in January of 2002 and it is conducted every two years. The first wave of the survey took place in 2004–2005, in 11 European countries ranging from Nordic to Mediterranean countries, while the fourth wave took place in 2010-2011. The main purpose of survey is to provide a full picture of all aspects of ageing process and its impact in the different cultures of Europe. Moreover, using the knowledge of its predecessors, the US Health and Retirement Study (HRS) and the English Longitudinal Survey on Ageing (ELSA), the survey aims to collect comparable data useful for the policies planned and applied in the European Union. In order to succeed its purposes, the survey divided into 21 modules. Except for the coverscreen (CV) and the demographic (DN) modules, it covers a large variety of subjects, such as physical and mental health, behavioural risks, employment and pensions, social support etc. The target population of the survey is all the non-institutionalised population aged more than 50 years old, as well as their spouse, regardless of their age.

SHARELIFE [12] is the third wave of data collection for SHARE, which focuses on people's life histories. SHARELIFE assembled more comprehensive information on significant areas of our respondents lives, including partners and children, housing and work history, detailed questions on health and health care, etc. SHARELIFE thus complements the SHARE panel data by providing life history information to enhance the understanding of how early life experiences and events throughout life influence the circumstances of older people. With this variety SHARELIFE constitutes an unique cross-national, interdisciplinary database for research in the fields of sociology, economics, gerontology, and demography. SHARELIFE links individual micro data over the respondents entire life with institutional macro data on the welfare state. It thereby allows assessing the full effect of welfare state interventions on the life of the individual. Changes in institutional settings that influence individual decisions are of specific interest to evaluate policies throughout Europe. SHARELIFE follows a Life History Calendar (LHC) approach, which has been

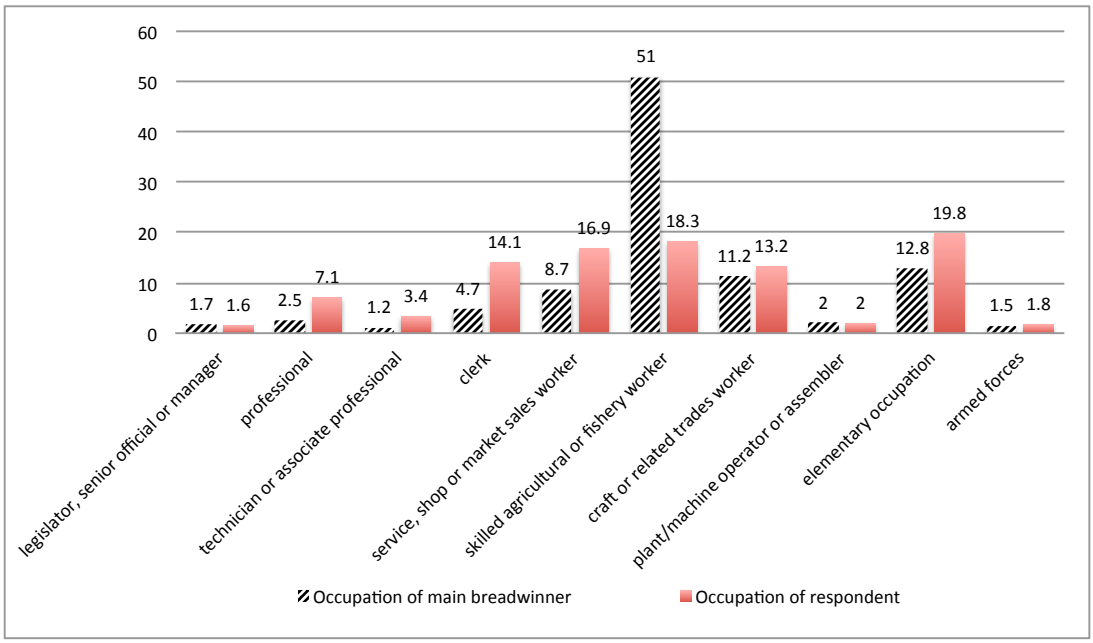

Fig. 1. Distribution of job description between main breadwinner and respondent. [2] *Source: SHARELIFE, release 1.0*, $N = 2,938$.

designed to help respondents in remembering past events more accurately. Using the life history calendar technique has been shown to improve the accuracy of the retrospective information given by respondents [12]. In the present section, we provide the experimental results obtained by using the similarity and distance measures of Section 3, with data drawn from SHARELIFE release 1.0 (SHARE, wave 3) for Greece, in respect to the respondent's occupation and the occupation of main breadwinner.

In Figure 1 the probability distributions of the main breadwinner and the respondent are exhibited. The categorisation used is the one provided in Table 2. The shortest distance, i.e. the Euclidean distance, for example will be equal to $d_{Euc} = 0.361$. Other distance measures can be found in Table 3 and Table 4. In the case of Chebyshev distance, only the maximum difference is estimated, and therefore $d_{Cheb} = 0.327$, being the difference in the proportions in the $6-$th occupational class, which is actually a considerable distance, caused by a notable drop in the percentage of individuals in the Agricultural or Fishery occupations.

5 Conclusions

The justification for using distance and similarity measures or similarity coefficients as a measure of intergenerational (or intragenerational) social mobility is established upon the understanding that high mobility indicates different distribution probabilities between siblings and parents (or different distributions

Table 2. Respondent's and main breadwinner's job description

Field of subject, highest qualification	**Main breadwinner**	**Respondent**
Legislator, senior official or manager	1.7	1.6
Professional	2.5	7.1
Technician or associate professional	1.2	3.4
Clerk	4.7	14.1
Service, shop or market sales worker	8.7	16.9
Skilled agricultural or fishery worker	51.0	18.3
Craft or related trades worker	11.2	13.2
Plant/machine operator or assembler	2.0	2.0
Elementary occupation	12.8	19.8
Armed forces	1.5	1.8
Total	100.0	100.0

[3] *Source: SHARELIFE, release 1.0*, $N = 2,938$.

Table 3. Distance and similarity measures between main breadwinners and respondents

1.	Euclidean distance	$d_{Euc} = 0.665$
2.	Manhattan distance	$d_{Man} = 0.361$
3.	Sorensen index	$d_{Mk} = 0.333$
4.	Gower simmilarity index	$d_{Gow} = 0.067$
5.	Chebyshev distance	$d_{Cheb} = 0.327$

[4] *Source: SHARELIFE, release 1.0*, $N = 2,938$.

during one's lifetime) across the occupational, educational or social classes; the more different the distributions, the more mobile individuals are in respect to the social ladder, the bigger the distance measures (or the smaller the similarity measures). Therefore, it is important to consider distance measures, to understand the meaning of their values and to be able to choose between them.

References

1.C. Barang, V. Eudier, N. Sirven. SHARE, the Survey of Health, Ageing, and Retirement in Europe goes longitudinal. *Issues in health economics*, n 137, Institute for research and information in health economics, IRDES, 2008.

2.D. J. Bartholomew, A. F. Forbes, S. I. McClean. *Statistical techniques for manpower planning*. 1991. John Wiley & Sons.

Table 4. The Minkowski distance for different values of p between main breadwinners and respondents

p	d_{Mk}
$p = 1$	$d_{Mk} = 0.361$
$p = 2$	$d_{Mk} = 0.815$
$p = 3$	$d_{Mk} = 0.19185$
$p = 4$	$d_{Mk} = 0.1064$
$p = 5$	$d_{Mk} = 0.06125$
$p = 6$	$d_{Mk} = 0.03498$
$p = 10$	$d_{Mk} = 0.00374$
$p = 20$	$d_{Mk} = 0.0000$

[5] *Source: SHARELIFE, release 1.0*, $N = 2,938$.

3.D. J. Bartholomew. *Stochastic Models for social processes*. London, 1982. Wiley.
4.A. Börsch-Supan and H. Jürges (eds.). *The Survey of Health, Ageing and Retirement in Europe - Methodology*. Mannheim, 2005. Mannheim Research Institute for the Economics of Aging (MEA).
5.R. Boudon. *Mathematical Structures of Social Mobility*. Amsterdam, 1973. Elsevier.
6.F. A. Cowell. Measures of distributional change: an axiomatic approach. *Review of Economic Studies*, 52:135-151, 1985.
7.G. S. Fields, E. Ok. Measurement movement of incomes. *Economica*, 66:455-471, 1999.
8.M. Frechet. Sur quelques points du calcul fonctionnel (These). *Rend. Circ. Mat. Palermo*, 22:1-74, 1906.
9.Gan, G., Ma, C. and Wu, J. (2007), Data Clustering: Theory, Algorithms, and Applications, ASA-SIAM Series on Statistics and Applied Probability, SIAM, Philadelphia, PA.
10.F. Hausdorff. *Grundzuege der Mengenlehre*. Leipzig, 1914. Viet.
11.G. Heineck and R. Riphahn. Intergenerational transmission of educational attainment in Germany - the last five decades. *Journal of Economic and Statistics*, 229:36-60, 2007.
12.SHARELIFE, Survey of Health, Ageing and Retirement in Europe, Release Guide 1, Mannheim Research Institute for the Economics of Aging (MEA).
13.A. F. Shorrocks. The measurement of social mobility. *Econometrica*, 46:1013-1024, 1978.
14.M. Symeonaki, O. Filopoulou and G. Stamatopoulou, Measuring Intergenerational Educational Mobility in Greece, ASMDA, Rome, Italy, 7-10 June, 2011.
15.M. Symeonaki, G. Stamatopoulou and K. Michalopoulou, Intergenerational Occupational Mobility in Greece: Evidence from EU-SILC, Demographic Analysis and Research International Conference, Chania, Greece, 5-8 June, 2012.
16.M. Symeonaki and G. Stamatopoulou, Exploring the transition to Higher Education in Greece: issues of intergenerational educational mobility In I. Lamprianou (ed.) "International perspectives of transition to Higher Education: issues of social justice and participation", Policy Futures in Education, 2013 in press.
17.A. F. Shorrocks. Ranking income distributions. *Economica* 50:3-17, 1983.